Targeted chromosome shredding to explore X chromosome aneuploidies in aging

Dissertation

Zur Erlangung des Grades

Doktor der Naturwissenschaften

Am Fachbereich Biologie

Der Johannes Gutenberg-Universität Mainz

José Héctor Gibrán Fritz García

geboren am 16.09.1998 in Mexiko Stadt, Mexiko

Mainz, 2025

Dekan: Prof. Dr. Eckhard Thines

1. Berichterstatterin: [redacted]

2. Berichterstatterin: [redacted]

Tag der mündlichen Prüfung: 12.02.2026

Summary

Aging is characterized by a gradual decline in cellular functions, and growing evidence shows that it does not affect men and women equally. Although women live, on average, five years longer than men, they often experience poorer health overall. Many age-associated diseases display sex biases. One contributing factor is the sex chromosome complement. Male mammals carry one X and one Y chromosome, whereas females possess two X chromosomes, one of which is largely transcriptionally inactivated, though some genes escape silencing. These escaper genes contribute to female resilience, yet their misregulation can also increase disease susceptibility. Notably, female cells with different X chromosome aneuploidies accumulate with age, with the preferential loss of the inactive X the most common. The causal relationship between X chromosome loss and aging remains unknown, and the immediate cellular consequences upon X chromosome loss are largely unexplored.

This work reports the first successful derivation and characterization of C3H/Bl6 hybrid mouse embryonic stem cells. Both male and female C3H/Bl6 cells express pluripotency markers, with only a minor differentiation bias toward the germ layers. The differentiation potential of these cells was evaluated through random differentiation into embryoid bodies, which expressed markers of all lineages; however, fewer beating cardiomyocyte-like structures were observed in embryoid bodies derived from female cells. Immunostainings confirmed the presence of cell types from all three germ layers. Analysis of X chromosome dynamics during the differentiation of female cells into epiblast-like stem cells showed that X chromosome silencing occurred progressively over seven days, following a heterogenous yet overall consistent kinetics.

Genome editing in the C3H/Bl6 background proved challenging and yielded low efficiencies. Nevertheless, we established a cellular system enabling allele-specific chromosome targeting and shredding in female hybrid cells. The system was activated through Cre recombinase delivery via baculovirus. We found that segmental aneuploidies of the targeted X chromosome constituted the predominant outcome, followed by complete X chromosome loss. Evidence of genomic instability was also observed, with a small proportion of cells exhibiting micronuclei containing X chromosome fragments.

Overall, we established a chromosome targeting and shredding system in *bona fide* C3H/Bl6 hybrids mouse embryonic stem cells. We demonstrated that generating X chromosome aneuploidies is feasible, with chromosome segmentation representing the primary event. This tool provides a foundation to dissect the causal relationship of sex chromosome loss and aging. In addition, these hybrid cells are a valuable model for studying stem cell biology, X chromosome dynamics and sex differences.

Zusammenfassung

Altern ist durch einen allmählichen Rückgang zellulärer Funktionen gekennzeichnet, und immer mehr Hinweise deuten darauf hin, dass Männer und Frauen davon nicht gleichermaßen betroffen sind. Obwohl Frauen im Durchschnitt fünf Jahre länger leben als Männer, weisen sie häufig eine insgesamt schlechtere Gesundheit auf. Viele altersassoziierte Erkrankungen zeigen Geschlechtsunterschiede. Ein Faktor der dazu beiträgt sind die Geschlechtschromosomen. Männliche Säugetiere besitzen ein X- und ein Y-Chromosom, während weibliche Säugetiere zwei X-Chromosomen aufweisen, von denen eines größtenteils transkriptionell inaktiviert ist - wenngleich einige Gene dieser Inaktivierung entgehen. Diese Escaper-Gene tragen zur Resilienz von Frauen bei, doch ihre Fehlregulation kann auch die Anfälligkeit für Krankheiten erhöhen. Bemerkenswerterweise häufen sich mit dem Alter weibliche Zellen mit unterschiedlichen X-Chromosomenvarianten an, einschließlich eines bevorzugten Verlusts des inaktiven X. Die kausale Beziehung zwischen dem Verlust des X-Chromosoms und dem Alterungsprozess ist bislang unbekannt, und die unmittelbaren zellulären Folgen eines solchen Verlusts sind weitgehend unerforscht.

Diese Arbeit beschreibt die erste erfolgreiche Etablierung und Charakterisierung von C3H/Bl6-Hybrid-Maus-embryonalen Stammzellen. Sowohl männliche als auch weibliche C3H/Bl6-Zellen exprimieren Pluripotenzmarker und zeigen nur eine geringe Differenzierungspräferenz hin zu den Keimblättern auf. Das Differenzierungspotenzial dieser Zellen wurde durch eine zufällige Differenzierung in Embryoid Bodies untersucht, die Marker aller Zelllinien exprimierten; jedoch wurden in Embryoid Bodies, die aus weiblichen Zellen stammten, weniger schlagende, kardiomyozytenähnliche Strukturen beobachtet. Immunfärbungen bestätigten das Vorhandensein von Zelltypen aller drei Keimblätter. Die Analyse der X-Chromosomendynamik während der Differenzierung weiblicher Zellen zu epiblast-ähnlichen Stammzellen zeigte, dass die X-Chromosomen-Inaktivierung über einen Zeitraum von sieben Tagen schrittweise erfolgte, wobei sie heterogen, aber insgesamt konsistent verlief.

Genome Editing im C3H/Bl6-Hintergrund erwies sich als anspruchsvoll und zeigte geringe Effizienzen. Dennoch etablierten wir ein zelluläres System, das allelspezifisches Chromosomen-Targeting und -Shredding in weiblichen Hybridzellen ermöglicht. Das System wurde durch die Einbringung einer Cre-Rekombinase über Baculoviren aktiviert. Wir stellten fest, dass segmentale Aneuploidien des anvisierten X-Chromosoms die häufigste Konsequenz waren, gefolgt vom vollständigen Verlust des X-Chromosoms. Hinweise auf genomische Instabilität wurden ebenfalls beobachtet, wobei ein kleiner Teil der Zellen Mikronuklei mit Fragmenten des X-Chromosoms aufwiesen.

Zusammenfassend etablierten wir ein System zum Targeting und Shredding von Chromosomen in bona fide C3H/Bl6-Hybrid-Maus-embryonalen Stammzellen. Wir zeigten, dass die Erzeugung von X-Chromosomen-Aneuploidien möglich ist, wobei Chromosomensegmentierungen das primäre Resultat darstellen. Dieses Werkzeug bildet eine Grundlage zur Untersuchung des kausalen Zusammenhangs zwischen dem Verlust von Geschlechtschromosomen und dem Alterungsprozess. Darüber hinaus stellen diese Hybridzellen ein wertvolles Modell für die Erforschung der Stammzellbiologie, der X-Chromosomendynamik und der Geschlechtsunterschiede dar.

Acknowledgements

[redacted]

[redacted]

Content

List of Figures

List of Tables

Abbreviations

AD	Alzheimer’s disease
AMPK	AMP-activated protein kinase
BAC	Bacterial artificial chromosome
Cas9	CRISPR-associated protein 9
cDNA	Complementary DNA
CMV	Cytomegalovirus promoter
CpG	Cytosine preceding guanine
CRISPR	Clustered Regularly Interspaced Short Palindromic Repeats
CVD	Cardiovascular disease
DC	Dosage compensation
DNA FISH	DNA fluorescence *in situ* hybridization
DNAme	DNA methylation
E	Embryonic day
EB	Embryoid body
EpiLSCs	Epiblast-like stem cells
FA	Fanconi anemia
FBS	Fetal bovine serum
gDNA	Genomic DNA
gRNA	Guide RNA
GWAS	Genome-wide association studies
HnRNP	Heterogeneous nuclear ribonucleoprotein
HSC	Hematopoietic stem cell
iPSC	Induced pluripotent stem cell

iXCI	Imprinted XCI
LIF	Leukaemia inhibitor factor
lncRNA	Long non-coding RNA
LOX	Loss of the X
LOY	Loss of the Y
MEF	Mouse embryonic fibroblast
mESC	Mouse embryonic stem cell
mTOR	Mammalian target of rapamycin
NHEJ	Non-homologous end joining
p	Passage
rXCI	Random XCI
RNA FISH	RNA fluorescence *in situ* hybridization
ROS	Reactive oxygen species
PAR	Pseudoautosomal region
qPCR	Quantitative PCR
RT-qPCR	Retrotrancriptase quantitative PCR
TAD	Topologically associating domain
UPR	Unfolded protein response
WT	Wild-type
XIC	X inactivation center
XCI	X chromosome inactivation
Xist/XIST	X-inactive specific transcript

Declaration

Parts of what is presented in the introduction sections **1.2 Sex bias in the hallmarks of aging** and **1.3 The X chromosome as a double balance**, together with Figure 1.4, have been published in the following peer-reviewed publication:

Fritz García JHG, Keller Valsecchi CI, Basilicata MF. 2024 Sex as a biological variable in ageing: insights and perspectives on the molecular and cellular hallmarks. *Open Biol*. **14**: 240177. https://doi.org/10.1098/rsob.24.

My contribution to that review involved conceptualization, investigation, writing—original draft, review and editing.

For the purpose of this thesis, some sections have been further expanded and updated since the publication of the review article and therefore they do not represent an identical version of the work presented herein. The original review article can be found in Appendix I.

1. Introduction

1.1 The mammalian X chromosome and X chromosome inactivation

1.1.1 Sex chromosomes and dosage compensation

Genetically, mammals only differ in a pair of chromosomes that, through a signaling pathway, define whether an organism develops as a male or a female. This pair, the X and Y, are known as sex the chromosomes. Male mammals contain a gene-rich X chromosome and a small, gene-poor Y chromosome; females, on the other hand, harbor two X chromosomes.

The sex chromosomes originated from a pair of autosomes where one of them —the future Y chromosome in this case —acquired a sex-determining region. Over time, other male-benefiting genes evolved. Linkage between the sex-determining locus and the other male-beneficial alleles suppressed recombination between the future pair of sex chromosomes, resulting in a shorter and degenerated Y chromosome; some genes, however, have been retained on the pseudoautosomal regions (PARs) (Figure 1.1) (Furman et al. 2020). In fact, the X chromosome is about 100 megabases larger than the Y chromosome, yet a handful of X-linked genes, known as gametologs, are also present in the Y (Balaton et al. 2018). Out of the approximately 70 protein-coding genes found on the Y chromosome (Maan et al. 2017), 17 in humans and 8 in the mouse

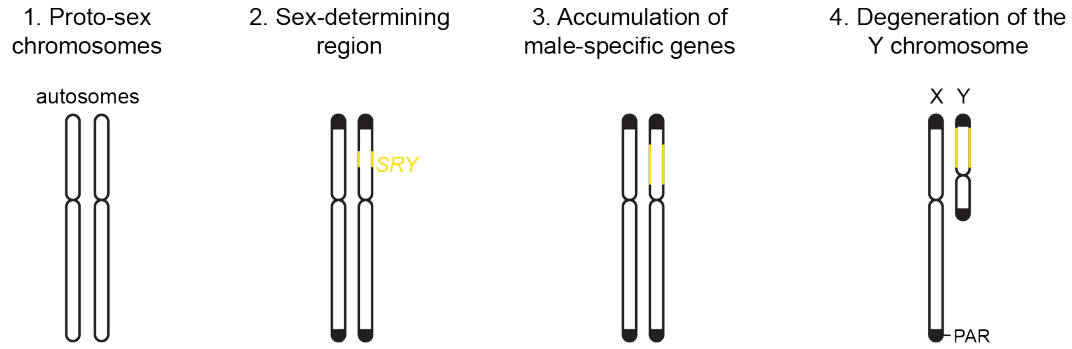

Figure 1.1. Evolution of the sex chromosomes. (1) Sex chromosomes originated from a pair of ancestral autosomes. (2) The future Y chromosomes acquired a sex-determining region (the *SRY* locus) and overtime (3) male-benefitting genes appeared, suppressing recombination between the chromosomes. (4) Lack of recombination resulted in degeneration of the Y chromosome. In the pseudoautosomal regions (PAR) recombination still takes place.

have a homolog on the X chromosome, known as gametologs (Bellott et al. 2014). Given the presence of conserved genes between the X and Y chromosomes in the PARs, they behave like autosomes and undergo recombination during meiosis (Dos Santos, Mendes, and Antunes 2022).

Eukaryotes generally have two copies of each gene, one paternally inherited and the other of a maternal origin. Gene dosage is the number of gene copies present in a genome and deviations from an *n* euploid karyotype results in gene dosage alterations. The main evidence of gene dosage deviations is whole chromosome aneuploidies during development; of note, chromosome arm losses result in copy number variations and can also be considered as aneuploidies (Ben-David and Amon 2020). Aneuploidies are incompatible with embryonic development, resulting in premature differentiation and cell cycle arrest, which can be cell-type specific, affecting either the cells that will give rise to the embryo, or extraembryonic tissue such as the placenta (Shahbazi et al. 2020). When they are tolerated, however, diseases manifest. The only three known viable human autosomal aneuploidies are present in Patau, Edwards and Down syndromes, accounting for trisomies of human chromosomes 13, 18 and 21, respectively (Basilicata and Keller Valsecchi 2021). This piece of evidence suggests that organisms cannot cope with gene dosage changes. Of note, aneuploidies can also arise during lifespan resulting in different diseases, being cancer the most well-known consequence (Ben-David and Amon 2020; Sdeor et al. 2024).

1.1.2 X chromosome inactivation (XCI)

By definition, the XY karyotype is an aneuploidy that is, surprisingly, well-tolerated. This perception, together with the fact that females have an additional X chromosome, raised the idea that a compatible mechanism simultaneously evolved to ensure similar expression levels between males and females (Susumu Ohno 1967). Without it, the XX genotype would lead to a gene dosage imbalance between the sexes since, compared to higher expression in females, the only X copy present in males would result in monoallelic gene expression. Molecularly, and in agreement with autosomal aneuploidies, the X-linked gene imbalance may disrupt protein stoichiometric ratios and perturbation of molecular networks affecting, in turn, organismal fitness (Gu and Walters 2017; Chunduri, Barthel, and Storchova 2022).

Seminal work by Mary F. Lyon discussed that a mechanism to equalize the gene expression between the XX and XY genotypes must exist (Lyon 1961, 1962). Her law was based on the realization that X-linked mutations would result in a patched coat color in mice, rather than a homogenous tone. She proposed that the difference in color spots arises from different

populations of cells inactivating different parental X chromosomes, resulting in a distribution of color patches (Lyon 1961). This is complemented with earlier work indicating that X0 mice are fertile (Welshons and Russell 1959) and the observation that sex-specific X chromosome condensation patterns exist (Barr and Bertram 1949; S. Ohno and Hauschka 1960). Years later, this process is now known and has been coined X chromosome inactivation (XCI). Most of the existing knowledge of XCI comes from the mice but its study in other mammalian species provides an evolutionary perspective of this process. The following sections mostly discuss findings from the mouse, but other relevant models are discussed appropriately.

1.1.2.1 Mechanism of XCI

As proposed by [redacted], XCI works by the transcriptional silencing of one random X chromosome. XCI starts with the upregulation of the master regulator *Xist*/*XIST* (or X-inactive specific transcript), a long non-coding RNA (lncRNA) transcribed from the future inactive X, coating the X chromosome from which it is produced in *cis* (Galupa and Heard 2018).

Xist/*XIST* is 17-kb long lncRNA, divided into several domain repeats (A-F) that help establish XCI (Figure 1.2a) (Galupa and Heard 2018; Loda, Collombet, and Heard 2022). *Xist*/*XIST* does not, *per se*, induce all the chromatin changes needed for gene silencing. The process is rather orchestrated by the breadth of ribonucleoproteins *Xist*/*XIST* associates with via the repeats and these proteins work in different phases of the XCI process. Systematic screening of proteins interacting with *Xist*/*XIST* have allowed the identification and validation of interactors during gene silencing (Chu et al. 2015; McHugh et al. 2015; Minajigi et al. 2015). A-repeats are needed for chromosome heterochromatinization and silencing and their deletion do not affect spreading (Wutz, Rasmussen, and Jaenisch 2002); A-repeats interact with the protein SPEN which induces deacetylation on the future inactive X (Chu et al. 2015; McHugh et al. 2015; Minajigi et al. 2015). B-repeats are required for *Xist* coating, spreading and deposition of repressive chromatin marks by interacting with Polycomb (Almeida et al. 2017; Colognori et al. 2019) and heterogeneous nuclear ribonucleoprotein RNA-binding (hnRNP) proteins (Pintacuda et al. 2017); the B-repeats have been also recently found to regulate autosomal expression by *Xist* binding to promoters in 3D proximity from the *Xist* locus (Yao et al. 2025). C-repeats, and its interacting partner YY1, help tether *Xist* to the inactive X (Jeon and Lee 2011); C-repeats also promote the enrichment of hnRNPs to the inactive X (Helbig and Fackelmayer 2003; Chu et al. 2015; Minajigi et al. 2015). E-repeats give specificity towards the inactive X by interaction with CIP1-interacting zinc-finger protein 1 as its depletion results in *Xist* diffusion (Ridings-Figueroa et al. 2017; Sunwoo

et al. 2017). Therefore, *Xist*/*XIST* is a scaffold molecule important for the recruitment of different ribonucleoproteins involved in X-linked gene silencing.

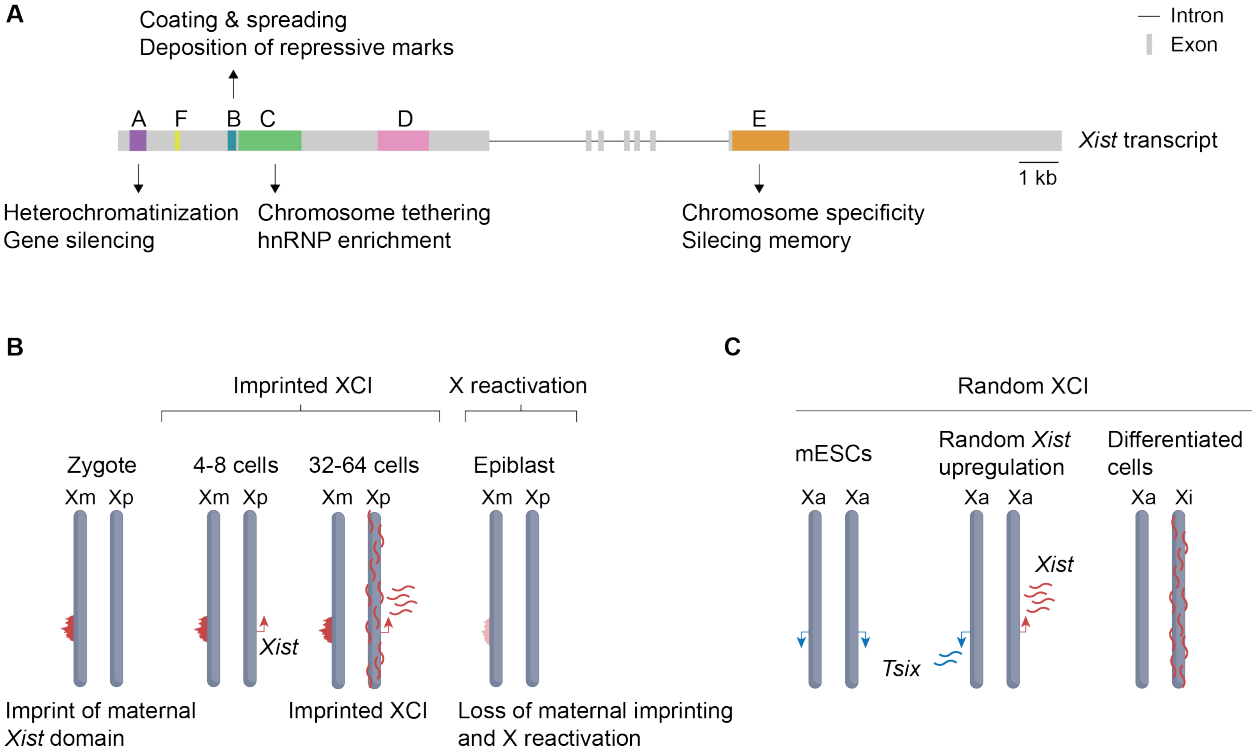

Figure 1.2. *Xist* is a multi-repeat long non-coding RNA involved in X chromosome inactivation. (A) *Xist* has six repeats, named A to F, which play different roles in X chromosome inactivation. The function of each domain is provided if available. Exons and introns are depicted. The figure was adapted from (Jacobson et al. 2022). (B) In the mouse, the first wave of X chromosome inactivation (XCI) is imprinted and the paternal X (Xp) is silenced, leaving the maternal X (Xm) active. Reactivation of the imprinted Xp occurs in the epiblast stage. (C) After reactivation, XCI is random. Mouse embryonic stem cells (mESCs) contain two active X chromosomes (Xa) expressing *Tsix*, which inhibits *Xist* from triggering XCI. Upon differentiation, random XCI occurs and *Xist* is upregulated from one of the X chromosomes which will become the inactive X (Xi). Figures B and C were adapted from (Loda et al. 2022).

After *Xist*/*XIST* expression, a simple diffuse mechanism ensure its spreading: it initially becomes enriched locally before spreading to specific genomic sites located in close 3D proximity of the *Xist*/*XIST* locus (Engreitz et al. 2013). Only after targeting a subset of entry sites, it then diffuses to the rest of the chromosome (Rodermund et al. 2021), leading to a cascade of different epigenetic mechanisms resulting in gene silencing (Figure 1-3). Knockout experiments revealed that SPEN is essential for initial gene silencing (Dossin et al. 2020) and for restricting *Xist* to the X chromosome by limiting *Xist* expression (Jachowicz et al. 2022). The loss of active histone marks (such as H3K27ac) is one of the first responses upon XCI. SPEN-induced silencing of a handful of genes is achieved by interacting with the histone deacetylase 3, prebound to the

inactive X (McHugh et al. 2015; Żylicz et al. 2019) but other mechanisms independently of the histone deacetylase 3 exist (Żylicz et al. 2019; Dossin et al. 2020). Histone acetylation is then replaced by the accumulation of monoubiquitylation of H2AK119 (H2AK119ub) through recruitment of the noncanonical Polycomb proteins via hnRNPs (Nesterova et al. 2019; Żylicz et al. 2019). Next, gene silencing becomes more prominent via trimethylation of H3K27 (H3K27me3), also deposited by the Polycomb proteins. Finally, late epigenetic changes include dimethylation of H3K9 (Escamilla-Del-Arenal et al. 2013), accumulation of the histone variant macroH2A (Mermoud et al. 1999) and DNA methylation of CpG (cytosine residues preceding guanine nucleotides) islands (Norris, Brockdorff, and Rastan 1991; Gendrel et al. 2012).

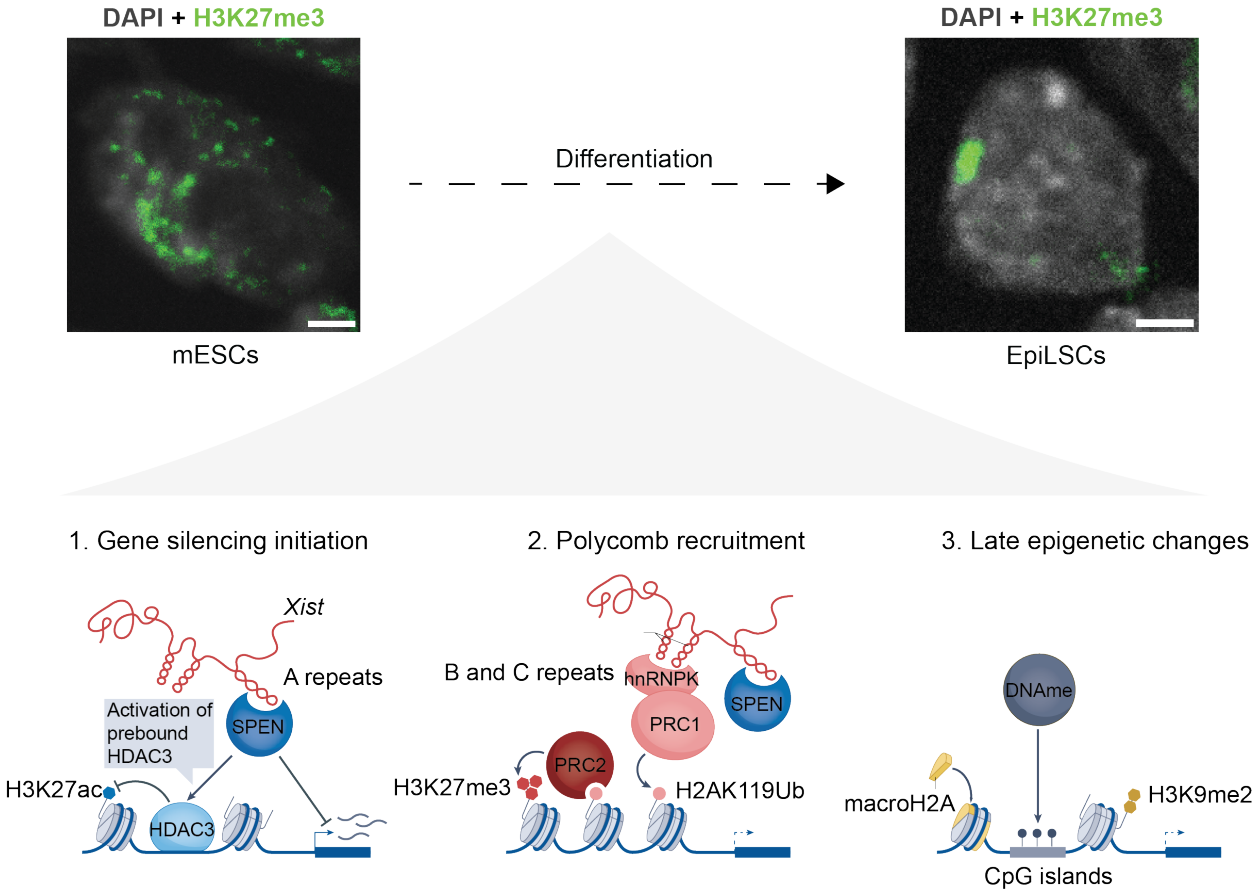

Figure 1.3. Mechanism of X chromosome inactivation. (Top) *In vitro* differentiation of mouse embryonic stem cells (mESCs) to epiblast-like stem cells (EpiLSCs) has revealed some mechanistic insights into inactivation of the X chromosome (bottom). 1. One of the earliest responses is removal of active chromatin marks (H3K27ac) by histone deacetylates 3 (HDAC3) which is activated by the protein SPEN, via *Xist* A repeats. 2. Silencing is also achieved by deposition of repressive marks (H3K27me3 and H2AK119Ub) by the Polycomb complexes. 3. The last steps of silencing include deposition of the histone H2A variant macroH2A, DNA methylation (DNAme) at CpG islands and deposition of H3K9me2. The illustration in the bottom was adapted from (Loda et al. 2022).

1.1.2.2 XCI as a dynamic process during development

In mammals, dosage compensation of the X chromosome takes place during female embryonic development. XCI exists in two different flavors in the mouse: imprinted and random (Figure 1.2b-c). Imprinted XCI (iXCI) is the selective choice of one parental X chromosome, and in the mouse is always the paternal allele. On the other hand, during random XCI (rXCI), either X chromosome has the same probability to be chosen for inactivation, a phenomenon initially proposed by Lyon (Lyon 1961). As a result, females are said to be mosaic. Once XCI is established, the chosen allele is kept genetically inactivated and propagated through each cell division (Kaufmann and Wutz 2023).

The choice of either X chromosome selection for inactivation is restricted to the developmental stage. In the mouse, the first wave of inactivation occurs shortly after zygotic genome activation in preimplantation embryos, which takes place between the 2- and 4-cell stage. At this point, iXCI is the default program and remains up until the late blastocyst stage (Harper, Fosten, and Monk 1982; Huynh and Lee 2003). Afterwards, the inactive X chromosome is reactivated rendering cells with two active Xs (Mak et al. 2004) but the iXCI remains in extraembryonic tissues (the trophoblast and the primitive endoderm) (Okamoto et al. 2004). After chromosome reactivation and at around the time of implantation, rXCI takes place in the cells of the epiblast, which will go on and form the embryo proper.

XCI is elastic, demonstrating remarkable diversity across mammals. Compared to the monoallelic expression in the mouse, *Xist* coats both X chromosomes in the rabbit and therefore iXCI is not possible; this occurs at the 8-cell stage and monoallelic expression is seen from the blastocyst stage (Okamoto et al. 2011). Similar to the rabbit, the two X chromosomes are *Xist*-coated in the pig at the blastocyst stage and no evidence of iXCI has been reported in the placenta (Zou et al. 2019). Similarly, in the horse and the mule, rXCI is found in the placenta with no information regarding *Xist* distribution (X. Wang et al. 2012). The story is completely different in marsupials. These mammals lack *Xist* and instead, another lncRNA with *Xist*-like features ensures XCI (Grant et al. 2012). The default program in marsupials is iXCI and starts from embryonic day (E) 3.5, concomitant with genome activation (Mahadevaiah et al. 2020); iXCI remains until the adult stages (X. Wang et al. 2014) implying that iXCI is the only mechanism of inactivation. These studies highlight the evolutionary diversification of dosage compensation and set the way for understanding how one process is tweaked for divergence across species.

Despite high synteny and gene orthology between the mouse and the human (Mouse Genome Sequencing Consortium et al. 2002), the murine XCI insights cannot be fully scalable to humans and they require special consideration. Similar to rabbits, human embryos do not necessarily undergo iXCI as both X chromosomes are coated by *XIST* from the 8-cell stage (Okamoto et al. 2011; Petropoulos et al. 2016). However, iXCI is possible and will be a matter of discussion in section **1.3.1 Skewing of X chromosome inactivation**. This evidence suggests that the choice of which human X to silence is downstream of *XIST*. In addition, other human-specific factors play a role in XCI (Vallot et al. 2013). Single cell RNA sequencing of human embryos revealed a similar XCI process to that of the nematode (Meyer 2010): the transcriptional output of both X chromosome remained constant and similar to the male X suggesting that dampening, instead of inactivation, is responsible for dosage compensation in humans (Petropoulos et al. 2016). Importantly, discrepancies have been reported after reanalysis of the data provided by (Petropoulos et al. 2016) and dampening has been a matter of debate (Moreira de Mello et al. 2017; Reinius and Sandberg 2019). Closely related to humans, the two X chromosomes in female cynomolgus monkeys also exhibit *XIST*-coating at E7 which is resolved by *XIST* repression on the active X at around day 11 together with X chromosome upregulation, instead of dampening (Okamoto et al. 2021). Whether human X dampening is the actual mechanism requires further investigation but pinpoint to an evolutionary diversification of the XCI where dampening is not favored.

Not only are the dynamics of XCI different across mammals but also gene silencing. In the mouse, silencing is achieved after about two rounds of cell division once XCI starts and occurs at a gene-to-gene basis with some genes being transcriptionally repressed earlier than others (Loda, Collombet, and Heard 2022; Severino et al. 2022). In the rabbit, both X chromosomes are initially downregulated —consistent with biallellic *Xist* expression— before gene upregulation from the active X kicks in (Okamoto et al. 2011). In the pig, silencing is also uncoupled from *Xist* expression as monoallelic expression is found at the late epiblast (Ramos-Ibeas et al. 2019). The exact onset of XCI in humans is not known but follows a similar trend to those of the rabbit and pig where gene silencing does not follow *XIST* expression (Petropoulos et al. 2016; Vallot et al. 2017; Alfeghaly et al. 2024). In the cynomolgus monkey both X chromosomes remain coated by *XIST* from day 7 and the dynamics of silencing differ between the lineages: in the placenta one *XIST* cloud is found at day 11 with gene-dependent monoallelic expression; the presence of one *XIST* cloud in the epiblast and hypoblast were completed by day 17 (Okamoto et al. 2021). All in all, the timing difference of silencing of the X chromosome is an intriguing area of research and

suggests that the timing of XCI is linked to species-specific onset of genome activation with iXCI present only in species with early silencing events (like the mouse and rabbit). Further establishments of other mammalian organisms will expand the field and refute or support that hypothesis.

1.1.2.3 Structural organization of the X chromosome in females

XCI does not only induce gene silencing on the X chromosome but also results in a reorganization of the X chromosome topology inside the nucleus and a shift in replication timing. Early work demonstrated the difference of chromatin structure between the sexes. A single "nucleolar satellite" close to the nucleolus was present only in the nuclei of neuron female cats, now known as the Barr body (Barr and Bertram 1949). Ten years later, it was recognized that the Barr body was indeed one of the two X chromosomes (S. Ohno and Hauschka 1960). These discoveries have laid the foundation to understand how XCI changes the structure of the inactive X.

Apart from inducing gene silencing, *Xist*/*XIST* works by repositioning the chromosome within the nucleus, bringing it to and associating with the nucleolus (Barr and Bertram 1949; Belmont, Bignone, and Ts'o 1986; Rego et al. 2008). The localization of the inactive X seems dynamic as it can also be located at the nuclear lamina given that *Xist* itself interacts with the lamin B receptor (McHugh et al. 2015; C.-K. Chen et al. 2016). How important is and whether the positioning of the inactive X in specific nuclear compartments during XCI play a role in silencing are open but interesting questions.

Topologically associating domains (TADs) are folded regions of the genome with high intra-domain chromatin interactions and advances in chromosome conformation techniques have allowed the understanding of how distant regions in the same chromosome, or even between chromosomes, interact together within the nucleus (Tena and Santos-Pereira 2021). As a transcriptionally dynamic entity, the active X chromosome contains several TADs involved in long-range interactions whereas the inactive X is mostly depleted of them (Splinter et al. 2011). Instead, the inactive X is partitioned into two megadomains separated by the conserved microsatellite repeats locus *Dxz4*/*DXZ4* (X. Deng et al. 2015; S. S. P. Rao et al. 2015; Giorgetti et al. 2016).

The inactive X was initially discovered microscopically using chemical chromatin stainings (Barr and Bertram 1949; S. Ohno and Hauschka 1960). However, the most common methods nowadays are immunofluorescence (IF) and RNA fluorescence *in vitro* hybridization (RNA FISH).

IF takes advantage of the overrepresentation of the repressive mark H3K27me that, although is found across the genome, is mostly present in the inactive X and can be identified as a strong dot usually close to the nuclear periphery. On the other hand, RNA FISH uses a fluorescently labeled RNA probe that, in this case, specifically recognizes *Xist*/*XIST*, appearing as a large cloud in the nuclei. The addition of RNA probes hybridizing with monoallelic X-linked genes helps discern the active from the inactive allele; the use of DNA probes in DNA fluorescence *in vitro* hybridization (DNA FISH) can also help differentiate both alleles.

1.1.2.4 Gene escapers from the inactive X chromosome

A fascinating fact is that XCI is incomplete, leading to expression of some genes from the inactive X, known as escapers. Escapers are, by definition, biallelically expressed in females and are important female drivers in sexual dimorphism, homeostasis and disease. Escaper expression is not consistent and escapers have been classified into two major groups: escapers that are expressed in most tissues regardless of the cell type, developmental stage or between individuals are referred as “constitutive” and are usually conserved in mice and humans whereas genes escaping in a specific contexts are considered “facultative” (Galupa and Heard 2018; Fang, Disteche, and Berletch 2019; Peeters, Posynick, and Brown 2023). In that sense, facultative escapers initially undergo XCI and only become reactivated depending on the content in which they are needed (Carrel and Brown 2017). The commonly accepted cutoff to determine escaping is at least 10% expression of the gene residing in the inactive X in comparison to that same gene in the active X (Carrel and Willard 2005). The X chromosome contains around a thousand genes and the number of escaper genes in humans is estimated to be around 20% and much less in the mouse, with 3-8% (Berletch et al. 2015; Tukiainen et al. 2017).

The most evident escaper genes are conserved genes usually found in the PARs together with gametologs, ancestral sex chromosomes genes that retained a copy on the Y allele (Bellott et al. 2014; Tukiainen et al. 2017). In males, the expression of the gametologs together with the conserved X-Y pair results in their double dose. The conservation of such genes during evolution, together with their roles in cellular processes such as splicing, transcription and translation (Bellott et al. 2014), clearly denotes their essentiality and ensures that escaping from inactivation in females attenuates a gene dosage imbalance between the sexes. These genes are, however, not the only escapers.

An important consideration is the chromatin landscape defining escaping. As discussed previously, the lack of TADs in the inactive X implies a depletion of *cis* and *trans* chromatin

interactions, consistent with the lack of gene expression. It is therefore not surprising that escapers have a chromatin conformation and profile similar to those on the active X. Escapers retain chromatin marks associated with gene expression, including H3K27ac, without deposition of repressive histone marks (H2AK119ub, H3K27me3, macroH2A) (Balaton and Brown 2016). This is in part by the lack of *Xist*/*XIST* coating, suggesting that a mechanism impedes this lncRNA to act on them. In addition, specific features of the genomic location of these genes may dictate escaping in different ways. In the mouse, most of the escapers are distributed along the chromosome as single units whereas in humans they are encompassed as gene blocks (Lopes et al. 2011; Marks et al. 2015). This implies that local mechanisms promote escaping in single genes while in block-grouped genes, domain mechanisms serve as a reference. Two important elements determining gene silencing and escaping are widely recognized and are also applicable to XCI. Repetitive elements such as long-interspaced nuclear elements have been found to colocalize with loci prone to silencing and are absent in escaper regions. Alternatively, Alu elements are close to escaper genes and are known to contribute to gene expression (for a deeper insight on these elements on XCI, see (Peeters, Posynick, and Brown 2023)).

A major consideration is the phenotypic importance of escaper genes. While a more detailed analysis is provided in **1.3 The X chromosome as a double balance**, it is important to point out that if escapers as biallelically expressed genes are needed in female homeostasis, their misregulation should impair normal physiology and hence, can be considered as dosage sensitive. Individuals with sex chromosome aneuploidies are the perfect subject to understand the importance of escaper dosage. Indeed, many of their clinical manifestations have been attributed for a long time to escaper dysregulation whether this is a decrease (in the X0 Turner's syndrome) or increased expression (in XXY Klinefelter's syndrome or supernumerary X chromosome) (Navarro-Cobos, Balaton, and Brown 2020; Gravholt et al. 2023).

Understanding the underlying mechanisms and requirements for genes resisting inactivation is an important avenue for expanding the world of gene regulation at the intersection of chromatin biology and its impact on sex differences.

1.1.2.5 Regulation of XCI

Cells with two active X chromosomes need to possess a regulatory network that controls when to silence one X. This section focuses on rXCI happening in the cells of the epiblast but does not underscore the importance of iXCI in the supporting extraembryonic tissues, especially

in light of novel mechanist insights of paternal X chromosome selection for imprinted inactivation (Wei et al. 2024).

Much of the knowledge of XCI regulation comes from *in vitro* work of isolated mouse cells. More specifically, mouse embryonic stem cells (mESCs) have become an ideal system to understand XCI. mESCs are cells isolated from the epiblast of the inner cell mass of preimplantation embryos and share the same characteristics as their *in vivo* counterpart: they can be propagated indefinitely *in vitro*, are pluripotent and retain developmental potential, allowing scientists to differentiate them to many cell types in the laboratory (Czechanski et al. 2014). Pluripotency allows them to give rise to three germ layers that will generate a whole organism: endoderm, mesoderm and ectoderm. As such, mESCs are versatile and when transferred back to the embryo, they contribute to the germline. Consequently, these cells are exploited for the development of transgenic mouse models after clonal selection of genetically edited cells. mESCs are isolated from the developmental window after iXCI has been removed and the two female Xs are therefore active. As one would expect, when mESCs are differentiated, one X chromosome is chosen for silencing and XCI takes place. This is the key characteristic that represents mESCs, making them the ideal model to understand XCI dynamics in a dish.

Considering that *Xist* upregulation is needed for XCI, a mechanism controlling its expression should exist. As such, the transcriptional regulation of *Xist* occurs at different levels. One important aspect is the genomic location of the lncRNA: *Xist* is part of a large locus known as the X inactivation center (XIC), the minimal critical region that is sufficient and necessary for XCI when at least two copies are present (Galupa and Heard 2018). Before XCI, TADs are also present in the future inactive X and *Xist* lies at the intersection of two important regulatory TADs: the promoter of this lncRNA is present in the activator TAD-E, containing protein-coding and non-coding genes that promoter its expression; on the vicinity, the repressor TAD-D contains negative regulators of *Xist* expression (Nora et al. 2012) (an in-depth review of the XIC and its elements is presented elsewhere (Galupa and Heard 2018; Schwämmle and Schulz 2023)).

One of the most studied repressors of *Xist* is *Tsix*, a lncRNA transcribed antisense of *Xist*. *Xist* is lowly expressed in mESCs, following a similar trend to their *in vivo* counterpart (Panning and Jaenisch 1996; Panning, Dausman, and Jaenisch 1997). The low *Xist* expression in mESCs is due through the deposition of repressive marks induced by *Tsix* expression (Sado, Hoki, and Sasaki 2005; Ohhata et al. 2015; Kesler, Adams, and Neuert 2025) together with instability of spliced *Xist* (Panning, Dausman, and Jaenisch 1997; Sheardown et al. 1997). Another layer of

regulation demonstrates that pluripotency is directly linked to X silencing. Pluripotency is controlled by a regulatory network that drives mESC identity with the transcription factors Oct4, Nanog and Sox2 as the main regulators (C.-Y. Chen et al. 2017). These factors are important negative regulators of XCI as they bind to *Xist* intron 1 in mESCs, repressing its expression (Navarro et al. 2008). Additionally, other pluripotency factors bind to *Tsix*, resulting in its upregulation (Navarro et al. 2010). In turn, the presence of two active X chromosomes stabilizes the pluripotency network (Schulz et al. 2014) by inhibition of MAPK signalling pathway and continuous expression of pluripotency factors, both mediated by X-linked genes (Genolet et al. 2021). Upregulation of *Xist* upon differentiation is multidynamic: levels of pluripotency factors decrease suggesting that occupancy at the *Xist* and *Tsix* is limited allowing for *Xist* RNA to become stable. Moreover, activation of the MAPK signalling pathway is achieved by expression of the fibroblast growth factor family, directed by Oct4 (Kunath et al. 2007), and surrounding cells in the embryo (Kunath et al. 2007), implying that differentiation, and hence XCI, are to some extent autoinductive.

The process of XCI is more than just gene silencing: it is a hierarchical framework involving many factors that need to properly act in time and space to ensure equilibrated X dosage between the sexes. Yet, some genes can resist inactivation and are therefore important regulators of sex differences in females. How these genes, and the X chromosome, achieve so will be a matter of debate in the following sections.

1.2 Sex bias in the hallmarks of aging

Aging is the decrease of cellular functions over time, comprising an organism's integrity (López-Otín et al. 2013, 2023). It is increasingly evident that males and females across species do not age similarly. Depending on the species, the lifespan of one sex is favored (Xirocostas, Everingham, and Moles 2020). Several hypotheses have been proposed and addressed to understand sex-specific lifespan and one of them explores the sex chromosome complement (Austad and Fischer 2016).

As introduced earlier, in the XY determination system, females are genetically XX while males harbor one X and one Y chromosome. The sex chromosome theory postulates that the heterogametic species, that is the XY males, have a shorter lifespan. Owing to the extra X chromosome, females are better at buffering the effect of sex-linked deleterious mutations whereas the same mutation in males would result in detrimental fitness or death.

In humans, women live on average 5 years longer than men (Rochelle et al. 2015). Paradoxically, women are more susceptible to health vulnerabilities and their healthspan worsens along aging (Austad 2006; Gordon and Hubbard 2020). As a matter of fact, age-associated illnesses are often sex-biased. For instance, higher death rates are seen in males within leading death-causing diseases, including but not limited to, heart diseases, cancer, septicemia and diabetes, while females die more from Alzheimer's disease (AD) and stroke. In addition, females suffer more from autoimmunity than males and the prevalence of neurodegenerative diseases—such as Parkinson's disease and autism— is higher in men (Austad and Fischer 2016; Mauvais-Jarvis et al. 2020).

Understanding human aging from a genomics perspective is tricky for two main reasons. Women inclusion in clinical trials has been historically limited to preserve reproduction and the sex chromosomes are often omitted in genome-wide association studies (GWAS) (Mazure and Jones 2015; L. Sun et al. 2023). These two factors restrict the development and limit the application of current therapies, especially when a female bias disease is encountered. This is highly relevant when considering that sex-biased expression exists in human tissues (Oliva et al. 2020), making it hard to link sex-specific effects and aging.

The hallmarks of aging are a set of molecular features that identify different roots of aging. They are grouped into three different categories and possess a slight hierarchy. The primary hallmarks hinder genome, telomere, epigenetic, protein and autophagic functions, directly resulting in aging. The antagonistic ones aim to alleviate the damage from the primary hallmarks but their functions tend to be malignant over lifespan; they include nutrient sensing, mitochondria function and cellular senescence. Ultimately, when the consequence of damage are higher than the repair provided, the integrative hallmarks lead to stem cell pool exhaustion, chronic inflammation, dysbiosis and alteration of cell communication (López-Otín et al. 2013, 2023).

Considering that aging is not an equal process between the sex, the following sections briefly discuss the hallmarks of aging in a sex-specific manner. A summary is provided in Figure 1.4.

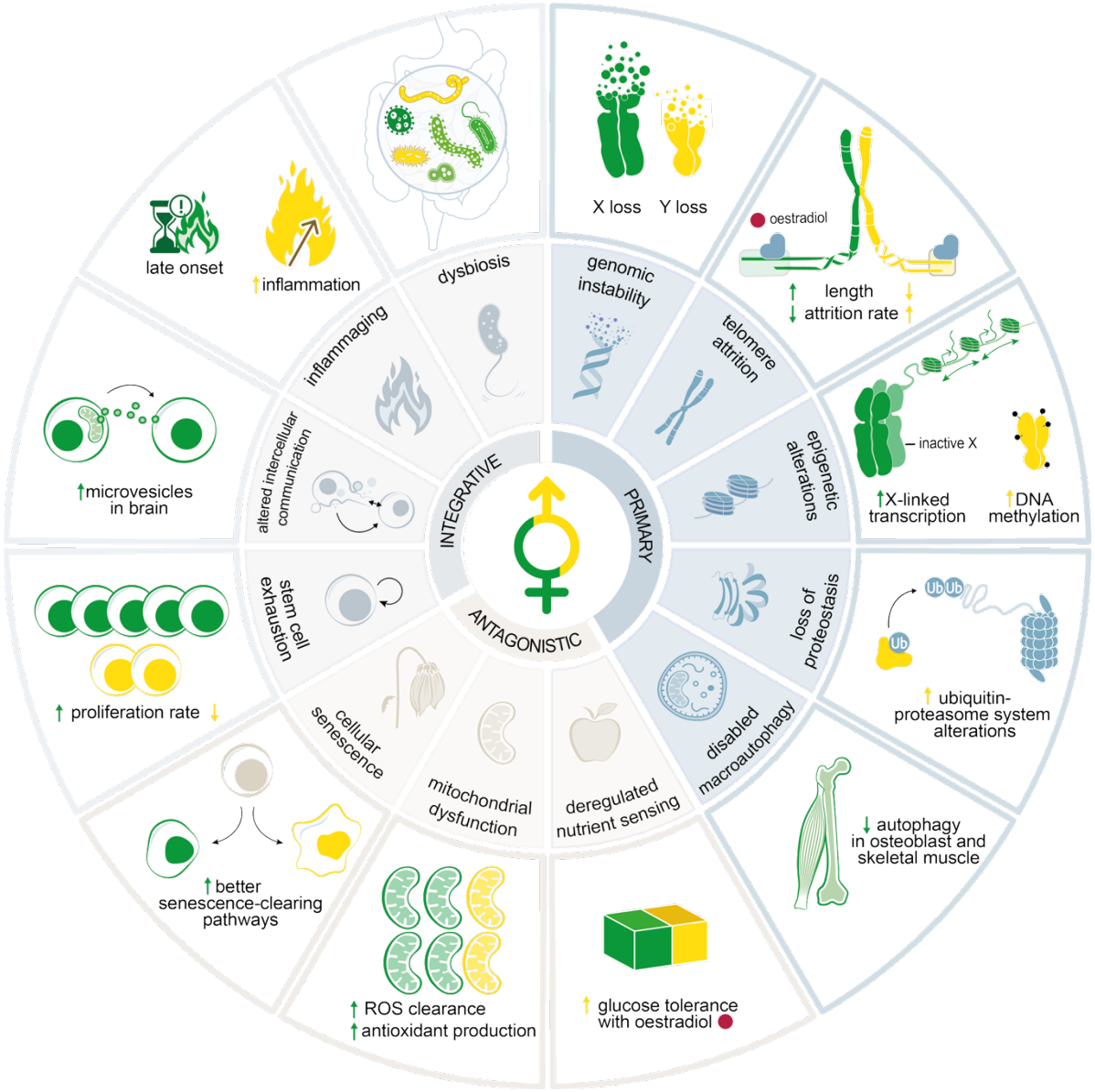

Figure 1.4. The sex-specific hallmarks of aging. One illustration per hallmark is provided; females are represented in green and males in yellow. Primary hallmarks are shown in light blue. Genomic instability results in Y chromosome loss in men and X chromosome loss in females. Males undergo telomere attrition faster than females as the TERT subunit of the telomerase complex is oestrogen-responsive. Epigenetic misregulations include Y chromosome hypermethylation and gene reactivation from the inactive X. Loss of proteostasis affects primarily men. Disabled macroautophagy is usually female-biased with lower activity in osteoblasts and skeletal muscle. Antagonistic hallmarks are depicted in beige. The onset of cellular senescence is earlier in males. Mitochondrial dysfunction in males is associated with impaired clearance of reactive oxygen species (ROS) and less production of antioxidants. Sex-specific nutrient sensing misregulation depends on the modulation of each pathway and the example shows oestradiol-mediated improved glucose tolerance in males. Integrative hallmarks are shown in light grey. Loss of stem cell potential is faster in males. Females have slower altered cellular communication by the increase in mitochondrial-derived microvesicles in aged astrocytes. Inflammaging affects males faster. Dysbiosis starts later in females because microbial diversity is affected by menopause.

1.2.1 Genomic instability

Genome instability is the result of alterations at the DNA level posed by intrinsic and extrinsic cellular factors (Vijg and Suh 2013). Sex differences in the DNA damage response have been shown, especially in the context of aging. Gene expression profiling of DNA damage repair pathways showed that they tend to be upregulated in peripheral blood lymphocytes in old human males compared to females but these changes are not seen in young individuals (Rall-Scharpf et al. 2025), implying that these differences are specific to aging. Quantification of DNA damage, assessed by the replication stress marker γH2AX (Gagou, Zuazua-Villar, and Meuth 2010), was also higher in female cells (Rall-Scharpf et al. 2025). This is partially attributed to lower levels of the FANCD2 protein involved in resolving interstrand crosslinks in the Fanconi anemia (FA) pathway. The FA pathway is an interesting repair mechanism because mutated X-encoded factors of the pathway result in male-biased FA (Jung et al. 2020). The FA pathway is not the only affected system. A previous study demonstrated that human female lymphocytes have a decreased activity in repairing double-stranded breaks using the non-homologous end joining (NHEJ) pathway. More specifically, this was a consequence of decreased expression of *ATM*, *BLM* and *KU70*, players involved in the pathway (Rall-Scharpf et al. 2021).

One of the consequences of unrepaired DNA damage is the generation of cells with different mutations or mosaic clones that, over time, become amplified and result in clonal mosaicism. Clonal mosaicism can be identified in a sex-specific fashion. Sex chromosome loss is the main form of somatic aneuploidies in humans, happening at a higher frequency in the elderly population and found primarily in blood cells (Guttenbach et al. 1995).

In human males, loss of the Y chromosome (LOY) rapidly increases from around 50 years and the incidence can reach 25% with up to 95% of analyzed cells with LOY (Guttenbach et al. 1995; Herens et al. 1999). LOY is correlated with diabetes, cardiovascular disease (CVD), AD, a shorter lifespan and other phenotypes (Dumanski et al. 2016; Forsberg et al. 2014). How does loss of a highly heterochromatic chromosome exert many diseases? And is LOY a cause or consequence of such phenotypes? (Maan et al. 2017) These have been two long-standing questions with some answers to them. Recently, a direct association between LOY in blood cells and non-hematological conditions has been described. Transplantation of hematopoietic stem cells (HSCs) with LOY to irradiated male mice led to cardiac malfunctioning and fibrosis as they aged (Sano et al. 2022). This reflects that Y-encoded genes regulate genes from other chromosomes, which is in agreement with previous reports (Dumanski et al. 2021; Sano et al.

2022; Vermeulen et al. 2022; Celli et al. 2024). Finally, LOY is a clonal driver in uveal melanoma while in other types of cancer LOY is a consequence (M. Qi et al. 2023). What makes some cell types more sensitive to LOY than others is unclear but opens up new avenues for understanding Y-dependent gene regulation.

In females, loss of the X chromosome (LOX) is more of a mystery box. The frequency of LOX is less than 3% in women younger than 40 years old that increases to more than 30% in women older than 80 years (A. Liu et al. 2023). While LOX can include partial chromosomal losses and gains, the most overrepresented event is the loss of one of the two Xs (Machiela et al. 2016). Cytological and sequencing approaches have revealed that the inactive X is the preferential lost allele (Abruzzo, Mayer, and Jacobs 1985; Machiela et al. 2016). The consequences of LOX are less known but some studies report an increased risk of lymphoid leukemia and acute tonsillitis (Zekavat et al. 2020; S.-H. Lin et al. 2021). Conversely, the story becomes more complex. LOX in acute myeloid leukemia has a favorable outcome (G. Chen et al. 2020). However, this was reported in the t(8;21) translocation, which is an underrepresented event in this type of leukemia (Reikvam et al. 2011). How LOX affects other types of leukemia is unknown.

Advances in different sequencing technologies and integration of sex chromosomes will provide a better understanding of the causal mechanism between sex chromosome loss and aging (Muyas et al. 2024).

1.2.2 Telomere attrition

Located at the end of each chromosome, telomeres comprise a stretch of DNA repeats with associated nucleoproteins that protects chromosome ends from fusing and activating the DNA damage response pathways (Benetos et al. 2001). Telomeres shorten with each somatic cell division as DNA polymerase is unable to replicate them and eventually, cells undergo senescence or die (Harley, Futcher, and Greider 1990; Allsopp et al. 1995; López-Otín et al. 2023). Telomere length measurements have shown that telomere shortening is an age-dependent event but whether sex is a biological variable is a topic of debate (Harley, Futcher, and Greider 1990; Cawthon et al. 2003). However, some data point to sex-specific factors affecting primarily men.

Telomere shortening can lead to chromosome aneuploidies with shorter and heterochromatic chromosomes, like the Y chromosome, having a higher frequency of being lost (Leach et al. 2004). While females harbor two X chromosomes that are larger than the Y allele,

the inactive X becomes heterochromatic upon XCI as previously discussed. Indeed, telomeres from the inactive X shorten at a faster rate than the active X during aging (Surrallés et al. 1999). More importantly, telomere shortening disrupts XCI maintenance by reducing the deposition of H3K27me3, allowing for the reactivation of genes that under normal XCI dynamics are silenced (Schoeftner et al. 2009).

Dyskeratosis congenita is a disease characterized by defective telomerase activity. Mutations in the X-linked *DKC1* gene lead to rapid telomere shortening in men (Mitchell, Wood, and Collins 1999). Women remain unaffected due to iXCI. Moreover, the telomerase subunits possess an estrogen-responsive element providing better clearance mechanisms in females of reactive oxygen species (ROS), important drivers of telomere shortening (Nawrot et al. 2004).

Addressing the contribution of telomere shortening in aging is needed and the use of important models is important. Mouse models are not an ideal system to understand telomere-mediated replicative aging. The telomerase activity in mice is higher compared to the restricted activity in human tissue and mouse telomeres are longer than those of humans (Gomes et al. 2011; Horikawa et al. 2005). However, the introduction of relevant humanized mouse models resembling human telomere biology (Cheng et al. 2024; F. Zhang et al. 2025) will provide a better understanding of how exactly age-dependent telomere shortening affects each sex.

1.2.3 Epigenetic alterations

Epigenetics refers to the chemical modifications that alter gene expression without changing the DNA sequence itself. The study of different histone modifications falls under the umbrella of epigenetics and has revealed, for example, that decreasing acetylation levels of H4K16 in aged yeast cells increases lifespan (Dang et al. 2009). However, the most well-known epigenetic biomarker of aging is DNA methylation (DNAme), where CpG islands become methylated for gene silencing (Vitorakis and Piperi 2023). By integrating DNAme data on CpG islands from different tissues and cell types, trained machine learning algorithms can predict the biological age of the sample to be analyzed (of note, chronological age is the amount of years lived, that is different from the real biological age) (Hannum et al. 2013; Horvath 2013). These algorithms are known as epigenetic clocks and have been useful in identifying relevant differentially methylated regions that change over time as promising aging predictors. The lack of inclusion of sex chromosomes in sequencing analysis has limited the potential of these epigenetic clocks but some insights exist. In males, the majority of CpG regions analyzed on the Y chromosome become hypermethylated with age (Lund et al. 2020; Vidaki et al. 2021). Correlation

analysis showed, interestingly, that their hypomethylation decreases the risk of death (Lund et al. 2020).

In females, the process of XCI provides the perfect landscape to study epigenetic aging as re-expression of inactivated genes can take place. Gene reactivation is variable and dependent on the tissue context and the set of genes analyzed (Wareham et al. 1987; B. R. Migeon, Axelman, and Beggs 1988; Bennett-Baker, Wilkowski, and Burke 2003). For example, *Xist* expression levels were found to increase in some brain cell types but these results were not reproduced in another study (Hajdarovic et al. 2022; Eckersley-Maslin et al. 2024). However, increasing evidence suggests that derepression of the inactive X is a widespread mechanism in different aged tissues (Hoelzl et al. 2025). Additionally, while disruption of the heterochromatic context of the inactive X can stem from *Xist* misregulation (e.g., macroH2A localization is dispersed upon *Xist* loss (Csankovszki et al. 1999)), it is not the solely cause. For instance, laminar disruption in HSCs results in hypomethylation, chromatin relaxation and variable gene reactivation of the inactive X (Grigoryan et al. 2021). As such, the components that ensure X inactivation, regardless of whether they induce XCI or directly modify the chromatin landscape of the X to promote silencing, are important triggers for epigenetic alterations.

While identifying the dynamics of epigenetic changes across the genome provide correlation with aging, mechanistic experiments that causally connect locus-specific methylation changes with aging and sex are still lacking. This is exemplified by the identification and, importantly, validation of the role of the sex chromosome dosage compensation of the fruit fly in longevity (Tennant et al. 2024).

1.2.4 Loss of proteostasis

Proteostasis regulates protein synthesis and folding, cellular location, maintenance and degradation (Dormann and Lemke 2024). The inability to keep the proteome in check is an age-related process that fails to remove misfolded proteins and protein aggregates (Hipp, Kasturi, and Hartl 2019). One way to look at proteostasis is by evaluating degradation activity through the 26S proteasome, a eukaryotic large protease complex responsible for degrading the majority of proteins in the cells (Finley and Prado 2020). In this sense, by measuring the activity of specific proteins in the proteasome, it was reported that female mice have an overall higher tissue-specific proteasome activity than males, including the spinal cord, intestine, spleen and kidney but higher activity was seen in male kidney (Jenkins et al. 2020).

Proteostasis can also be assessed by protein turnover dynamics, the replacement of old proteins with newly synthesized ones. Turnover rates are different across mouse tissues (W. Li et al. 2025), suggesting that protein regulation is not the same organismically and tissue specificity has to be considered. For instance, compared to the heart and the liver, the protein turnover in the brain is less dynamic (N. R. Rao, Upadhyay, and Savas 2024). This is a double-edged sword because it can initially be interpreted as a slower aging process but it can become detrimental if spontaneously damaged proteins are present for longer. In fact, many proteins in the brain that are long-lasting are important in AD, a female-biased disease (X. Liu et al. 2024).

Linked to protein turnover, degradation pathways can be informative in revealing key aspects of protein removal. Protein synthesis at the endoplasmic reticulum serves as a quality control of protein production: different stimuli can stress the cells and lead to accumulation of misfolded proteins; stressed cells, in turn, activate one major clearance pathway known as the unfolded protein response (UPR) (Xingyi Chen et al. 2023) which is gaining attention for its function in a sex-specific manner. In the adult nematodes, mechanisms to cope with proteostasis extend their lifespan in a male-specific fashion which is mediated by proteins acting in the sex determination pathway (Qu et al. 2025). However, this is context-dependent as XX hermaphrodite worms are more sensitive to activating the UPR from mitochondrial stress in the germline compared to X0 males (Charmpilas et al. 2024). These studies indicate that the source of protein stress dictates the benefits each sex experiences.

In normal conditions, as well as cellular stress upon protein aggregation, the cells activate the ubiquitin-proteosome system (UPS) for protein elimination. Degradation of misfolded proteins is achieved by labeling them with long chains of activated ubiquitin (Lozada Ortiz et al. 2023). Mutations in the X-linked gene *UBA1*, responsible for ubiquitin activation for protein tagging, lead to the male-biased spinal muscular atrophy resulting in a shorter lifespan (X. H. Wang et al. 2020). Importantly, its impaired activity can be partially restored by small molecules usually used for treating rheumatoid arthritis, showing promising therapeutic potential (W. Yan et al. 2023). After ubiquitin activation, ubiquitin conjugation to E2 ligases serves as an intermediate step before tagging the targeted protein. Mutations in the responsible gene, *UBQLN2*, lead to X-linked intellectual disability affecting males (Nascimento et al. 2006; Zhao et al. 2016) as well as age-associated dementia (H.-X. Deng et al. 2011), but the underlying aging conditions are not clear. The only loss-of-proteostasis-related phenotype affecting females, to my knowledge, involves the X-encoded deubiquitinase USP11, which removes ubiquitin chains from tagged proteins, promoting their stabilization (Chiang et al. 2021). *USP11* is an escaper gene (X. Li et al. 2016)

important for neurogenesis (Chiang et al. 2021). Paradoxically, USP11 dephosphorylates the microtubuline-stabilizing Tau protein leading to Tau aggregation (Y. Yan et al. 2022). Tau aggregation is an important driver of AD, a female-biased disease, providing evidence of how the X complement plays a role in sex-biased brain pathologies.

Developing therapies for ameliorating the symptoms of age-associated diseases is needed especially when proteins, as the key players in each of our cells, are affected. Importantly, some therapeutics approaches targeting enzymes involved in the UPS pathway have been reported (Liao et al. 2022; W. Yan et al. 2023). In addition, the X seems to be overrepresented in genes participating in proteostasis. In the future, drug repurposing, together with the identification and screening of factors contributing to proteostasis will be important, enabling in turn the development of targeted therapies against pathologies.

1.2.5 Disable macroautophagy

The delivery of the cell's component to the lysosome refers to autophagy (Levine and Kroemer 2019). As proteins are also subjected to degradation, proteostasis is tightly linked to autophagy and therefore a positive correlation between the proteasome activity and autophagy is somewhat expected. Age-dependent decline in autophagy is, in part, due to reduced expression of autophagy-associated genes as well as autophagic activity (López-Otín et al. 2023). Reduced autophagic activity in aging organisms tends to be tissue-specific. In the adipose tissue, decrease in autophagic levels result in metabolic disorders with no sex specificity provided (Yamamuro et al. 2020). In the skeletal muscle and in osteoblasts, however, the activity is lower only in old female mice (Oliván et al. 2014; Camuzard et al. 2016). In aging male mice, on the other hand, autophagic activity in the blood increased, decreased in heart and had no effect in motor cortex neurons while it remained unchanged in old females (Carosi et al. 2025; Rodriguez and Stavoe 2025).

Selective degradation of cellular components is an alternative pathway known as chaperone-mediated autophagy (CMA) and declines as well during aging (Kaushik and Cuervo 2018). One protein involved in this process, the lysosome-associated protein 2 splicing variant A is an X-encoded protein that is gaining attention in aging. Mutations in this gene result in Danon disease, characterized by impaired autophagy, affecting more males (Rowland et al. 2016). More recently, it was shown that the male murine aging brain and liver have a reduced CMA activity compared to females as a result of reduction in *Lamp2a* expression (Khawaja et al. 2025). The study also reported that lower levels of *Xist* expression correlates with higher CMA activity

(Khawaja et al. 2025). This study highlights the importance of how the heterochromatic environment of the inactive X provides female resilience.

The integration of sex and tissue in the process of autophagy will be a key approach to understanding how the chromosome complement, hormones and relaxation of the inactive X contribute to a female resilience in the clearance of cellular compartments.

1.2.6 Nutrient sensing dysregulation

The ability to sense nutrients is an important characteristic of cells and known to be essential in regulating lifespan. The main nutrient sensors are the AMP-activated protein kinase (AMPK), sirtuins and mammalian target of rapamycin (mTOR) pathways.

When the nutrient availability is low (e.g., during a fasting event), females have a higher basal activity of mTOR (Baar et al. 2016). Diminished mTOR activity either directly, indirectly, genetically or by chemical inhibition by rapamycin increases longevity in a wide range of species. For example, rapamycin extends the lifespan of female fruit flies (Bjedov et al. 2010) and induces increased autophagy in enterocytes (Regan et al. 2022). Additionally, deletion of the ribosomal protein S6, which is phosphorylated by mTOR, results in a female-specific increase of lifespan (Selman et al. 2009). This mutation is phenocopied as well in the worms (McQuary et al. 2016) and only in the adipose tissue of the fruit fly (P. Zhang et al. 2024).

The AMPK pathway is known to suppress the mTOR pathway (González et al. 2020) and has sex-specific effects. Constant activation of the AMPK pathway, and therefore reduced mTOR activity, has a stronger lifespan effect in the female killifish (Ripa et al. 2023), in female rat livers (Gustavsson et al. 2010) and female oysters (Guévélou et al. 2013) which is consistent with the rapamycin-mediated inhibition of mTOR. However, the naturally high activity renders females less reactive of enhanced metabolic functions of AMPK (Astre et al. 2023).

While these studies highlight the importance of specific players within the mTOR pathway, some are genetically induced and therefore more research is needed to understand how to translate those findings into actual applications. Moreover, whether genes encoded by the sex chromosomes play a role is unknown making it hard to link sex-specific gene products to nutrient sensing. Importantly, the sex hormone estrogen (S. Yang and Wang 2015) activates the AMPK pathway implying that the longer presence of this hormone in females may help explain, to some extent, female longevity.

1.2.7 Mitochondrial dysfunction

Mitochondria are pleiotropic organelles. Not only are they the main producers of energy via respiration but they also generate ROS, iron-containing cofactors and are mediators of apoptosis; mitochondria are also central regulators of different metabolic pathways (Pahal et al. 2025). As the primary organelle for cellular respiration and the generator of energy, properly working mitochondria are essential for cellular processes, especially in energetically demanding tissues. Therefore, the respiratory activity of the mitochondria is one approach to understanding the effects of age in a sex-specific fashion.

Mitochondria are the house of the respiratory complexes needed to produce energy. For instance, respiratory activity is higher in peripheral blood cells of old human females compared to men (Mahapatra et al. 2024). In the mouse, a pan-atlas evaluating the activity of respiratory complexes in males and females across different tissues reported that, at a first glance, the activity of the respiratory complexes is generally similar between the sexes although some specificities exist (Sarver et al. 2024). Old male mice have a higher activity in the colon, lung, eyes, pancreas, kidney and heart where the adipose tissue, stomach and the majority of brain regions in females have a higher capacity (Sarver et al. 2024). This study clearly exemplifies the relationship of respiration and tissue at the sex level and offers a valuable collection of energetics across lifespan. Complementary to that, more efficient respiratory complexes reside in the brains of aging female baboon primates compared to those of males (Adekunbi et al. 2025). These findings have wide implications for understanding resilience of sex-specific diseases in the context of neurodegeneration and suggest an evolutionary preservation of female brain activity. How female-specific neurodegenerative diseases exhibit its sex-specific effect is unclear and underscore how they interfere with functions that make females resilient, especially in the context of female-biased diseases. Moreover, the generation of ROS as by-products of metabolic processes require antioxidants to keep them at proper amounts that do not compromise cellular functions through oxidative stress. In plasma, males have higher amounts of oxidative damage than females (Martínez de Toda et al. 2023; Y. Huang et al. 2025) suggesting that antioxidants are either more abundant in females or have a better role at protecting them from oxidative damage.

Another way to look at age-specific mitochondrial dynamics is through their genome. Mitochondria contain their own DNA and are maternally transmitted through the germline highlighting a sexual benefit for females towards preserving the organelle for generational

inheritance (Tower, Pomatto, and Davies 2020). This dimorphism renders refined cellular processes acting on females including higher energy production, better clearance of ROS and better responses to mitochondrial-induced stress. In fact, men are worse at dealing with proapoptotic signals and ROS production, making them more prone to age-related illnesses (Ventura-Clapier et al. 2017). Finally, mitochondrial resilience via antioxidant expression in females can also be attributed to estrogen. This is demonstrated by estrogen administration to women experiencing a menopause-like state, reaching expression of antioxidants similar to females prior to menopause (Borrás et al. 2021).

A handful of genes have been attributed to the better mitochondria and mitochondrial-related functions. Gene expressions are decreased in menopause and their levels are increased upon estrogen administration; these autosomal-encoded antioxidants include superoxide dismutase 2, glutathione peroxidases and sestrin-2 (Borrás et al. 2021). The expression signature of those genes in males was not provided but it is important to investigate if estrogen would have the same effect on them. Two other autosomal and metabolic genes whose product act in the mitochondria, *Hk2* and *Pdk4*, have increased expression by the presence of the Y chromosome and correlate with increased adiposity but the extent of their mechanism in XY mice is unclear (Xuqi Chen et al. 2013). As such, little proof exists of how sex chromosomes and their genes may benefit and protect mitochondria. Therefore, screens on how X- and Y-linked genes protect or affect mitochondrial function will be needed, especially in the context of metabolic disorders.

1.2.8 Cellular senescence and inflammation

Senescence is the permanent arrest of cell division and senescent cells are eliminated by means of the immune system via pro-inflammatory programs. The accumulation of senescent cells occurs at a greater incidence in males, hinting to better female-specific clearance pathways (Yousefzadeh et al. 2020). Aging amplifies the consequences of constant inflammation resulting in inflammaging, a pro-inflammatory condition with an unbalanced ratio of secreted inflammatory and anti-inflammatory cytokines. Indeed, a higher accumulation of senescent cells results in higher levels of pro-inflammatory molecules in males (Márquez et al. 2020). These outcomes can be, in part, supported by increased gene expression and chromatin accessibility in aging-related genes in immune cells; while these changes occur in both sexes, they are more pronounced in males (Márquez et al. 2020; Z. Huang et al. 2021).

At the sex chromosome level, 15% of the gene content of the X chromosome accounts for immune-related genes (Bost et al. 2022). Additionally, a great proportion of brain genes are

expressed from the X chromosome and have been associated to sex bias in homeostasis, aging and disease (Skuse 2005; Abdulai-Saiku et al. 2025; Jiang et al. 2025). Therefore, it is no wonder why females have a greater immune robustness to fight off pathogens more efficiently, yet it makes them more prone to autoimmunity (Klein and Flanagan 2016). Moreover, certain regions of the brain, like the cortex and hippocampus, have higher inflammation levels in aging female mice (Cyr and de Rivero Vaccari 2023; Kang et al. 2024), suggesting that disrupted X chromosomal dynamics occur over time. Indeed, differential gene expression of aged female microglia compared to the ones in males revealed that female-biased genes are enriched in senescent and disease-associated signatures with genes encoded from both autosomal and sex chromosomes (Ocañas et al. 2023). Finally, normal physiology also results in sex-specific phenotypes. The constant remodeling the uterus undergoes with each reproductive cycle makes females prone to fibrosis and inflammation (Winkler et al. 2024).

A more detailed explanation on the role of X chromosome misregulation is provided in **1.2.3 Epigenetic alterations** and **1.3 Epigenetic alterations**, however the understanding of senescence and inflammaging in a sex-specific manner is needed as I believe that these processes are a direct manifestation of disease, important for the development of personalized medicine.

1.2.9 Stem cell exhaustion

Cells in the body are constantly exposed to damage, and it is imperative that stem cells in different tissues are able to proliferate and differentiate to keep a balanced environment. While little is known about how sex affects stem cell pools in different tissues, previous work has shown that hematopoietic, neural and muscle stem cells proliferate faster in female rodents, with estrogen playing a role (Dulken and Brunet 2015; Sullivan et al. 2025).

Most of the information on stem cell aging comes from HSCs because, as part of the immune system, they are the progenitor cells of blood cells that circulate throughout the body. Aging disrupts a balanced HSC potential since cell division tends to be biased towards the myeloid lineage occurring earlier in females (Cho, Sieburg, and Muller-Sieburg 2008; C. Zhang et al. 2025). In addition, aged male HSCs have a higher tendency to uncontrollably divide and result in leukemias (C. Zhang et al. 2025). However, aging HSCs are more quiescent and decreased their proliferation suggesting that additional mechanisms push less cycling HSCs into an active state (Lv et al. 2024; Scherer et al. 2025).

The analysis of different stem cell niches and integration of lineage tracing technologies, using sex as a variable, will provide a better understanding of how tissue-residing stem cells change over time and affect tissue homeostasis and function.

1.2.10 Dysbiosis

The commensal bacteria found in the mammalian gastrointestinal tract regulates nutrient absorption and digestion, protects against pathogens and synthesizes beneficial metabolites. More recently, the microbiome has gained attention because it can act a messenger to other organs highlighting it as a great area of interest (Jašarević, Morrison, and Bale 2016).

Disruption of the microbiome can generally be evaluated from two different perspectives: bacterial communities and intestinal function. The microbiome of females is richer than that of males and remains stable until menopause (de la Cuesta-Zuluaga et al. 2019; Mayneris-Perxachs et al. 2020; X. Zhang et al. 2021). Similarly, remodeling of the microbiota during aging is sex-specific, with implications in physiology. Old female mice have a higher abundance of taxonomic bacterial groups associated with mouse models of AD while probiotic-related taxa decreased in males but remained the same in females (Ma et al. 2020; Webster et al. 2022). A functional and healthy intestinal barrier permeability is needed to selectively allow the absorption of nutrients without the passage of bacteria, affecting not only the gut but also other systems. Female rodents have a reduced barrier integrity, leading to leakage of intestinal-derived bacterial products and in consequence inflammation (Webster et al. 2022; Quin et al. 2024). How this inflammation is dealt with is unknown, considering that inflammation is less abundant in females in the early stages of aging.

While the consequences of the synergetic effect of an XX or XY genotype, in combination with the microbiome, has started to be studied, the introduction of aging as a variable is needed (Amato-Menker et al. 2024). Moreover, translating such findings is challenging but needed, considering that the microbiome is highly shaped by population-specific diets.

1.2.11 Altered cellular communication

The crosstalk between different cells in an organism is an important feature of responding to different stimuli, whether those are to maintain homeostasis or to induce cellular repair when an injury is made. Communication between cells can initially be hindered by a cell intrinsic factor

that can affect the expression of a certain ligand or receptor and therefore diminish or completely abrogate cell-cell interactions.

Identification of cell types based on transcriptomic signature using single-cell sequencing allows for the identification of gene changes that can interfere with cell communication. Although they are limited, sex-specific findings have been reported. In the aging immune system, females experience increased expression of ligands that mediate the pathogenesis of autoimmunity, leading to its higher incidence in females (Z. Huang et al. 2021). In males, on the other hand, there is increased expression of ligands linked to tumorigenesis (Z. Huang et al. 2021) which can explain the male-biased incidence of cancer. The enhanced immunity response also occurs in the retina. In the eye, retinal glial cells have a more pronounced cell-cell communication due to increased expression of ligand-receptor pairs resulting in immune inflammation in the female retina (H. Liu et al. 2025). In aged female mice, the quality of the oocyte is compromised with its surrounding somatic cells because of communication decline between them; supplementation of melatonin helped maintain the germline-soma communication, which can be clinically relevant in reproductive-assisted technologies.

Another form of communication, that is perhaps more long-range than the ones present previously, is through extracellular vesicles. These structures are lipid bilayer particles encapsulating different macromolecules and mediate cell-to-cell communication and transfer of molecules (Kumar et al. 2024); as such, they constitute an important source of communication between cells. The aging brain in female mice produces more astrocyte-derived vesicles than that of males, assessed by increased protein levels of the machinery that produces vesicles and more specifically, the vesicles were of mitochondrial origin (Y. Kim et al. 2022). What the vesicles contain and which cells they target has not been described but open up new avenues to understanding brain resilience and pathogenesis considering that females, compared to males, experience a higher vesicle-induced inflammatory response upon injury (Y. Li et al. 2023).

1.3 The X chromosome as a double balance

1.3.1 Skewing of X chromosome inactivation

As introduced earlier, XCI generates mosaic female cells, each with a 50% probability of having either X chromosome inactivated. Skewing towards one allele, however, is possible and is either of embryo origin (direct) or acquired. Direct skewing involves the presence of mutation in regulators of or *Xist*/*XIST* itself, resulting in the inactivation of the chromosome with the mutated

gene (Plenge et al. 1997). Acquired skewing arises from the negative selection of cells expressing pathogenic X-linked variants from the outgrowth of WT cells (Barbara R. Migeon 2020). Skewing is generally beneficial to females: pathogenic variants affects males more frequently since they only have one X chromosome and unless the variant is lethal to them or females are homozygous, they tend to show little to no diseases at all as a result of skewed XCI towards the WT allele (Barbara R. Migeon 2020). Nonetheless, in some instances selective advantage to the mutant cells can also happen (Barbara R. Migeon 2020).

When not influenced by deleterious mutations, XCI was initially thought to be a random process in young individuals (Amos-Landgraf et al. 2006; Bolduc et al. 2008), with skewing becoming more prominent during aging and correlating with CVD and cancer (Busque et al. 1996; Mengel-From et al. 2021; Roberts et al. 2022). However, advances in DNA sequencing technologies, coupled with parental genomes to generate haplotypes, have revealed that skewing in the population occurs at a frequency of nearly 1 women for every 50, which is more common than previously estimated (Shvetsova et al. 2019). One aspect of analyzing the transcriptome of cells with completely skewed XCI has allowed the identification of new gene escapers (Bjorn Gylemo, Bensberg, and Nestor 2025), expanding the list. Moreover, traceability of complete skewed inactivation along development helps understand the plasticity of escaping. A recent study using thymocytes with full skewed XCI and comparisons to XY and X0 samples, showed that previously identified escapers are dispensable during T cell development (Björn Gylemo et al. 2024). This is quite unexpected if one considers the noncanonical XCI dynamics in lymphocytes (Savarese et al. 2006; Syrett et al. 2017), which is a topic of discussion at the end of this section, but highlights the flexibility of XCI during differentiation in a cell type-specific fashion.

1.3.2 Above and beyond: *Xist*/*XIST* roles outside of induction of XCI

XCI renders a similar X-linked transcriptomic landscape between the sexes and yet, the regulation of the inactive X, in terms of *Xist*/*XIST* is unclear. Once inactivation and gene silencing have taken place, it was believed that the master regulator is indispensable for silencing. This was based on the observations that conditional deletion of *Xist* in mouse fibroblasts after XCI had occurred, resulted in no apparent reactivation of *Pgk1* and *Hprt* genes from the inactive X by RNA FISH, genes that are subjected to silencing (Csankovszki et al. 1999). The development of more sensitive techniques challenged that notion. For example, by fluorescently tagging the inactive copy of the *Mecp2* gene with *EGFP*, conditional and tissue-specific *Xist* deletion led to up to 5%

of neurons with EGFP signal suggesting that at least *Mecp2* had been reactivated (Adrianse et al. 2018). These results were phenocopied in mouse HSCs where *in vivo Xist* deletion resulted in hematologic cancer (Yildirim et al. 2013). Human mammary stem cells lacking *XIST* after chromosome inactivation had increasing tumorigenic potential, in part due to the expression of X-linked genes involved in chromatin remodeling and transcription (Richart et al. 2022). The previous experiments were carried out by genome editing approaches and point out to a protective role of the lncRNA in female homeostasis, however, understanding whereas the *in vivo* female epigenetic undergoes natural rearrangements is important to link female-specific mechanisms to homeostasis and disease. These studies highlight the contribution of *Xist*/*XIST* in maintaining the heterochromatin landscape of the inactive X after the initiation phase of XCI. However, while dysregulation of *Xist*/*XIST* induces the reactivation of some X-linked genes, the consequences are lineage-specific and become amplified upon stress (L. Yang et al. 2020).

In vitro culturing of WT female cells from humans have different epigenetic profiles and natural loss of *XIST*, defined as erosion, is a common phenotype (Anguera et al. 2012; Brenes et al. 2021). Upregulation of oncogenes found in the X is correlated with *XIST* erosion (Anguera et al. 2012), supporting the previous evidence that *Xist*/*XIST* has a protective tumorigenic effect. Not only is the X content affected upon erosion but autosomal-encoded proteins also show a higher abundance and were found to be disease-relevant (Brenes et al. 2021). This is in agreement with the hypothesis that an imbalance of X-linked gene expression disrupts molecular networks, affecting an organism's homeostasis (Gu and Walters 2017; Chunduri, Barthel, and Storchova 2022). Whether erosion is a true epigenetic mechanism or an artifact of culturing female cells outside of its natural cellular environment is not known but it has provided important evidence of the consequences of misregulation of the inactive X.

Finally, different lines of evidence have reported that *Xist*/*XIST* plays roles outside of inducing X silencing. Recently, some reports have shown that it also binds to autosomal genes that are in close spatial proximity to its locus (Dror et al. 2024; Yao et al. 2025), however these results come from cells resembling the preimplantation embryo and are not found in the soma. Moreover, one of the reasons why the onset of inflammation is delayed in females might be due to *Xist* as the lncRNA attenuates acute inflammation by translocating to the cytoplasm from the nucleus (Shenoda et al. 2021). Importantly, inflammation in males was reduced when cells overexpressed the 5' of the *XIST* gene (Shenoda et al. 2021).

Although they have largely relied on genetic manipulation, all those findings show how important keeping the inactive X chromosome in check is, to rely on a proper silencing and expression only of the escapers. The following sections therefore provide information on how escapers contribute to an array of positive, but also detrimental, phenotypes in females.

1.3.3 Sex bias in homeostasis

The notion that female cells have an additional X that helps them deal with pathogenic mutations suggests that XCI is, in general, a female-beneficial event. One of the most obvious advantages is a protective effect in developing cancer. Except for gonadal and thyroid cancer, this disease is male-biased (Clocchiatti et al. 2016). Sequencing projects have revealed that the inactive X is highly mutated in cancer suggesting that inactivation of one allele buffers the expression of mutated proteins that promote cancer development (Jäger et al. 2013). This idea is supported by the interplay between the X chromosome and p53, a tumor suppressor protein (Hernández Borrero and El-Deiry 2021). Through direct interaction, p53 regulates XCI and loss-of-function mutations in the *TP53* gene perturb it (Delbridge et al. 2019). Moreover, the X chromosome encodes ubiquitinases and kinases which are regulators of p53 (Haupt et al. 2019). Finally, some escaper genes are known to act as tumor suppressor genes, providing enhanced protections in females (Dunford et al. 2017). Since males have only one X chromosome, cancer-promoting mutations cannot be masked and ultimately result in cancer. However, a balance must be present. The X contains many oncogenes and XCI ensures that a proper dosage does not lead to enhanced cell proliferation (Anguera et al. 2012; Richart et al. 2022). On the other hand, the loss of the inactive X makes females prone to ovarian and breast cancer (Pageau et al. 2007; Chaligné et al. 2015). Collectively, these data support a selective pressure to ensure expression of functional X-linked cancer suppressor genes.

Besides cancer, relaxation of the inactive X chromosome can be beneficial, although to some extent. Recent studies have shown that derepression of neural genes in specific regions of the brain confers advantage to age-associated memory decline (Gadek et al. 2025). Another example is considering the presence of the X chromosome, rather than its genes, in longevity. The lifespan of mice with an additional X chromosome, regardless of the gonads, is lengthened (E. J. Davis, Lobach, and Dubal 2019). These biological processes exemplified the protective effect of having an additional, yet almost transcriptionally silenced, X chromosome. However, the extra X chromosome can also have an opposing effect in female physiology. A correct gene dosage of escaper is needed for female homeostasis. The most clear example is seen in

individuals with sex chromosome aneuploidies, lacking or having one additional X chromosome, leading to Turner's syndrome and Klinefelter's syndrome, respectively; supernumerary X chromosome syndromes also exist (Tallaksen et al. 2023; Viuff et al. 2023).

1.3.4 Sex bias in disease

The clearest example involves the immune system as the X chromosome encodes 15% of immune-related genes (Bost et al. 2022). Mice with an extra X, independently of the gonads, have a greater susceptibility to suffer from autoimmune diseases (Smith-Bouvier et al. 2008). Moreover, individuals with multiple X chromosomes are more likely to develop lupus, an immune-mediated disease, in comparison to XY, XX and X0 individuals (Vieira et al. 2024). This can be explained, in part, to the nature of the exceptional XCI process in lymphocytes. Generally, naïve lymphocyte cells lack the canonical *Xist*/*XIST* RNA cloud, which is only detectable upon antigen stimulation (Savarese et al. 2006; Syrett et al. 2017). Interestingly, the inactive X chromosome is largely dosage-compensated despite the lack of visible *Xist*/*XIST* RNA clouds; only a few genes that are relevant in the context of autoimmunity are biallelically expressed (Sierra et al. 2022; Forsyth et al. 2024). While the dynamics of XCI in the immune system do not seem to affect dosage compensation, it is plausible that it predisposes them to aberrant transcriptional programs over time.

Not only the misregulation of XCI upon aging (see **1.2.3 Epigenetic alterations**) but also its components add another layer of complexity. Beyond its role in inducing XCI, *Xist*/*XIST* can also attenuate inflammation as described previously (Shenoda et al. 2021), nonetheless this lncRNA and its associated proteins serve as autoantigens, resulting in the production of autoantibodies commonly found in lupus (Shenoda et al. 2021; Dou et al. 2024). *Xist*/*XIST* misregulation relaxes the heterochromatin on the inactive X and thus, gene reactivation takes place. The consequence of escaping of genes that are not normally considered as escapers can also lead to autoimmunity (Yu et al. 2021; Huret et al. 2024).

1.3.5 Tissue-specific activity of gene escapers

Understanding how X-linked genes promote female resilience is important and will lay a foundation to target them for therapeutic purposes, especially in the context of individuals harboring only one X chromosome. Only a handful of genes have been described with tissue-specific roles.

Kdm6a is an X-linked histone demethylase, identified as a constitutive escape (Berletch et al. 2015; Tukiainen et al. 2017). *Kdm6* expression is higher in CD4+ cells from XX individuals and its deletion ameliorates neuropathology symptoms in mouse models of multiple sclerosis, suggesting that escapers can be modulators of autoimmunity (Itoh et al. 2019). However, Kdm6a prevents female bladder cancer development and improves memory and learning when overexpressed in the brains of aging males (Kaneko and Li 2018; Shaw et al. 2023). Importantly, Kdm6 has been proposed a buffering protein in the later onset of AD in females (E. J. Davis et al. 2020)

Kdm5c is another sexually dimorphic X-linked demethylase with higher expression in XX cells (Berletch et al. 2015; Tukiainen et al. 2017). Dosage modulation of the extra copy of *Kdm5c* results in reduced fat content and body weight to that of males with a single copy (Link et al. 2020). Moreover, Kdm5c and Kdm6a have been proposed to have a protective role to the coronary heart disease in young females (J. Li et al. 2014; S. Qi et al. 2021)

These data demonstrate how the context of X chromosome escapers influence beneficial or detrimental outcomes. However, there is an incomplete understanding of how escaping from the inactive X contributes to disease manifestation in a sex-specific fashion during aging.

1.4 Generation of chromosome aneuploidies

Studying how any chromosome contributes to sexual dimorphism in aging as chromosomal entities, rather than their encoded genes, is challenging. Different methods have been developed from chemical inhibition of different mitotic proteins to DNA editing technologies. The following sections include a description of how these methods work.

1.4.1 Microcell-mediated chromosome transfer

One of the initial methods to generate cells with an additional chromosome was microcell-mediated chromosome transfer. In this approach, human chromosomes from fibroblasts are tagged with a drug-resistant gene, followed by chemically induced micronucleation. These micronuclei are then enucleated generating microcells with intact plasma membranes. Fusing the microcells to recipient cells creates hybrid clones, which are further isolated by drug selection (Suzuki et al. 2020). Transferring the microcells to cancer cells allowed the identification and mapping of tumor suppressor genes when the growth of cancer cells was reduced (Kugoh, Ohira, and Oshimura 2015).

1.4.2 Centromere inactivation

In the case of the Y chromosome, one initial method has been developed and is known as centromere inactivation. In humans, the centromere of autosomes and chromosome X contain the centromere proteins A and B that are recognized by the centromere protein C found in kinetochores, allowing chromosome segregation in each division. The Y chromosome stands out as it is the only human chromosome containing only the centromere protein A. Using this approach, inducible degradation of the centromere protein A leads to Y chromosome loss as no backup mechanisms, such as the centromere protein B in the remaining chromosomes, can account for proper segregation (Ly et al. 2017, 2019).

Using this methodology, it has been shown that chromosome segregation errors result in Y chromosome micronucleation, chromosome shattering and DNA repair of the broken pieces. These events ultimately lead to chromothripsis and genomic instability and have been used as a proxy to study complex karyotypes commonly found in cancer (Ly et al. 2017, 2019).

1.4.3 Chromosome-specific aneuploidies using CRISPR-Cas

CRISPR stands for Clustered Regularly Interspaced Short Palindromic Repeats, a bacterial locus containing specific DNA sequences separated from one another. These sequences are DNA-derived viral pieces that bacteria have acquired from past infections. CRISPR uses the viral-transcribed RNA pieces, together with the CRISPR-associated protein 9 (Cas9), to target viral DNA upon a new round of infection. Cas9 specifically targets the viral DNA by the presence of a protospacer adjacent motif (PAM) upstream of the complementary RNA base pairs in the viral genome. Once the viral sequence has been recognized, Cas9 induces double-stranded breaks (DSBs) in the target sequence, subsequently leading to its degradation. This is a mechanism used for bacteria to deal with pathogen infections. However, the CRISPR-Cas system has been exploited since the RNA pieces can be programmable into a single guide RNA (gRNA), making any sequence with a PAM-specific motif targetable. Many Cas proteins exist, nonetheless Cas9 has been the most adaptable Cas protein (J. Y. Wang and Doudna 2023).

The identification of repetitive sequences along the mouse Y chromosome, and in the centromere, have allowed the use of the CRISPR-Cas9 technology to induce massive DSBs that ultimately result in chromosome elimination, a process termed chromosome shredding (Adikusuma et al. 2017). This technology has been used to generate both female X0 mice from XY zygotes and embryos as well as the elimination of an extra chromosome 14 in mouse

embryonic stem cells and an extra chromosome 21 in human pluripotent stem cells (Zuo et al. 2017). Moreover, this technique was used to causally link LOY and aging in HSCs (Sano et al. 2022).

Engineering of the CRISPR-Cas9 includes the catalytic inactivation of Cas9 by mutating the amino acids required for cleavage activity. This dead version can then be coupled to transcriptional activators or repressors to tweak gene-specific transcription programs (Gilbert et al. 2013; L. S. Qi et al. 2013). In humans, tethering a mutated kinetochore protein to a catalytically inactive Cas9 protein, together with chromosome-specific gRNAs has enabled partial and whole human chromosomes aneuploidies (Bosco et al. 2023; Truong et al. 2023).

2. Aim of thesis

Different methods have been applied to generate chromosome-specific aneuploidies. Yet, while some of them have been shown to induce X chromosome aneuploidies, they have some caveats (Zuo et al. 2017; Bosco et al. 2023).

First, female cells contain two X chromosomes and therefore, it is essential to be able to differentiate the two parental alleles. This is important in a sequence-dependent targeting, such as in the CRISPR-Cas system. The presence of single nucleotide polymorphisms ensures that allele-specific gRNAs bring Cas9 to one X chromosome and target it, leaving the other X chromosome intact. In this sense, this approach has an advantage as the targeting relies only on endogenous sequences.

Second, the previous methods to generate aneuploid cells rely on clonal expansion and cell line verification (Viuff et al. 2023). This limits the study of the initial consequences upon aneuploidy because only adaptation events, rather than acute effects, can be studied. Therefore, an inducible approach where the expression of the targeting system can be controlled provides a powerful tool to understand chromosome aneuploidies at one specific time.

Finally, identifying the most suitable system is important. Generation of X chromosome aneuploidies has been reported by fusing a mutant kinetochore protein to a catalytically inactive Cas9. In this system, the chromosome recognized by the gRNA-Cas9 complex is missegregated by the destabilization of the kinetochore-microtubule interaction with the mutant kinetochore protein (Bosco et al. 2023). The experiments relied, however, on human colonic epithelial cells and retinal pigment epithelial cells suggesting that the consequences of aneuploidy can be cell-type specific. While induced pluripotent cells (iPSCs) can be obtained from the said epithelial cells, the reactivation of the inactive X by erosion (see page 47) in iPSCs changes the gene expression of the cells, hindering its application (Brenes et al. 2021). Instead, mESCs are a better system for our project for several reasons. Firstly, these cells are isolated from the epiblast of the inner cell mass of preimplantation embryos and share the same characteristics as their *in vivo* counterpart. Secondly, similar to iPSCs, they can be propagated indefinitely *in vitro* and retain developmental potential, allowing scientists to differentiate them to many cell types in a dish (Czechanski et al. 2014). Specifically, the use of female hybrid cells is essential. Hybrid mESCs are isolated from the first-generation offspring by crossing two genetically distant inbred strains. This is a major advantage because we gain allele resolution, allowing us to target only one allele—

either autosomal or sex chromosome—of each chromosomal pair. Third, mESCs can be transferred back to an embryo and generate mouse models (Takahashi et al. 2023). Lastly, genome editing in mESCs is relatively easy compared to other cellular systems. For instance, gene delivery in cells isolated from human and adult tissues requires optimization of gene delivery and editing; more importantly, they undergo senescence (Z. Zhang et al. 2024).

The aim of my PhD project was to develop an inducible system for the targeting of one X chromosome in mESCs. Previously, unique gRNA sites in the X chromosome of the C57BL/6 mouse genome were reported and used for chromosome shredding to generate X0 mice from XX (Zuo et al. 2017). We exploited the unique sites in the X chromosome to target the X^{Bl6} allele in female cells. Therefore, we used hybrid mESCs of the cross of female C3H/HeJ with male C57BL/6 (referred as C3H/Bl6 from now on) which are strains distantly related in evolution with sufficient numbers of polymorphisms to distinguish each parental allele. To reach our aim, C3H/Bl6 mESC cultures were established and cells were characterized to further use females to establish our inducible CRISPR-targeting system for X chromosome shredding. Ultimately, this system will make it possible to link the contribution of the second and inactive X chromosome to sexual dimorphism in aging.

3. Results

3.1 Generation of targeting vectors

To enable X chromosome targeting in a timely manner, we generated plasmids from a previously generated mouse line (available in the lab [redacted]) that allows the Cre-dependent expression of Cas9 (Platt et al. 2014). In brief, in this mouse line, Cas9 and EGFP are produced as two different proteins from the same transcript via a T2A ribosome skipping event (Donnelly, Hughes, et al. 2001; Donnelly, Luke, et al. 2001). Upstream of the *Cas9-T2A-EGFP* cassette, three polyadenylation sites are present and are flanked by loxP sites. Under normal conditions, the presence of the polyadenylation sites hinders the translation of *Cas9* and *EGFP*. Their transcription is inducible only by the presence of the protein Cre recombinase, which recognizes the loxP sites flanking the polyadenylation sites, removing them by DNA recombination. Only after loxP site removal, the *Cas9-T2A-EGFP* transcript is expressed. We then inserted the previously published Bl6-specific gRNA (referred to as gRNA X-C in (Zuo et al. 2017)) in the construct under the human *U6* promoter, commonly used for driving the constitutive expression of gRNAs. We designated this construct as the shredder system.

We employed two different inducible systems to generate X chromosome aneuploidies, differing in the integration approach and the promoters driving the expression of *Cas9-T2A-EGFP*.

3.1.1 X chromosome shredder donor plasmid for Rosa26 targeting

The *Rosa26* locus is a commonly used harboring genomic site for single-copy transgene insertion, as the locus transcribes RNAs with no coding potential. Moreover, modification of the WT loci does not result in any abnormal phenotype in mice (Zambrowicz et al. 1997), making it a safe genomic location for transgene insertion. The *Rosa26* locus is lowly expressed and its promoter can be used to drive the expression of the desired transgenes. This is one of the major advantages of using the *Rosa26* locus as transgene expression using highly active promoters can result in gene silencing (Cabrera et al. 2022).

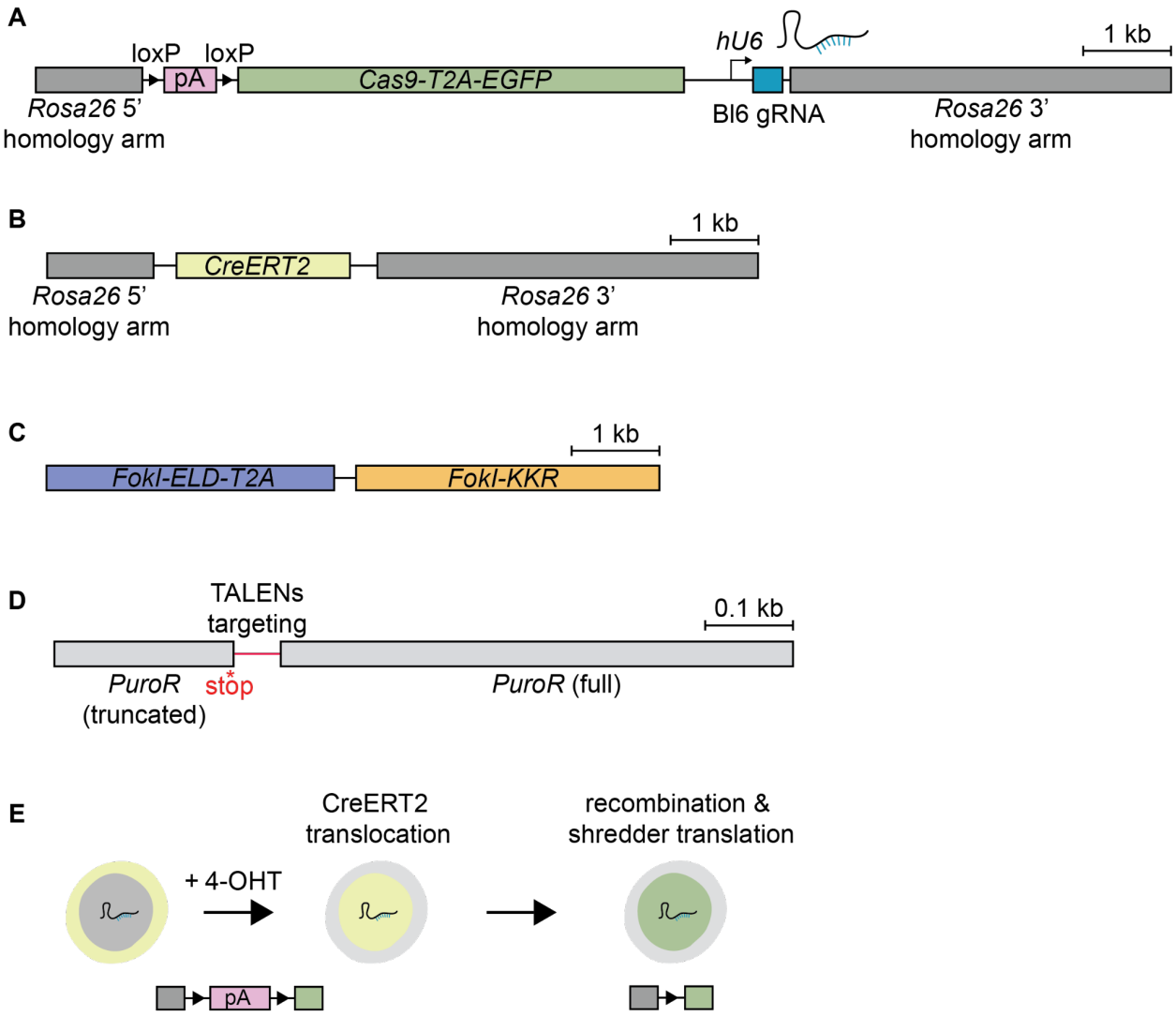

Figure 3.1. Vectors for targeting the *Rosa26* loci. **(A)** Shredder construct containing three polyadenylation sites (pA) flanked by loxP sites. Downstream of the pA sites, the coding sequence of the protein Cas9 is tethered to a T2A and the coding sequence of EGFP. The Bl6-specific gRNA is constitutively expressed. The shredder fragment is flanked on both ends by the *Rosa26* homology arms. **(B)** *CreERT2* recombinase vector for loxP site recombination. The fused protein is flanked on both ends by the *Rosa26* homology arms. **(C)** Plasmid encoding the two TALEN proteins for Rosa26 targeting. The ELD TALEN protein targets the forward strand while KKR TALEN targets the reverse strand. **(D)** Puromycin-resistance (*PuroR*) vector for selecting transfected cells. The plasmid encodes a truncated version of puromycin-resistant protein. The TALEN proteins target as well the red sequence in the reporter vector. **(E)** (left) Bl6 gRNA is expressed at all times and CreERT2 is present in the nucleus. (middle) Upon 4-hydrotamoxifen (4-OHT) addition, CreERT2 is translocated to the nucleus, recombining the loxP sites flanking the pA site. (right) *Cas9-T2A-EGFP* is then translated and present in the cells. The TALENs targeting the Rosa26 loci as well as the puromycin reporter vector have been previously reported in (Flemr and Bühler 2015) and were kindly donated. The fragments for bacterial amplification are omitted.

My supervisor, [redacted], initially constructed the shredder vector with homology arms to the *Rosa26* loci, aiming to integrate the construct in one of the parental alleles (Figure 3.1a). The second other allele is engineered to encode a modified version of Cre recombinase protein that will remove the loxP sites (Figure 3.1b), using a plasmid previously reported and kindly donated from Marc Bühler (Flemr and Bühler 2015). Fusion of Cre to a mutated version of the human estrogen receptor, ERT2, results in Cre-ERT2. Cre-ERT2 is normally present in the cytoplasm and upon addition of tamoxifen, which recognizes and binds to ERT2, the fused protein translocates to the nucleus. Only then, the Cre recombinase protein is able to mediate loxP site recombination (Feil et al. 1997; Indra et al. 1999) (Figure 3.1e).

In this setup, targeting of the *Rosa26* alleles cannot be aided by generating a double stranded break with the standard CRISPR system because the Bl6 gRNA is constitutively expressed and X chromosome shredding would be induced from the donor vectors as soon as the Cas9 protein is present. Therefore, we employed another cutting strategy using transcription activator-like effector nucleases (TALENs). In this approach, previously reported TALENs proteins target *Rosa26*-specific sequences in exon 1 similarly to CRISPR (Figure 3.1c) (Flemr and Bühler 2015). A selection strategy is employed to enrich cells after transfection and gene targeting (Figure 3.1d). The *Rosa26* TALENs, besides targeting the endogenous *Rosa26* loci, also target a truncated version of a puromycin-resistance reporter. Once the puromycin-resistance reporter plasmid has been targeted and after homologous recombination has taken place, the WT puromycin-resistance sequence is restored and growth in puromycin-containing medium is possible. The TALEN *Rosa26* targeting and puromycin reporter vectors have been previously designed, reported and were kindly donated from Marc Bühler (Flemr and Bühler 2015).

This approach renders five plasmids: the shredder vector, the Cre-ERT2 plasmids, two *Rosa26* TALEN vectors (one for each strand) and the puromycin selection plasmid. To reduce the number of plasmids, I generated one single TALEN plasmid containing both TALEN nucleases separated by a T2A skipping event. An illustration of TALENs targeting and cell selection after transfection is presented in Figure 3.2.

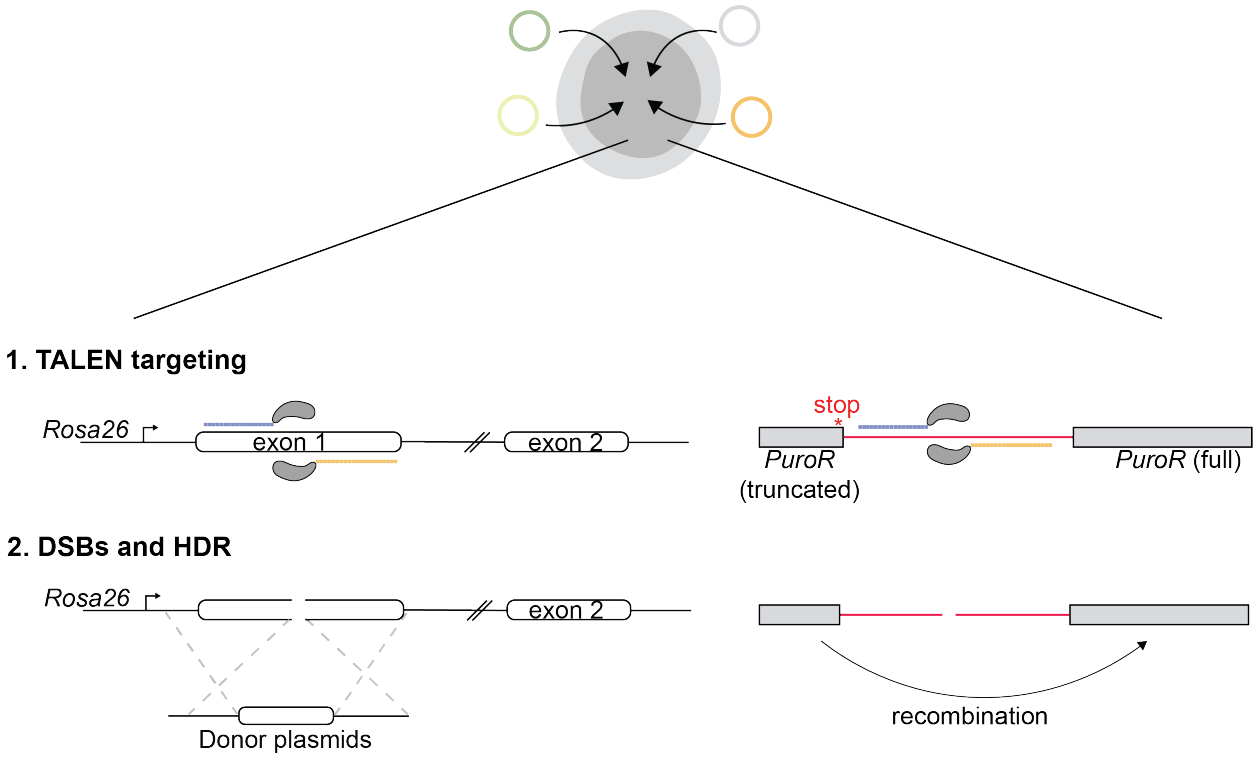

Figure 3.2. TALEN-mediated *Rosa26* targeting approach. Once transfected **(1)** the TALEN proteins will target a specific region within exon 1 of the *Rosa26* locus (left) as well as the reporter vector (right) that will result in double stranded breaks (DSBs) and homology-directed repair (HDR). **(2)** In the case of the *Rosa26* targeting, the DSBs are repaired by recombination via the homology arms present in the donor plasmids; the puromycin-resistant (*PuroR*) reporter plasmid will under recombination with the downstream sequence after TALEN targeting. **(3)** The result of homologous recombination is expected to generate one *Rosa26* allele containing the shredder construct and one allele with the *CreERT2* sequence while in the reporter a full *PuroR* cassette will be generated. The TALENs targeting the *Rosa26* loci as well as the puromycin reporter vector have been previously reported in (Flemr and Bühler 2015) and were kindly donated. The fragments for bacterial amplification are omitted.

3.1.2 X chromosome shredder piggyBac plasmid for transposition

Gene targeting in mESCs is a low-efficiency process as cells prefer NHEJ over homologous-mediated repair (Miyaoka et al. 2016). Therefore, we also employed a transposon strategy.

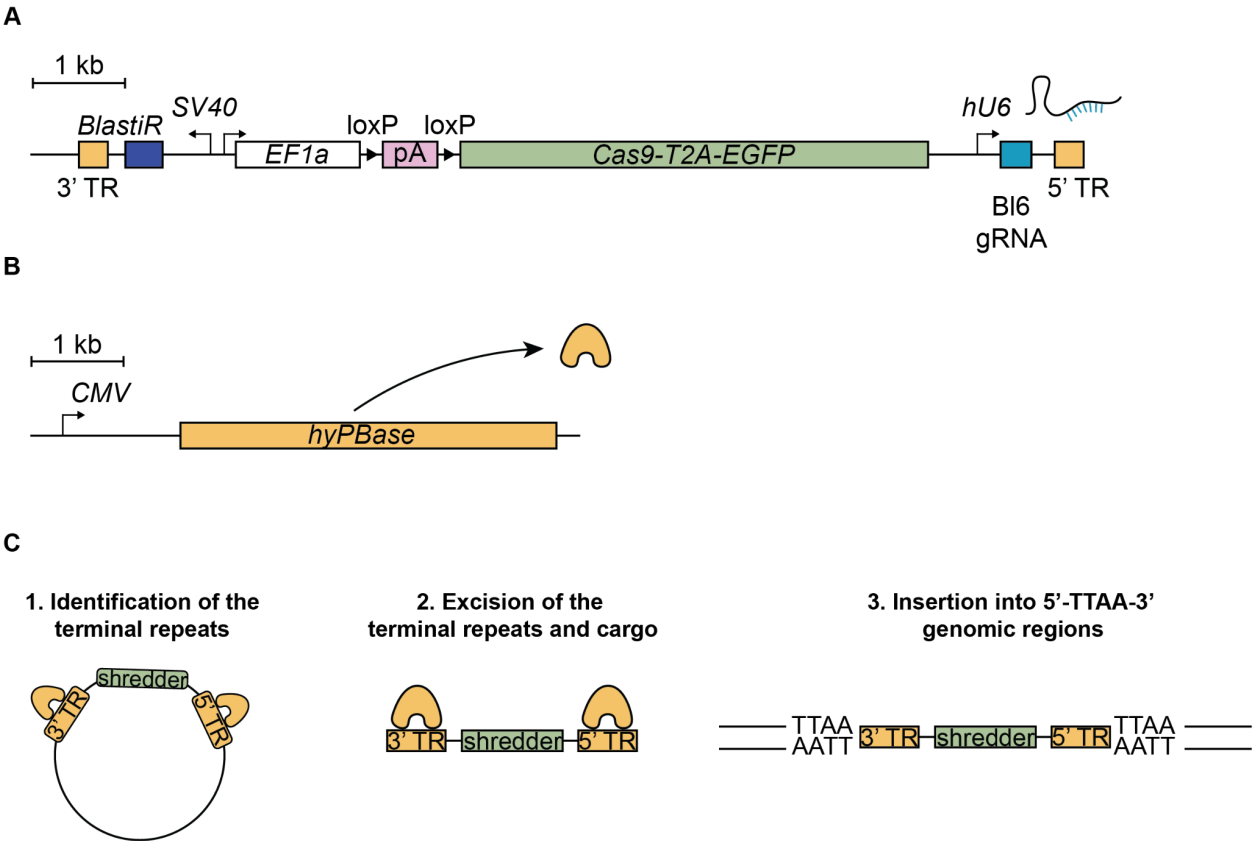

Figure 3.3. Vectors for transposition of the shredder construct.(A) Cargo: shredder construct under the human *EF1a* promoter containing three polyadenylation sites (pA) flanked by loxP sites. Downstream of the pA sites, the coding sequence of the Cas9 protein is tethered to a T2A-EGFP coding sequence. The Bl6-specific gRNA is constitutively expressed by the human *U6* promoter. Upstream of the shredder construct, a blasticidin-resistance cassette (*BlastiR*) is present. The cargo is flanked by 3' and 5' terminal repeats (TR). (B) Hyperactive *piggyBac* transposase sequence (*hyPBase*) is expressed under the *cytomegalovirus* promoter (*CMV*) (C) Mechanism of transposition: 1. The transposase recognizes the TRs and 2. excises them out, including the cargo, of the vector. 3. The transposase integrates the cargo in a random 5'-TTAA3-' genomic region.

The shredder construct from the *Rosa26* donor plasmid was cloned into a *piggyBac* backbone containing terminal inverted repeats flanking the construct. The terminal repeats are recognized by a transposase which excises the inverted repeats out, along with the cargo (the shredder system in our case), and integrates the fragment into the host genome. The integration is not completely random as the transposase targets 5'-TTAA-3' sites. The original shredder

construct does not contain a promoter as it relies on that from the *Rosa26* locus so the human *EF1a* promoter was added upstream of the polyadenylation sites. In addition, a blasticidin-resistance cassette was added to enrich for transfected cells (Figure 3.3).

3.2 Establishment of hybrid mESCs

3.2.1 Derivation of hybrid C3H/Bl6 mESCs

Traditionally, mESCs were derived using medium containing fetal calf or bovine serum on a layer of mitotically inactivated fibroblasts (feeders) that provide trophic factors for ESC growth and pluripotency maintenance. The replacement of feeders with gelatin and supplementation of leukaemia inhibitor factor (LIF) provided the minimum and essential factors for self-renewal of mESCs (Williams et al. 1988). However, ESC cultures grown in these conditions contain a heterogeneous population of pluripotent cells and only classical inbred mouse strains (typically of the 129 background) can be derived in serum conditions without feeders and LIF (Gardner and Brook 1997). Efforts to derive mESCs from non-classical strains have resulted in the development of the known 2i medium supplemented with LIF. The addition of two small molecules (Ying et al. 2008), inhibiting the FGF/ERK signal transduction pathway and activating the WNT pathway by inhibition of the GSK3 protein, have allowed the derivation, stabilization and propagation of different mammalian ESCs, making it the go-to medium for ESCs; the 2i/LIF medium is also supplemented with lipids supporting pluripotency maintenance (Zhong et al. 2023). Canonical mESCs used in the field are typically isogenic 129 or C57BL/6 cells of XY karyotype, or XX 129/Cast hybrids, for which culture conditions are established. Culture conditions and growth factor requirements, however, vary between mouse strains (Ortmann et al. 2020). We therefore chose to grow cells in the traditional serum medium supplemented with LIF on a layer of feeders.

We obtained cryopreserved 2-cell stage C3H/Bl6 embryos from the Janvier company and cultured them until the blastocyst stage, after which they were allowed to hatch and form outgrowths on a layer of feeders under serum/LIF. We chose these culture conditions because they promote a stable karyotype and genomic stability (Guo et al. 2018), which are important for the generation of a mouse model and critical points to answer our questions. Once outgrowths were visible, mESCs from each embryo were picked and expanded, where four of them could be stabilized to establish cell lines (Figure 3.4).

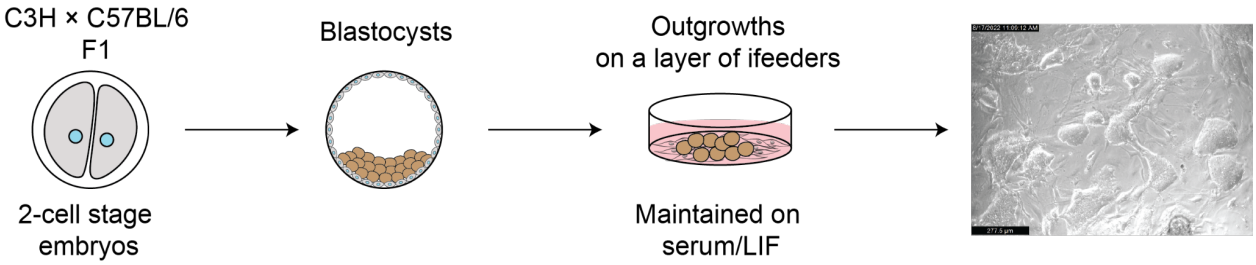

Figure 3.4. Derivation of C3H/Bl6 mouse embryonic stem cells. 2-cell stage embryos were obtained and cultured until the blastocyst stage before transferring to feeder plates in serum/LIF. Over time, outgrowths were identified and single colonies were picked and expanded. A representative picture is presented. Scale bar: 277.5 µm

3.2.2 The X chromosome content remains stable over passaging in C3H/Bl6 mESCs

X chromosome instability in female cells is a common phenomenon of *in vitro* mESC cultures (Robertson, Evans, and Kaufman 1983; Rastan and Robertson 1985; Kawase et al. 1994; Keniry et al. 2022). Having established the four C3H/Bl6 cell lines, we used DNA FISH to evaluate the X chromosomal content in the cells over passaging. Having female cells with an euploid X chromosome content is of great importance considering the focus of our project. DNA FISH uses a fluorescent probe that is complementary to one specific locus in the genome of interest; the DNA:fluorescent probe complex can then be visualized by microscopy. In the case of the X chromosome, one dot is expected to be present in males and two dots in females as each dot represents one specific locus within the X chromosome. In this sense, DNA FISH also allows us to genotype the cells based on the number of X chromosome dots. In addition, we used chromosome 6 as an euploid autosomal control, which is visualized as two dots.

We chose three different passages: early (p9 for cell lines 1-3 and p11 for cell line 4), medium (p14 for cell lines 1-3 and p16 for cell line 4) and late (p24 for cell lines 1-3 and p26 for cell line 4) and performed DNA FISH, followed by confocal microscopy and analysis, on the cells. DNA FISH revealed that lines 1 and 3 contain two X chromosomes while lines 2 and 4 have only one X chromosome. Moreover, around 80% of cells of lines 1 and 3 remained XX over long passaging, suggesting that the culture conditions chosen by us do not profoundly affect the stability of the X chromosome (Figure 3.5a, 3.5c). As expected, chromosome 6 remained euploid over time (Figure 3.5b).

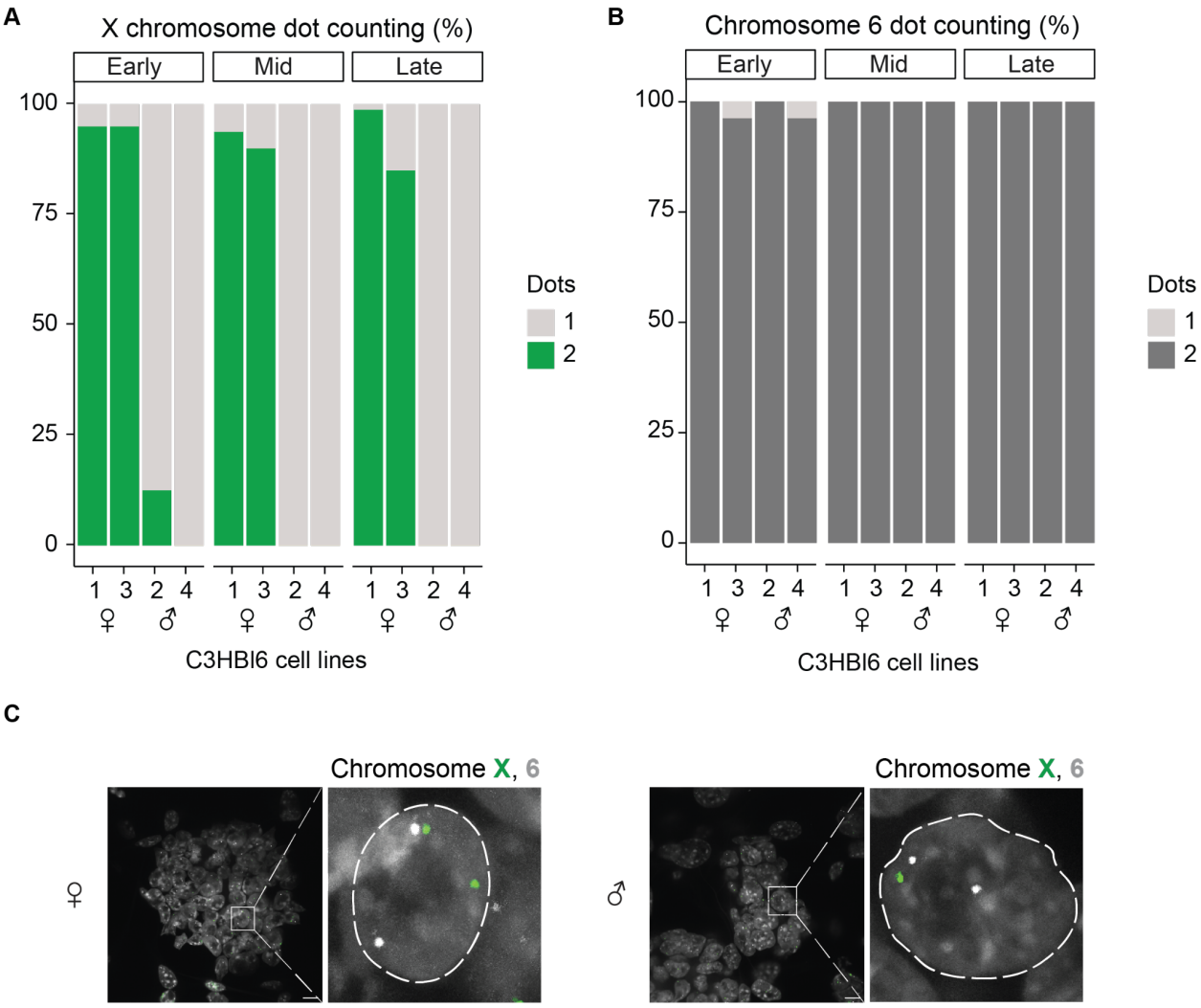

Figure 3.5. The X chromosome remains stable over passaging in C3H/Bl6 mESCs. **(A)** Bar plots showing the proportion of cells per line with one or two chromosome X dots in terms of percentage (three biological replicates, 240 total cells were counted). **(B)** Bar plots showing the proportion of cells per line with one or two chromosome 6 dots in terms of percentage (three biological replicates, 240 total cells were counted). (**C**) Representative *Z*-stack microscopy image of female (left) or male (right) cells with one or two X chromosome dots (in green) or chromosome 6 (grey dots). Scale bar: 10 µm.

3.2.3 Karyotype by long-read sequencing

After identification of the X chromosomal stability in the hybrids upon passaging, we confirmed the sex and determined karyotype of the cells by Oxford Nanopore long-read sequencing; we compared our cells to gDNA extracted from lung tissues of isogenic C57BL/6 male or female mice. After running quality control metrics, removing sequencing adapters and mapping to the mouse genome, we found that reads from cell lines 2 and 4 were similar to the lung male samples with almost 50% of the reads mapping to Y chromosome (Figure 3.6a). This

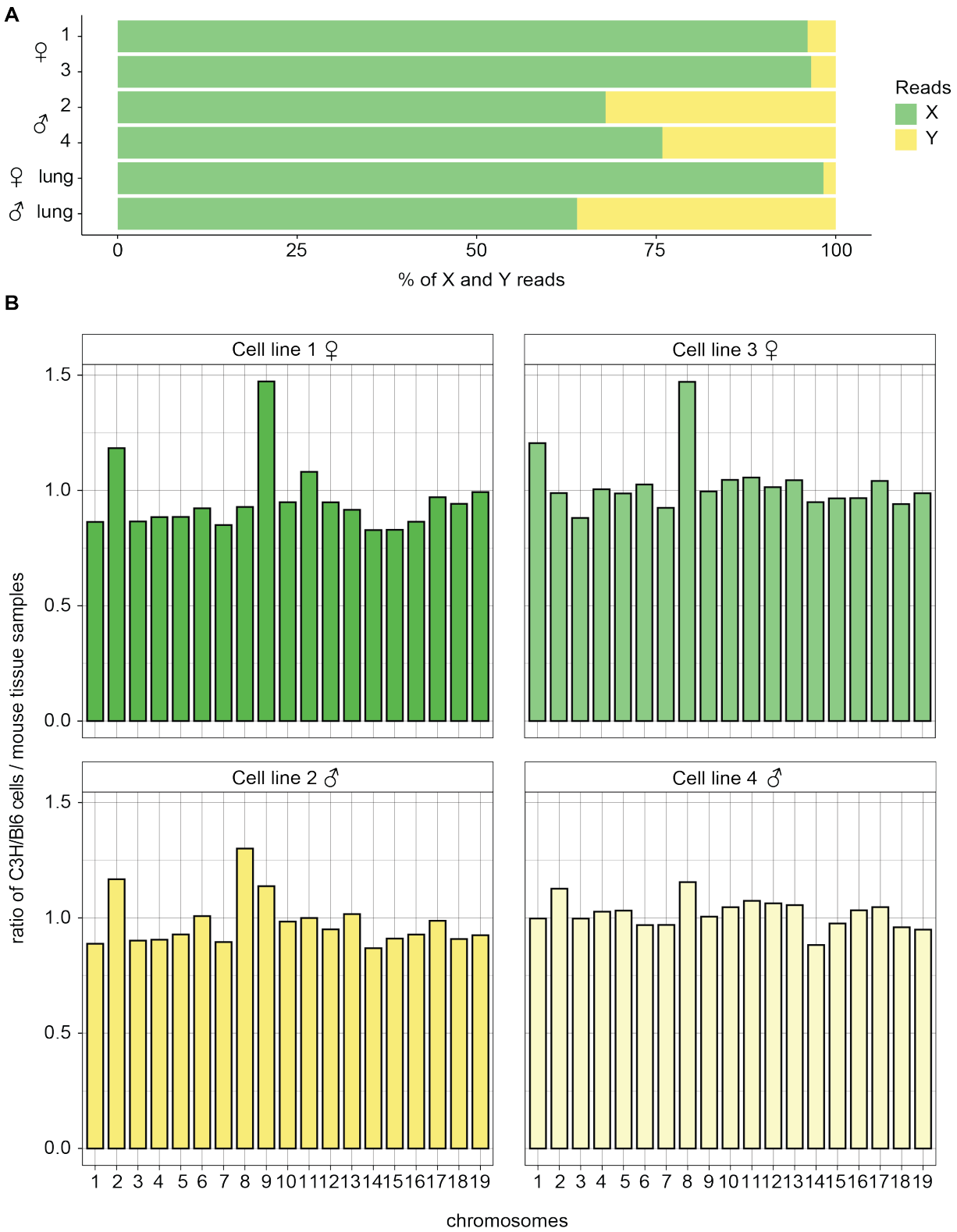

Figure 3.6. Sex chromosome content and karyotype of C3H/Bl6 mESC by long-read sequencing. **(A)** Bar plots showing the ratio of reads from C3H/Bl6 cells or mouse tissues mapped to the X or Y chromosomes. **(B)** Bar plots showing the ratio of C3H/Bl6 chromosome number over mouse tissues. A value of 1 represents chromosome diploidy.

result supported the DNA FISH counting where those cell lines had one X chromosome dot

(Figure 3.5a). Female cell lines 1 and 3 had almost all reads mapping to the X chromosome as expected by the DNA FISH results. The approximately 5% reads that mapped to the Y chromosome in females or the increase of the X reads in males could represent sequences with high degree of homology (PARs, for example).

We also evaluated the karyotype of the autosomes by dividing the ratio of autosome reads in the hybrids over the reads from the tissue samples. Out of the male lines, cell line 4 had the most euploid karyotype with most of the chromosome reaching a value of 1. In females, both lines had ratio values of 1.5 for chromosome 8 in cell line 1 and 1.5 for chromosome 9 in cell line 3 suggesting an extra copy of chromosome 8 and 9 in cell lines 1 and 3, respectively. Trisomy of chromosome 8 is a common aneuploidy of *in vitro* mESC cultures that is selected in the population as it provides a proliferative advantage over a WT karyotype (Y. M. Kim et al. 2013).

3.3 Characterization of the C3H/Bl6 mESC lines

The C3H/Bl6 mESCs have not been previously reported in the literature. Therefore, we verified that the C3H/Bl6 cells we isolated behave like typical mESC in terms of pluripotency and differentiation potential. Moreover, since we are interested in the X chromosome, we verified whether the X chromosomal dynamics can also be recapitulated in these cells.

3.3.1 C3H/Bl6 cells are pluripotent mESCs

Pluripotency, the inherited characteristic of mESCs to give rise to three germ layers (endoderm, mesoderm and ectoderm), is controlled by the regulatory network driving mESC identity with the transcription factors Oct4, Nanog and Sox2 as the main regulators (C.-Y. Chen et al. 2017).

We used retrotranscriptase quantitative PCR (RT-qPCR) to quantify the relative RNA levels of pluripotency markers and compared them to fibroblasts, a terminally-differentiated cell type. Contrary to fibroblasts, all four cell lines expressed pluripotency markers (Figure 3.7a). mESCs cultured in serum/LIF fluctuate in and out of the pluripotency network (Hackett and Surani 2014), so we also tested the expression of some genes associated to the three germ layers. Genes from the ectoderm layer had the highest expression among the three germ layers, yet pluripotency genes were the most highly expressed genes (Figure 3.7a). At the protein level, Nanog was present in the nuclei of the mESCs and the pluripotency-related epithelial cadherin was present at the rim of the colonies. These stainings did not colocalize with F-actin filaments

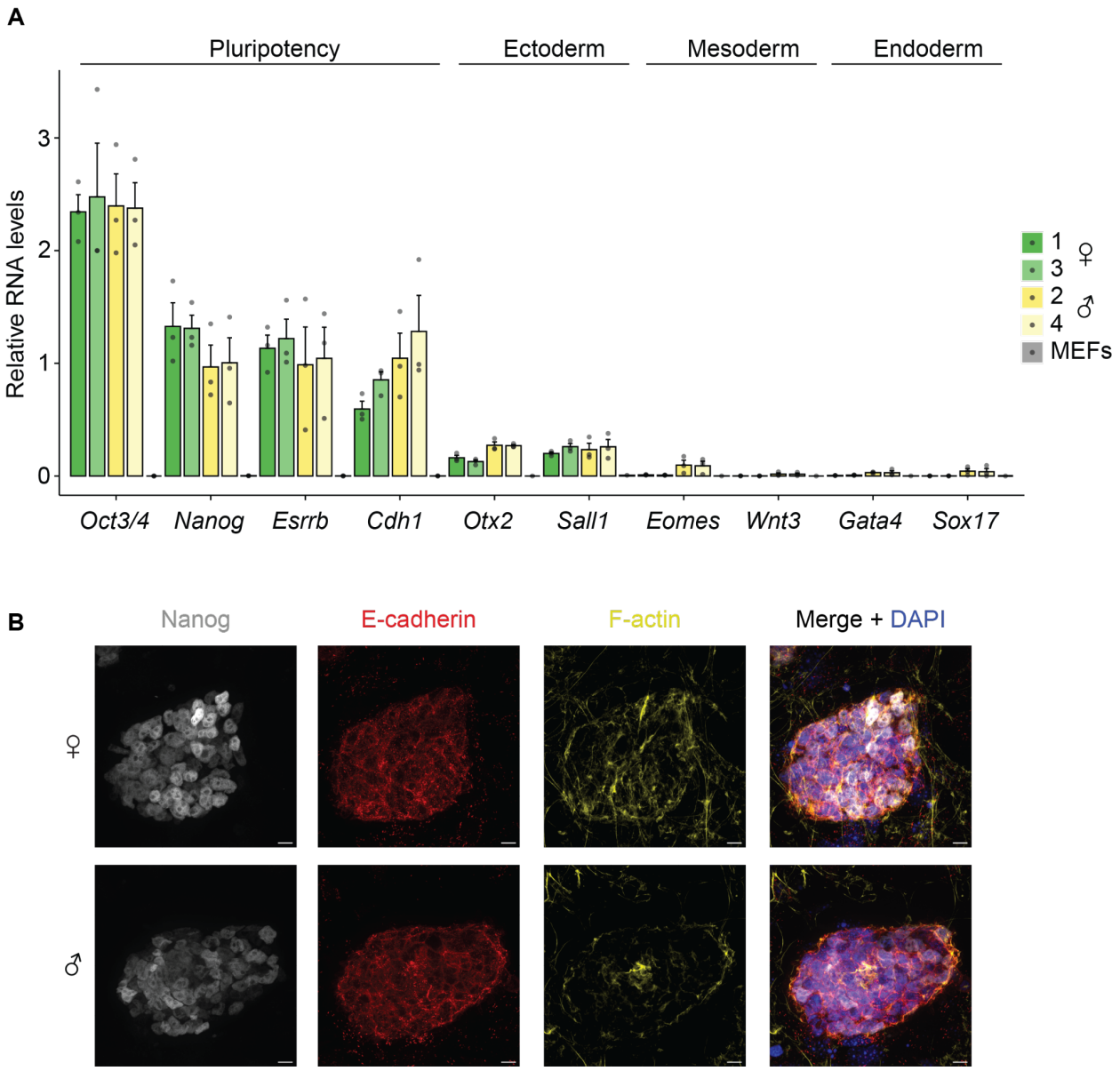

Figure 3.7. C3H/Bl6 mESCs express pluripotent-specific genes. **(A)** Bar plots showing the relative RNA levels of some genes associated with pluripotency or germ layers. Each dot represents one biological replicate. *TBP*, *Rplp0* and *Hprt* were used as normalization genes. **(B)** Representative merged immunofluorescence images of mESC colonies stained with antibodies anti-Nanog or anti-E-cadherin; phalloidin was used to stain F-actin filaments present in feeders. E-cadherin: epithelial cadherin. MEFs, mouse embryonic fibroblasts. Scale bar: 10 µm.

which are present in feeder cells, supporting the stem cell specificity of the Nanog and epithelial cadherin stainings (Figure 3.7b). These results showed that the C3H/Bl6 cells express pluripotency genes and have a minor differentiation bias towards the germ layers.

3.3.2 C3H/Bl6 mESCs exhibit developmental potential for the germ layers

Pluripotency is accompanied by the ability of cells to differentiate into the three germ layers upon signaling cues. LIF, together with the trophic factors provided by the feeders and serum, ensure the self-renewal of mESCs and support pluripotency (Hackett and Surani 2014). We

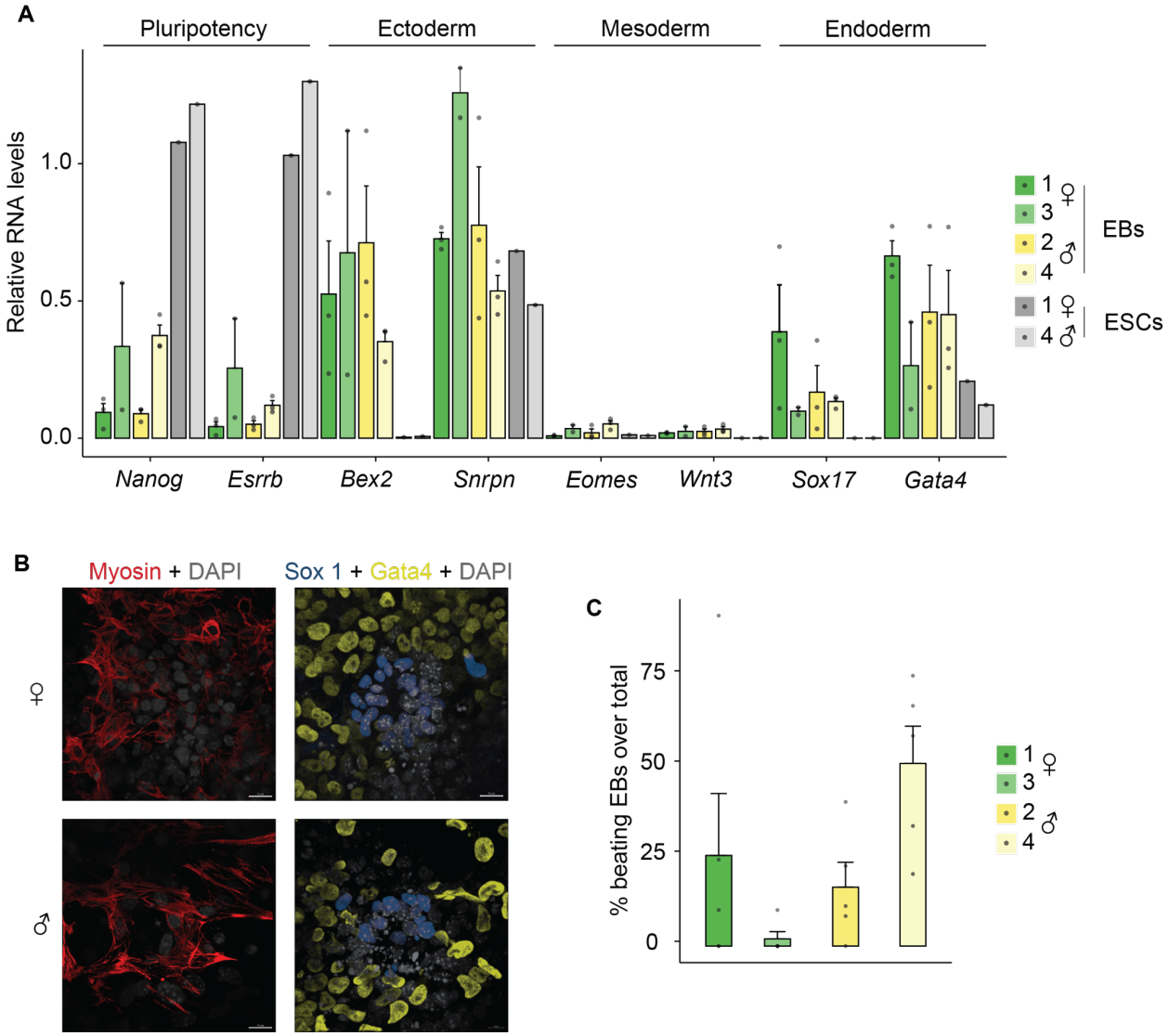

Figure 3.8. C3H/Bl6 mESCs differentiate into the three germ layers via EBs. **(A)** Bar plots showing the relative RNA levels of some genes associated with pluripotency or germ layers. Each dot represents one EB. mESCs prior to differentiation were used as controls. *TBP*, *Rplp0* and *Hprt* were used as normalization genes. **(B)** Representative merged immunofluorescence images of EBs stained with antibodies anti-myosin (mesoderm), anti-Sox1 (ectoderm) or anti-Gata4 (endoderm). **(C)** Bar plots showing the percentage of beating structures per total amount of EBs. Each dot represents one biological replicate of EB differentiation. EBs, embryoid bodies; ESCs, embryonic stem cells. Scale bar: 10 µm.

assessed the developmental potential of cells by removing the feeders and withdrawing LIF and let the cells form embryoid bodies (EBs).

EBs are cell aggregates containing progenitors cells of the three germ layers (Brickman and Serup 2017). Our consideration for successful EB differentiation was evaluated based on the appearance of beating-like structure on the plate. Female cells had a lower differentiation efficiency than males yet some beating-like structures were found (Figure 3.8c).

Pluripotency genes were downregulated in EBs while lineage-specific genes were upregulated (Figure 3.8a). Although mesodermal genes were upregulated in EBs, their expression levels were minimal compared to the other germ layers. We then immunostained EBs and found Sox1-, Myosin- and Gata4-positive cells representing the ectoderm, mesoderm and endoderm layers, respectively, which were present in all cell lines (Figure 3.9b). These pieces of evidence demonstrate that the functionality of the beating-like structure, rather than lack of myosin fibers, was impaired in the female-derived EBs. Finally, these results show that C3H/Bl6 mESCs are pluripotent and can be differentiated *in vitro* to the three germ layers.

3.4 X chromosome dynamics in hybrid C3H/Bl6 cells

Female mESCs provide a unique system to study the dynamics of XCI. mESCs are derived from the inner cell mass before random XCI occurs, therefore as their *in vivo* counterpart, females contain two X chromosomes that are transcriptionally active. This has offered an ideal system to understand the regulatory mechanisms of XCI upon cellular differentiation (Pintacuda and Cerase 2015).

3.4.1 C3H/Bl6 mESCs contain two active X chromosomes and downregulation occurs upon differentiation to epiblast-like stem cells

The process of XCI is not as stable across cell types as previously thought (J. Wang et al. 2016; Syrett et al. 2017, 2018, 2019; Sierra et al. 2023). Given that EBs may contain different cell types in which the process of XCI might not be canonical, we decided to differentiate the mESCs to epiblast-like stem cells (EpiLSCs). EpiLSCs share a transcriptome profile similar to that of post-implantation epiblast (Hayashi et al. 2011) and have been used as a system to study the dynamics of X chromosome regulation upon differentiation as they undergo XCI (Schulz et al. 2014).

We first evaluated the efficiency of differentiation of mESCs to EpiLSCs over seven days. Morphology changed from 3D round mESCs to flat EpiLSC colonies (Figure 3.9a), in agreement

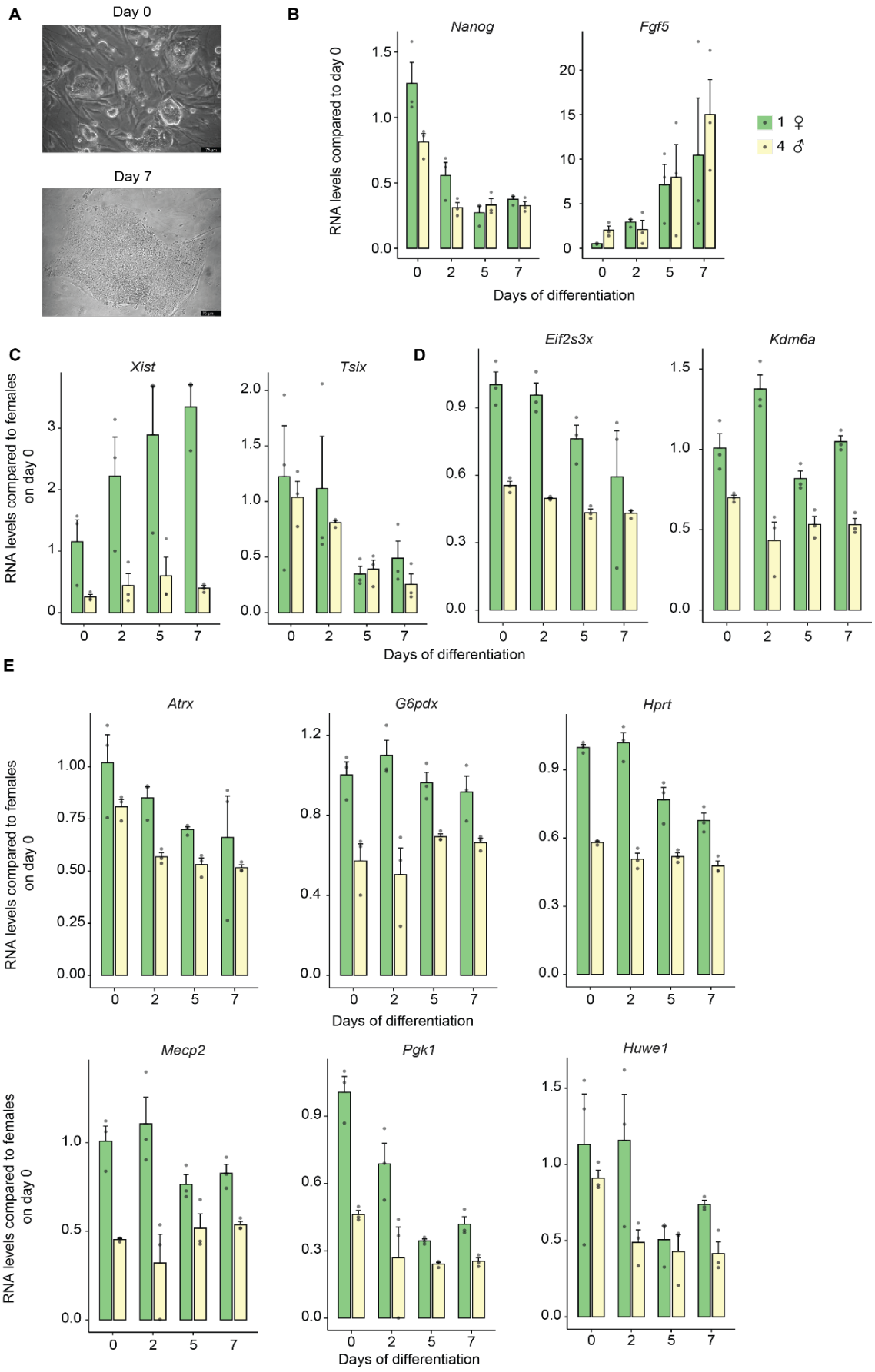
A
Day 0
Day 7
B
Nanog
Fgf5
RNA levels compared to day 0
Days of differentiation
1 ♀
4 ♂
C
Xist
Tsix
RNA levels compared to females on day 0
D
Eif2s3x
Kdm6a
Days of differentiation
E
Atrx
G6pdx
Hprt
Mecp2
Pgk1
Huwe1
RNA levels compared to females on day 0
Days of differentiation

Figure 3.9. Differentiation dynamics of C3H/Bl6 mESCs into EpiLSCs. **(A)** Representative pictures of colony morphology prior (day 0) and after differentiation (d7). Scaler bar: 75 µm. **(B)** Bar plots showing the expression levels of pluripotency (*Nanog*) or epiblast markers (*Fgf5*) over seven days of differentiation measured at four different timepoints. *TBP*, *Rplp0* and *Hprt* were used as normalization genes. Samples were further normalized to timepoint 0 of differentiation. Each dot represents one biological replicate. **(C)** Bar plots showing the expression levels of positive (*Xist*) or negative (*Tsix*) regulators of X chromosome inactivation. *TBP* and *Rplp0* were used as normalization genes. Samples were further normalized to timepoint 0 of female differentiation. Each dot represents one biological replicate. **(D)** Bar plots showing the expression levels of X-linked escapers (*Kdm6a* or *Ei2fs3x*) or **(E)** genes subjected to inactivation. *TBP* and *Rplp0* were used as normalization genes. Samples were further normalized to timepoint 0 of female differentiation. Each dot represents one biological replicate.

with previous reports (Brons et al. 2007; Sugimoto et al. 2015). Pluripotency, assessed by *Nanog* expression, was progressively lost which is in agreement with the expected expression profile (Morgani, Nichols, and Hadjantonakis 2017). Moreover, the epiblast marker *Fgf5* became upregulated over time, suggesting that mESCs transitioned into a late epiblast-like phenotype (Figure 3.9b). The master regulator of XCI, *Xist*, became upregulated in females as differentiation happened while the opposite occurred to its negative regulator, *Tsix*.

In general, X-linked genes underwent silencing given that expression was reduced (Figure 3.9c-d) but the silencing is not homogenous. Downregulation of X-linked genes was observed independently of whether they belong to the inactive class (*Atrx*, *G6pdx*, *Hprt*, *Mecp2*, *Pgk1* or *Huwe1*) (Figure 3.9e) or are known escapers (*Kdm6a* or *Ei2fs3x*) (Figure 3.9d). Only *Atrx* reached levels close to the expression in males by day 7. The escapers, *Kdm6a* and *Ei2fs3x*, also underwent inactivation as expected but the downregulation was milder. *Kdm6a* expression at day 7 of differentiation was similar to day 0 while *Ei2fs3x* expression was only downregulated by approximately 25%. These results indicate that the dynamics occurred on a gene-to-gene basis, as previously shown (Severino et al. 2022) and suggest that complete silencing of the inactive genes requires more than a week. Increased expression of some X-linked genes from the single male X was seen, however this is in agreement with previous reports (H. Lin et al. 2007; Marks et al. 2015).

3.5 Generation of X-shredder cells in female C3H/Bl6 mESCs

Having characterized our cellular system, we then moved forward with the generation of the shredder cell line. Out of the two female cell lines, we chose cell line 1 as it showed the highest developmental potential out of the two female lines. From now on, this cell line will be referred to as the female line.

3.5.1 Rosa26 targeting was not an efficient approach for cell line generation

We initially targeted the *Rosa26* loci (Figure 3.2) together with another mESC line. This is a hybrid F2 129/Bl6 background male cell line and is the one of the traditional cell lines used for *in vitro* studies. This 129/Bl6 cell line has been selected for its relatively easy genetic manipulation so we tested whether the intended targeting was possible. Treatment of the cells with tamoxifen after gene targeting and selection revealed that some colonies were green while others were not (Figure 3.10a). The gDNA of all the cells on the plate was used to optimize a PCR strategy to screen for edited *Rosa26* alleles.

Gene targeting relies on homology-mediated repair, however, the main DNA repair mechanism upon DSBs is the NHEJ pathway (Miyaoka et al. 2016). Moreover, a double dose of X-linked genes further reduces homology-mediated repair (Tamura et al. 2021). To target the *Rosa26* loci, female cells were targeted using liposome-mediated transfection with different approaches: (1) the majority of the experiments were done with the Lipofectamine™ 3000 Transfection Reagent kit (Life Technologies, L3000001); (2) in one round of transfection with that kit, the cells were also treated with inhibitors of the NHEJ pathway to increase the targeting efficiency and (3) lastly, one round of transfection was treated with the jetOPTIMUS® DNA Transfection kit (Poyplus, 101000051) which we later found to be a better reagent than the Lipofectamine™ 3000 Transfection Reagent.

In total around 1,000 colonies after transfection and puromycin selection were screened. Out of them and from the cells transfected with the jetOPTIMUS® DNA Transfection kit (Polyplus, 101000051), we found two positive colonies (Figure 3.10b): one colony had only one integration event of the shredder vector (colony A6) while the other colony had one integration event of the of *CreERT2* plasmid and one of the shredder vector (colony A11). Cells were screened while they were growing in 2i/LIF medium and the PCR fragment corresponded to the expected size (Figure 3.10b). Clone A11 was then transferred to serum/LIF medium for expansion and treatment. However, the shredder locus was already recombined in these cells as the colonies were already

fluorescent even before treatment (Figure 3.10c). The low editing efficiency of the *Rosa26* loci suggests that gene targeting, at least in a TALEN-dependent fashion and together with the C3H/Bl6 genetic background, is not straightforward.

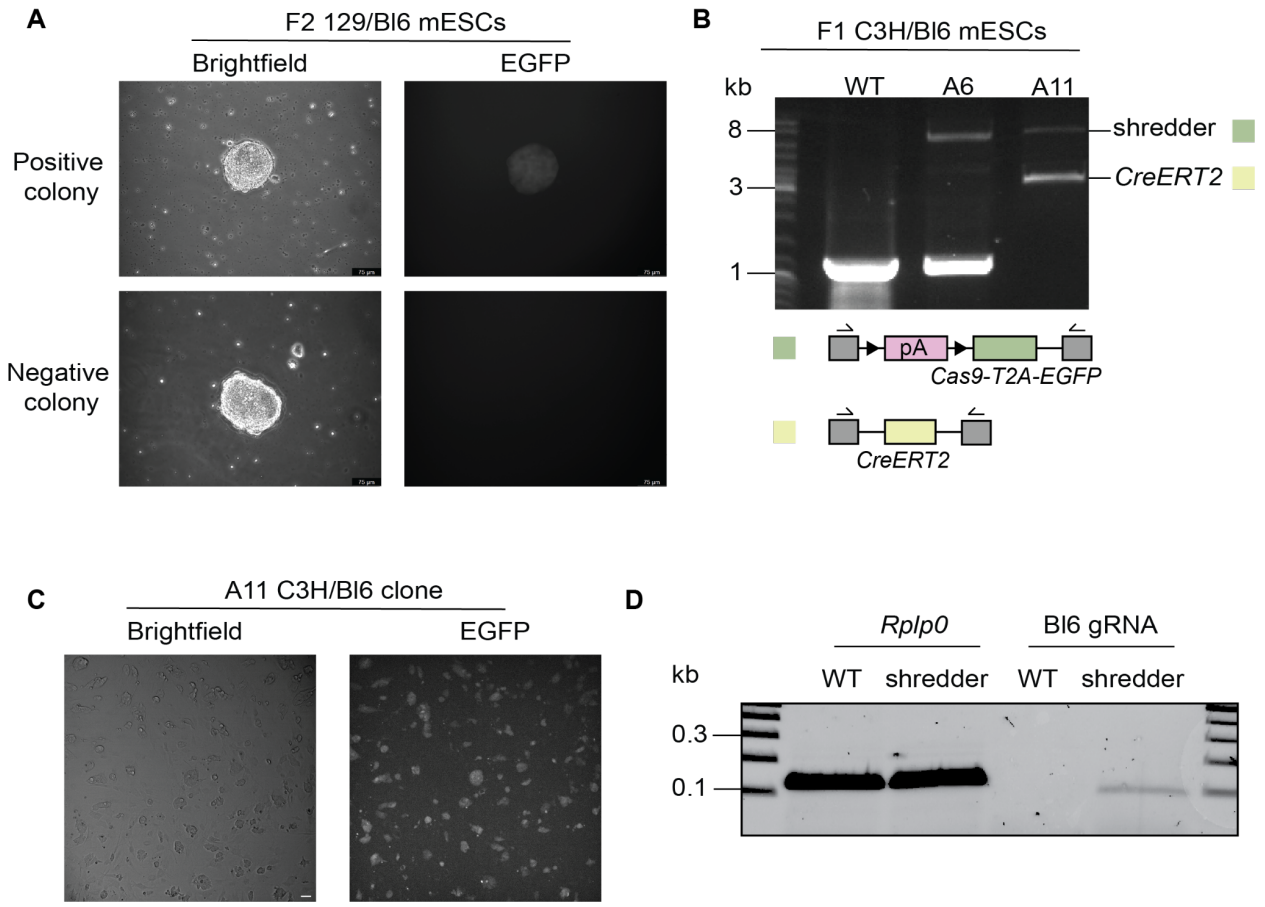

Figure 3.10. Shredder integration in mESCs. **(A-C)** *Rosa26* targeting; see Fig. 2.2; **(A)** Representative pictures of a positive or negative colony after *Rosa26* targeting and treatment with 4-hydrotamoxifen. Scaler bar: 75 µm. **(B)** Agarose gel of WT or *Rosa26*-targeted clones positive for the shredder or *CreERT2* integrations. The drawing underneath the gel picture represents the genotyping strategy where the primers (arrows) bind to *Rosa26* regions that are not present in the homology arms of the donor plasmids. **(C)** Representative pictures showing the leakiness of the shredder construct prior to 4-hydrotamoxifen addition. Scaler bar: 50 µm. **(D)** Representative agarose gel of expression of the Bl6 gRNA in the *piggyBac* shredder clone.

3.5.2 *PiggyBac* transposition

We then proceeded with the integration of the shredder construct in a *piggyBac* background (Figure 3.3). Different colonies after blasticidin selection were picked and screened for copy-number integration of the shredder cargo by qPCR. We chose a clone that had one

integration event in the genome. RT-PCR showed that the clone expressed the Bl6-specific gRNA (Figure 3.10d).

3.6 X chromosome shredding in C3H/Bl6 mESCs

3.6.1 Segmental aneuploidies of the X chromosome are the main type of aneuploidy upon X shredding

After establishing the shredder system in female cells, we needed to deliver the Cre recombinase to the cells to induce the loxP recombination of the shredder vector. We employed infection by baculovirus for its high efficiency of transduction (Mansouri and Berger 2018). The baculovirus contains the Cre recombinase coding sequence under the cytomegalovirus promoter (CMV) promoter.

Infection was performed in suspension and on 8-well µ-slide ibidi chambers because scalability to a larger format was not possible. Nevertheless, the shredder cells were infected with the baculovirus and fixed two days later after infection for DNA FISH analysis. We used two different X chromosome probes that bind to regions upstream and downstream of the gRNA targeting sites. While the cells should turn green upon induction, EGFP fluorescence was lost upon fixation and both uninfected and infected fixed cells exhibited autofluorescence when excited at the corresponding wavelength. Therefore, colonies were counted regardless of whether the shredder construct had been recombined in all cells.

In untreated female cells, two dots per probe should appear in the cells and the dots per cell and condition were counted (Figure 3.11a). Aneuploidies were classified depending on the number of probe dots. Compared to uninfected shredder or WT cells, infected shredder cells were overrepresented with segmental aneuploidies, in which one chromosomal region (respective to the gRNA targeting sites) was lost (Figure 3.11b and 3.11e). Around 25% of the aneuploid shredder cells had one X chromosome lost (Figure 3.11b and 3.11e) followed by cells with more than copies of the X chromosome. A minor aneuploidy event included micronuclei, small nucleus-derived structures associated with genomic instability (Krupina, Goginashvili, and Cleveland 2021). These structures contained either one X chromosome arm, one complete X chromosome or a chromosome region that cannot be detected with our probes (Figure 3.11d-e). These results suggest that our tool can generate X chromosome aneuploidies in which segmentation of the X chromosome, rather than whole chromosome loss, is the main type of aneuploidy. The application

of this tool using inbred mouse strains reported a similar result in which indels, rather than complete X loss, occurred (Bunting et al. 2024).

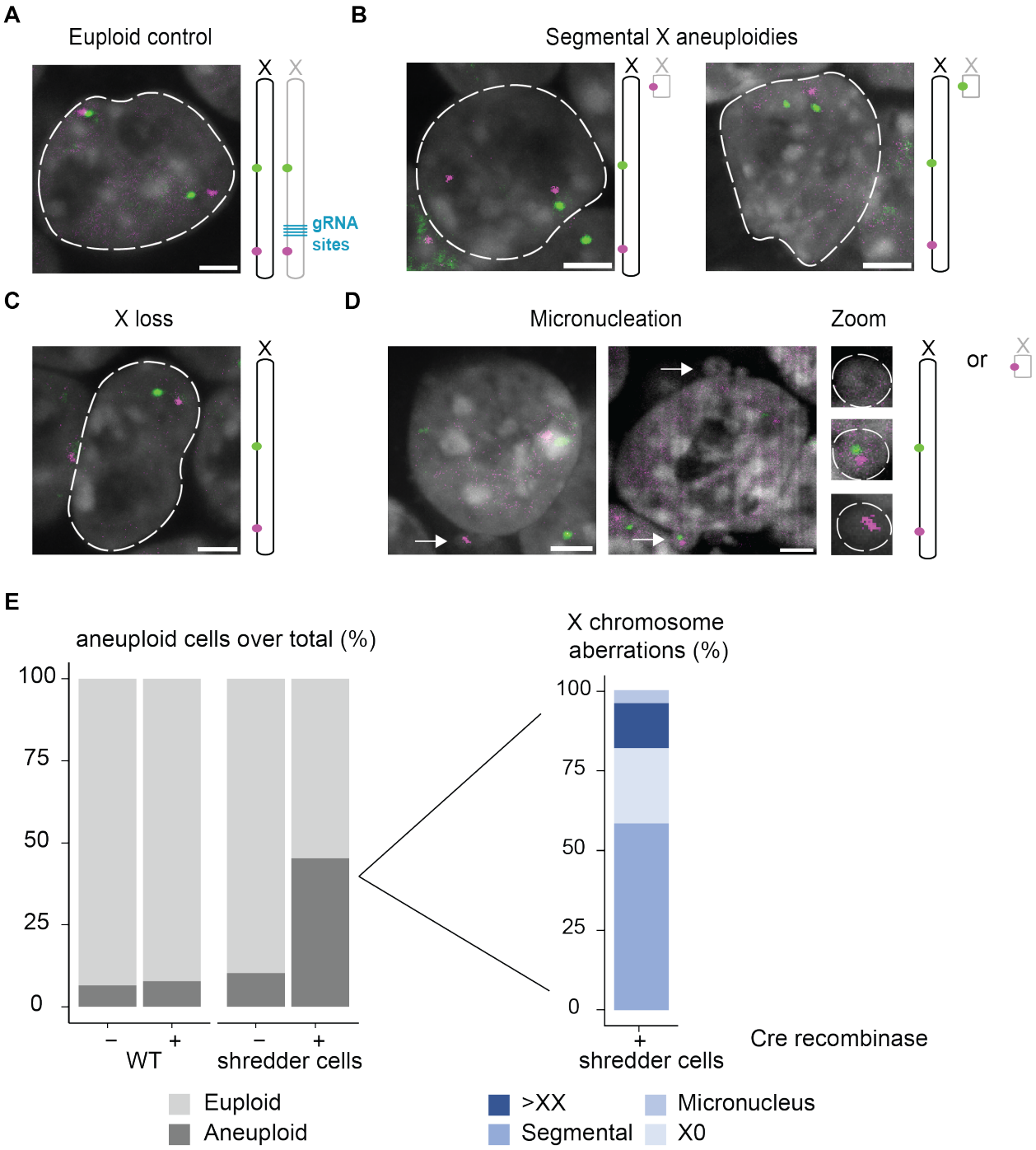

Figure 3.11. X chromosome aneuploidies occur in shredder cells. Representative microscopy images of DNA-FISH using two probes for the X chromosome with different outcomes: **(A)** euploid X cells **(B)** segmental X aneuploidies **(C)** whole X chromosome loss **(D)** Micronucleation events. The arrows depict the zoomed pictures on the right; scaler bar: 5 µm. **(E)** Stacked bar plots of counted cells after DNA FISH. The blue plots show the aneuploidy events recorded in infected shredder cells. Data obtained from two biological replicates.

4. Discussion

4.1 Characterization of hybrid mESCs for stem cell biology

4.1.1 *Bona fide* isolation of hybrid mESCs

This study reports the first successful derivation and characterization of C3H/Bl6 hybrid mESC lines, both males and females, establishing a model for studying stem cell biology, X chromosome dynamics and sex differences. As pluripotent cells, mESCs are widely used in the context of developmental biology to understand and model differentiation dynamics *in vitro* but can be also used to generate mouse models. Historically, establishing C3H/Bl6 hybrid mESCs has been considered challenging with up to 3% of success rate of either isogenic C3H strains or C3H/Bl6 hybrids. These cells had been previously maintained in a conditioned culture, that is a medium that had been used for embryonal carcinoma cell culture, resulting in its enrichment with growth factors and cytokines released by the carcinoma cells (Martin 1981). Changing to 2i/LIF medium (see definition on page 60) on a layer of feeders increases derivation of isogenic C3H mESCs by up to 90% (Czechanski et al. 2014) while isolation on feeders and serum/LIF is a process with poor efficiencies as the conditioned medium (Yagi et al. 2017). Constant culturing in 2i/LIF medium results in irreversible impaired developmental potential by widespread loss of DNA methylation, especially at imprinting regions (Choi et al. 2017; Yagi et al. 2017). We therefore decided to use serum/LIF medium together with feeders to strategically promote genomic stability, which is critical for both generating mouse models and for investigating X chromosome dosage effects without confounding chromosomal instabilities.

Out of 20 two-cell stage embryos, we obtained a 20% efficiency by deriving and stabilizing four cell lines with the expected Mendelian ratios: two males and two females. C3H/Bl6 cells were characterized to ensure that they behave as typical mESCs which is essential to validating them as a relevant biological model. The C3H/Bl6 lines demonstrated robust expression of core pluripotency factors by RNA quantification, together with immunostainings of pluripotency-related proteins (Figure 3.7). Furthermore, differentiation of mESCs and formation into EBs resulted in gene expression of the three germ layers, along with populations of cells positively stained for germ layer-specific markers (Figure 3.8). Despite parallel differentiation, female-derived EBs showed fewer beating structures than male-derived EBs, suggesting impaired functional maturation rather than inappropriate mesodermal differentiation. Intrinsic sex-biased differences

in cardiac differentiation have been reported in human iPSCs with two active X chromosomes resulting in higher efficiencies (D'Antonio-Chronowska et al. 2019) along with differential expression of cardiac-related metabolic genes (Givens et al. 2025). While our differentiation protocol is different and specific to mouse cells, they highlight that X dosage and sex-specific metabolic requirements need to be met and our culture conditions may not completely fulfill them, leading to disrupted cardiomyocyte maturation. This result also shows the importance of fine-tuning differentiation protocols, especially when working with ESC-derived cells from non-classical mouse strains.

Lastly, our hybrid cells, specifically male cell line 4, remained genomically stable at passage 25. While the female cell line that was used for establishing the shredder system has an autosomal trisomy, it aligns with well-known selection pressures in mESC cultures, particularly the frequent occurrence of an additional chromosome 8 as a culture-adapted aneuploidy (Kim et al. 2013). This is, however, counterintuitive as higher X chromosome dosage protects against the recurrent *in vitro* duplications of chromosomes 8 and 11 (Stanton et al. 2024). Analysis of earlier passages will reveal if the chromosome 8 aneuploidy was acquired, and selected for, upon passing. All in all, these results support the isolation and identity of *bona fide* hybrid C3H/Bl6 mESCs.

4.1.2 X chromosome dynamics in hybrid mESCs and EpiLSCs

We observe high stability of the X chromosome karyotype in the female lines, where a maximum of 20% of the cells lost one X chromosome by passage 26 (Figure 3.5 and 3.6). This stability is experimentally crucial when studying XCI-related mechanisms, as mixed populations of XX and X0 cells would result in confounded interpretations of gene expression and chromatin modification changes during differentiation. Although earlier works showed a tendency of spontaneous X chromosome loss in cultured female mESCs (Robertson et al. 1983; Rastan and Robertson 1985; Kawase et al. 1994; Keniry et al. 2022), the high ratio of XX cells in our mESCs hybrids is in line with reports showing that serum/LIF, paired with feeders, provides factors that allow genome stability at two different levels (Choi et al. 2017; Yagi et al. 2017; Guo et al. 2018). Feeders secrete follistatin-like 1 and bone morphogenetic protein 4 both of which activate the SMAD signaling pathway in mESCs for self-renewal and pluripotency maintenance (Hackett and Surani 2014; Guo et al. 2018). In addition, feeders activate the 2-cell stage gene *Zscan4* which promotes telomere elongation, resulting in chromosomal stability (Guo et al. 2018; Stanton et al. 2024). The hybrid background also plays an important role as they are generally more resilient

and robust than their parental inbred strains (Corder et al. 2023). This is also consistent with our results and that of others where lower rates of spontaneous X chromosome loss have been reported (Halter et al. 2024; Koshiguchi et al. 2024).

One of the major advantages of this work is that we have parallelically isolated and characterized cells of the same genetic background and different sex. As such, we can study X chromosome dynamics along differentiation in females and compare the expected gene silencing to males of the same genetic background, providing the ideal matching control. Other works have used males as control cell lines but they are usually of a closely related background and therefore not identical. For instance, in (Schulz et al. 2014) the Pgk12.1 XX and X0 cell lines were obtained from crossing a 129 female mouse with a (PGK×129) male F1 hybrid (Penny et al. 1996) whereas the male XY control was derived from an inbred 129/Ola mice. In (Y. Sun et al. 2023) the male cell lines were derived from crossing a female CAST/EiJ mouse to a male C57BL/6 mouse (the reciprocal crosses were of the same genetic background) whereas the reciprocal cross in female cell lines was derived from the cross of a female 129S1/SvImJ mouse to a male CAST/EiJ mouse. A matching genetic background is highly important as it has been reported to be a variable affecting the outcome of different experiments (Ortmann et al. 2020; Byers et al. 2022).

We further differentiated the mESCs to EpiLSCs to understand the X chromosomal dynamics in females. There are no standard ways to differentiate cells but protocols rely on chemically defined media (where the basal medium is not consistent) supplemented with cytokines to promote self-renewal. Fgf is present consistently with concentrations varying depending on the presence of feeders, while activin A is only supplemented in feeder-free conditions (Johansson and Wiles 1995; Chenoweth and Tesar 2010; Sugimoto et al. 2015). C3H/Bl6 only survived differentiation when cultured with DMEM/F12 and on a layer of feeders. Differentiation of mESCs to EpiLSCs over seven days resulted in the expected morphological shift of cell colonies, alongside loss of pluripotency by downregulation of the core factor *Nanog* with upregulation of the epiblast marker *Fgf5* (Figure 3.9). These results indicate a faithful transition to the post-implantation epiblast state in which random XCI should initiate. We recapitulated the canonical XCI process in female EpiLSCs to some extent: we observed clear and constant upregulation of the master regulator *Xist*, concomitant with decreased expression of its antisense regulator *Tsix* (Figure 3.9). Five (*Eif2s3x*, *G6pdx*, *Hprt*, *Mecp2* and *Pgk1*) out of the eight X-linked genes tested here had almost a double dose of expression prior to differentiation which supports the two active X chromosomes model in mESCs (Lentini et al. 2022). Silencing over the seven days of differentiation followed a heterogenous but progressive

kinetics. In differentiated cells, expression levels of monoallelic genes is expected to be similar between the sexes (Lentini et al. 2022). However, after seven days of differentiation, the levels of monoallelic genes (*Atrx*, *Hprt*, *Pgk1*) were still higher in females suggesting that fine-tuning of dosage compensation in this specific background requires more than a week. Complete optimization of EpiLSC differentiation, including RNA FISH of *Xist* and monoallelic genes to determine gene silencing over time, together with H3K27me3 staining, is needed to establish the C3H/Bl6 mESCs as a tractable *in vitro* model to dissect the underlying mechanisms of XCI initiation and propagation.

The notion of a burst of X-linked gene expression in males along differentiation, while it can be initially counterintuitive, is consistent with previous reports describing X chromosome upregulation as a compensatory mechanism in males, both in EBs and EpiLSCs (Lin et al. 2007; Marks et al. 2015). This underscores the complex regulatory landscape of X chromosome dosage control, which extends beyond simple gene silencing in females to include active regulatory processes in both sexes. Upregulation of the single X chromosome in males is an evolutionary adaptation to correct the X-to-autosome dosage imbalance posed by the degeneration of the Y chromosome during sex chromosome evolution, a theory initially proposed by (Ohno 1967). Indeed, tuning of the X chromosome expression by upregulation also takes place in the single male X (Lentini et al. 2022; Naik et al. 2022; Allsop et al. 2025) and is consistent with increased X-linked gene expression during EpiLSC differentiation in C3H/Bl6 males.

An important aspect of female mESCs undergoing differentiation is which X chromosome will be transcriptionally silenced. While we indeed reported X-linked gene silencing (Figure 3.9), we do not know if the X^{C3H} and X^{Bl6} alleles were equally chosen for inactivation, but this is important to determine for various reasons. As discussed in page 25, in WT conditions either allele has a 50% chance of inactivation but allele-specific deletion of *Xist* in CAST/EiJ×C57BL/6 hybrid cells (Pacini et al. 2021), as well as doxycycline-mediated $Bl6^{Xist}$ expression in the same cells have been used to induce skewed XCI (Schulz et al. 2014). Moreover, structural variations in the XIC exist resulting in alleles with varying functionality degrees in the different mouse species, whether they are wild or laboratory-adapted strains (Calaway et al. 2013). This is exemplified by skewed XCI towards the X^{Bl6} allele in hybrid C57BL/6×CAST/EiJ mESCs (Pacini et al. 2021) as a result of different XIC alleles (Plenge et al. 2000; Chadwick et al. 2006). Our allele-specific gRNA brings Cas9 to the X^{Bl6} allele, therefore if skewing in our cells towards the C3H allele occurs, our system will then induce aneuploidies in the Bl6 active X. Given that we are interested in the age-dependent mosaicism of the inactive X, deleting *Xist* in the C3H allele would

need to be done prior to differentiation as this will result in skewed XCI towards the Bl6 allele. To estimate X chromosome silencing, amplification of monoallelic transcripts (such as *Pgk1* and *Hprt*) in EpiLSCs, coupled to Sanger sequencing and accounting for the polymorphisms between the C3H and Bl6 genomes, will allow the identification of the active and inactive X. Complementary to this experiment, amplification of the *Xist* transcript can also be used and will reveal which X chromosome, and consequently the inactive X, is expressing the master regulator of XCI.

4.2 Genetic engineering of hybrid mESCs

4.2.1 Gene targeting in C3H/Bl6 mESCs

Generating genetically engineered cell lines in the C3H/Bl6 background was an important goal in my work. The C3H/Bl6 hybrid background had not been previously used in gene editing applications. Additionally, gene editing for *in vitro* studies with mESCs relies on a well-established mixed F2 129Tr/Bl6 (male) cell line (Bibel et al. 2004). To study XCI, mESCs with allele-specific deletion or upregulation of *Xist* in the CAST/EiJ×C57BL/6 hybrid cells (see previous paragraph) were obtained by electroporation (Wutz et al. 2002; Pacini et al. 2021). We attempted to target the *Rosa26* locus and introduce the shredder system directly to female C3H/Bl6 cells, which brought upon several barriers specific to this genetic background. We found that TALEN-mediated gene targeting in hybrid C3H/Bl6 is intrinsically hard to achieve as we only found two positive colonies out of 1,000 screened ones. While the genetic background can play a role in editing efficiency, the nature of genome targeting itself could have been limited by the presence of four plasmids that needed to be present in the same cell. Treatment with puromycin was used as a selection marker for *Rosa26* targeting, however resistance to puromycin can occur in the absence of the resistance cassette. Similar to our puromycin selection strategy (Fig 3.2), EGFP fluorescence has also been used as reporter strategy and in this case, colony picking or sorting based on green signal can be used to narrow down the number of colonies to screen. Isolation of the resistant colonies and RT-qPCR specific to the TALENs sequence will inform about the presence and expression of both nucleases. After that, the identification and presence of insertion and deletions by PCR and Sanger sequencing of the *Rosa26* locus is expected. The presence of the integration plasmids can be screened by primer-specific PCR.

Liposome-mediated transfection is a commonly used method for gene delivery in mESCs and we found that the reagent used greatly affects efficiency. Lipofectamine™ 3000 Transfection Reagent kit is a liposome-generating reagent widely used for transfection. This kit had low

efficiency rates in the C3H/Bl6 hybrids and no properly edited clones were found. On the other hand, liposome-mediated transfection with the jetOPTIMUS® DNA Transfection kit, resulted in less puromycin-resistant colonies but there were two positive clones with the plasmids of interest integrated. In epithelial cells, jetOPTIMUS® outperformed Lipofectamine™ 3000 at the cost of cell viability (Guo et al. 2025) and similar transfection efficiencies were reported in hard-to-transfect cells (Cocchiararo et al. 2022). The actual composition of the jetOPTIMUS® buffer is not provided but it is chemically defined and compatible with serum-containing medium, unlike Lipofectamine™ 3000 in which reduced-serum medium is usually recommended. These results suggest that, at least in the conditions tested by us, the jetOPTIMUS® DNA Transfection kit is a better choice for the generation of cell lines in C3H/Bl6 hybrids. Delivery efficiency of the vector can be increased by electroporation, which has allowed the generation of genome edited female mESCs (Wutz et al. 2002; Pacini et al. 2021).

TALEN proteins work by binding to DNA via repeats and cleaving the target sequence by the FokI endonuclease. Each repeat has a repeat-variable di-residue region, a two-amino acid residue that recognizes one nucleotide in the target DNA sequence. Therefore, when targeting, for example, a 20-bp sequence, 20 repeats are needed. Unlike the PAM recognition sequence needed by Cas9 for targeting, TALENs do not need any PAM-like locus and can virtually target any region of interest. However, efficiency highly depends on specific combinations of repeat-variable di-residues (Becker and Boch 2021). As such, the choice of repeat-variable di-residues is limited when DSBs at specific locations are needed, which can bring down targeting efficiencies. In addition, the TALEN-mediated approach employed here may be inherently less efficient than alternative nuclease platforms for this genetic background.

Another layer of regulation for cell line engineering is the DNA damage repair pathway. DSBs, of either CRISPR or TALENs origin, are mainly repaired via NHEJ over HDR (Davis and Chen 2013). This is a drawback for gene targeting approaches where repair templates containing desired gene-edits of choice are intended to be introduced by HDR. Attempts at increasing HDR have been described employing inhibition of factors involved in the NHEJ pathway (Arai and Nakao 2021; Wimberger et al. 2023). While we similarly attempted to increase HDR by chemically inhibiting the autosomal proteins DNA-dependent protein-kinase catalytic subunit together with the DNA polymerase theta, this did not increase the editing efficiency in the single experiment performed in our C3H/Bl6 cells. Possibly the concentrations and/or timings were not enough to limit the proteins' activity; these experiments were also performed with the Lipofectamine™ 3000

Transfection Reagent kit. This suggests that a prior optimization of inhibition is needed to check if the protein levels of the targeted proteins is reduced.

Lastly, sex differences can also be part of the low transfection efficiencies. As shown by (Tamura et al. 2021) a double dosage of X-linked DNA repair genes promoting NHEJ in females drastically reduces successful targeting. Increased efficiency is met upon XCI reaching similar levels to that of males (Tamura et al. 2021). Here we targeted the *Rosa26* locus only in female mESCs and the double dose of X-linked genes might have brought down the efficiency of HDR. Considering that EpiLSCs can be reverted back to mESCs a few days after differentiation, gene targeting in cells where transcriptional shutdown of the X is happening would be one option to increase gene targeting efficiency. Besides chemically inhibiting the autosomal NHEJ proteins, temporal and partial inhibition of X-linked gene repair genes (Tamura et al. 2021) in mESCs via RNA interference a few days prior to gene editing, together with assessment of decreased protein levels by western blot, could enhance targeting efficiency.

Taken together, my observations reinforce the notion that in a female hybrid background, gene targeting by the conditions tested here is not a straightforward route for generating engineered cell lines and further optimization is needed to enhance gene targeting efficiency.

4.2.2 Vector transposition in C3H/Bl6 mESCs

The implementation of the *piggyBac* transposon-mediated integration provided an alternative solution to bypass the multifactorial hurdles encountered with the *Rosa26* targeting. Contrary to the *Rosa26* targeting, transposition of the *piggyBac* vector relied on transfecting the cargo (shredder) vector and the transposase to cut-and-paste the cargo into a sequence-specific location (Fig. 3.3). Those two vectors were transfected using Lipofectamine™ 3000 and only one colony was positive for integration of the cargo into the genome of the female C3H/Bl6 cells. Despite obtaining one positive colony, the *piggyBac* transposition rather than site-specific integration also has important caveats. Unlike the *Rosa26* locus, which provides moderate expression levels across tissues, the *piggyBac* shredder backbone integrated semi-randomly at a 5'-TTAA-3' sequence somewhere in the mouse genome. We did not map the insertion site of the shredder vector, yet derived clones could be subjected to position effect. In addition, the *piggyBac* shredder construct also depended on transient Cre delivery for temporal loxP site recombination and system induction.

Due to time constraints, we attempted to provide a proof-of-concept for the transient induction and expression of the shredder construct targeting the X^{Bl6} allele. Thus, we chose to use a commercially available baculovirus to deliver the Cre recombinase sequence. Infection with baculovirus results in high infection rates and do not replicate nor integrate into the host genome (Mansouri and Berger 2018). While this served as a proof-of-concept showing the generation of X chromosome aneuploidies (see next section), this system also has some limitations to overcome for future experiments. The commercial construct expresses the Cre recombinase under the CMV promoter which can only be used for short-term expression in mESCs as it gets rapidly silenced. In the long run another viral system would be advantageous, such an adeno-associated virus system. As preliminary work, I tested several adeno-associated viruses, which however did not result in high transduction efficiencies. Lentiviruses can also be used and although lentiviruses are biosafety level 2 and integrate into the host genome, they have high infection rates and approaches to develop non-integrating viruses exist (Dong and Kantor 2021). Thus, I would propose to move forward with a lentivirus approach where delivery of the Cre recombinase sequence together with a selection marker (e.g., dsRED expression) can potentially allow us to focus only on infected cells. The addition of a dsRED-only expressing adenovirus is also needed to account for possible cellular consequences, as well as infection responses, raised by the virus. Alternatively, the cell-permeant TAT-NLS-Cre recombinase could be useful. In this setup, the recombinase is fused with the basic TAT peptide from the human immunodeficiency virus to allow it to cross the cell membrane (Schwarze et al. 1999), along with a nuclear localization signal to specifically target the nucleus compartment (Peitz et al. 2002). This approach has been previously used in mESCs, where loxP site recombination occurred in about 90% of the cells at a concentration of 1-2 μM of TAT-NLS-Cre (Peitz et al. 2002).

4.3 X chromosome aneuploidies in mouse embryonic stem cells

Despite the challenges of generating the shredder cell line and Cre recombinase delivery to those cells, we evaluated the consequences of targeting and shredding of the X chromosome by DNA FISH. The cells should turn green after Cre recombinase expression, however EGFP fluorescence was lost upon fixation and cells exhibited autofluorescence when excited at the corresponding wavelength. Therefore, colonies were counted regardless of whether the shredder construct had been recombined in all cells.

Almost 50% of the total counted cells had an X chromosome aneuploidy, results consistent with *in vivo* X shredding using the same gRNA in isogenic inbred mouse zygotes (Zuo et al. 2017).

The aneuploid cells were further classified into the type of aneuploidy they had. Given the increasing rates of LOX upon female aging (Abruzzo et al. 1985; Machiela et al. 2016; Liu et al. 2023), we were interested in generating whole chromosome losses. One round of cell cycle in mESCs cultured in serum/LIF takes approximately 12 hours (Stead et al. 2002; Kolodziejczyk et al. 2015) and baculoviruses delay the cell cycle of the host they infect (Rohrmann 2019). While cells were fixed for analysis two days after infection, we estimate that the fixation was performed two cell cycles after infection. By DNA FISH we found that segmental X chromosome aneuploidies—partial loss of chromosomal regions that are relative to the gRNA targeting sites—constituted the predominant outcome of the shredding system. LOX represented the second most abundant aneuploidy with a frequency of 25%, followed by supernumerary X chromosomes (Figure 3.11). About 5% of the events accounted for a micronucleus, of which half of them contained either a piece of the X or the whole chromosome and the remaining half were not positive for any of the probes used. Previously, centromere staining of the X chromosome in female peripheral lymphocytes showed that 40-60% of the micronuclei contain an X chromosome (Tucker et al. 1996), suggesting that the LOX in peripheral lymphocytes may result in micronucleation. The fact that half of the micronuclei were not positive for the X does not mean that the X is not present. The probes upstream of the gRNA sites are of 100-200 bp spanning a total of 185 kilobases while the probes downstream span 195 kilobases. It is plausible that the DNA piece(s) present in the micronuclei correspond to regions that do not span any of the DNA FISH probes used herein. Whole chromosome painting will provide information if those micronuclei contain any X chromosome fragment. In addition, purification and sequencing of these structures by flow cytometry (Toufektchan and Maciejowski 2021) will reveal which specific region(s) of the X the micronuclei contain. It will also inform us whether those pieces have undergone chromothripsis, that is, fragmentation and rearrangement of the missegregated locus (Kwon et al. 2020). Along the same line, whether the missing piece in segmental aneuploidies was completely lost or underwent chromothripsis and remained in the primary nucleus is unclear; whole genome sequence can reveal if this is the case.

The mechanistic basis for the outcome of segmental aneuploidies in our shredder system can be attributed to different causes. First, our results differ from X chromosome targeting in zygotes. Microinjection of the same gRNA used in this work in zygotes, followed by transfer to pseudopregnant female donors one cell cycle later resulted in almost 43% of X0 mice (Zuo et al. 2017). The zygotes used are isogenic and thus both X chromosomes are targeted, which can generate an extensive DNA damage response. In this sense, it is likely that one X chromosome

is preferentially lost while the other is efficiently repaired and kept. Indeed, in some cells, insertions and deletion occurred in the remaining X chromosome (Zuo et al. 2017). Second, as previously mentioned, hybrids are more resilient than the parental strains (Corder et al. 2023) and in this sense, they could have better mechanisms at repairing DSBs without the pressure for preferential chromosome loss. For instance, the untargeted allele could serve as a template for repairing the targeted X chromosome. Third, female mESCs have two active X chromosomes and genes involved in NHEJ are more abundant in mESCs (Tamura et al. 2021), rather than in differentiated cells. Therefore, higher DNA damage repair pathways in mESCs could provide an additional mechanism for resecting the DSBs after shredding, leading to segmental aneuploidies rather than LOX. Targeting the single X chromosome in males should prove or refute this theory expecting an increased number of cells with X chromosome aneuploidies or cell death in whole chromosome loss. However, this experiment cannot be performed in our C3H/Bl6 mESCs given that the X chromosome in these male cells, the X chromosome is inherited from the female C3H/HeJ mouse, and our gRNA targets the X^{Bl6} allele. Cells isolated from a reciprocal cross, in which a female C57BL/6 mouse is mated with a male C3H/HeJ mouse (and therefore, the X chromosome is provided by the female mouse), can be used for this experiment. Finally, the gRNA recognizes approximately 67 sites spanning 2.1 Mb on the end of the X chromosome. Since the gRNAs are not distributed along the X chromosome, it is highly plausible that the chromosome arm downstream of the gRNA sites will have a higher likelihood of being lost. A fourth insight is the role of p53. As a tumor suppressor, p53 is activated upon DNA damage and ensures that aneuploid cells do not proliferate either by inducing senescence, cell cycle arrest or apoptosis. In fact, many reports knock out *TP53* prior to inducing chromosome missegregation to select for aneuploid cells. While we are not directly generating whole chromosome losses, it is likely that the DNA damage induced by CRISPR activates p53 for end resectioning and DSB repair leading to segmental aneuploidies.

5. Conclusions and future perspectives

5.1 Conclusions

In this work, we have described the first successful derivation and characterization of C3H/Bl6 male and female hybrid mESC lines. These cells can be exploited to model stem cell biology, X chromosome dynamics and sex differences. We have also reported the generation of plasmids for the inducible Cas9-mediated chromosome targeting and shredding in C3H/Bl6 cells. We used this system to target the X^{Bl6} allele, while leaving the X^{C3H} copy intact, to generate X chromosome aneuploidies that are relevant in the context of aging. One of the biggest advantages of our cells is the fact that they are hybrid. Consequently, their polymorphisms allow the targeting and shredding of only one parental allele of any chromosome in the C3H/Bl6 genome.

We established the inducible system in the female hybrids cells and generated shredder cells. Inducibility by baculovirus-mediated Cre recombinase delivery, we showed that our system is able to generate X chromosome aneuploidies. While we are interested in whole chromosome loss, we found that segmentation of the X chromosome was the predominant outcome with some cells undergoing LOX.

5.2 Future perspectives

The main optimization still required is to increase the number of cells with complete LOX. Chemical inhibition of DNA repair pathways has been shown to increase whole chromosome aneuploidies (Zuo et al. 2017), hence this approach can be useful after Cre delivery in the shredder cells. Alternatively, a second gRNA, closer to the centromere (Zuo et al. 2017), can be cloned into the shredder vector to increase the likelihood of whole chromosome loss. For *in vitro* studies, the shredder cells can be further transfected with a *piggyBac* vector encoding Cre-ERT2. In this scenario, supplementation of 4-hydrotamoxifen should be sufficient to induce the system, overcoming Cre delivery in each experiment. On the other hand, for *in vivo* studies, shredder cells can be transferred back to an embryo for the generation of a mouse shredder model. Crossing this shredder mouse to tissue-specific Cre-ERT2 models will allow the expression of the shredder construct in a cell type-specific manner upon 4-hydrotamoxifen feeding. For both approaches,

generating a non-shredder system (cells with the shredder without X targeting gRNA) is the essential comparison control.

In vitro experiments using the shredder cells can provide several answers to LOX. Ideally, these experiments would need to be performed in HSCs, where LOX has been reported and although protocols for *in vitro* differentiation of mESCs to HSCs have been reported (Gordon-Keylock et al. 2010), they need to be adapted to C3H/Bl6 hybrids. Instead, these experiments could be performed in EpiLSCs with the X^{Bl6} allele inactive to be as close to the *in vivo* phenotype as possible. An important question is whether female cells are able to sense X chromosome dosage upon LOX and restore expression levels to WT levels. Reactivation of the inactive X is a well-established aging phenomenon (Hoelzl et al. 2025) but decreased X expression after LOX has not been shown. Targeting the inactive X, followed by RNA sequencing at different timepoints, will reveal if the X-to-autosome transcriptional output is maintained or decreases. If the latter occurs, the consequences of LOX can be attributed to X chromosome haploinsufficiency.

A second point to address is selection of aneuploid cells. Given the increasing frequencies of LOX during female aging (Abruzzo et al. 1985; Machiela et al. 2016; Liu et al. 2023), it is expected that this aneuploidy confers a selective proliferative advantage. To test this hypothesis, one would need to count the number of EGFP+ cells in shredder and control cells two to four cell cycles after system induction. The number of cell cycles is chosen based on previously reported Y chromosome loss dynamics (Ly et al. 2017), where one cycle after chromosome shredding results in LOY. If expansion of X0 cells relative to XX occurs, it would suggest that LOX confers a proliferative advantage to X0 cells, mimicking the clonal expansion seen in aging. What factors are involved in this selection is unknown, but it has been previously shown that increased expression of DNA repair genes, together with mitotic DNA synthesis, allows aneuploid cells to proliferate (Garribba et al. 2023).

Whether LOX is a cause or consequence of aging is an important question to answer. The X is the chromosomal home to immune genes (Bost et al. 2022) and haploinsufficiency of escapers can lead to disease. With the mouse shredder model, elimination of the X chromosome in HSCs would result in aneuploid X0. If this aneuploidy triggers aging, the mouse model, compared to the control mice, should present a faster pro-inflammatory phenotype (measured by increased markers of inflammation and/or immune X0 cells involved in this process), accompanied with an autoimmunity-like state (by the identification of autoantibodies) or leukemia (Sopena-Rios et al. 2024). Inflammaging has an earlier onset in males. Whether the delay in

female inflammaging requires a threshold to exert in a phenotype is unclear. Co-culturing different amounts of isolated macrophages with LOX from the mouse model with XX fibroblasts and monitoring senescence or secretion of pro-inflammatory cytokines over time will reveal if this is the case.

Finally, using the shredder mouse model to understand organismic aging is a great tool. HSC-derived cell types are virtually present throughout the body and their misregulation can affect different parts of an organism. LOY in male mice results in earlier cardiac malfunction and fibrosis (Sano et al. 2022). How HSCs will react to LOX can directly link X chromosome aneuploidy to leaukemia (Zekavat et al. 2020; Lin et al. 2021).

Understanding how aging affect each sex is an important need for the upcoming years. More research will lay the foundation for the generation of therapies that will enable equal treatment between males and females.

6. Materials

6.1 Devices

Table 1. Devices used in this work

Devices	Manufacturer	Catalogue Number
Balance	Sartorius	ED822-0CE
Biological Safety Cabinets	Dometic	BSC-SG403 N
Centrifuge	Eppendorf	5427 R
Centrifuge	Thermo Scientific	Heraeus Multifuge X3
ChemiDoc™ Touch Gel Imaging System	Bio-Rad	
Color Sprout Plus Mini Centrifuge	Biozym	552031
Concentrator Plus	Eppendorf	5305000703
DS-11 FX+ Spectrophotometer/Fluorometer	DeNovix	DS-11 FX+
DynaMag™-2 Magnet	Thermo	12321D
Forma™ Steri-Cult™ CO2 Incubator, 232L	Thermo Scientific	3308
Freezer (-20)	Liebherr	LIE-LGex3410
Freezer (-80)	Sanyo	MDF-U74V
Fridge (4°C)	Liebherr	LIE-FKex3600-20
Fume Hood	Wesemann Laboreinrichtungen	Delta System 30
LightCycler 480 System	Roche	5015243001
Microwave	Samsung	MS8F303TAS
MinION sequencer	Oxford Nanopore Technologies	MN24510
Multipette® E3x	Eppendorf	4987000029
Objective	Leica Microsystems	10450167
Pellet Mixer	VWR	431-0100

Pico™ 21 Microcentrifuge	Thermo Fisher	75002475
PIPETBOY acu	Integra	612-0928
Pipette (10 µL)	Eppendorf	3125000010
Pipette (2.5 µL)	Eppendorf	123000012
Pipette (20 µL)	Eppendorf	3123000039
Pipette (200 µL)	Eppendorf	3123000055
Pipettes (1000 µL)	Eppendorf	3123000063
PowerPac™ Basic Power Supply	Bio-Rad	1645050
Rotator Test Tube Rotator	Kisker Biotech Gmbh	Test Tube Rotator
ThermoMixer	Eppendorf® ThermoStat C	EP5383000035
Tissue Culture Coverslips 13 mm (Plastic)	Starstedt	83.1840.002
Transmitted Light Base	Leica Microsystems	TL5000
VisiScope 5 Elements Fluorescence Spinning Disc confocal microscope	Visitron Systems	
Vortex Genie 2	Scientific Industries	P505.1
HC PL APO CS2 100x/1.4 NA oil-immersion objective	Leica Microsystems	11506372

6.2 Consumables

Table 2. Consumables used in this work.

Consumables	Manufacturer	Catalogue Number
6-well plate	Sarstedt	83.392
12-well plate	Sarstedt	83.3921
24-well plate	Sarstedt	83.3922
48-well plate	Falcon	353078
96-well plate	Sarstedt	83.3924
Bacteria Tubes	Sarstedt	62.515.006

Bottle Top Filter 500 mL	Fisher Scientific	FB12566510
Cell Culture Dish 35-mm	Greiner	627160
Cell Culture Dish 60-mm	Falcon	353004
Cell Culture Dish 100-mm	Falcon	353003
Cell Culture Dish 150-mm	Falcon	353025
Combitips (0.1 mL)	Eppendorf	0030089405
Combitips (0.2 mL)	Eppendorf	0030089626
Combitips (0.5 mL)	Eppendorf	0030089421
Combitips (1 mL)	Eppendorf	0030089430
Combitips (5 mL)	Eppendorf	0030089456
Combitips (10 mL)	Eppendorf	0030089464
Cryovials (1.8 mL)	Sarstedt	72.397.992
Dressing tissue forceps	Merck	F4267
Falcon™ Round-Bottom Polystyrene Test Tubes	Fisher Scientific	10186360
Filter tips (2.5 µL)	Starlab	S1121-2710
Filter tips (200 µL)	Starlab	S1120-8710
Filter tips (1000 µL)	Starlab	S1122-1730
Filter tips low retention (2.5 µL)	Sarstedt	703.010.285
Filter tips low retention (200 µL)	Sarstedt	703.031.275
Filter tips low retention (1000 µL)	Sarstedt	703.050.375
Ibidi µ-slide 8-well chamber	Ibidi	80806
LB plates	IMB Media Lab	L-20_P
LightCycler® 480 Multiwell Plate 384, white	Roche	04 729 749 001
LightCycler® 480 sealing foil	Roche	04 729 757 001
Luer-Lock Syringe	BD Plastipak	300865

PCR Tube, Flat Cap 0.2 mL	Starlab	I1402-8100
PCR Tubes, with Flat Caps, 0.2 mL 8-Strip	Starlab	I1402-3700
Pipette tips (for agarose-TBE-gels)	Sarstedt	703.03
SafeSeal Tube (1.5 mL)	Sarstedt	72.706
SafeSeal Tube (2 mL)	Sarstedt	72.695.500
Screw Cap Tube (15 mL)	Sarstedt	62.554.502
Screw Cap Tube (50 mL)	Sarstedt	62.547.254
Serological pipette (5 mL)	Corning	CLS4487
Serological pipette (10 mL)	Corning	CLS4488
Serological pipette (25 mL)	Corning	CLS4489
Serological pipette (50 mL)	Corning	CLS4490
Syringe filter 0.2 µm	Starlab	83.1826.001
Tips (10 µL)	Starlab	S1111-3210
Tips (200 µL)	Starlab	S1111-1716
Tips (1000 µL)	Starlab	S1111-8701

6.3 Chemicals, inhibitors, antibiotics and enzymes

Table 3. Chemicals, inhibitors, antibiotics and enzymes used in this work.

Chemicals, inhibitors and antibiotics	Company	Catalogue Number
Accutase	Sigma Aldrich	A6964-100ML
Agarose	Sigma Aldrich	cas 9012 366
Alexa Flour 555-aha-dUTP	Thermo Fisher	A32763
Alexa Flour 647-aha-dUTP	Invitrogen	10654193
Ampicillin	IMB Media Lab	A-10_A
AscI	NEB	R0558L

Attachment Factor Protein 1×	Thermo Scientific	S006100
AZD-7648	MedChemExpress	HY-111783
BbsI-HF	NEB	R3539S
Blasticidin	Thermo Fisher	J67216.XF
CHIR99021	Axon Medchem	1386
Chloramphenicol	IMB Media Lab	n.a.
DAPI (4',6-Diamidin-2-phenylindol, Dihydrochlorid)	Invitrogen	10184322
Dextran sulfate	Sigma Aldrich	67578-5G
Dimethylsulfoxide (DMSO)	Sigma Aldrich	D8418-100ML
DL-Dithiothreitol (DTT)	Sigma Aldrich	D0632-25G
DMEM, high glucose, no glutamine	Gibco	11960044
DMEM/F-12 GlutaMAX	Life Technologies	10565018
DNA ladder	Thermo Fisher	SM0331
dNTP mix	NEB	N0447S
DPBS, calcium, magnesium	Gibco	14040117
Dulbeccos's Phosphate Buffered Saline	Sigma Aldrich	D8662
EDTA (0.5 M, pH 8)	IMB	
EmbryoMax® Acidic Tyrode's Solution	Millipore	MR-004-D
EmbryoMax® Filtered Light Mineral Oil	Sigma Aldrich	ES-005-C
EmbryoMax® KSOM Mouse Embryo Media	Millipore	637429
EmbryoMax® M2 Medium	Sigma Aldrich	MR-015-D
EmbryoMax® 2-Mercaptoethanol (100×)	Sigma Aldrich	ES-007-E
Ethanol 100%	Thermo Fisher	10342652
FastStart Universal SYBR Green Master	Roche	4913914001
Fetal Bovine Serum (fibroblasts)	Gibco	A5256701
Fetal Bovine Serum (mESCs)	Life Technologies	10270106
FGF2	IMB	n.a.
Gelatin	Sigma Aldrich	G1890
Gibson Assembly 2× MasterMix	IMB Protein Production	n.a.

GlutaMAX™ Supplement 100×	Gibco	35050061
Glycerol	Sigma Aldrich	G5516
Green Taq buffer (5×)	IMB Protein Production	n.a.
HCl, 32%	Merck	1.00319.1000
Insulin	Sigma Aldrich	I0516
KnockOut DMEM	Life Technologies	10829018
KnockOut Serum Replacement	Life Technologies	10828028
LB agar	IMB Media Lab	L-12_M
LB without Antibiotics	IMB Media Lab	L-10_M
LB plates supplemented with ampicillin	IMB Media Lab	L-20_P
Leukaemia inhibitor factor	Sigma Aldrich	ESG1107
Mitomycin	Fisher Scientific	226940020
NEB® 10-Beta Competent *E. coli* (High Efficiency)	NEB	C3019H
NheI	NEB	R3131S
Non-essential Amino Acids (NEAA) 100x	Gibco	11140050
Novobiocin	MedChemExpress	HY-B0425A
Nuclease-Free Water	Qiagen	129115
Opti-MEM™	Gibco	31985062
PacI	NEB	R0547S
Paraformaldehyde 16% solution	Electron Microscopy Sciences	15710
PBS (5×)	IMB Media Lab	P-20_L
PD0325901	Axon Medchem	Axon 1408
Penicillin-Streptomycin (10.000 U/ml)	Gibco	15140122
Pierce™ 16% Formaldehyde (w/v), Methanol-free	Thermo Scientific	28906
ProLong™ Diamond Antifade Mountant	Invitrogen	P36930
Puromycin	Sigma Aldrich	P8833
QuickCIP	NEB	M0525S
QuickExtract™ DNA Extraction Solution	Byozim	QE09050
rCutSmart™ Buffer	NEB	B6004S

RNaseZAP™	Sigma Aldrich	R2020-250ML
RNasin® Ribonuclease Inhibitor	Promega	N2515
Rubber solution	Mibenco	1297848 - 62
Saline sodium citrate (SSC, 20×)	IMB Protein Production	n.a.
ScreenBlend	IMB Protein Production	n.a.
Sodium acetate anhydrous	Sigma Aldrich	S2889
SYBR Safe DNA Gel Stain	Thermo Fisher	S33102
Taq DNA Polymerase	IMB Protein Production	n.a.
TBE Buffer (10×)	IMB Media Lab	T-40_L
Triton-X	Sigma-Aldrich	X100-500ML
TRIZol™ Reagent	Invitrogen	15596026
Trypsin/EDTA	Life Technologies	25200056
TWEEN® 20	Merck	P1379-1L
Ultrapure Water	IMB Protein Production	n.a.
VECTASHIELD Vibrance® Antifade Mounting Medium with DAPI	Vector Laboratories	H-1800-10
Yeast tRNAs	Invitrogen	AM7118

6.4 Kits

Table 4. Kits used in this work.

Kits	Manufacturer	Catalogue Number
Direct-zol RNA MicroPrep Kit	Zymo Research	R2062
EasySep™ Mouse PE Positive Selection Kit II	STEMCELL Technologies	17666
Flow Cell Wash Kit	Oxford Nanopore Technologies	n.a.
jetOPTIMUS® DNA Transfection Kit	Poyplus	101000051
Ligation Sequencing Kit V14	Oxford Nanopore Technologies	
Lipofectamine™ 3000 Transfection Reagent Kit	Life Technologies	L3000001
Nick Translation Reagent Kit	Abbott Molecular	07J0001

NucleoBond Xtra BAC Kit	Takara	740436.10
Oligo Clean & Concentrator Kit	Zymo Research	D4061
Rapid DNA Dephos & Ligation Kit	Roche	4898117001
TaKaRa LA Taq ® DNA Polymerase Hot-Start Version	Takara	RR042A
Takara PrimeSTAR® GXL DNA Polymerase	Takara	R050A
ZR Plasmid Miniprep-Classic	Zymo Research	D4054
Zymoclean Gel DNA Recovery Kit	Zymo Research	D4001

6.5 Homemade solutions

Table 5. Homemade solutions used in this work.

Homemade solutions	Recipe
Annealing solution	1 M Tris pH 8, 50 mM NaCl, 1 mM EDTA
Antigen retrieval buffer	10 mM sodium citrate, 0.05% Tween 20.
DAPI, 1:2000	1 µL of DAPI in 1,999 µL of PBS -Ca^{2+} -Mg^{2+} (1×)
Equilibrating solution	2× SSC buffer supplemented with 50% formamide
gDNA dilution buffer	Tris 10 mM pH 8, NaCl 100 mM, EDTA 25 mM, SDS 0.5%
Gelatin, 0.1%	0.5 g of gelatin in 500 mL of miliQ water; autoclaved
HCl, 0.1 N	98 µL of HCl 32% in 9,902 µL of water
Hybridization buffer	1% dextran sulfate, 50% formamide, 0.1% Tween 20 in 2× SSC
Isolation buffer	2% FBS and EDTA 1 mM in 1× PBS -Ca^{2+} -Mg^{2+}
PBS -Ca2+ -Mg2+ (1×)	5x PBS -Ca^{2+} -Mg^{2+} was diluted with Ultrapure Water to 1x and autoclaved
PBS + EDTA	1× PBS -Ca^{2+} -Mg^{2+} supplemented with EDTA 1:1000
PBS + Triton X-100 0.1% + saponin 0.1%	1 µL of Tritox X-100, 10 µL of saponin 10%, 989 µL of 1× PBS -Ca^{2+} -Mg^{2+}
PFA, 4%	1 mL of Paraformaldehyde 16% solution, EM grade were diluted with 3 mL of 1× PBS -Ca^{2+} -Mg^{2+}

Sodium acetate, 3M	8.2 g of sodium acetate anhydrous in 20 mL of water
0.1× SSC	1 mL of 2× SSC in 19 mL of water
1× SSC	10 mL of 10× SSC in 10 mL of water
2× SSC	2 mL of 20× SSC in 18 mL of water

6.6 Plasmids

Table 6. Vectors used and created in this work.

pCK number	Common name
176	pMF-Rosa26-splitRecombination Reporter Puromycin
178	pMF-TALEN-Rosa26 F (ELD)
179	pMF-TALEN-Rosa26 R (KKR)
180	pMF-Rosa26 HR - CreERT2
181	pMF-Rosa26 HR - BirA-V5
185	pSpCas9(BB)-3HA
545	pSpCas9(BB)-3HA-Bl6-gRNA
579	Rosa26(tg)-loxP-stop-loxP-Cas9-2A-EGFP-U6-Bl6-gRNA
580	Rosa26(tg)-hEF1a-loxP-stop-loxP-Cas9-2A-EGFP-U6-Bl6-gRNA
602	PBJ123-Piggbac/Puro
603	pCMV-hyPBase
668	pSpCas9(BB)-2A-Puro (PX459)
693	5'TR-EF1a-loxP-stop-loxP-Cas9-2A-EGFP-U6-Bl6-gRNA-BlastiR
704	SV40p-TALEN-Rosa26F-ELD-2A-TALEN-Rosa26R-KKR

6.7 Oligonucleotides

Table 7. Oligonucleotides used in this work.

Target	Forward primer		Reverse primer	
	Internal name	Sequence (5'-3')	Internal name	Sequence (5'-3')
AmpR	q455	TGATAACACTGCGGCCAACT	q456	TTCATTCAGCTCCGGTTCCC
Atrx	q1070	AGTGGCAGTGACAACGATGTT	q1073	AATCTGGAGCTGGGCTACTTG
Bex2	q104	CAGATTGACTGGAAACCGAGAG	q105	CACGCCTTGTTCCACTTTG
BlastiR	q399	CCACACATAACCAGAGGGCAGCA	q031	TCGCGATCGGAAATGAGAAC
BlastiR (cloning)	s157	tgcagacaaatggctctagaAACTTGTTTATTGCAGCTTATAATG	s158	GCGGCAATCAGAGAGATCATTAAGCTTGGGCTGCAGGTCG
***Bl6 gRNA* (cloning)**	s033	caccgCTGGGAATTAGAATGCCAGA	s034	aaacTCTGGCATTCTAATTCCCAGc
***Bl6 gRNA* (qPCR)**	q354	GCTGGGAATTAGAATGCCAGAGT	q355	CGACTCGGTGCCACTTTTTC
***Bl6 gRNA* (subcloning)**	s055	ataatGGCGCGCCgagggcctatttcccatgattccttca	s056	ataatGGCGCGCCtctagagccatttgtctgcagaattggc
Cas9	q040	TACAACAAGCACCGGGATAAG	q041	GTCGATGGTGGTGTCAAAGTA
Cdh1	q088	AGACTTTGGTGTGGGTCAGG	q089	CATGCTCAGCGTCTTCTCTG
EF1a	s088	gtatgTTAATTAAgtctccaggcgatctgacggt	s089	gtatgTTAATTAAgagcttgggcccattgcatacgtt
EGFP	q042	GACAACCACTACCTGAGCAC	q043	CAGGACCATGTGATCGCG

Ei2fs3x	q1066	CAGGATCTCGCCACATTGGA	q1067	GCCTTCACCACAGTGGACTT
Eomes	q086	GGATATCACCCAGCTAAAGATCG	q087	CTGTCATTTTCTGAAGCCGTG
Esrrb	q082	TGGCAGGCAAGGATGACAGA	q083	TTTACATGAGGGCCGTGGGA
Fgf5	q711	CGGATGGCAAAGTCAATGGC	q712	TCCCCTGAGACACAGCAAAT
Gata4	q110	CCTCTATCACAAGATGAACGGC	q111	GTGGTAGTCTGGCAGTTGG
G6pdx	q669	GGTGACCTGGCCAAGAAGAA	q670	GGCTCACTCTGCTTTCGGAT
Hbb-g	q221	TGATCAGAAGGAAACAGATGAGTC	q222	ATGAGAGCTTTCTGCCAATGA
Hprt	q074	GTATACCTAATCATTATGCCGAGGA	q075	GACATCTCGAGCAAGTCTTTCA
Huwe1	q1054	GGGTGGAAAGGAGAATGGCT	q1055	GTGGTTGCACTGGGTGGATA
Kdm6a	q1052	CCTTTTCGGGTTCGTGAGGT	q1053	GATTCGTAGCAGCGAACAGC
Mecp2	q1058	GGCCGATCTGCTGGAAAGTA	q1059	AGGAGGTGTCTCCCACCTTT
***Nanog* (gDNA)**	q223	ACAGCTTCTTTTGCATTACAATGTCC	q224	TATTCTCCCAGGCACCCAGGC
***Nanog* (cDNA)**	q078	GAACTCTCCTCCATTCTGAACC	q079	TTGCTAGTCTTCAACCACTGG
Oct3/4	q076	TCTCCAGACTCCACCTCACAC	q077	AGCCGACAACAATGAGAACC
Otx2	q094	GGTGGCACTGAAAATCAACTTG	q095	TGTTCTGACCTCCATTCTGC
PiggyBac	s153	AAATCATTTAAAACATCAGAggatcctttgttactttatagaaga	s154	gtatgcaatgggccaagctccttaagcgcgcaattaaccc

Pgk1	q693	ATGCTTTCCGAGCCTCACTG	q694	TCACACCCACCATGGAGCTA
***Rosa26* (gDNA)**	p99	GGTAGGGGATCGGGACTCTG	p58	CCCTCCAATTTTACACCTGTTCA
***Rosa26* (homology arms)**	s35	ctttgggccgcctccccgcaACCGGTTCGAGATCCAGGCG	s36	catacattatacgaagttatCACCTGCAGGAGTACTGGAAA
***Rosa26* (TALEN EKD FokI)**	s374	gtatgGctagccaccatggactataaggaccacg	s375	catacgctagCgggccaggattctcctcgacgtcaccgcatgttagcagacttcctctgccctctccactgccgaattctgagcggaaattgatctcgccattg
Rplp0	q072	ACTGGTCTAGGACCCGAGAAG	q073	CTCCCACCTTGTCTCCAGTC
RP23-378I14	p116	CTCCTCTGTACTCCCTGGCT	p117	AGGTGGGTAGGAAGGCTAGG
RP23-391D18	q444	CCGTGGCTGTATGTGGGAAT	q445	GCAAGCGATGGGACTCCATA
RP24-169C1	p134	CTCACGTGGTCAGACGTCAA	p135	ATAGCGGAGCACCACTTTCC
Sall1	q090	GCCTCAACATTTCCAATCCG	q091	CACAGACATGGGCATCCTT
Shredder fragment 1	s37	TTCCAGTACTCCTGCAGGTGataacttcgtataatgtatgctatacgaagttattcgcgatga	p51	CTCAGCTGCAGTTTGGCAT
Shredder fragment 2	p42	CCAGACTGAGCAAGAGCAGA	q41	GTCGATGGTGGTGTCAAAGTA
Shredder fragment 4	q40	TACAACAAGCACCGGGATAAG	s38	CGCCTGGATCTCGAACCGGTtgcggggaggcggcccaaag
Snprn	q122	CTAGCATTGCAGGAGCCC	q123	GGTCTCATACCAGGTGGAGG

Sox17	q096	CGATGAACGCCTTTATGGTG	q097	TTCTCTGCCAAGGTCAACG
TBP	q068	CACCAATGACTCCTATGACCC	q069	AGCCAAGATTCACGGTAGATAC
Tsix	q231	ATGGCTCAAATGGATGCCTG	q232	TTAGTGACCTCCCAGTACCC
Wnt3	q080	CCCGCTCAGCTATGAACAAG	q081	CCCGTGGCATTTACACTTTAG
Xist	q360	CTATCGCCCCAGGTCACATC	q361	CCAGTGCAGAGGTTTTTGGC

6.8 Antibodies

Table 8. Antibodies used in this work.

Antibody	Clone	Manufacturer	Catalogue Number	Dilution	Host
anti-Goat IgG (H+L) Cross-Adsorbed Secondary Antibody, Alexa Fluor™ 488	n.a.	ThermoFisher	A11055	1:500	Donkey
anti-Mouse IgG (H+L) Highly Cross-Adsorbed Secondary Antibody, Alexa Fluor™ 555	n.a.	ThermoFisher	A31570	1:500	Donkey
anti-mouse IgG (H+L) Highly Cross-Adsorbed Secondary Antibody, Alexa Fluor™ 647	n.a.	ThermoFisher	A31571	1:500	Donkey

anti-rabbit IgG (H+L) Cross-Adsorbed Secondary Antibody, Alexa Fluor™ 555	n.a.	ThermoFisher	A21430	1:500	Goat
E-cadherin	n.a.	BD Transduction Laboratories	610182	1:500	Mouse
Gata4	n.a.	Santa Cruz	sc-25310	1:150	Mouse
Nanog	D2A3	Cell Signaling Technology	8822T	1:500	Rabbit
PE-conjugated feeder cells	mEF-SK4	Miltenyi Biotec	130-120-166	0.3 µg	Mouse
Skeletal Myosin Heavy Chain	EPR22697-17	Abcam	ab234431	1:50	Rabbit
Sox1	n.a.	R&D Systems	AF3369	1:250	Goat

7. Methods

7.1 Cloning of different constructs

7.1.1 X^{Bl6}-specific gRNA cloning

The primers s033 and s034 were annealed together by mixing equimolar concentrations of the plasmid in annealing solution. The mix was placed in a thermocycle by incubating for 2 min at 95 °C followed by a 45-min gradient from 95 to 25 °C. The annealed primers were kept at -20 °C until further use.

1 µg of the plasmid pCK185 was digested with BbsI (NEB, R3539S) in rCutSmart™ Buffer (NEB, B6004S) with QuickCIP (NEB, M0525S) for 1 h at 37 °C and the digested plasmid was purified from an agarose gel using the Zymoclean Gel DNA Recovery Kit (Zymo Research, D4001). The eluted plasmid was measured using a DS-11 FX+ Spectrophotometer/Fluorometer. The annealed primer mix contains compatible ends with the BbsI-digested plasmid and they were ligated using the Rapid DNA Dephos & Ligation Kit (Roche, 4898117001) and used for bacterial transformation. The resulting plasmid was named pCK545.

7.1.2 *Rosa26* shredder plasmid cloning

The 8.6 kb fragment containing the *Rosa26* homology arms for recombination was amplified from pCK181, which is a plasmid previously reported and kindly provided by (Flemr and Bühler 2015). The plasmid was used as a template for PCR amplification with s35 and s36 using the Takara PrimeSTAR® GXL DNA Polymerase (Takara, R050A); the manufacturer's conditions were used with primers at a final concentration of 0.5 µM, 1 µL of polymerase and 25 cycles with 1 min/kb of extension time. This fragment contains the bacterial resistance cassette (ampicillin) as well as the origin of replication for bacterial amplification.

The floxed polyadenylation sites together with *Cas9*, *T2A* and *EGFP* were amplified from different sources and the *Cas9* sequence was amplified in different fragments. Fragment 1 (1.6 kb) used isolated mouse DNA (kindly provided from [redacted] from (Platt et al. 2014)) to PCR amplify the floxed polyadenylation sites with the first nucleotides of the *Cas9* sequence with s37 and p51 using the Takara PrimeSTAR® GXL DNA Polymerase (Takara, R050A); the manufacturer's conditions were used with primers at a final concentration of 0.5 µM, 0.5 µL of polymerase and 25 cycles with 1 min/kb of extension time. Fragment 2 (3.7 kb) containing the

remaining *Cas9* sequence was amplified from the commercially available PX459 (pCK668) plasmid with p42 and q41 using the Takara PrimeSTAR® GXL DNA Polymerase (Takara, R050A); the manufacturer's conditions were used with primers at a final concentration of 0.5 µM, 0.5 µL of polymerase and 25 cycles with 1 min/kb of extension time. Fragments 1 and 2 were fused by PCR using s37 and q41 using the Takara PrimeSTAR® GXL DNA Polymerase (Takara, R050A) resulting in fragment 3 (4.8 kb); the manufacturer's conditions were used with templates at equimolar concentrations, primers at a final concentration of 0.5 µM, 0.5 µL of polymerase and 20 cycles with 1 min/kb of extension time. For fragment 4 (1.7 kb) containing the *T2A-EGFP* sequence, the same mouse DNA used in fragment 1 was used as template with q40 and s38 using the TaKaRa LA Taq ® DNA Polymerase Hot-Start Version (Takara, RR042A) with the provided 10× $MgCl_2$ buffer; the manufacturer's conditions were used with primers at a final concentration of 0.5 µM, 0.5 µL of polymerase and 33 cycles with 1 min/kb of extension time.

The *Rosa26* homology arms PCR product together with fragments 3 and 4 were used for gibson assembly. For the assembly, 100 ng of total DNA were combined in a 0.2 mL thin walled PCR tube kept on ice containing the Gibson Assembly 2× Master Mix (IMB Protein Production Core Facility) and equimolar concentrations of all the fragments. The reaction mixture was incubated at 50 °C for 30-60 min. The whole reaction was further used for bacterial transformation. 1 µg of this plasmid was digested with AscI (NEB, R0558L) in rCutSmart™ Buffer (NEB, B6004S) with QuickCIP (NEB, M0525S) for 1 h at 37 °C and the digested plasmid was purified from an agarose gel using the Zymoclean Gel DNA Recovery Kit (Zymo Research, D4001). The eluted plasmid was measured using a DS-11 FX+ Spectrophotometer/Fluorometer.

The Bl6-gRNA (0.5 kb) was amplified from pCK545 using s55 and s56 using the Takara PrimeSTAR® GXL DNA Polymerase (Takara, R050A); the manufacturer's conditions were used with primers at a final concentration of 0.5 µM, 0.5 µL of polymerase and 25 cycles with 1 min/kb of extension time. The fragment was digested with AscI (NEB, R0558L) in rCutSmart™ Buffer (NEB, B6004S) for 1 h at 37 °C and ligated to the *Rosa26* plasmid using the Rapid DNA Dephos & Ligation Kit (Roche, 4898117001) and used for bacterial transformation. The resulting plasmid was named pCK579.

7.1.3 *PiggyBac* shredder plasmid cloning

The human *EF1a* promoter (1.5 kb) was added to pCK579 by amplifying it from another plasmid with s88 and s89 using the TaKaRa LA Taq ® DNA Polymerase Hot-Start Version (Takara, RR042A) with the provided GC buffer; the manufacturer's conditions were used with

primers at a final concentration of 0.5 µM, 0.5 µL of polymerase and 25 cycles with 1 min/kb of extension time. The purified PCR fragment was digested with PacI (NEB, R0547S) in rCutSmart™ Buffer (NEB, B6004S) for 1 h at 37 °C. 1 µg of the plasmid pCK579 was digested with PacI (NEB, R0547S) in rCutSmart™ Buffer (NEB, B6004S) with QuickCIP (NEB, M0525S) for 1 h at 37 °C and the digested plasmid was purified from an agarose gel using the Zymoclean Gel DNA Recovery Kit (Zymo Research, D4001). The eluted plasmid was measured using a DS-11 FX+ Spectrophotometer/Fluorometer and ligated with the *EF1a* promoter using the Rapid DNA Dephos & Ligation Kit (Roche, 4898117001) and used for bacterial transformation. The resulting plasmid was named pCK580.

A *piggyBac* plasmid (Cary et al. 1989) containing the terminal repeats was kindly provided by [redacted] and named pCK602. A fragment (3.6 kb) containing the terminal repeats, the bacterial resistance cassette (ampicillin) as well as the origin of replication was amplified from pCK602 with s153 and s154 using the Takara PrimeSTAR® GXL DNA Polymerase (Takara, R050A); the manufacturer's conditions were used with primers at a final concentration of 0.3 µM, 1 µL of polymerase and 25 cycles with 1 min/kb of extension time. The blasticidin resistance cassette (1.8 kb) was amplified from a previous plasmid with s157 and 158 using the Takara PrimeSTAR® GXL DNA Polymerase (Takara, R050A); the manufacturer's conditions were used with primers at a final concentration of 0.3 µM, 1 µL of polymerase and 25 cycles with 1 min/kb of extension time. The shredder construct with the *EF1a* promoter was amplified (8.6 kb) from pCK580 with s155 and 156 using the Takara PrimeSTAR® GXL DNA Polymerase (Takara, R050A); the manufacturer's conditions were used with primers at a final concentration of 0.3 µM, 1 µL of polymerase and 25 cycles with 1 min/kb of extension time.

The fragments were used for gibson assembly. For the assembly, 100 ng of total DNA were combined in a 0.2 mL thin walled PCR tube kept on ice containing the Gibson Assembly 2× Master Mix (IMB Protein Production Core Facility) and equimolar concentrations of all the fragments. The reaction mixture was incubated at 50 °C for 30-60 min. The whole reaction was further used for bacterial transformation. The resulting plasmid was named pCK693.

7.1.4 Double *Rosa26* TALEN plasmid cloning

The *Rosa26* TALEN plasmids (pCK178 and pCK179) have been previously reported and kindly provided by (Flemr and Bühler 2015).

The *Rosa26* TALEN EKD FokI was PCR amplified (3.1 kb) from pCK178 with s374 and s375 using the Takara PrimeSTAR® GXL DNA Polymerase (Takara, R050A); the manufacturer's

conditions were used with primers at a final concentration of 0.3 µM, 1 µL of polymerase and 25 cycles with 1 min/kb of extension time. The PCR fragment was purified from an agarose gel using the Zymoclean Gel DNA Recovery Kit (Zymo Research, D4001). The eluted plasmid was measured using a DS-11 FX+ Spectrophotometer/Fluorometer and used for digestion with NheI (NEB, R3131S) in rCutSmart™ Buffer (NEB, B6004S) for 1 h at 37 °C.

1 µg of the plasmid pCK179 was digested with NheI (NEB, R3131S) in rCutSmart™ Buffer (NEB, B6004S) with QuickCIP (NEB, M0525S) for 1 h at 37 °C and the digested plasmid was purified from an agarose gel using the Zymoclean Gel DNA Recovery Kit (Zymo Research, D4001). The eluted plasmid was measured using a DS-11 FX+ Spectrophotometer/Fluorometer and used for ligation together with the PCR fragment from pcK178 using the Rapid DNA Dephos & Ligation Kit (Roche, 4898117001) and used for bacterial transformation. The resulting plasmid was named pCK704.

7.1.5 Bacterial transformation

Cloned vectors were transformed into NEB® 10-beta Competent *Escherichia coli* (High Efficiency) (NEB, C3019H) following the manufacturers' protocol.

7.1.6 Colony PCR and plasmid DNA isolation

Following bacterial transformation, individual colonies were picked using a pipette tip and placed into 10 µL of nuclease free water. Per 100 µL, a PCR master mix was prepared by combining 75 µL nuclease free water, 20 µL of Green Taq buffer (5×) (IMB Protein Production Core Facility), 2 µL of dNTP mix (NEB, N0447S), 1 µL of 100 µM forward primer, 1 µL of 100 µM reverse primer and 1 µL of Taq DNA Polymerase (IMB Protein Production Core Facility); per colony, 6 µL of the master mix were used and added to a PCR tube. The same pipet tip used to pick the colony was then transferred into the PCR mixture. After removing the tip, the samples underwent PCR with the following thermal cycling conditions: initially denaturation at 95 °C for 3 min, followed by 24 cycles of denaturation at 94 °C for 20 s, annealing at 55 °C for 20 s, and elongation at 68 °C for 1 min/kb. A final extension at 68 °C for 5 min was followed by holding the samples at 10 °C. The PCR products were analyzed by running them on an agarose gel, with the gel percentage selected based on the size of PCR product.

Two selected plasmids were inoculated into LB medium (IMB Media Lab, L-10_M) supplemented with ampicillin (IMB Media Lab, A-10_A). The cultures were incubated at 37 °C with orbital shaking at 200 rpm for 16 h. Plasmid DNA was isolated using the ZR Plasmid Miniprep-

Classic (Zymo, D4054) kit according to the manufacturer's instructions. DNA concentrations were measured using a DS-11 FX+ Spectrophotometer/Fluorometer (DeNovix), and plasmid sequences were verified by Sanger sequencing.

7.1.7 Plasmid maintenance

Bacterial stocks were prepared by combining 500 µL of liquid bacterial culture with 800 µL of glycerol (Sigma Aldrich, G5516) in cryovials (Sarstedt, 72.397.992). The mixture was gently rotated to ensure even distribution before storage at -80oC.

For bacterial recovery, a small portion of the frozen stock was scraped using a pipet tip and streaked on LB plates (IMB Media Lab, L-20_P) supplemented with ampicillin (IMB Media Lab, A-10_A) and grown for 15 h at 37 °C. A single colony was used to inoculate LB medium (IMB Media Lab, L-10_M) supplemented with ampicillin (IMB Media Lab, A-10_A). The culture was incubated at 37 °C with orbital shaking at 200 rpm for 16 h. For artificial chromosomes, the LB medium (IMB Media Lab, L-10_M) was supplemented with chloramphenicol at a final concentration of 12.5 µg/mL (IMB Media Lab).

For the bacterial artificial chromosomes, chloramphenicol plates were prepared by melting LB agar (IMB Media Lab, L-12_M) and adding chloramphenicol at a final concentration of 12.5 µg/mL (IMB Media Lab) and pouring the mixture in 100-mm bacterial plates.

7.2 Composition of media and plate coating

7.2.1 Fibroblast medium

For culturing mouse embryonic fibroblasts (MEFs), fibroblast medium was prepared with 4.5 g/L glucose DMEM (Gibco, 11960044) supplemented with 10% heat-inactivated fetal bovine serum (FBS) (Gibco, A5256701), 1% Penicillin/Streptomycin (Gibco, 15140122), and 1% GlutaMAX™ Supplement (Gibco, 35050061). The medium was sterilized by filtering using bottle filters (Fisher Scientific, FB12566510). The medium was stored at 4°C and brought to room temperature prior to using.

7.2.2 Inactivation medium

For mitotic inactivation of MEFs, mitomycin C (Fisher Scientific, 226940020) was dissolved to a final concentration of 10 µg/mL using fibroblast medium; the solution was frozen in 40 mL aliquots.

7.2.3 Mouse embryonic stem cell in serum medium

Medium was prepared with 4.5 g/L glucose DMEM (Gibco, 11960044) supplemented with 15% heat-inactivated FBS (Life Technologies, 10270106), 1% Penicillin/Streptomycin (Gibco, 15140122), 1% GlutaMAX™ Supplement (Gibco, 35050061), 1% Non-essential Amino Acid (Gibco, 11140050) and 1% EmbryoMax® 2-Mercaptoethanol (Sigma, ES-007-E). The medium was sterilized by filtering using bottle filters (Fisher Scientific, FB12566510). After filtering, leukaemia inhibitor factor (LIF; Sigma Aldrich, ESG1107) was added to a final concentration of 500 U/mL. The medium was stored at 4°C and brought to room temperature prior to using.

7.2.4 Mouse embryonic stem cell in 2i medium

The 2 inhibitors (2i) were initially prepared by dissolving lyophilized powders. PD0325901 (Axon Medchem, Axon 1408) was dissolved in DMSO (Sigma Aldrich, D8418-100ML) to a final concentration of 1 mM. The lyophilized CHIR99021 (Axon Medchem, 1386) was dissolved to a final concentration of 3 mM: first, approximately 30% of the final volume of DMSO was added (Sigma Aldrich, D8418-100ML) and the solution was incubated for 5 min in the water bath until the white solution turned crystal clear. After that, the remaining amount of DMSO was added.

The 2i medium was prepared with KnockOut DMEM (Life Technologies, 10829018) supplemented with 15% KnockOut serum replacement (Life Technologies, 10828028), 1% Penicillin/Streptomycin (Gibco, 15140122), 1% GlutaMAX™ Supplement (Gibco, 35050061), 1% Non-essential Amino Acid (Gibco, 11140050), 1% EmbryoMax® 2-Mercaptoethanol (Sigma, ES-007-E) and 5 µg/mL insulin (Sigma Aldrich, I0516). The medium was sterilized by filtering using bottle filters (Fisher Scientific, FB12566510). After filtering, LIF (Sigma Aldrich, ESG1107) was added to a final concentration of 1000 U/mL together with PD0325901 (Axon Medchem, Axon 1408) at final concentration of 1 µM and CHIR99021 (Axon Medchem, 1386) at final concentration of 3 µM were added to the medium. The medium was stored at 4°C and brought to room temperature prior to using.

7.2.5 Differentiation media for assessment of developmental potential

Differentiation medium 1 was prepared as the serum medium without LIF (Sigma Aldrich, ESG1107) and 1% EmbryoMax® 2-Mercaptoethanol (Sigma, ES-007-E). Differentiation medium 2 was prepared as the serum medium without LIF (Sigma Aldrich, ESG1107).

7.2.6 Mouse epiblast-like stem cell medium

For differentiating and culturing mESCs to EpiLSCs, medium was prepared with 4.5 g/L glucose DMEM/F-12 GlutaMAX (Life Technologies, 10565018) supplemented with 15% KnockOut serum replacement (Life Technologies, 10828028), 0.5% Penicillin/Streptomycin (Gibco, 15140122), 1% Non-essential Amino Acid (Gibco, 11140050) and 1% EmbryoMax® 2-Mercaptoethanol (Sigma, ES-007-E). The medium was sterilized by filtering using bottle filters (Fisher Scientific, FB12566510). After filtering, FGF2 (IMB) was added to a final concentration of 7 ng/mL. The medium was stored at 4°C and brought to room temperature prior to using.

7.2.7 Freezing medium

For fibroblasts and mESCs (in either serum or 2i), freezing medium was prepared by supplementing each of them with 10% DMSO (Sigma Aldrich, D8418-100ML). For EpiLSCs, medium without FGF2 was prepared and supplemented with 10% DMSO (Sigma Aldrich, D8418-100ML) and 15% KnockOut serum replacement (Life Technologies, 10828028).

7.2.8 Plate coating

For mESCs (when needed) and EpiLSCs, 2 mL of 0.1% gelatin solution (Sigma, G1890) or Attachment Factor 1X (Gibco, S-006-100 100mL) were added in a 35- or 60-mm plate and placed for at least 30 min in the incubator. The plates can be left for longer taking care of the gelatin not drying up in the incubator. Afterwards, plates were coated with gelatin and then inactivated feeders MEFs were seeded: for mESCs at a density of $1x10^5/cm^2$ and for EpiLSCs at a density of $4x10^4/cm^2$. Coating for mESCs was only done for transfection and differentiation experiments.

7.3 Mouse work

Animal experiments were conducted in compliance with local and European animal welfare regulations and were approved by the relevant authorities (ethical committees on animal care and use of the federal state of Rhineland-Palatinate, Germany; covered under LUA license G 23-5-049). Mice, aged 7–24 weeks for MEF isolation or 7-month old for lung isolation, were housed in ventilated cages with enrichment materials under controlled conditions (humidity 40–70%, temperature 22 ± 2 °C) on a 12-hour light/dark cycle and provided food and water *ad libitum*.

WT female mice in a C57BL/6J background were transferred to cages with WT males of the same background and allowed to mate overnight. The morning after, plugs were checked and

plug-positive female mice were separated in a new cage; this is referred to as E0.5. Non-positive females were transferred to their old cage. On E13.5, females were sacrificed by CO_2 inhalation; 7-month-old mice were directly sacrificed (no mating). Females were placed in a CO_2 chamber until no breathing was seen. Females were taken out of the cage, sprayed with 70% ethanol (Sigma Aldrich, ES-007-E) and the ventral abdominal skin was cut and opened using dissecting scissors. The uterine horn containing the embryo strings popped out and the horns were isolated and separated from the uterus using dissecting scissors. The horns were placed in PBS -Ca^{2+} -Mg^{2+} string and taken to the laminar hood for the isolation of fibroblasts. The lungs were directly cut into two pieces and snap-frozen in dry ice.

7.4 Cell culture

All cells were grown in a humidifier incubator (Thermo Scientific, 3308) at 37 °C and 5% CO_2. For mESCs and EpiLSCs, the media were changed daily. For fibroblasts, the medium was changed every 2-3 days. Splitting of either cell type was performed with they reached a confluency of around 80% percentage.

7.4.1 Isolation of mouse embryonic fibroblasts

After isolating the horns from the uterus and inside the laminar hood, the string was transferred to a 100-mm cell culture dish (Falcon, 353003) with PBS -Ca^{2+} -Mg^{2+} and embryos were individually isolated from the yolk sac with the help of tweezers and the placenta and umbilical cords were removed. Afterwards, the embryos were transferred to a 100-mm cell culture dish (Falcon, 353003) with PBS -Ca^{2+} -Mg^{2+}. For each embryo, the head was removed with a scalpel and the heart with tweezers and the remaining body parts were cut into smaller pieces with the scalpel until a homogeneous mixture was obtained and transferred to 15-mL falcon tubes. Per embryo, 900 µL of 0.25% Trypsin/EDTA (Life Technologies, 25200056) was added to each tube together with DNAse I to a final concentration of 0.1 µg/mL and the mixture was incubated in a water bath at 37 °C for 15-20 min. The reaction was neutralized with fibroblast medium and the resulting cells were plated in a 6-well plate (one well per embryo); this is referred to as p0. When the wells were approximately 85% confluent, cells were frozen at a density of $2.2x10^6$ cells per vial.

7.4.2 Expansion and splitting of mouse embryonic fibroblasts

One vial of fibroblasts p1, was thawed and grown in a 150-mm plate and two days later cells were split 1:2 to two 150-mm plates (p2) and the process was repeated once more until p3. The four plates at a confluency of 90% were detached and frozen at a density of 2×10^6 cells per vial. Fibroblasts were split when the wells reached a confluency of around 85% and were never used beyond passage 8 (p8). For splitting, the medium was removed, rinsed once with PBS $-Ca^{2+}$ $-Mg^{2+}$ and enough accutase (Sigma Aldrich, A6964-100ML) to cover the plate was added; the plate was incubated in the incubator until detached, floating cells were visible under the microscope. For expansion, cells were transferred usually at a 1:2 ratio to new plates containing fibroblast medium; for freezing, cells were pelleted (1,000 rpm for 3 min), the medium was removed and frozen with freezing medium at the desired density.

7.4.3 Inactivation of fibroblasts (feeders)

One vial of MEFs at p4, was thawed and grown in a 150-mm plate and two days later cells were split 1:2 to two 150-mm plates (p5) and the process was repeated once more until p6. Two days later, the fibroblast medium was removed and per plate, 20 mL of inactivation medium was added to each plate. Cells were incubated for 3 hours and afterwards the inactivation medium was removed, cells were washed twice with DPBS $+Ca^{2+}$ $+Mg^{2+}$ and cells were detached. The resulting feeders were frozen at a density of 2.15×10^6 cells per vial.

7.4.4 Isolation of hybrid mESCs

Prior to embryo thawing, EmbryoMax® M2 Medium (Sigma, MR-015-D) was added to 35-mm plates and placed in the incubator for equilibration for 30 min. In addition, plates containing small drops of KnockOut serum replacement (Life Technologies, 10828028) covered with EmbryoMax® Filtered Light Mineral Oil (Sigma, ES-005-C) and placed in the incubator for equilibration for 30 min.

Cryopreserved C3H/Bl6 2-cell stage embryos in embryo straws, obtained from Janvier Labs, were thawed by placing them in a distilled water bath for 15 s. The straws contained a cotton plug, and the plug was cut with scissors; the other end of the straw was also cut and with the help of a syringe, the embryos were pumped out of the straw into a 35-mm plate containing equilibrated M2 medium (Sigma, MR-015-D). Embryos were allowed to settle and then were washed three times by consecutive transfers to equilibrated M2-containing medium before placing them in EmbryoMax® KSOM Mouse Embryo Media (Millipore, 637429) drops in the incubator. Embryos were monitored each day and further processed until the blastocyst stage. Blastocyst were

washed one by one in EmbryoMax® Acidic Tyrode's Solution (Millipore, MR-004-D) before seeding them in individual feeder-coated wells of a 48-well plate with serurm/LIF medium. The blastocysts were allowed to attach for two days and afterwards, the medium was changed to a fresh aliquot daily until outgrowths were visible. Cell lines were split and mESCs were expanded.

7.4.5 Expansion and splitting of hybrid mESCs

For every splitting event, feeders were thawed the day before at a density of $1x10^5$ cells/cm^2; if needed, gelatin coating was performed. Cells were then split and passaged usually every 2-3 days, depending on the density of seeding. mESCs were split when the wells reached a confluency of around 85%. For splitting, cells were detached by removing the medium, rinsing once with PBS -Ca^{2+} -Mg^{2+} and enough accutase (Sigma Aldrich, A6964-100ML) to cover the plate was added; if two or less plates were handled, they were placed in the incubator for 2-3 min, otherwise they were incubated in the hood and when the accutase was added to the last plate, the first one was already ready for detaching. For each plate, 1 volume of serum medium was added and cells were detached by gently pipetting up and down until a single-celled suspension was obtained; the process was repeated with all plates. For expansion, cells were transferred usually at a 1:5 ratio to new feeder plates containing serum/LIF medium; for freezing, cells were pelleted (1,000 rpm for 3 min), the medium was removed and frozen with freezing medium at the desired density.

7.4.6 Isolation of mESCs from feeders

mESCs were isolated from feeders when the either 6-well or 60-mm plates reached a confluency of around 75-80% using the EasySep™ Mouse PE Positive Selection Kit II (STEMCELL Technologies, 17666) with some modification. Cells were detached with accutase and centrifuged at 1,000rpm for 3 min and the pellets were resuspended in 300 µL of isolation buffer. The mixtures were transferred to polystyrene round-bottom tubes (Fisher Scientific, 10186360) with 3 µL of the provided FcR blocker, mixing them carefully before adding 0.3 µg of the provided conjugated anti-mouse antibody and samples were incubated for 15 min in the dark. Each sample was topped up with a 10-fold excess of isolation buffer and centrifuged at 300×g for 10 min using low brake. The supernatant was removed and the pellets were resuspended in 200 µL of isolation buffer before adding 20 µL of the provided selection cocktail and samples were incubated in the dark for 15 min. The vial of the provided RapidSpheres was vortexed for 30 s prior to using and 15 µL of them were used per 200 µL of buffer; samples were carefully mixed and incubated in the dark for 10 min before topping up to 2.5 mL of isolation buffer. The samples

were placed in a magnetic rack for 10 min; mESCs remain in the suspension while the fibroblast remain in the bound beads-antibody complex, therefore the supernatants were transferred to falcon tubes and cells were centrifuged at 1,000rpm for 3 min. The pellets were either frozen until further processing for RNA extraction or cultured for 3 additional days for embryoid bodies.

7.4.7 Differentiation of mESCs to embryoid bodies (EBs)

EBs were generated as previously described with some modifications (Bedzhov et al. 2013). C3H/Bl6 mESCs isolated from feeders and cultured for up to three days in gelatin-coated plates with 2i/LIF medium were resuspended differentiation medium 1 at a concentration of 1×10^6 cells/mL. Drops of 30 µL were plated on the lid of 10-cm bacterial plates and the plate was filled with PBS -Ca^{2+} -Mg^{2+}; the lid was flipped in order to form hanging drops and cells were allowed to aggregate for 3 days in the incubator. Cells that aggregated and formed “balls” were transferred to 10-cm bacterial dishes with differentiation medium 1 and with shaking for 3 more days in the incubator; cells were constantly monitored for growth. After three days, the cell bodies were plated on gelatin-coated wells or coverslips in differentiation medium 2 for 3 days. If needed, the medium was changed and EBs were cultured for 3 more additional days. Beating structures were counted at the end of the experiment. Cells were either fixed with 4% PFA or TRIzol™ (Invitrogen, 15596026) was added to the plates.

7.4.8 Differentiation of mESCs to EpiLSCs and splitting

mESCs were detached at 125,000 cells were seeded for timepoints 0 and 2 days of differentiation and an additional well for day 5 and 7. All cells were seeded, as specified for EpiLSCs, in serum/LIF medium. For days 2 and the additional well, the medium was changed to EpiLSC medium while for day 0 it was changed to a fresh aliquot of serum/LIF medium; the medium was changed daily. For the additional well, cells were split, as specified for EpiLSCs, and colonies were seeded for days 5 and 7. Cells were collected at the respective points after differentiation was induced by removing the medium from the wells, rinsing carefully once with PBS -Ca^{2+} -Mg^{2+} and proceeding with the splitting procedure for EpiLSCs. After two rounds of washing, cells were centrifuged for freezing but instead of freezing medium, TRIzol™ (Invitrogen, 15596026) was added and cells were snap frozen.

EpiLSCs were split when the wells reached a confluency of around 80%. If differentiated cells were found, the plates were cleaned with a pipet tip before proceeding. For splitting, the medium was removed, rinsed once with PBS -Ca^{2+} -Mg^{2+} and cells were incubated with PBS/EDTA solution for exactly 2 min. Afterwards, the detaching solution is removed and epiblast-like medium

without FGF2 is added to the plate; using a cell scraper, cells are gently detached from the plate and resuspended with a 5 mL serological pipette to triturate cells making sure to obtain a mixture with smaller colonies and not single cells. Cells are then transferred to a falcon tube and washed twice with epiblast-like medium without FGF2 (200×g, 15-30 s) and then cell pellets are gently resuspended in complete epiblast-like medium and seeded to new feeder plates with complete epiblast-like medium. For freezing, after the two washes, cells were centrifuged at 200×g for 5 min and the pellet was gently resuspended in the EpiLSC freezing medium.

7.4.9 Liposome-mediated transfection

In a DNA LoBind Eppendorf 1.5 mL tube, 3.74 µL of Lipofectamine™ 3000 reagent was mixed with 125 µL of Opti-MEM™ I (Gibco, 31985062) supplemented with LIF (Sigma Aldrich, ESG1107) at final concentration of 1000 U/mL. In a second tube and for *Rosa26* targeting 800 ng of pCK704, 200 ng of pCK176, 2.062 µg of pCK180 and 3 µg of pCK579 were added to a tube containing P3000 reagent (2 µL/µg DNA) and 125 µL of Opti-MEM™ I (Gibco, 31985062) supplemented with LIF (Sigma Aldrich, ESG1107) at final concentration of 1000 U/mL. The contents of the first tube were then transferred into the second tube, vortexed for 30 s, briefly centrifuged, and incubated at room temperature for 20 min. In the meantime, 1×10^6 cells were centrifuged at 1,000 rpm for 3 min, the supernatant was discarded, and the pellet was resuspended in 500 µL of Opti-MEM™ I (Gibco, 31985062) supplemented with LIF (Sigma Aldrich, ESG1107) at final concentration of 1000 U/mL. For *piggyBac* transposition, 2 µg of pCK693 and 352 ng of pCK603 were used. The DNA–lipofectamine mixture was added to the cell suspension, which was gently mixed by pipetting and incubated at room temperature for 2 minutes. In the meantime, the fibroblast medium was removed from the culture plate, and 2 mL of fresh Opti-MEM™ I (Gibco, 31985062) supplemented with LIF (Sigma Aldrich, ESG1107) at final concentration of 1000 U/mL was added to the 60-mm plate. After incubation, the transfection mixture was carefully added dropwise onto the plate, and cells were incubated for 6 hours. Following this incubation, the medium was replaced with serum/LIF medium.

For the jetOPTIMUS® DNA Transfection Kit, 500 µL of the provided buffer were mixed with 800 ng of pCK704, 200 ng of pCK176, 2.062 µg of pCK180 and 3 µg of pCK579 and the tube was vortexed for 1 s and spun down. The provided reagent was vortexed for 5 s and span down and 7.5 µL of the reagent were added to the DNA-buffer mix. The mixture was vortexed for 1 s and spun down and incubated at room temperature for 10 min. In the meantime, cells were detached and collected and 1 million cells in serum/LIF medium without antibiotics were added to the mixture and pipetted up and down to get a single-celled suspension. In addition, the fibroblast medium

was removed from the culture plate, and 1 mL of serum/LIF medium without antibiotics was added to the 60-mm plate. After incubation, the transfection mixture was carefully added dropwise onto the plate, and cells were incubated for 4 hours. Following this incubation, the medium was replaced with serum/LIF medium.

For both kits, the next morning after transfection, selection with the respective antibiotic (1 µg/mL of puromycin for the *Rosa26* targeting or 5 µg/mL of blasticidin for the *piggyBac* transposition) was initiated and maintained for 2 days, changing to fresh aliquots daily. Single colonies were then picked and transferred individually into gelatin coated 96-well plates containing 2i/LIF medium for expansion. The plate was then divided into two: one on gelatin and 2i/LIF medium for genotyping and one with feeders and serum/LIF medium for expansion. For NHEJ inhibition, 200 µM of Novobiocin and 1 µM of AZD-7648 were used from the liposome generation step until selection was done.

7.5 DNA fluorescence in situ hybridization (DNA FISH)

7.5.1 Isolation of bacterial artificial chromosomes (BACs)

The BACs RP23-378I14 and RP23-391D18 for the X chromosome and RP24-169C1 for chromosome 6 were used. For each, one isolated colony from agar plates was taken and used for inoculating 4 mL of LB supplemented with chloramphenicol for around 8 h. 500 µL of the culture were taken and added to 250 mL of LB supplemented with chloramphenicol in a 1000 mL flask and incubated for 16-18 h. Next day, the cultures were centrifuged at 5,000×g for 10 min at 4 °C and the supernatant was removed and the bacterial pellets were snap frozen until further processing. Isolation of the BACs was performed using the NucleoBond Xtra BAC kit (Takara, 740436.10) according to manufacturer's instructions. BAC DNA concentrations were measured using a DS-11 FX+ Spectrophotometer/Fluorometer (DeNovix).

7.5.2 Verification of BACs by PCR

100-150 ng of BAC DNA were used for BAC verification by PCR. A PCR master mix was prepared by combining 11.5 µL nuclease free water, 4 µL of 5× Green Taq buffer (IMB Protein Production Core Facility), 0.4 µL of dNTP mix (NEB, N0447S), 0.4 µL of 10 µM forward primer, 0.4 µL of 10 µM reverse primer and 0.3 µL of ScreenBlend DNA Polymerase (IMB Protein Production Core Facility). The samples underwent PCR with the following thermal cycling conditions: initially denaturation at 94 °C for 1 min 30 s, followed by 33 cycles of denaturation at 94 °C for 30 sec, annealing at 55 °C for 30 sec, and elongation at 68 °C for 1 min/kb. A final

extension at 68 °C for 5 min was followed by holding the samples at 10 °C. The PCR products were analyzed by running them on an agarose gel, with the gel percentage selected based on the size of PCR product.

7.5.3 Nick translation and purification of BACs

Alexa Flour 647-aha-dUTP 1 mM (Thermo Fisher, A32763) and Alexa Flour 555-aha-dUTP 1 mM (Invitrogen, 10654193) were used; RP23-378I14 was labeled with Alexa Fluor 647 while RP23-391D18 and RP24-169C1 with Alexa Fluor 555. The fluorophores were diluted to 0.1 mM with nuclease-free water. A 0.1 mM dNTP mix from the nick translation kit (Abbott Molecular, 07J0001) was prepared by mixing 10 µL of 0.3 mM of dATP, 10 µL of 0.3 mM of dCTP and 10 µL of 0.3 mM of dGTP; dTTP 0.1 mM was prepared by diluted 10 µL of 0.2 mM dTTP with 20 µL of nuclease-free water.

1 µg of BAC DNA were used for fluorophore labeling using a nick translation kit (Abbott Molecular, 07J0001). Per reaction, a master mix together with the BAC was prepared by adding 2.5 µL of fluorophores 0.1 mM, 5 µL of 0.1 mM dTTP, 10 µL of 0.1 mM dNTP mix, 5 µL of 10x reaction buffer, 10 µL of enzyme mix; the mix was topped up to 50 µL with nuclease-free water. Nick translation was performed by incubating the samples at 15 °C and the timing varied between samples (6 h for RP23-378I14 and RP24-169C1 and 14 h for RP23-391D18) and the reaction was stopped by a 10-min incubation at 70 °C.

Purification was done using the Oligo Clean & Concentrator kit (Zymo Research, D4061) according to the manufacturer's instructions. 200 µL of ethanol were used for the purification. Samples were eluted in 50 µL of nuclease-free water and kept at -20 °C until further use.

7.5.4 Hybridization

For fixation, the medium was removed and cells were rinsed once with PBS -Ca^{2+} -Mg^{2+} and 4% PFA was added to the wells and incubated for 15 min in the fume hood. Cells were washed twice with -Ca^{2+} -Mg^{2+}, 5 min each and the samples were kept in -Ca^{2+} -Mg^{2+} or processed immediately.

The hybridization probes were prepared by adding the purified probe(s), 3 µg of COT human DNA (Sigma, 11581074001), 20 µg of yeast tRNAs (Invitrogen, AM7118) and topped up with water to 40 µL; if cells were seeded on coverslips, 5 µL per probe were used and 10 µL if cells were seeded on 8-well µ-slide ibidi chambers. 0.1× of total volume of 3 M sodium acetate were added and 3× of total volume of ice-cold 100% ethanol (kept at -20 °C) were added. The mix

was vortexed on the highest setting and spun down before centrifuging at maximum speed for 30 min at 4 °C. The supernatant was carefully removed by pipetting and the probes were carefully washed with cold 70% ethanol and centrifuging at maximum speed for 5 min at 4 °C. The supernatant was carefully removed by pipetting and the probes were air dried and resuspended in a hybridization buffer; if cells were seeded on coverslips, the probes were resuspended in 7 µL of hybridization buffer per coverslip and in 200 µL of hybridization buffer for 8-well µ-slide ibidi chambers.

Cells were permeabilized for 10 min with freshly prepared PBS supplemented with Triton X-100 0.1% and saponin 0.1% and cells were washed twice with -Ca^{2+} -Mg^{2+}, 5 min each. Proteins were then precipitated with HCl 0.1 N for 15 min and washed once with 2× SSC buffer for 10 min afterwards. Cells were then incubated in the equilibrating solution for 30-45 min. The equilibrating solution was removed and the probes were added to the samples: for coverslips, the probe in hybridization buffer was added to a glass slide and the cells facing the solution were placed on top, sealing the coverslips with rubber solution; for 8-well µ-slide ibidi chambers, the probe in hybridization buffer was added. Samples were light-protected and incubated for 10 min at 85 °C and then transferred to a humid hybridization oven for 16 h. After incubation, the rubber solution on the coverslips was removed by soaking the glass slide in 2× SSC buffer and the coverslips and placed facing upwards; for the 8-well µ-slide ibidi chambers the hybridization solution was removed. Samples were washed twice with 2× SSC buffer, each for 5 min; washed three times with 1× SSC buffer at 45 °C, each for 5 min; washed three times with 0.1× SSC buffer at 45 °C, each for 5 min. Samples were counterstained with DAPI 1:2000 for 10 min and afterwards they were rinsed once with PBS -Ca^{2+} -Mg^{2+}, rinsed once with miliQ water, rinsed once with PBS -Ca^{2+} -Mg^{2+} and finally mounted with ProLong Gold Antifade Mountant (Invitrogen, P36930) or VECTASHIELD Vibrance® Antifade Mounting Medium with DAPI (Vector Laboratories, H-1800-10). Before imaging, samples mounted with ProLong were cured for at least 24 h and at least 1 h for VECTASHIELD.

7.6 Nucleic acid work

7.6.1 Genomic DNA (gDNA) isolation

The medium from cells growing on 96-well plates was removed and 50 µL of QuickExtract™ DNA Extraction Solution (Biozym, QE09050) were added. Plates were incubated at 55 °C for 1 h followed by 15 min at 75 °C. gDNA was either used immediately and can be stored

at 4 °C for short-term or at -20 °C for long-term. For RT-qPCR, gDNA was diluted 1:30 with nuclease-free water.

7.6.2 Isolation of high molecular weight gDNA and library preparation

C3H/Bl6 cells were purified from feeders and grown on gelatin-coated plates in 2i/LIF for no more than five days and gDNA was isolated as previously described (passage 24). For lungs, 300 µL of QuickExtract™ DNA Extraction Solution (Biozym, QE09050) were added and samples were grinded, followed by an incubation at 55 °C for 1 h followed by 15 min at 75 °C.

gDNA samples were topped up to 500 µL with gDNA dilution buffer and 1 mL of the lower phase of pre-equilibrated phenol:chloroform:isoamyl alcohol pH 8 were added to each sample; samples were shaken to homogeneize and transferred to a phase lock tube. Samples were centrifuged and the upper phase was transferred to a LoBind tube containing 50 µL of sodium acetate 3 M and 1 volume of isopropanol was added; samples were incubated for 1 h at - 20 °C. The gDNA was pelleted by centrifugation at maximum speed for 1 h at 4 °C, with two washing steps with 70% ethanol for 10 min at maximum speed at 4 °C; gDNA was incubated at 37 °C for 5 min to remove all liquid. Tris pH 8 was added to the pellets (50 µL for lung samples and 40 µL for cell samples) and the samples were incubated at 50 °C for 2 h. Samples were run on a gel to assess integrity of the high molecular weight gDNA.

Size selection of fragments larger than 30 kb, adapter ligation and barcode ligation were done according to the manufacturer's instruction using the Ligation Sequencing Kit V14 from Oxford Nanopore Technologies.

7.6.3 RNA isolation and complementary DNA (cDNA) preparation

TRIzol™ Reagent was added directly to the samples; for EBs, RNA was added directly to the plate and equally distributed to cover the entire cell surface. Plates were either stored at −80°C or immediately processed for RNA extraction. EBs remained attached to the well of the plates so with a pipette tip, they were detached and transferred to a 1.5-mL tube and homogenized using a handheld pestle. An equal volume of 99.9% ethanol was added to the TRIzol™ lysates and total RNA was subsequently extracted according to the manufacturer's instructions using the Direct-zol™ RNA MicroPrep Kit. RNA was eluted in nuclease-free water. RNA concentration and purity were measured using a DS-11 FX+ Spectrophotometer/Fluorometer (DeNovix). RNA samples with 260/280 ratios between 1.8 and 2.0 were considered acceptable for downstream applications.

Complementary DNA (cDNA) was synthesized from the isolated RNA. For each reaction, 500 ng of total RNA in a final volume of 5 µL was mixed with 0.435 µL of 0.1 mM oligo(dT) and 0.435 µL of 10 mM dNTP (NEB, N0447S) mix. The mixture was briefly vortexed, incubated at 65°C for 5 min, and immediately chilled on ice on a 96-well metal rack. Following a brief centrifugation, the reverse transcription master mix was added to each sample: 1.739 µL of 5× reverse transcription buffer (IMB Protein Production Core Facility), 0.87 µL of 0.1 mM DTT (Sigma Aldrich, D0632-25G), 0.109 µL of RNasin® Ribonuclease Inhibitor (Promega, N2515) and 0.25 µL of M-MLV reverse transcriptase (IMB Protein Production Core Facility). Samples were mildly vortexed, briefly centrifuged, and incubated sequentially at 25°C for 10 min, 42°C for 50 min, and 70°C for 15 min in a thermocycler. The resulting cDNA was diluted to 300 µL of nuclease-free water and used for RT-qPCR analysis.

7.7 Quantitative PCR (qPCR)

RT-qPCR was performed using the LightCycler 480 System (Roche) in a final volume of 7 µL. 3.5 µL of either diluted cDNA or gDNA together with 3.5 µL of a master mix containing FastStart Universal SYBR Green Master (Roche, 4913914001) and primers at a final concentration of 300 nM were mixed and added to a LightCycler® 480 Multiwell 384-well plate (Roche, 04729749001). Plates were sealed before quantification with LightCycler® 480 sealing foil (Roche, 04729757001).

The samples were initially denatured at 95 °C for 10 min (ramp rate 4.8 °C/s), followed by 45 cycles of denaturation at 95 °C for 15 s (ramp rate 4.8 °C/s), and annealing-elongation at 60 °C for 1 min (ramp rate 2.5 °C/s), with single signal acquisition at each cycle. For the melting curve analysis, the samples were denatured at 95 °C for 15 s (ramp rate 4.8 °C/s), then held at 60 °C for 1 min (ramp rate 2.5 °C/s), followed by a gradual melt at 95 °C (ramp rate 0.11 °C/s) with continuous signal acquisition every 5 °C. Finally, the samples were cooled at 40 °C for 30 s (ramp rate 2.5 °C/s). Cp values were determined using the Abs Quant/2nd Derivative Max analysis mode in the LightCycler 480 software (version 1.5.1.62). The values were normalized against the geometric mean of Cp values from housekeeping genes. If needed, further normalizing was performed against WT controls.

7.8 Genotyping

For *Rosa26* genotyping, the TaKaRa LA Taq ® DNA Polymerase Hot-Start Version with the 10× buffer was used (Takara, RR042A) following manufacturer's instructions with some modifications. Per 100 µL of master mix, 0.25 µL of La Taq-HS enzyme were used, primers were

used at a final concentration of 0.6 µM and depending on the cell confluency before gDNA extraction, 0.8 to 2 µL of template solution were used; p99 was used as a forward primer and p58 as a reverse primer. The following thermal cycling conditions were used: initially denaturation at 94 °C for 3 min, followed by 33 cycles of denaturation at 98 °C for 10 s, annealing at 60 °C for 15 s, and elongation at 68 °C for 8 min 30 s. A final extension at 72 °C for 10 min was followed by holding the samples at 10 °C. The PCR products were analyzed by running them on an agarose gel, with the gel percentage selected based on the size of PCR product.

For *piggyBac* transposition, qPCR on gDNA was used. All genes on the shredder vector (*Cas9*, *EGFP*, *Bl6 gRNA*, *BlastiR*) were amplified; *AmpR* was also added to ensure that only transposition of the shredder vector occurred. Samples were normalized to autosomal *Hbb-g* and *Nanog* genes.

7.9 Immunofluorescence stainings

For mESCs, cells were seeded onto ifeeder-coated 8-well µ-slide ibidi chambers and for EBs, they were seeded on gelatin-coated coverslips (Starstedt, 83.1840.002). Once they were at around 85% confluency, samples were washed twice with PBS -Ca^{2+} -Mg^{2+}. The cells were then fixed with 4% paraformaldehyde in PBS -Ca^{2+} -Mg^{2+} for 15 minutes at room temperature. After three washes with PBS -Ca^{2+} -Mg^{2+}, samples were stored at 4 °C in PBS -Ca^{2+} -Mg^{2+} until staining.

For permeabilization, the samples were incubated in 0.3% Triton X-100 in PBS -Ca^{2+} -Mg^{2+} for 3 minutes, followed by two PBS -Ca^{2+} -Mg^{2+} of 5 min each. Blocking was performed using 1% BSA (Pan Biotech, P06-1391500) in PBS -Ca^{2+} -Mg^{2+} for 30 minutes at room temperature. After one additional wash in PBS -Ca^{2+} -Mg^{2+}, samples were incubated overnight at 4 °C with the respective primary antibodies, diluted in 0.1% BSA in PBS -Ca^{2+} -Mg^{2+}. Following three washes with PBS -Ca^{2+} -Mg^{2+}, samples incubated with the respective secondary antibodies, diluted in 0.1% BSA in PBS -Ca^{2+} -Mg^{2+}, for 1 hour at room temperature. They were then washed three times with PBS -Ca^{2+} -Mg^{2+} and counterstained with DAPI 1:2000 for 10 min and afterwards they were rinsed once with PBS -Ca^{2+} -Mg^{2+}, rinsed once with miliQ water, rinsed once with PBS -Ca^{2+} -Mg^{2+} and finally mounted with ProLong Gold Antifade Mountant (Invitrogen, P36930) or VECTASHIELD Vibrance® Antifade Mounting Medium with DAPI (Vector Laboratories, H-1800-10). Before imaging, samples mounted with ProLong were cured for at least 24 h and at least 1 h for VECTASHIELD.

For myosin stainings, an antigen retrieval step was performed. After fixation, the antigen retrieval buffer was boiled to 115 °C and once it was boiling it was added to the EBs and incubated for 20 min at 98 °C; more buffer was added during the incubation time if needed. The samples were then placed on a water-filled chamber for 20 min and washed three times with PBS -Ca^{2+} -Mg^{2+} and the protocol continued from the permeabilization step.

7.10 Long read sequencing and analysis

Sequencing was performed using a minION flow cell on two rounds. 400 ng (~15 fmol) of library pool were loaded on a minion flow cell (sequencer ID: MN24510, flow cell type: FLO-MIN114, flow cell ID: FAX59673) and the sequencing was run for 26 h 10 min. The flow cell was then washed with the DNAse I solution from the Flow Cell Wash Kit (Oxford Nanopore Technologies). The library pool was loaded again for a total running time of 72 h.

For base calling, demultiplexing and adaptor trimming: dorado v0.3.4 was used for base calling the raw pod5 input files in 'hac' accuracy mode using the "dna_r10.4.1_e8.2_400bps_hac@v4.2.0" model to produce bam files that include information about base modifications. Base modification information was extracted from bam files using modkit v0.1.12 using the options "--cpg --ignore h --combine-strands" to produce pileup information in the form of bedMethyl files. To produce sequencing reads in fastq format, guppy v6.5.7 was used for demultiplexing and adaptor trimming.

Sequencing reads were mapped against the *Mus musculus* GRCm39 genome assembly (release 109) using minimap2 v2.26 with the options "-y -ax map-ont --MD --cs --secondary=no".

pycoQC v2.5.2, nanoplot v1.41.3 and FastQC v0.12.1 were used to obtain metrics for read length distribution and assess overall sequencing quality. To estimate sequencing depth per chromosome, mosdepth v0.3.3 was used after alignment, and ratios of mapped versus total reads per chromosome were obtained using samtools idxstats v1.17. MultiQC v1.15 was used to visualize results.

7.11 Microscopy and image analysis

Images were acquired taking *Z*-planes using a fluorescence spinning disc confocal microscope, VisiScope 5 Elements (Visitron Systems), which is based on a Ti-2E (Nikon) stand and equipped with a spinning disc unit (CSU-W1, 50 µm pinhole; Yokogawa). The set-up was controlled using VisiView 5.0 software, and images were acquired with a ×100/1.49 NA oil-

immersion objective and a sCMOS camera (BSI; Photometrics). 3D stacks of images were recorded for each sample. Raw .companion.ome files were processed using Fiji (ImageJ2, v2.16) and converted to .tif files using a macro program. The intensity of all channels was equally adjusted for all images per replicate. For DNA FISH, the resulting .tif merged files containing intensity projections were produced from *Z*-stacks and further used for quantification experiments. For immunostainings, the resulting .tif merged files contained maximum intensity projections.

mESCs grow as 3D colonies, therefore for DNA FISH dot counting, a region of *Z*-stacks was defined. Within that *Z*-stack, using the Cell Counter tool, cells with one or two X dots as well as cells with one or two chromosome 6 dots were counted and recorded. The process was repeated for all acquired images in each passage, in each replicate or for each sex, depending on the experiment.

7.12 Software

R Studio Version 2022.12.0+353 (2022.12.0+353) was used to plot graphs.

Adobe Illustrator 2025 was used to generate and assemble figures.

8. References

Abdulai-Saiku, Samira, Shweta Gupta, Dan Wang, et al. 2025. “The Maternal X Chromosome Affects Cognition and Brain Ageing in Female Mice.” Nature 638 (8049): 152–159.

Abruzzo, M. A., M. Mayer, and P. A. Jacobs. 1985. “Aging and Aneuploidy: Evidence for the Preferential Involvement of the Inactive X Chromosome.” Cytogenetics and Cell Genetics 39 (4): 275–278.

Adekunbi, Daniel A., Hillary F. Huber, Gloria A. Benavides, et al. 2025. “Sex-Specific Decline in Prefrontal Cortex Mitochondrial Bioenergetics in Aging Baboons Correlates with Walking Speed.” Neurobiology of Aging 151 (July): 1–12.

Adikusuma, Fatwa, Nicole Williams, Frank Grutzner, James Hughes, and Paul Thomas. 2017. “Targeted Deletion of an Entire Chromosome Using CRISPR/Cas9.” Molecular Therapy: The Journal of the American Society of Gene Therapy 25 (8): 1736–1738.

Adrianse, Robin L., Kaleb Smith, Tonibelle Gatbonton-Schwager, et al. 2018. “Perturbed Maintenance of Transcriptional Repression on the Inactive X-Chromosome in the Mouse Brain after Xist Deletion.” Epigenetics & Chromatin 11 (1): 50.

Alfeghaly, Charbel, Gaël Castel, Emmanuel Cazottes, et al. 2024. “XIST Dampens X Chromosome Activity in a SPEN-Dependent Manner during Early Human Development.” Nature Structural & Molecular Biology 31 (10): 1589–1600.

Allsopp, R. C., E. Chang, M. Kashefi-Aazam, et al. 1995. “Telomere Shortening Is Associated with Cell Division in Vitro and in Vivo.” Experimental Cell Research 220 (1): 194–200.

Allsop, Ryan N., Jeffrey Boeren, Beatrice F. Tan, et al. 2025. “X-Chromosome Upregulation Operates on a Gene-by-Gene Basis at RNA and Protein Levels.” Nature Communications 16 (1): 8352.

Almeida, Mafalda, Greta Pintacuda, Osamu Masui, et al. 2017. “PCGF3/5-PRC1 Initiates Polycomb Recruitment in X Chromosome Inactivation.” Science (New York, N.Y.) 356 (6342): 1081–1084.

Amato-Menker, Carly J., Quinn Hopen, Andrea Pettit, et al. 2024. “XX Sex Chromosome Complement Modulates Immune Responses to Heat-Killed Streptococcus Pneumoniae Immunization in a Microbiome-Dependent Manner.” Biology of Sex Differences 15 (1): 21.

Amos-Landgraf, James M., Amy Cottle, Robert M. Plenge, et al. 2006. “X Chromosome-Inactivation Patterns of 1,005 Phenotypically Unaffected Females.” The American Journal of Human Genetics 79 (3): 493–499.

Anguera, Montserrat C., Ruslan Sadreyev, Zhaoqing Zhang, et al. 2012. “Molecular Signatures of Human Induced Pluripotent Stem Cells Highlight Sex Differences and Cancer Genes.” Cell Stem Cell 11 (1): 75–90.

Arai, Daisuke, and Yoichi Nakao. 2021. “Efficient Biallelic Knock-in in Mouse Embryonic Stem Cells by in Vivo-Linearization of Donor and Transient Inhibition of DNA Polymerase θ/DNA-PK.” Scientific Reports 11 (1): 18132.

Astre, Gwendoline, Tehila Atlan, Uri Goshtchevsky, et al. 2023. “Genetic Perturbation of AMP Biosynthesis Extends Lifespan and Restores Metabolic Health in a Naturally Short-Lived Vertebrate.” Developmental Cell 58 (15): 1350–1364.e10.

Austad, Steven N. 2006. “Why Women Live Longer than Men: Sex Differences in Longevity.” Gender Medicine 3 (2): 79–92.

Austad, Steven N., and Kathleen E. Fischer. 2016. “Sex Differences in Lifespan.” Cell Metabolism 23 (6): 1022–1033.

Baar, Emma L., Kathryn A. Carbajal, Irene M. Ong, and Dudley W. Lamming. 2016. “Sex- and Tissue-Specific Changes in mTOR Signaling with Age in C57BL/6J Mice.” Aging Cell 15 (1): 155–166.

Balaton, Bradley P., and Carolyn J. Brown. 2016. “Escape Artists of the X Chromosome.” Trends in Genetics: TIG 32 (6): 348–359.

Balaton, Bradley P., Thomas Dixon-McDougall, Samantha B. Peeters, and Carolyn J. Brown. 2018. “The eXceptional Nature of the X Chromosome.” Human Molecular Genetics 27 (R2): R242–R249.

Barr, M. L., and E. G. Bertram. 1949. “A Morphological Distinction between Neurones of the Male and Female, and the Behaviour of the Nucleolar Satellite during Accelerated Nucleoprotein Synthesis.” Nature 163 (4148): 676.

Basilicata, M. Felicia, and Claudia Isabelle Keller Valsecchi. 2021. “The Good, the Bad, and the Ugly: Evolutionary and Pathological Aspects of Gene Dosage Alterations.” PLoS Genetics 17 (12): e1009906.

Becker, Sebastian, and Jens Boch. 2021. “TALE and TALEN Genome Editing Technologies.” Gene and Genome Editing 2 (100007): 100007.

Bedzhov, Ivan, Hani Alotaibi, M. Felicia Basilicata, et al. 2013. “Adhesion, but Not a Specific Cadherin Code, Is Indispensable for ES Cell and Induced Pluripotency.” Stem Cell Research 11 (3): 1250–1263.

Bellott, Daniel W., Jennifer F. Hughes, Helen Skaletsky, et al. 2014. “Mammalian Y Chromosomes Retain Widely Expressed Dosage-Sensitive Regulators.” Nature 508 (7497): 494–499.

Belmont, A. S., F. Bignone, and P. O. Ts’o. 1986. “The Relative Intranuclear Positions of Barr Bodies in XXX Non-Transformed Human Fibroblasts.” Experimental Cell Research 165 (1): 165–179.

Ben-David, Uri, and Angelika Amon. 2020. “Context Is Everything: Aneuploidy in Cancer.” Nature Reviews. Genetics 21 (1): 44–62.

Benetos, A., K. Okuda, M. Lajemi, et al. 2001. “Telomere Length as an Indicator of Biological Aging: The Gender Effect and Relation with Pulse Pressure and Pulse Wave Velocity: The Gender Effect and Relation with Pulse Pressure and Pulse Wave Velocity.” Hypertension 37 (2 Pt 2): 381–385.

Bennett-Baker, Pamela E., Jodi Wilkowski, and David T. Burke. 2003. “Age-Associated Activation of Epigenetically Repressed Genes in the Mouse.” Genetics 165 (4): 2055–2062.

Berletch, Joel B., Wenxiu Ma, Fan Yang, et al. 2015. “Escape from X Inactivation Varies in Mouse Tissues.” PLoS Genetics 11 (3): e1005079.

Bibel, Miriam, Jens Richter, Katrin Schrenk, et al. 2004. “Differentiation of Mouse Embryonic Stem Cells into a Defined Neuronal Lineage.” Nature Neuroscience 7 (9): 1003–1009.

Bjedov, Ivana, Janne M. Toivonen, Fiona Kerr, et al. 2010. “Mechanisms of Life Span Extension by Rapamycin in the Fruit Fly Drosophila Melanogaster.” Cell Metabolism 11 (1): 35–46.

Bolduc, Véronique, Pierre Chagnon, Sylvie Provost, et al. 2008. “No Evidence That Skewing of X Chromosome Inactivation Patterns Is Transmitted to Offspring in Humans.” The Journal of Clinical Investigation 118 (1): 333–341.

Borrás, C., M. Ferrando, M. Inglés, et al. 2021. “Estrogen Replacement Therapy Induces Antioxidant and Longevity-Related Genes in Women after Medically Induced Menopause.” Oxidative Medicine and Cellular Longevity 2021 (1): 8101615.

Bosco, Nazario, Aleah Goldberg, Xin Zhao, et al. 2023. “KaryoCreate: A CRISPR-Based Technology to Study Chromosome-Specific Aneuploidy by Targeting Human Centromeres.” Cell 186 (9): 1985–2001.e19.

Bost, Chloé, Marina I. Arleevskaya, Wesley H. Brooks, Samuel Plaza, Jean-Charles Guery, and Yves Renaudineau. 2022. “Long Non-Coding RNA Xist Contribution in Systemic Lupus Erythematosus and Rheumatoid Arthritis.” Clinical Immunology (Orlando, Fla.) 236 (108937): 108937.

Brenes, Alejandro J., Harunori Yoshikawa, Dalila Bensaddek, et al. 2021. “Erosion of Human X Chromosome Inactivation Causes Major Remodeling of the iPSC Proteome.” Cell Reports 35 (4): 109032.

Brickman, Joshua M., and Palle Serup. 2017. “Properties of Embryoid Bodies.” Wiley Interdisciplinary Reviews. Developmental Biology 6 (2). https://doi.org/10.1002/wdev.259.

Brons, I. Gabrielle M., Lucy E. Smithers, Matthew W. B. Trotter, et al. 2007. “Derivation of Pluripotent Epiblast Stem Cells from Mammalian Embryos.” Nature 448 (7150): 191–195.

Bunting, Mark D., Gelshan I. Godahewa, Nicole O. McPherson, et al. 2024. “Investigating the Potential of X Chromosome Shredding for Mouse Genetic Biocontrol.” Scientific Reports 14 (1): 13466.

Busque, L., R. Mio, J. Mattioli, et al. 1996. “Nonrandom X-Inactivation Patterns in Normal Females: Lyonization Ratios Vary with Age.” Blood 88 (1): 59–65.

Byers, Candice, Catrina Spruce, Haley J. Fortin, et al. 2022. “Genetic Control of the Pluripotency Epigenome Determines Differentiation Bias in Mouse Embryonic Stem Cells.” The EMBO Journal 41 (2): e109445.

Cabrera, Alan, Hailey I. Edelstein, Fokion Glykofrydis, et al. 2022. “The Sound of Silence: Transgene Silencing in Mammalian Cell Engineering.” Cell Systems 13 (12): 950–973.

Calaway, John D., Alan B. Lenarcic, John P. Didion, et al. 2013. “Genetic Architecture of Skewed X Inactivation in the Laboratory Mouse.” PLoS Genetics 9 (10): e1003853.

Camuzard, Olivier, Sabine Santucci-Darmanin, Véronique Breuil, et al. 2016. “Sex-Specific Autophagy Modulation in Osteoblastic Lineage: A Critical Function to Counteract Bone Loss in Female.” Oncotarget 7 (41): 66416–66428.

Carosi, Julian M., Alexis Martin, Leanne K. Hein, et al. 2025. “Autophagy across Tissues of Aging Mice.” PloS One 20 (6): e0325505.

Carrel, Laura, and Carolyn J. Brown. 2017. “When the Lyon(ized Chromosome) Roars: Ongoing Expression from an Inactive X Chromosome.” Philosophical Transactions of the Royal Society of London. Series B, Biological Sciences 372 (1733). https://doi.org/10.1098/rstb.2016.0355.

Carrel, Laura, and Huntington F. Willard. 2005. “X-Inactivation Profile Reveals Extensive Variability in X-Linked Gene Expression in Females.” Nature 434 (7031): 400–404.

Cary, L. C., M. Goebel, B. G. Corsaro, H. G. Wang, E. Rosen, and M. J. Fraser. 1989. “Transposon Mutagenesis of Baculoviruses: Analysis of Trichoplusia Ni Transposon IFP2 Insertions within the FP-Locus of Nuclear Polyhedrosis Viruses.” Virology 172 (1): 156–169.

Cawthon, Richard M., Ken R. Smith, Elizabeth O’Brien, Anna Sivatchenko, and Richard A. Kerber. 2003. “Association between Telomere Length in Blood and Mortality in People Aged 60 Years or Older.” Lancet 361 (9355): 393–395.

Celli, Ludovica, Patrizia Gasparini, Ginevra Biino, Laura Zannini, and Miriana Cardano. 2024. “CRISPR/Cas9 Mediated Y-Chromosome Elimination Affects Human Cells Transcriptome.” Cell & Bioscience 14 (1): 15.

Chadwick, Lisa Helbling, Lisa M. Pertz, Karl W. Broman, Marisa S. Bartolomei, and Huntington F. Willard. 2006. “Genetic Control of X Chromosome Inactivation in Mice: Definition of the Xce Candidate Interval.” Genetics 173 (4): 2103–2110.

Chaligné, Ronan, Tatiana Popova, Marco-Antonio Mendoza-Parra, et al. 2015. “The Inactive X Chromosome Is Epigenetically Unstable and Transcriptionally Labile in Breast Cancer.” Genome Research 25 (4): 488–503.

Charmpilas, Nikolaos, Aggeliki Sotiriou, Konstantinos Axarlis, Nektarios Tavernarakis, and Thorsten Hoppe. 2024. “Reproductive Regulation of the Mitochondrial Stress Response in Caenorhabditis Elegans.” Cell Reports 43 (6): 114336.

Chen, Chen-Yun, Yuan-Yuan Cheng, Christopher Y. T. Yen, and Patrick C. H. Hsieh. 2017. “Mechanisms of Pluripotency Maintenance in Mouse Embryonic Stem Cells.” Cellular and Molecular Life Sciences: CMLS 74 (10): 1805–1817.

Chen, Chun-Kan, Mario Blanco, Constanza Jackson, et al. 2016. “Xist Recruits the X Chromosome to the Nuclear Lamina to Enable Chromosome-Wide Silencing.” Science (New York, N.Y.) 354 (6311): 468–472.

Cheng, De, Fan Zhang, Kenneth I. Porter, et al. 2024. “Humanization of the Mouse Tert Gene Reset Telomeres to Human Length.” Research Square, ahead of print, January 5. https://doi.org/10.21203/rs.3.rs-3617723/v1.

Chen, Guofeng, Wei Zhou, Dan Gong, et al. 2020. “Loss of X Chromosome Predicts Favorable Prognosis in Female Patients with t(8;21) Acute Myeloid Leukemia.” Leukemia & Lymphoma 61

(5): 1168–1177.

Chenoweth, Josh G., and Paul J. Tesar. 2010. “Isolation and Maintenance of Mouse Epiblast Stem Cells.” Methods in Molecular Biology (Clifton, N.J.) 636: 25–44.

Chen, Xingyi, Chaoran Shi, Meihui He, Siqi Xiong, and Xiaobo Xia. 2023. “Endoplasmic Reticulum Stress: Molecular Mechanism and Therapeutic Targets.” Signal Transduction and Targeted Therapy 8 (1): 352.

Chen, Xuqi, Rebecca McClusky, Yuichiro Itoh, Karen Reue, and Arthur P. Arnold. 2013. “X and Y Chromosome Complement Influence Adiposity and Metabolism in Mice.” Endocrinology 154 (3): 1092–1104.

Chiang, Shang-Yin, Hsin-Chieh Wu, Shu-Yu Lin, et al. 2021. “Usp11 Controls Cortical Neurogenesis and Neuronal Migration through Sox11 Stabilization.” Science Advances 7 (7): eabc6093.

Choi, Jiho, Aaron J. Huebner, Kendell Clement, et al. 2017. “Prolonged Mek1/2 Suppression Impairs the Developmental Potential of Embryonic Stem Cells.” Nature 548 (7666): 219–223.

Cho, Rebecca H., Hans B. Sieburg, and Christa E. Muller-Sieburg. 2008. “A New Mechanism for the Aging of Hematopoietic Stem Cells: Aging Changes the Clonal Composition of the Stem Cell Compartment but Not Individual Stem Cells.” Blood 111 (12): 5553–5561.

Chu, Ci, Qiangfeng Cliff Zhang, Simão Teixeira da Rocha, et al. 2015. “Systematic Discovery of Xist RNA Binding Proteins.” Cell 161 (2): 404–416.

Chunduri, Narendra Kumar, Karen Barthel, and Zuzana Storchova. 2022. “Consequences of Chromosome Loss: Why Do Cells Need Each Chromosome Twice?” Cells 11 (9). https://doi.org/10.3390/cells11091530.

Clocchiatti, Andrea, Elisa Cora, Yosra Zhang, and G. Paolo Dotto. 2016. “Sexual Dimorphism in Cancer.” Nature Reviews. Cancer 16 (5): 330–339.

Cocchiararo, Ilaria, Mélanie Cornut, Hadrien Soldati, Alessandro Bonavoglia, and Perrine Castets. 2022. “Back to Basics: Optimization of DNA and RNA Transfer in Muscle Cells Using Recent Transfection Reagents.” Experimental Cell Research 421 (2): 113392.

Colognori, David, Hongjae Sunwoo, Andrea J. Kriz, Chen-Yu Wang, and Jeannie T. Lee. 2019. “Xist Deletional Analysis Reveals an Interdependency between Xist RNA and Polycomb Complexes for Spreading along the Inactive X.” Molecular Cell 74 (1): 101–117.e10.

Corder, Katelynn M., Jessica M. Hoffman, Anamarija Sogorovic, and Steven N. Austad. 2023. “Behavioral Comparison of the C57BL/6 Inbred Mouse Strain and Their CB6F1 Siblings.” Behavioural Processes 207 (104836): 104836.

Csankovszki, G., B. Panning, B. Bates, J. R. Pehrson, and R. Jaenisch. 1999. “Conditional Deletion of Xist Disrupts Histone macroH2A Localization but Not Maintenance of X Inactivation.” Nature Genetics 22 (4): 323–324.

Cuesta-Zuluaga, Jacobo de la, Scott T. Kelley, Yingfeng Chen, et al. 2019. “Age- and Sex-Dependent Patterns of Gut Microbial Diversity in Human Adults.” mSystems 4 (4). https://doi.org/10.1128/mSystems.00261-19.

Cyr, Brianna, and Juan Pablo de Rivero Vaccari. 2023. “Sex Differences in the Inflammatory Profile in the Brain of Young and Aged Mice.” Cells (Basel, Switzerland) 12 (10). https://doi.org/10.3390/cells12101372.

Czechanski, Anne, Candice Byers, Ian Greenstein, et al. 2014. “Derivation and Characterization of Mouse Embryonic Stem Cells from Permissive and Nonpermissive Strains.” Nature Protocols 9 (3): 559–574.

Dang, Weiwei, Kristan K. Steffen, Rocco Perry, et al. 2009. “Histone H4 Lysine 16 Acetylation Regulates Cellular Lifespan.” Nature 459 (7248): 802–807.

D’Antonio-Chronowska, Agnieszka, Margaret K. R. Donovan, William W. Young Greenwald, et al. 2019. “Association of Human iPSC Gene Signatures and X Chromosome Dosage with Two Distinct Cardiac Differentiation Trajectories.” Stem Cell Reports 13 (5): 924–938.

Davis, Anthony J., and David J. Chen. 2013. “DNA Double Strand Break Repair via Non-Homologous End-Joining.” Translational Cancer Research 2 (3): 130–143.

Davis, Emily J., Lauren Broestl, Samira Abdulai-Saiku, et al. 2020. “A Second X Chromosome Contributes to Resilience in a Mouse Model of Alzheimer’s Disease.” Science Translational Medicine 12 (558). https://doi.org/10.1126/scitranslmed.aaz5677.

Davis, Emily J., Iryna Lobach, and Dena B. Dubal. 2019. “Female XX Sex Chromosomes Increase Survival and Extend Lifespan in Aging Mice.” Aging Cell 18 (1): e12871.

Delbridge, Alex R. D., Andrew J. Kueh, Francine Ke, et al. 2019. “Loss of p53 Causes Stochastic Aberrant X-Chromosome Inactivation and Female-Specific Neural Tube Defects.” Cell Reports 27 (2): 442–454.e5.

Deng, Han-Xiang, Wenjie Chen, Seong-Tshool Hong, et al. 2011. “Mutations in UBQLN2 Cause Dominant X-Linked Juvenile and Adult-Onset ALS and ALS/dementia.” Nature 477 (7363): 211–215.

Deng, Xinxian, Wenxiu Ma, Vijay Ramani, et al. 2015. “Bipartite Structure of the Inactive Mouse X Chromosome.” Genome Biology 16 (1): 152.

Dong, Wendy, and Boris Kantor. 2021. “Lentiviral Vectors for Delivery of Gene-Editing Systems Based on CRISPR/Cas: Current State and Perspectives.” Viruses 13 (7): 1288.

Donnelly, Michelle L. L., Lorraine E. Hughes, Garry Luke, et al. 2001. “The ‘Cleavage’ Activities of Foot-and-Mouth Disease Virus 2A Site-Directed Mutants and Naturally Occurring ‘2A-like’ Sequences.” The Journal of General Virology 82 (Pt 5): 1027–1041.

Donnelly, Michelle L. L., Garry Luke, Amit Mehrotra, et al. 2001. “Analysis of the Aphthovirus 2A/2B Polyprotein ‘Cleavage’ Mechanism Indicates Not a Proteolytic Reaction, but a Novel Translational Effect: A Putative Ribosomal ‘Skip.’” The Journal of General Virology 82 (Pt 5): 1013–1025.

Dormann, Dorothee, and Edward Anton Lemke. 2024. “Adding Intrinsically Disordered Proteins to Biological Ageing Clocks.” Nature Cell Biology, ahead of print, May 23. https://doi.org/10.1038/s41556-024-01423-w.

Dos Santos, Carla S., Tito Mendes, and Agostinho Antunes. 2022. “The Genes from the

Pseudoautosomal Region 1 (PAR1) of the Mammalian Sex Chromosomes: Synteny, Phylogeny and Selection." Genomics 114 (4): 110419.

Dossin, François, Inês Pinheiro, Jan J. Żylicz, et al. 2020. "SPEN Integrates Transcriptional and Epigenetic Control of X-Inactivation." Nature 578 (7795): 455–460.

Dou, Diana R., Yanding Zhao, Julia A. Belk, et al. 2024. "Xist Ribonucleoproteins Promote Female Sex-Biased Autoimmunity." Cell 187 (3): 733–749.e16.

Dror, Iris, Tsotne Chitiashvili, Shawn Y. X. Tan, et al. 2024. "XIST Directly Regulates X-Linked and Autosomal Genes in Naive Human Pluripotent Cells." Cell 187 (1): 110–129.e31.

Dulken, Ben, and Anne Brunet. 2015. "Stem Cell Aging and Sex: Are We Missing Something?" Cell Stem Cell 16 (6): 588–590.

Dumanski, Jan P., Jonatan Halvardson, Hanna Davies, et al. 2021. "Immune Cells Lacking Y Chromosome Show Dysregulation of Autosomal Gene Expression." Cellular and Molecular Life Sciences: CMLS 78 (8): 4019–4033.

Dumanski, Jan P., Jean-Charles Lambert, Chiara Rasi, et al. 2016. "Mosaic Loss of Chromosome Y in Blood Is Associated with Alzheimer Disease." The American Journal of Human Genetics 98 (6): 1208–1219.

Dunford, Andrew, David M. Weinstock, Virginia Savova, et al. 2017. "Tumor-Suppressor Genes That Escape from X-Inactivation Contribute to Cancer Sex Bias." Nature Genetics 49 (1): 10–16.

Eckersley-Maslin, Melanie A., Simão Teixeira da Rocha, Samantha Mancino, et al. 2024. "Exploring the Stability of Genomic Imprinting and X-Chromosome Inactivation in the Aged Brain." Aging Biology 2 (1): 20240030.

Engreitz, Jesse M., Amy Pandya-Jones, Patrick McDonel, et al. 2013. "The Xist lncRNA Exploits Three-Dimensional Genome Architecture to Spread across the X Chromosome." Science (New York, N.Y.) 341 (6147): 1237973.

Escamilla-Del-Arenal, M., S. T. da Rocha, C. G. Spruijt, et al. 2013. "Cdyl, a New Partner of the Inactive X Chromosome and Potential Reader of H3K27me3 and H3K9me2." Molecular and Cellular Biology 33 (24): 5005–5020.

Fang, He, Christine M. Disteche, and Joel B. Berletch. 2019. "X Inactivation and Escape: Epigenetic and Structural Features." Frontiers in Cell and Developmental Biology 7 (October): 219.

Feil, R., J. Wagner, D. Metzger, and P. Chambon. 1997. "Regulation of Cre Recombinase Activity by Mutated Estrogen Receptor Ligand-Binding Domains." Biochemical and Biophysical Research Communications 237 (3): 752–757.

Finley, Daniel, and Miguel A. Prado. 2020. "The Proteasome and Its Network: Engineering for Adaptability." Cold Spring Harbor Perspectives in Biology 12 (1): a033985.

Flemr, Matyas, and Marc Bühler. 2015. "Single-Step Generation of Conditional Knockout Mouse Embryonic Stem Cells." Cell Reports 12 (4): 709–716.

Forsberg, Lars A., Chiara Rasi, Niklas Malmqvist, et al. 2014. "Mosaic Loss of Chromosome Y in

Peripheral Blood Is Associated with Shorter Survival and Higher Risk of Cancer.” Nature Genetics 46 (6): 624–628.

Forsyth, Katherine S., Natalie E. Toothacre, Nikhil Jiwrajka, et al. 2024. “Maintenance of X Chromosome Inactivation after T Cell Activation Requires NF-κB Signaling.” Science Immunology 9 (100): eado0398.

Furman, Benjamin L. S., David C. H. Metzger, Iulia Darolti, et al. 2020. “Sex Chromosome Evolution: So Many Exceptions to the Rules.” Genome Biology and Evolution 12 (6): 750–763.

Gadek, Margaret, Cayce K. Shaw, Samira Abdulai-Saiku, et al. 2025. “Aging Activates Escape of the Silent X Chromosome in the Female Mouse Hippocampus.” Science Advances 11 (10): eads8169.

Gagou, Mary E., Pedro Zuazua-Villar, and Mark Meuth. 2010. “Enhanced H2AX Phosphorylation, DNA Replication Fork Arrest, and Cell Death in the Absence of Chk1.” Molecular Biology of the Cell 21 (5): 739–752.

Galupa, Rafael, and Edith Heard. 2018. “X-Chromosome Inactivation: A Crossroads Between Chromosome Architecture and Gene Regulation.” Annual Review of Genetics 52 (November): 535–566.

Gardner, R. L., and F. A. Brook. 1997. “Reflections on the Biology of Embryonic Stem (ES) Cells.” The International Journal of Developmental Biology 41 (2): 235–243.

Garribba, Lorenza, Giuseppina De Feudis, Valentino Martis, et al. 2023. “Short-Term Molecular Consequences of Chromosome Mis-Segregation for Genome Stability.” Nature Communications 14 (1): 1353.

Gendrel, Anne-Valerie, Anwyn Apedaile, Heather Coker, et al. 2012. “Smchd1-Dependent and -Independent Pathways Determine Developmental Dynamics of CpG Island Methylation on the Inactive X Chromosome.” Developmental Cell 23 (2): 265–279.

Genolet, Oriana, Anna A. Monaco, Ilona Dunkel, Michael Boettcher, and Edda G. Schulz. 2021. “Identification of X-Chromosomal Genes That Drive Sex Differences in Embryonic Stem Cells through a Hierarchical CRISPR Screening Approach.” Genome Biology 22 (1): 110.

Gilbert, Luke A., Matthew H. Larson, Leonardo Morsut, et al. 2013. “CRISPR-Mediated Modular RNA-Guided Regulation of Transcription in Eukaryotes.” Cell 154 (2): 442–451.

Giorgetti, Luca, Bryan R. Lajoie, Ava C. Carter, et al. 2016. “Structural Organization of the Inactive X Chromosome in the Mouse.” Nature 535 (7613): 575–579.

Givens, Sophie E., Abygail A. Andebrhan, Eric G. Schmuck, et al. 2025. “Healthy Human Induced Pluripotent Stem Cell-Derived Cardiomyocytes Exhibit Sex Dimorphism Even without the Addition of Hormones.” Stem Cells (Dayton, Ohio) 43 (9). https://doi.org/10.1093/stmcls/sxaf038.

Gomes, Nuno M. V., Oliver A. Ryder, Marlys L. Houck, et al. 2011. “Comparative Biology of Mammalian Telomeres: Hypotheses on Ancestral States and the Roles of Telomeres in Longevity Determination.” Aging Cell 10 (5): 761–768.

González, Asier, Michael N. Hall, Sheng-Cai Lin, and D. Grahame Hardie. 2020. “AMPK and TOR: The Yin and Yang of Cellular Nutrient Sensing and Growth Control.” Cell Metabolism 31

(3): 472–492.

Gordon, Emily H., and Ruth E. Hubbard. 2020. “Differences in Frailty in Older Men and Women.” The Medical Journal of Australia 212 (4): 183–188.

Gordon-Keylock, Sabrina A. M., Melany Jackson, Caoxin Huang, et al. 2010. “Induction of Hematopoietic Differentiation of Mouse Embryonic Stem Cells by an AGM-Derived Stromal Cell Line Is Not Further Enhanced by Overexpression of HOXB4.” Stem Cells and Development 19 (11): 1687–1698.

Grant, Jennifer, Shantha K. Mahadevaiah, Pavel Khil, et al. 2012. “Rsx Is a Metatherian RNA with Xist-like Properties in X-Chromosome Inactivation.” Nature 487 (7406): 254–258.

Gravholt, Claus H., Mette Viuff, Jesper Just, et al. 2023. “The Changing Face of Turner Syndrome.” Endocrine Reviews 44 (1): 33–69.

Grigoryan, Ani, Johannes Pospiech, Stephen Krämer, et al. 2021. “Attrition of X Chromosome Inactivation in Aged Hematopoietic Stem Cells.” Stem Cell Reports 16 (4): 708–716.

Guévélou, Eric, Arnaud Huvet, Clara E. Galindo-Sánchez, et al. 2013. “Sex-Specific Regulation of AMP-Activated Protein Kinase (AMPK) in the Pacific Oyster Crassostrea Gigas.” Biology of Reproduction 89 (4): 100.

Gu, Liuqi, and James R. Walters. 2017. “Evolution of Sex Chromosome Dosage Compensation in Animals: A Beautiful Theory, Undermined by Facts and Bedeviled by Details.” Genome Biology and Evolution 9 (9): 2461–2476.

Guo, Renpeng, Xiaoying Ye, Jiao Yang, et al. 2018. “Feeders Facilitate Telomere Maintenance and Chromosomal Stability of Embryonic Stem Cells.” Nature Communications 9 (1): 2620.

Guo, Tony J. F., Wan Yi Liang, Gurpreet K. Singhera, Jasmine Memar Vaghri, Janice M. Leung, and Del R. Dorscheid. 2025. “Optimization of Chemical Transfection in Airway Epithelial Cell Lines.” BMC Biotechnology 25 (1): 10.

Gustavsson, Carolina, Kamal Yassin, Erik Wahlstrom, et al. 2010. “Sex-Different Hepatic Glycogen Content and Glucose Output in Rats.” In The Endocrine Society’s 92nd Annual Meeting, June 19–22, 2010 - San Diego. Endocrine Society.

Guttenbach, M., B. Koschorz, U. Bernthaler, T. Grimm, and M. Schmid. 1995. “Sex Chromosome Loss and Aging: In Situ Hybridization Studies on Human Interphase Nuclei.” American Journal of Human Genetics 57 (5): 1143–1150.

Gylemo, Björn, Maike Bensberg, Viktoria Hennings, et al. 2024. “A Landscape of X-Inactivation during Human T Cell Development.” Nature Communications 15 (1): 10527.

Gylemo, Bjorn, Maike Bensberg, and Colm E. Nestor. 2025. “A Whole-Organism Landscape of X-Inactivation in Humans.” eLife 14 (RP102701). https://doi.org/10.7554/eLife.102701.

Hackett, Jamie A., and M. Azim Surani. 2014. “Regulatory Principles of Pluripotency: From the Ground State up.” Cell Stem Cell 15 (4): 416–430.

Hajdarovic, Kaitlyn H., Doudou Yu, Lexi-Amber Hassell, et al. 2022. “Single-Cell Analysis of the Aging Female Mouse Hypothalamus.” Nature Aging 2 (7): 662–678.

Halter, Kevin, Jingyi Chen, Tadeas Priklopil, Asun Monfort, and Anton Wutz. 2024. “Cdk8 and Hira Mutations Trigger X Chromosome Elimination in Naive Female Hybrid Mouse Embryonic Stem Cells.” Chromosome Research: An International Journal on the Molecular, Supramolecular and Evolutionary Aspects of Chromosome Biology 32 (4): 12.

Hannum, Gregory, Justin Guinney, Ling Zhao, et al. 2013. “Genome-Wide Methylation Profiles Reveal Quantitative Views of Human Aging Rates.” Molecular Cell 49 (2): 359–367.

Harley, C. B., A. B. Futcher, and C. W. Greider. 1990. “Telomeres Shorten during Ageing of Human Fibroblasts.” Nature 345 (6274): 458–460.

Harper, Mary I., Mandy Fosten, and Marilyn Monk. 1982. “Preferential Paternal X Inactivation in Extraembryonic Tissues of Early Mouse Embryos.” Development (Cambridge, England) 67 (1): 127–135.

Haupt, Sue, Franco Caramia, Alan Herschtal, et al. 2019. “Identification of Cancer Sex-Disparity in the Functional Integrity of p53 and Its X Chromosome Network.” Nature Communications 10 (1): 5385.

Hayashi, Katsuhiko, Hiroshi Ohta, Kazuki Kurimoto, Shinya Aramaki, and Mitinori Saitou. 2011. “Reconstitution of the Mouse Germ Cell Specification Pathway in Culture by Pluripotent Stem Cells.” Cell 146 (4): 519–532.

Helbig, Roger, and Frank O. Fackelmayer. 2003. “Scaffold Attachment Factor A (SAF-A) Is Concentrated in Inactive X Chromosome Territories through Its RGG Domain.” Chromosoma 112 (4): 173–182.

Herens, C., E. Brasseur, M. Jamar, L. Vierset, I. Schoenen, and L. Koulischer. 1999. “Loss of the Y Chromosome in Bone Marrow Cells: Results on 1907 Consecutive Cases of Leukaemia and Preleukaemia.” Clinical and Laboratory Haematology 21 (1): 17–20.

Hernández Borrero, Liz J., and Wafik S. El-Deiry. 2021. “Tumor Suppressor p53: Biology, Signaling Pathways, and Therapeutic Targeting.” Biochimica et Biophysica Acta. Reviews on Cancer 1876 (1): 188556.

Hipp, Mark S., Prasad Kasturi, and F. Ulrich Hartl. 2019. “The Proteostasis Network and Its Decline in Ageing.” Nature Reviews. Molecular Cell Biology 20 (7): 421–435.

Hoelzl, Sarah, Tim P. Hasenbein, Stefan Engelhardt, and Daniel Andergassen. 2025. “Aging Promotes Reactivation of the Barr Body at Distal Chromosome Regions.” Nature Aging 5 (6): 984–996.

Horikawa, Izumi, Y. Jeffrey Chiang, Tricia Patterson, et al. 2005. “Differential Cis-Regulation of Human versus Mouse TERT Gene Expression in Vivo: Identification of a Human-Specific Repressive Element.” Proceedings of the National Academy of Sciences of the United States of America 102 (51): 18437–18442.

Horvath, Steve. 2013. “DNA Methylation Age of Human Tissues and Cell Types.” Genome Biology 14 (10): R115.

Huang, Yiyao, Junjie Feng, Jiannan Xu, et al. 2025. “Associations of Age and Sex with Characteristics of Extracellular Vesicles and Protein-Enriched Fractions of Blood Plasma.” Aging

Cell 24 (1): e14356.

Huang, Zhaohao, Binyao Chen, Xiuxing Liu, et al. 2021. “Effects of Sex and Aging on the Immune Cell Landscape as Assessed by Single-Cell Transcriptomic Analysis.” Proceedings of the National Academy of Sciences of the United States of America 118 (33): e2023216118.

Huret, Christophe, Léa Ferrayé, Antoine David, et al. 2024. “Altered X-Chromosome Inactivation Predisposes to Autoimmunity.” Science Advances 10 (18): eadn6537.

Huynh, Khanh D., and Jeannie T. Lee. 2003. “Inheritance of a Pre-Inactivated Paternal X Chromosome in Early Mouse Embryos.” Nature 426 (6968): 857–862.

Indra, A. K., X. Warot, J. Brocard, et al. 1999. “Temporally-Controlled Site-Specific Mutagenesis in the Basal Layer of the Epidermis: Comparison of the Recombinase Activity of the Tamoxifen-Inducible Cre-ER(T) and Cre-ER(T2) Recombinases.” Nucleic Acids Research 27 (22): 4324–4327.

Itoh, Yuichiro, Lisa C. Golden, Noriko Itoh, et al. 2019. “The X-Linked Histone Demethylase Kdm6a in CD4+ T Lymphocytes Modulates Autoimmunity.” The Journal of Clinical Investigation 129 (9): 3852–3863.

Jachowicz, Joanna W., Mackenzie Strehle, Abhik K. Banerjee, Mario R. Blanco, Jasmine Thai, and Mitchell Guttman. 2022. “Xist Spatially Amplifies SHARP/SPEN Recruitment to Balance Chromosome-Wide Silencing and Specificity to the X Chromosome.” Nature Structural & Molecular Biology 29 (3): 239–249.

Jacobson, Elsie C., Amy Pandya-Jones, and Kathrin Plath. 2022. “A Lifelong Duty: How Xist Maintains the Inactive X Chromosome.” Current Opinion in Genetics & Development 75 (101927): 101927.

Jäger, Natalie, Matthias Schlesner, David T. W. Jones, et al. 2013. “Hypermutation of the Inactive X Chromosome Is a Frequent Event in Cancer.” Cell 155 (3): 567–581.

Jašarević, Eldin, Kathleen E. Morrison, and Tracy L. Bale. 2016. “Sex Differences in the Gut Microbiome-Brain Axis across the Lifespan.” Philosophical Transactions of the Royal Society of London. Series B, Biological Sciences 371 (1688): 20150122.

Jenkins, Edmund Charles, Nagma Shah, Maria Gomez, et al. 2020. “Proteasome Mapping Reveals Sexual Dimorphism in Tissue-Specific Sensitivity to Protein Aggregations.” EMBO Reports 21 (4): e48978.

Jeon, Yesu, and Jeannie T. Lee. 2011. “YY1 Tethers Xist RNA to the Inactive X Nucleation Center.” Cell 146 (1): 119–133.

Jiang, Zhiwen, Patrick F. Sullivan, Tengfei Li, et al. 2025. “The X Chromosome’s Influences on the Human Brain.” Science Advances 11 (4): eadq5360.

Johansson, B. M., and M. V. Wiles. 1995. “Evidence for Involvement of Activin A and Bone Morphogenetic Protein 4 in Mammalian Mesoderm and Hematopoietic Development.” Molecular and Cellular Biology 15 (1): 141–151.

Jung, Moonjung, Ramanagouda Ramanagoudr-Bhojappa, Sylvie van Twest, et al. 2020. “Association of Clinical Severity with FANCB Variant Type in Fanconi Anemia.” Blood 135 (18):

1588–1602.

Kaneko, Satoshi, and Xue Li. 2018. “X Chromosome Protects against Bladder Cancer in Females via a KDM6A-Dependent Epigenetic Mechanism.” Science Advances 4 (6): eaar5598.

Kang, Seokjo, Emily Y. Ko, Amelia E. Andrews, et al. 2024. “Microglia Undergo Sex-Dimorphic Transcriptional and Metabolic Rewiring during Aging.” Journal of Neuroinflammation 21 (1): 150.

Kaufmann, Corinne, and Anton Wutz. 2023. “IndiSPENsable for X Chromosome Inactivation and Gene Silencing.” Epigenomes 7 (4): 28.

Kaushik, Susmita, and Ana Maria Cuervo. 2018. “The Coming of Age of Chaperone-Mediated Autophagy.” Nature Reviews. Molecular Cell Biology 19 (6): 365–381.

Kawase, E., H. Suemori, N. Takahashi, K. Okazaki, K. Hashimoto, and N. Nakatsuji. 1994. “Strain Difference in Establishment of Mouse Embryonic Stem (ES) Cell Lines.” The International Journal of Developmental Biology 38 (2): 385–390.

Keniry, Andrew, Natasha Jansz, Peter F. Hickey, et al. 2022. “A Method for Stabilising the XX Karyotype in Female mESC Cultures.” Development (Cambridge, England) 149 (22). https://doi.org/10.1242/dev.200845.

Kesler, Benjamin K., John Adams, and Gregor Neuert. 2025. “Transcriptional Stochasticity Reveals Multiple Mechanisms of Long Non-Coding RNA Regulation at the Xist-Tsix Locus.” Nature Communications 16 (1): 4223.

Khawaja, Rabia R., Adrián Martín-Segura, Olaya Santiago-Fernández, et al. 2025. “Sex-Specific and Cell-Type-Specific Changes in Chaperone-Mediated Autophagy across Tissues during Aging.” Nature Aging 5 (4): 691–708.

Kim, Yohan, Rocío Pérez-González, Chelsea Miller, et al. 2022. “Sex Differentially Alters Secretion of Brain Extracellular Vesicles During Aging: A Potential Mechanism for Maintaining Brain Homeostasis.” Neurochemical Research 47 (11): 3428–3439.

Kim, Young Mi, Ji-Yun Lee, Lijun Xia, John J. Mulvihill, and Shibo Li. 2013. “Trisomy 8: A Common Finding in Mouse Embryonic Stem (ES) Cell Lines.” Molecular Cytogenetics 6 (1): 3.

Klein, Sabra L., and Katie L. Flanagan. 2016. “Sex Differences in Immune Responses.” Nature Reviews. Immunology 16 (10): 626–638.

Kolodziejczyk, Aleksandra A., Jong Kyoung Kim, Jason C. H. Tsang, et al. 2015. “Single Cell RNA-Sequencing of Pluripotent States Unlocks Modular Transcriptional Variation.” Cell Stem Cell 17 (4): 471–485.

Koshiguchi, Manami, Nao Yonezawa, Yu Hatano, Hikaru Suenaga, Kazuo Yamagata, and Shin Kobayashi. 2024. “A System to Analyze the Initiation of Random X-Chromosome Inactivation Using Time-Lapse Imaging of Single Cells.” Scientific Reports 14 (1): 20327.

Krupina, Ksenia, Alexander Goginashvili, and Don W. Cleveland. 2021. “Causes and Consequences of Micronuclei.” Current Opinion in Cell Biology 70 (June): 91–99.

Kugoh, Hiroyuki, Takahito Ohira, and Mitsuo Oshimura. 2015. “Studies of Tumor Suppressor Genes via Chromosome Engineering.” Cancers 8 (1): 4.

Kumar, Mudasir A., Sadaf K. Baba, Hana Q. Sadida, et al. 2024. “Extracellular Vesicles as Tools and Targets in Therapy for Diseases.” Signal Transduction and Targeted Therapy 9 (1): 27.

Kunath, Tilo, Marc K. Saba-El-Leil, Marwa Almousailleakh, Jason Wray, Sylvain Meloche, and Austin Smith. 2007. “FGF Stimulation of the Erk1/2 Signalling Cascade Triggers Transition of Pluripotent Embryonic Stem Cells from Self-Renewal to Lineage Commitment.” Development (Cambridge, England) 134 (16): 2895–2902.

Kwon, Mijung, Mitchell L. Leibowitz, and Jae-Ho Lee. 2020. “Small but Mighty: The Causes and Consequences of Micronucleus Rupture.” Experimental & Molecular Medicine 52 (11): 1777–1786.

Leach, Natalia T., Catherine Rehder, Keith Jensen, Shawn Holt, and Colleen Jackson-Cook. 2004. “Human Chromosomes with Shorter Telomeres and Large Heterochromatin Regions Have a Higher Frequency of Acquired Somatic Cell Aneuploidy.” Mechanisms of Ageing and Development 125 (8): 563–573.

Lentini, Antonio, Huaitao Cheng, J. C. Noble, et al. 2022. “Elastic Dosage Compensation by X-Chromosome Upregulation.” Nature Communications 13 (1): 1854.

Levine, Beth, and Guido Kroemer. 2019. “Biological Functions of Autophagy Genes: A Disease Perspective.” Cell 176 (1-2): 11–42.

Liao, Yihao, Diansheng Zhou, Pu Wang, Mengyue Yang, and Ning Jiang. 2022. “Ubiquitin Specific Peptidase 11 as a Novel Therapeutic Target for Cancer Management.” Cell Death Discovery 8 (1): 292.

Li, Jingyuan, Xuqi Chen, Rebecca McClusky, et al. 2014. “The Number of X Chromosomes Influences Protection from Cardiac Ischaemia/reperfusion Injury in Mice: One X Is Better than Two.” Cardiovascular Research 102 (3): 375–384.

Lin, Hong, Vibhor Gupta, Matthew D. Vermilyea, et al. 2007. “Dosage Compensation in the Mouse Balances up-Regulation and Silencing of X-Linked Genes.” PLoS Biology 5 (12): e326.

Link, Jenny C., Carrie B. Wiese, Xuqi Chen, et al. 2020. “X Chromosome Dosage of Histone Demethylase KDM5C Determines Sex Differences in Adiposity.” The Journal of Clinical Investigation 130 (11): 5688–5702.

Lin, Shu-Hong, Derek W. Brown, Brandon Rose, et al. 2021. “Incident Disease Associations with Mosaic Chromosomal Alterations on Autosomes, X and Y Chromosomes: Insights from a Phenome-Wide Association Study in the UK Biobank.” Cell & Bioscience 11 (1): 143.

Liu, Aoxing, Giulio Genovese, Yajie Zhao, et al. 2023. “Population Analyses of Mosaic X Chromosome Loss Identify Genetic Drivers and Widespread Signatures of Cellular Selection.” medRxiv : The Preprint Server for Health Sciences, ahead of print, January 31. https://doi.org/10.1101/2023.01.28.23285140.

Liu, Hongling, Xue Zhang, Qing Wang, Bowen Li, Baishijiao Bian, and Yong Liu. 2025. “A Comprehensive Analysis of Sex-Biased Gene Expression in the Aging Human Retina through a Combination of Single-Cell and Bulk RNA Sequencing.” Investigative Ophthalmology & Visual Science 66 (1): 28.

Liu, Xiaosong, Bozidar Novak, Christian Namendorf, Barbara Steigenberger, Yaoyang Zhang, and Christoph W. Turck. 2024. “Long-Lived Proteins and DNA as Candidate Predictive Biomarkers for Tissue Associated Diseases.” iScience 27 (4): 109642.

Li, Wenxue, Abhijit Dasgupta, Ka Yang, et al. 2025. “Turnover Atlas of Proteome and Phosphoproteome across Mouse Tissues and Brain Regions.” Cell 188 (8): 2267–2287.e21.

Li, Xin, Xiao-Long Cui, Jia-Qiang Wang, et al. 2016. “Generation and Application of Mouse-Rat Allodiploid Embryonic Stem Cells.” Cell 164 (1-2): 279–292.

Li, Yun, Niaz Khan, Rodney M. Ritzel, et al. 2023. “Sexually Dimorphic Extracellular Vesicle Responses after Chronic Spinal Cord Injury Are Associated with Neuroinflammation and Neurodegeneration in the Aged Brain.” Journal of Neuroinflammation 20 (1): 197.

Loda, Agnese, Samuel Collombet, and Edith Heard. 2022. “Gene Regulation in Time and Space during X-Chromosome Inactivation.” Nature Reviews. Molecular Cell Biology 23 (4): 231–249.

Lopes, Alexandra M., Sarah E. Arnold-Croop, António Amorim, and Laura Carrel. 2011. “Clustered Transcripts That Escape X Inactivation at Mouse XqD.” Mammalian Genome: Official Journal of the International Mammalian Genome Society 22 (9-10): 572–582.

López-Otín, Carlos, Maria A. Blasco, Linda Partridge, Manuel Serrano, and Guido Kroemer. 2013. “The Hallmarks of Aging.” Cell 153 (6): 1194–1217.

López-Otín, Carlos, Maria A. Blasco, Linda Partridge, Manuel Serrano, and Guido Kroemer. 2023. “Hallmarks of Aging: An Expanding Universe.” Cell 186 (2): 243–278.

Lozada Ortiz, Jenny, Marina Betancor, Sonia Pérez Lázaro, Rosa Bolea, Juan J. Badiola, and Alicia Otero. 2023. “Endoplasmic Reticulum Stress and Ubiquitin-Proteasome System Impairment in Natural Scrapie.” Frontiers in Molecular Neuroscience 16 (April): 1175364.

Lund, Jesper B., Shuxia Li, Kaare Christensen, et al. 2020. “Age-Dependent DNA Methylation Patterns on the Y Chromosome in Elderly Males.” Aging Cell 19 (2): e12907.

Lv, Jianjie, Chun Zhang, Xiuxing Liu, et al. 2024. “An Aging-Related Immune Landscape in the Hematopoietic Immune System.” Immunity & Ageing: I & A 21 (1): 3.

Lyon, M. F. 1961. “Gene Action in the X-Chromosome of the Mouse (Mus Musculus L.).” Nature 190 (4773): 372–373.

Lyon, M. F. 1962. “Sex Chromatin and Gene Action in the Mammalian X-Chromosome.” The American Journal of Human Genetics 14 (June): 135–148.

Ly, Peter, Simon F. Brunner, Ofer Shoshani, et al. 2019. “Chromosome Segregation Errors Generate a Diverse Spectrum of Simple and Complex Genomic Rearrangements.” Nature Genetics 51 (4): 705–715.

Ly, Peter, Levi S. Teitz, Dong H. Kim, et al. 2017. “Selective Y Centromere Inactivation Triggers Chromosome Shattering in Micronuclei and Repair by Non-Homologous End Joining.” Nature Cell Biology 19 (1): 68–75.

Maan, Akhlaq A., James Eales, Artur Akbarov, et al. 2017. “The Y Chromosome: A Blueprint for Men’s Health?” European Journal of Human Genetics: EJHG 25 (11): 1181–1188.

Machiela, Mitchell J., Weiyin Zhou, Eric Karlins, et al. 2016. “Female Chromosome X Mosaicism Is Age-Related and Preferentially Affects the Inactivated X Chromosome.” Nature Communications 7 (1): 11843.

Mahadevaiah, Shantha K., Mahesh N. Sangrithi, Takayuki Hirota, and James M. A. Turner. 2020. “A Single-Cell Transcriptome Atlas of Marsupial Embryogenesis and X Inactivation.” Nature 586 (7830): 612–617.

Mahapatra, Gargi, Zhengrong Gao, James R. Bateman 3rd, et al. 2024. “Peripheral Blood Cells from Older Adults Exhibit Sex-Associated Differences in Mitochondrial Function.” The Journals of Gerontology. Series A, Biological Sciences and Medical Sciences 79 (5). https://doi.org/10.1093/gerona/glae098.

Ma, Junli, Ying Hong, Ningning Zheng, et al. 2020. “Gut Microbiota Remodeling Reverses Aging-Associated Inflammation and Dysregulation of Systemic Bile Acid Homeostasis in Mice Sex-Specifically.” Gut Microbes 11 (5): 1450–1474.

Mak, Winifred, Tatyana B. Nesterova, Mariana de Napoles, et al. 2004. “Reactivation of the Paternal X Chromosome in Early Mouse Embryos.” Science (New York, N.Y.) 303 (5658): 666–669.

Mansouri, Maysam, and Philipp Berger. 2018. “Baculovirus for Gene Delivery to Mammalian Cells: Past, Present and Future.” Plasmid 98 (June): 1–7.

Marks, Hendrik, Hindrik H. D. Kerstens, Tahsin Stefan Barakat, et al. 2015. “Dynamics of Gene Silencing during X Inactivation Using Allele-Specific RNA-Seq.” Genome Biology 16 (1): 149.

Márquez, Eladio J., Cheng-Han Chung, Radu Marches, et al. 2020. “Sexual-Dimorphism in Human Immune System Aging.” Nature Communications 11 (1): 751.

Martínez de Toda, Irene, Mónica González-Sánchez, Estefanía Díaz-Del Cerro, Gemma Valera, Julia Carracedo, and Natalia Guerra-Pérez. 2023. “Sex Differences in Markers of Oxidation and Inflammation. Implications for Ageing.” Mechanisms of Ageing and Development 211 (111797): 111797.

Martin, G. R. 1981. “Isolation of a Pluripotent Cell Line from Early Mouse Embryos Cultured in Medium Conditioned by Teratocarcinoma Stem Cells.” Proceedings of the National Academy of Sciences of the United States of America 78 (12): 7634–7638.

Mauvais-Jarvis, Franck, Noel Bairey Merz, Peter J. Barnes, et al. 2020. “Sex and Gender: Modifiers of Health, Disease, and Medicine.” Lancet 396 (10250): 565–582.

Mayneris-Perxachs, Jordi, María Arnoriaga-Rodríguez, Diego Luque-Córdoba, et al. 2020. “Gut Microbiota Steroid Sexual Dimorphism and Its Impact on Gonadal Steroids: Influences of Obesity and Menopausal Status.” Microbiome 8 (1): 136.

Mazure, Carolyn M., and Daniel P. Jones. 2015. “Twenty Years and Still Counting: Including Women as Participants and Studying Sex and Gender in Biomedical Research.” BMC Women’s Health 15 (1): 94.

McHugh, Colleen A., Chun-Kan Chen, Amy Chow, et al. 2015. “The Xist lncRNA Interacts Directly with SHARP to Silence Transcription through HDAC3.” Nature 521 (7551): 232–236.

McQuary, Philip R., Chen-Yu Liao, Jessica T. Chang, et al. 2016. “C. Elegans S6K Mutants Require a Creatine-Kinase-like Effector for Lifespan Extension.” Cell Reports 14 (9): 2059–2067.

Mengel-From, Jonas, Rune Lindahl-Jacobsen, Marianne Nygaard, et al. 2021. “Skewness of X-Chromosome Inactivation Increases with Age and Varies across Birth Cohorts in Elderly Danish Women.” Scientific Reports 11 (1): 4326.

Mermoud, J. E., C. Costanzi, J. R. Pehrson, and N. Brockdorff. 1999. “Histone macroH2A1.2 Relocates to the Inactive X Chromosome after Initiation and Propagation of X-Inactivation.” The Journal of Cell Biology 147 (7): 1399–1408.

Meyer, Barbara J. 2010. “Targeting X Chromosomes for Repression.” Current Opinion in Genetics & Development 20 (2): 179–189.

Migeon, Barbara R. 2020. “X-Linked Diseases: Susceptible Females.” Genetics in Medicine: Official Journal of the American College of Medical Genetics 22 (7): 1156–1174.

Migeon, B. R., J. Axelman, and A. H. Beggs. 1988. “Effect of Ageing on Reactivation of the Human X-Linked HPRT Locus.” Nature 335 (6185): 93–96.

Minajigi, Anand, John Froberg, Chunyao Wei, et al. 2015. “Chromosomes. A Comprehensive Xist Interactome Reveals Cohesin Repulsion and an RNA-Directed Chromosome Conformation.” Science (New York, N.Y.) 349 (6245): aab2276.

Mitchell, J. R., E. Wood, and K. Collins. 1999. “A Telomerase Component Is Defective in the Human Disease Dyskeratosis Congenita.” Nature 402 (6761): 551–555.

Miyaoka, Yuichiro, Jennifer R. Berman, Samantha B. Cooper, et al. 2016. “Systematic Quantification of HDR and NHEJ Reveals Effects of Locus, Nuclease, and Cell Type on Genome-Editing.” Scientific Reports 6 (1): 23549.

Moreira de Mello, Joana C., Gustavo R. Fernandes, Maria D. Vibranovski, and Lygia V. Pereira. 2017. “Early X Chromosome Inactivation during Human Preimplantation Development Revealed by Single-Cell RNA-Sequencing.” Scientific Reports 7 (1): 10794.

Morgani, Sophie, Jennifer Nichols, and Anna-Katerina Hadjantonakis. 2017. “The Many Faces of Pluripotency: In Vitro Adaptations of a Continuum of in Vivo States.” BMC Developmental Biology 17 (1): 7.

Mouse Genome Sequencing Consortium, Robert H. Waterston, Kerstin Lindblad-Toh, et al. 2002. “Initial Sequencing and Comparative Analysis of the Mouse Genome.” Nature 420 (6915): 520–562.

Muyas, Francesc, Carolin M. Sauer, Jose Espejo Valle-Inclán, et al. 2024. “De Novo Detection of Somatic Mutations in High-Throughput Single-Cell Profiling Data Sets.” Nature Biotechnology 42 (5): 758–767.

Naik, Hemant Chandru, Kishore Hari, Deepshikha Chandel, Mohit Kumar Jolly, and Srimonta Gayen. 2022. “Single-Cell Analysis Reveals X Upregulation Is Not Global in Pre-Gastrulation Embryos.” iScience 25 (6): 104465.

Nascimento, Rafaella M. P., Paulo A. Otto, Arjan P. M. de Brouwer, and Angela M. Vianna-Morgante. 2006. “UBE2A, Which Encodes a Ubiquitin-Conjugating Enzyme, Is Mutated in a Novel

X-Linked Mental Retardation Syndrome.” The American Journal of Human Genetics 79 (3): 549–555.

Navarro-Cobos, Maria Jose, Bradley P. Balaton, and Carolyn J. Brown. 2020. “Genes That Escape from X-Chromosome Inactivation: Potential Contributors to Klinefelter Syndrome.” American Journal of Medical Genetics. Part C, Seminars in Medical Genetics 184 (2): 226–238.

Navarro, Pablo, Ian Chambers, Violetta Karwacki-Neisius, et al. 2008. “Molecular Coupling of Xist Regulation and Pluripotency.” Science (New York, N.Y.) 321 (5896): 1693–1695.

Navarro, Pablo, Andrew Oldfield, Julie Legoupi, et al. 2010. “Molecular Coupling of Tsix Regulation and Pluripotency.” Nature 468 (7322): 457–460.

Nawrot, Tim S., Jan A. Staessen, Jeffrey P. Gardner, and Abraham Aviv. 2004. “Telomere Length and Possible Link to X Chromosome.” Lancet 363 (9408): 507–510.

Nesterova, Tatyana B., Guifeng Wei, Heather Coker, et al. 2019. “Systematic Allelic Analysis Defines the Interplay of Key Pathways in X Chromosome Inactivation.” Nature Communications 10 (1): 3129.

Nora, Elphège P., Bryan R. Lajoie, Edda G. Schulz, et al. 2012. “Spatial Partitioning of the Regulatory Landscape of the X-Inactivation Centre.” Nature 485 (7398): 381–385.

Norris, D. P., N. Brockdorff, and S. Rastan. 1991. “Methylation Status of CpG-Rich Islands on Active and Inactive Mouse X Chromosomes.” Mammalian Genome: Official Journal of the International Mammalian Genome Society 1 (2): 78–83.

Ocañas, Sarah R., Kevin D. Pham, Jillian E. J. Cox, et al. 2023. “Microglial Senescence Contributes to Female-Biased Neuroinflammation in the Aging Mouse Hippocampus: Implications for Alzheimer’s Disease.” Journal of Neuroinflammation 20 (1): 188.

Ohhata, Tatsuya, Mika Matsumoto, Martin Leeb, et al. 2015. “Histone H3 Lysine 36 Trimethylation Is Established over the Xist Promoter by Antisense Tsix Transcription and Contributes to Repressing Xist Expression.” Molecular and Cellular Biology 35 (22): 3909–3920.

Ohno, S., and T. S. Hauschka. 1960. “Allocycly of the X-Chromosome in Tumors and Normal Tissues.” Cancer Research 20 (May): 541–545.

Ohno, Susumu. 1967. Sex Chromosomes and Sex-Linked Genes. 0077-1015. Springer Berlin Heidelberg.

Okamoto, Ikuhiro, Tomonori Nakamura, Kotaro Sasaki, et al. 2021. “The X Chromosome Dosage Compensation Program during the Development of Cynomolgus Monkeys.” Science (New York, N.Y.) 374 (6570): eabd8887.

Okamoto, Ikuhiro, Arie P. Otte, C. David Allis, Danny Reinberg, and Edith Heard. 2004. “Epigenetic Dynamics of Imprinted X Inactivation during Early Mouse Development.” Science (New York, N.Y.) 303 (5658): 644–649.

Okamoto, Ikuhiro, Catherine Patrat, Dominique Thépot, et al. 2011. “Eutherian Mammals Use Diverse Strategies to Initiate X-Chromosome Inactivation during Development.” Nature 472 (7343): 370–374.

Oliva, Meritxell, Manuel Muñoz-Aguirre, Sarah Kim-Hellmuth, et al. 2020. “The Impact of Sex on Gene Expression across Human Tissues.” Science (New York, N.Y.) 369 (6509). https://doi.org/10.1126/science.aba3066.

Oliván, Sara, Ana Cristina Calvo, Raquel Manzano, Pilar Zaragoza, and Rosario Osta. 2014. “Sex Differences in Constitutive Autophagy.” BioMed Research International 2014 (February): 652817.

Ortmann, Daniel, Stephanie Brown, Anne Czechanski, et al. 2020. “Naive Pluripotent Stem Cells Exhibit Phenotypic Variability That Is Driven by Genetic Variation.” Cell Stem Cell 27 (3): 470–481.e6.

Pacini, Guido, Ilona Dunkel, Norbert Mages, et al. 2021. “Integrated Analysis of Xist Upregulation and X-Chromosome Inactivation with Single-Cell and Single-Allele Resolution.” Nature Communications 12 (1): 3638.

Pageau, Gayle J., Lisa L. Hall, Shridar Ganesan, David M. Livingston, and Jeanne B. Lawrence. 2007. “The Disappearing Barr Body in Breast and Ovarian Cancers.” Nature Reviews. Cancer 7 (8): 628–633.

Pahal, Sonu, Nirjal Mainali, Meenakshisundaram Balasubramaniam, Robert J. Shmookler Reis, and Srinivas Ayyadevara. 2025. “Mitochondria in Aging and Age-Associated Diseases.” Mitochondrion 82 (102022): 102022.

Panning, B., J. Dausman, and R. Jaenisch. 1997. “X Chromosome Inactivation Is Mediated by Xist RNA Stabilization.” Cell 90 (5): 907–916.

Panning, B., and R. Jaenisch. 1996. “DNA Hypomethylation Can Activate Xist Expression and Silence X-Linked Genes.” Genes & Development 10 (16): 1991–2002.

Peeters, Samantha B., Bronwyn J. Posynick, and Carolyn J. Brown. 2023. “Out of the Silence: Insights into How Genes Escape X-Chromosome Inactivation.” Epigenomes 7 (4). https://doi.org/10.3390/epigenomes7040029.

Peitz, Michael, Kurt Pfannkuche, Klaus Rajewsky, and Frank Edenhofer. 2002. “Ability of the Hydrophobic FGF and Basic TAT Peptides to Promote Cellular Uptake of Recombinant Cre Recombinase: A Tool for Efficient Genetic Engineering of Mammalian Genomes.” Proceedings of the National Academy of Sciences of the United States of America 99 (7): 4489–4494.

Penny, G. D., G. F. Kay, S. A. Sheardown, S. Rastan, and N. Brockdorff. 1996. “Requirement for Xist in X Chromosome Inactivation.” Nature 379 (6561): 131–137.

Petropoulos, Sophie, Daniel Edsgärd, Björn Reinius, et al. 2016. “Single-Cell RNA-Seq Reveals Lineage and X Chromosome Dynamics in Human Preimplantation Embryos.” Cell 167 (1): 285.

Pintacuda, Greta, and Andrea Cerase. 2015. “X Inactivation Lessons from Differentiating Mouse Embryonic Stem Cells.” Stem Cell Reviews 11 (5): 699–705.

Pintacuda, Greta, Guifeng Wei, Chloë Roustan, et al. 2017. “HnRNPK Recruits PCGF3/5-PRC1 to the Xist RNA B-Repeat to Establish Polycomb-Mediated Chromosomal Silencing.” Molecular Cell 68 (5): 955–969.e10.

Platt, Randall J., Sidi Chen, Yang Zhou, et al. 2014. “CRISPR-Cas9 Knockin Mice for Genome Editing and Cancer Modeling.” Cell 159 (2): 440–455.

Plenge, R. M., B. D. Hendrich, C. Schwartz, et al. 1997. “A Promoter Mutation in the XIST Gene in Two Unrelated Families with Skewed X-Chromosome Inactivation.” Nature Genetics 17 (3): 353–356.

Plenge, R. M., I. Percec, J. H. Nadeau, and H. F. Willard. 2000. “Expression-Based Assay of an X-Linked Gene to Examine Effects of the X-Controlling Element (Xce) Locus.” Mammalian Genome: Official Journal of the International Mammalian Genome Society 11 (5): 405–408.

Qi, Lei S., Matthew H. Larson, Luke A. Gilbert, et al. 2013. “Repurposing CRISPR as an RNA-Guided Platform for Sequence-Specific Control of Gene Expression.” Cell 152 (5): 1173–1183.

Qi, Meifang, Jiali Pang, Irene Mitsiades, Andrew A. Lane, and Esther Rheinbay. 2023. “Loss of Chromosome Y in Primary Tumors.” Cell 186 (14): 3125–3136.e11.

Qi, Shaohua, Abdullah Al Mamun, Conelius Ngwa, et al. 2021. “X Chromosome Escapee Genes Are Involved in Ischemic Sexual Dimorphism through Epigenetic Modification of Inflammatory Signals.” Journal of Neuroinflammation 18 (1): 70.

Quin, Candice, Jessica A. Breznik, Allison E. Kennedy, et al. 2024. “Monocyte-Driven Inflamm-Aging Reduces Intestinal Barrier Function in Females.” Immunity & Ageing: I & A 21 (1): 65.

Qu, Zhi, Lu Zhang, Xue Yin, et al. 2025. “Male Sex Determination Maintains Proteostasis and Extends Lifespan of Daf-18/PTEN Deficient C. Elegans.” EMBO Reports 26 (4): 1084–1113.

Rall-Scharpf, Melanie, Thomas W. P. Friedl, Shahar Biechonski, Michael Denkinger, Michael Milyavsky, and Lisa Wiesmüller. 2021. “Sex-Specific Differences in DNA Double-Strand Break Repair of Cycling Human Lymphocytes during Aging.” Aging 13 (17): 21066–21089.

Rall-Scharpf, Melanie, Dominik Schlotter, Philipp Koch, et al. 2025. “Replication Stress Responses in Human Lymphocytes Change Sex-Specifically during Aging.” Nucleic Acids Research 53 (11). https://doi.org/10.1093/nar/gkaf498.

Ramos-Ibeas, Priscila, Fei Sang, Qifan Zhu, et al. 2019. “Pluripotency and X Chromosome Dynamics Revealed in Pig Pre-Gastrulating Embryos by Single Cell Analysis.” Nature Communications 10 (1): 500.

Rao, Nalini R., Arun Upadhyay, and Jeffrey N. Savas. 2024. “Derailed Protein Turnover in the Aging Mammalian Brain.” Molecular Systems Biology 20 (2): 120–139.

Rao, Suhas S. P., Miriam H. Huntley, Neva C. Durand, et al. 2015. “A 3D Map of the Human Genome at Kilobase Resolution Reveals Principles of Chromatin Looping.” Cell 162 (3): 687–688.

Rastan, Sohaila, and Elizabeth J. Robertson. 1985. “X-Chromosome Deletions in Embryo-Derived (EK) Cell Lines Associated with Lack of X-Chromosome Inactivation.” Development (Cambridge, England) 90 (1): 379–388.

Regan, Jennifer C., Yu-Xuan Lu, Enric Ureña, et al. 2022. “Sexual Identity of Enterocytes Regulates Autophagy to Determine Intestinal Health, Lifespan and Responses to Rapamycin.” Nature Aging 2 (12): 1145–1158.

Rego, Alena, Paul B. Sinclair, Wei Tao, Igor Kireev, and Andrew S. Belmont. 2008. “The Facultative Heterochromatin of the Inactive X Chromosome Has a Distinctive Condensed Ultrastructure.” Journal of Cell Science 121 (Pt 7): 1119–1127.

Reikvam, Håkon, Kimberley Joanne Hatfield, Astrid Olsnes Kittang, Randi Hovland, and Øystein Bruserud. 2011. “Acute Myeloid Leukemia with the t(8;21) Translocation: Clinical Consequences and Biological Implications.” Journal of Biomedicine & Biotechnology 2011 (1): 104631.

Reinius, Björn, and Rickard Sandberg. 2019. “Expression Reduction of Biallelically Transcribed X-Linked Genes during the Human Female Preimplantation Development.” In bioRxiv. BioRxiv, June 27. https://doi.org/10.1101/682286.

Richart, Laia, Mary-Loup Picod-Chedotel, Michel Wassef, et al. 2022. “XIST Loss Impairs Mammary Stem Cell Differentiation and Increases Tumorigenicity through Mediator Hyperactivation.” Cell 185 (12): 2164–2183.e25.

Ridings-Figueroa, Rebeca, Emma R. Stewart, Tatyana B. Nesterova, et al. 2017. “The Nuclear Matrix Protein CIZ1 Facilitates Localization of Xist RNA to the Inactive X-Chromosome Territory.” Genes & Development 31 (9): 876–888.

Ripa, Roberto, Eugen Ballhysa, Joachim D. Steiner, et al. 2023. “Refeeding-Associated AMPKγ1 Complex Activity Is a Hallmark of Health and Longevity.” Nature Aging 3 (12): 1544–1560.

Roberts, Amy L., Alessandro Morea, Ariella Amar, et al. 2022. “Age Acquired Skewed X Chromosome Inactivation Is Associated with Adverse Health Outcomes in Humans.” eLife 11 (November): e78263.

Robertson, E. J., M. J. Evans, and M. H. Kaufman. 1983. “X-Chromosome Instability in Pluripotential Stem Cell Lines Derived from Parthenogenetic Embryos.” Development (Cambridge, England) 74 (1): 297–309.

Rochelle, Tina L., Doris K. Y. Yeung, Michael Harris Bond, and Liman Man Wai Li. 2015. “Predictors of the Gender Gap in Life Expectancy across 54 Nations.” Psychology, Health & Medicine 20 (2): 129–138.

Rodermund, Lisa, Heather Coker, Roel Oldenkamp, et al. 2021. “Time-Resolved Structured Illumination Microscopy Reveals Key Principles of Xist RNA Spreading.” Science (New York, N.Y.) 372 (6547): eabe7500.

Rodriguez, Mya, and Andrea Kh Stavoe. 2025. “Sex Does Not Influence Neuronal Autophagosome Biogenesis throughout Aging in Mice.” Molecular Biology of the Cell 36 (11): mbcE25070312.

Rohrmann, George F. 2019. Baculovirus Infection: The Cell Cycle and Apoptosis. National Center for Biotechnology Information (US).

Rowland, Teisha J., Mary E. Sweet, Luisa Mestroni, and Matthew R. G. Taylor. 2016. “Danon Disease - Dysregulation of Autophagy in a Multisystem Disorder with Cardiomyopathy.” Journal of Cell Science 129 (11): 2135–2143.

Sado, Takashi, Yuko Hoki, and Hiroyuki Sasaki. 2005. “Tsix Silences Xist through Modification of Chromatin Structure.” Developmental Cell 9 (1): 159–165.

Sano, Soichi, Keita Horitani, Hayato Ogawa, et al. 2022. “Hematopoietic Loss of Y Chromosome Leads to Cardiac Fibrosis and Heart Failure Mortality.” Science (New York, N.Y.) 377 (6603): 292–297.

Sarver, Dylan C., Muzna Saqib, Fangluo Chen, and G. William Wong. 2024. “Mitochondrial Respiration Atlas Reveals Differential Changes in Mitochondrial Function across Sex and Age.” eLife 13 (RP96926). https://doi.org/10.7554/elife.96926.4.

Savarese, Fabio, Katja Flahndorfer, Rudolf Jaenisch, Meinrad Busslinger, and Anton Wutz. 2006. “Hematopoietic Precursor Cells Transiently Reestablish Permissiveness for X Inactivation.” Molecular and Cellular Biology 26 (19): 7167–7177.

Scherer, Michael, Indranil Singh, Martina Maria Braun, et al. 2025. “Clonal Tracing with Somatic Epimutations Reveals Dynamics of Blood Ageing.” Nature 643 (8071): 478–487.

Schoeftner, Stefan, Raquel Blanco, Isabel Lopez de Silanes, et al. 2009. “Telomere Shortening Relaxes X Chromosome Inactivation and Forces Global Transcriptome Alterations.” Proceedings of the National Academy of Sciences of the United States of America 106 (46): 19393–19398.

Schulz, Edda G., Johannes Meisig, Tomonori Nakamura, et al. 2014. “The Two Active X Chromosomes in Female ESCs Block Exit from the Pluripotent State by Modulating the ESC Signaling Network.” Cell Stem Cell 14 (2): 203–216.

Schwämmle, Till, and Edda G. Schulz. 2023. “Regulatory Principles and Mechanisms Governing the Onset of Random X-Chromosome Inactivation.” Current Opinion in Genetics & Development 81 (August): 102063.

Schwarze, S. R., A. Ho, A. Vocero-Akbani, and S. F. Dowdy. 1999. “In Vivo Protein Transduction: Delivery of a Biologically Active Protein into the Mouse.” Science (New York, N.Y.) 285 (5433): 1569–1572.

Sdeor, Eran, Hajime Okada, Ron Saad, Tal Ben-Yishay, and Uri Ben-David. 2024. “Aneuploidy as a Driver of Human Cancer.” Nature Genetics 56 (10): 2014–2026.

Selman, Colin, Jennifer M. A. Tullet, Daniela Wieser, et al. 2009. “Ribosomal Protein S6 Kinase 1 Signaling Regulates Mammalian Life Span.” Science (New York, N.Y.) 326 (5949): 140–144.

Severino, Jacqueline, Moritz Bauer, Tom Mattimoe, et al. 2022. “Controlled X-Chromosome Dynamics Defines Meiotic Potential of Female Mouse in Vitro Germ Cells.” The EMBO Journal 41 (12): e109457.

Shahbazi, Marta N., Tianren Wang, Xin Tao, et al. 2020. “Developmental Potential of Aneuploid Human Embryos Cultured beyond Implantation.” Nature Communications 11 (1): 3987.

Shaw, Cayce K., Samira Abdulai-Saiku, Francesca Marino, et al. 2023. “X Chromosome Factor Kdm6a Enhances Cognition Independent of Its Demethylase Function in the Aging XY Male Brain.” The Journals of Gerontology. Series A, Biological Sciences and Medical Sciences 78 (6): 938–943.

Sheardown, S. A., S. M. Duthie, C. M. Johnston, et al. 1997. “Stabilization of Xist RNA Mediates Initiation of X Chromosome Inactivation.” Cell 91 (1): 99–107.

Shenoda, Botros B., Sujay Ramanathan, Richa Gupta, et al. 2021. “Xist Attenuates Acute Inflammatory Response by Female Cells.” Cellular and Molecular Life Sciences: CMLS 78 (1): 299–316.

Shvetsova, Ekaterina, Alina Sofronova, Ramin Monajemi, et al. 2019. “Skewed X-Inactivation Is

Common in the General Female Population." European Journal of Human Genetics: EJHG 27 (3): 455–465.

Sierra, Isabel, Son C. Nguyen, R. Jordan Barnett, et al. 2022. "Remodeling and Compaction of the Inactive X Is Regulated byXistduring Female B Cell Activation." In bioRxiv. October 21. https://doi.org/10.1101/2022.10.19.512821.

Sierra, Isabel, Sarah Pyfrom, Aaron Weiner, et al. 2023. "Unusual X Chromosome Inactivation Maintenance in Female Alveolar Type 2 Cells Is Correlated with Increased Numbers of X-Linked Escape Genes and Sex-Biased Gene Expression." Stem Cell Reports 18 (2): 489–502.

Skuse, David H. 2005. "X-Linked Genes and Mental Functioning." Human Molecular Genetics 14 Spec No 1 (suppl_1): R27–32.

Smith-Bouvier, Deborah L., Anagha A. Divekar, Manda Sasidhar, et al. 2008. "A Role for Sex Chromosome Complement in the Female Bias in Autoimmune Disease." The Journal of Experimental Medicine 205 (5): 1099–1108.

Sopena-Rios, Maria, Aida Ripoll-Cladellas, Fatemeh Omidi, et al. 2024. "Single-Cell Atlas of the Human Immune System Reveals Sex-Specific Dynamics of Immunosenescence." In bioRxiv. November 8. https://doi.org/10.1101/2024.11.06.622096.

Splinter, Erik, Elzo de Wit, Elphège P. Nora, et al. 2011. "The Inactive X Chromosome Adopts a Unique Three-Dimensional Conformation That Is Dependent on Xist RNA." Genes & Development 25 (13): 1371–1383.

Stanton, Alexander, Selcan Aydin, Daniel A. Skelly, et al. 2024. "Chromosome X Dosage Modulates Development of Aneuploidy in Genetically Diverse Mouse Embryonic Stem Cells." In bioRxiv. July 3. https://doi.org/10.1101/2024.06.29.601344.

Stead, Elaine, Josephine White, Renate Faast, et al. 2002. "Pluripotent Cell Division Cycles Are Driven by Ectopic Cdk2, Cyclin A/E and E2F Activities." Oncogene 21 (54): 8320–8333.

Sugimoto, Michihiko, Masayo Kondo, Yumiko Koga, et al. 2015. "A Simple and Robust Method for Establishing Homogeneous Mouse Epiblast Stem Cell Lines by Wnt Inhibition." Stem Cell Reports 4 (4): 744–757.

Sullivan, Brian P., Alexie A. Larson, Ahmed S. Shams, et al. 2025. "Estradiol Deficiency as a Consequence of Aging Contributes to the Depletion of the Satellite Cell Pool in Female Mice." Aging Cell 24 (4): e14441.

Sun, Lei, Zhong Wang, Tianyuan Lu, Teri A. Manolio, and Andrew D. Paterson. 2023. "eXclusionarY: 10 Years Later, Where Are the Sex Chromosomes in GWASs?" The American Journal of Human Genetics 110 (6): 903–912.

Sunwoo, Hongjae, David Colognori, John E. Froberg, Yesu Jeon, and Jeannie T. Lee. 2017. "Repeat E Anchors Xist RNA to the Inactive X Chromosomal Compartment through CDKN1A-Interacting Protein (CIZ1)." Proceedings of the National Academy of Sciences of the United States of America 114 (40): 10654–10659.

Sun, Yidan, Meike Wiese, Raed Hmadi, et al. 2023. "MSL2 Ensures Biallelic Gene Expression in Mammals." Nature 624 (7990): 173–181.

Surrallés, J., M. P. Hande, R. Marcos, and P. M. Lansdorp. 1999. “Accelerated Telomere Shortening in the Human Inactive X Chromosome.” The American Journal of Human Genetics 65 (6): 1617–1622.

Suzuki, Teruhiko, Yasuhiro Kazuki, Takahiko Hara, and Mitsuo Oshimura. 2020. “Current Advances in Microcell-Mediated Chromosome Transfer Technology and Its Applications.” Experimental Cell Research 390 (1): 111915.

Syrett, Camille M., Bam Paneru, Donavon Sandoval-Heglund, et al. 2019. “Altered X-Chromosome Inactivation in T Cells May Promote Sex-Biased Autoimmune Diseases.” JCI Insight 4 (7). https://doi.org/10.1172/jci.insight.126751.

Syrett, Camille M., Vishal Sindhava, Suchita Hodawadekar, et al. 2017. “Loss of Xist RNA from the Inactive X during B Cell Development Is Restored in a Dynamic YY1-Dependent Two-Step Process in Activated B Cells.” PLoS Genetics 13 (10): e1007050.

Syrett, Camille M., Vishal Sindhava, Isabel Sierra, Aimee H. Dubin, Michael Atchison, and Montserrat C. Anguera. 2018. “Diversity of Epigenetic Features of the Inactive X-Chromosome in NK Cells, Dendritic Cells, and Macrophages.” Frontiers in Immunology 9: 3087.

Takahashi, Yuta, Mariana Morales Valencia, Yang Yu, et al. 2023. “Transgenerational Inheritance of Acquired Epigenetic Signatures at CpG Islands in Mice.” Cell 186 (4): 715–731.e19.

Tallaksen, Helene Bandsholm Leere, Emma B. Johannsen, Jesper Just, Mette Hansen Viuff, Claus H. Gravholt, and Anne Skakkebæk. 2023. “The Multi-Omic Landscape of Sex Chromosome Abnormalities: Current Status and Future Directions.” Endocrine Connections 12 (9). https://doi.org/10.1530/EC-23-0011.

Tamura, Yuka, Tatsuya Ohhata, Hiroyuki Niida, et al. 2021. “Homologous Recombination Is Reduced in Female Embryonic Stem Cells by Two Active X Chromosomes.” EMBO Reports 22 (9): e52190.

Tena, Juan J., and José M. Santos-Pereira. 2021. “Topologically Associating Domains and Regulatory Landscapes in Development, Evolution and Disease.” Frontiers in Cell and Developmental Biology 9 (July): 702787.

Tennant, Nikolai, Ananya Pavuluri, Kate O’Connor-Giles, Gunjan Singh, Erica Larschan, and Ritambhara Singh. 2024. “TimeFlies: An snRNA-Seq Aging Clock for the Fruit Fly Head Sheds Light on Sex-Biased Aging.” In Genomics, No. Biorxiv;2024.11.25.625273v3. BioRxiv, November 27. https://www.biorxiv.org/content/10.1101/2024.11.25.625273v3.full.

Toufektchan, Eléonore, and John Maciejowski. 2021. “Purification of Micronuclei from Cultured Cells by Flow Cytometry.” STAR Protocols 2 (1): 100378.

Tower, John, Laura C. D. Pomatto, and Kelvin J. A. Davies. 2020. “Sex Differences in the Response to Oxidative and Proteolytic Stress.” Redox Biology 31 (101488): 101488.

Truong, My Anh, Paula Cané-Gasull, Sippe G. de Vries, et al. 2023. “A Kinesin-Based Approach for Inducing Chromosome-Specific Mis-Segregation in Human Cells.” The EMBO Journal 42 (10): e111559.

Tucker, J. D., J. Nath, and J. C. Hando. 1996. “Activation Status of the X Chromosome in Human

Micronucleated Lymphocytes." Human Genetics 97 (4): 471–475.

Tukiainen, Taru, Alexandra-Chloé Villani, Angela Yen, et al. 2017. "Landscape of X Chromosome Inactivation across Human Tissues." Nature 550 (7675): 244–248.

Vallot, Céline, Christophe Huret, Yann Lesecque, et al. 2013. "XACT, a Long Noncoding Transcript Coating the Active X Chromosome in Human Pluripotent Cells." Nature Genetics 45 (3): 239–241.

Vallot, Céline, Catherine Patrat, Amanda J. Collier, et al. 2017. "XACT Noncoding RNA Competes with XIST in the Control of X Chromosome Activity during Human Early Development." Cell Stem Cell 20 (1): 102–111.

Ventura-Clapier, Renée, Elke Dworatzek, Ute Seeland, et al. 2017. "Sex in Basic Research: Concepts in the Cardiovascular Field." Cardiovascular Research 113 (7): 711–724.

Vermeulen, Michael C., Richard Pearse, Tracy Young-Pearse, and Sara Mostafavi. 2022. "Mosaic Loss of Chromosome Y in Aged Human Microglia." Genome Research 32 (10): 1795–1807.

Vidaki, Athina, Diego Montiel González, Benjamin Planterose Jiménez, and Manfred Kayser. 2021. "Male-Specific Age Estimation Based on Y-Chromosomal DNA Methylation." Aging 13 (5): 6442–6458.

Vieira, Adriana A., Inês Almada-Correia, Joana Inácio, Patrícia Costa-Reis, and S. T. da Rocha. 2024. "Female-Bias in Systemic Lupus Erythematosus: How Much Is the X Chromosome to Blame?" Biology of Sex Differences 15 (1): 76.

Vijg, Jan, and Yousin Suh. 2013. "Genome Instability and Aging." Annual Review of Physiology 75 (1): 645–668.

Vitorakis, Nikolaos, and Christina Piperi. 2023. "Insights into the Role of Histone Methylation in Brain Aging and Potential Therapeutic Interventions." International Journal of Molecular Sciences 24 (24). https://doi.org/10.3390/ijms242417339.

Viuff, Mette, Anne Skakkebæk, Emma B. Johannsen, et al. 2023. "X Chromosome Dosage and the Genetic Impact across Human Tissues." Genome Medicine 15 (1): 21.

Wang, Jianle, Camille M. Syrett, Marianne C. Kramer, Arindam Basu, Michael L. Atchison, and Montserrat C. Anguera. 2016. "Unusual Maintenance of X Chromosome Inactivation Predisposes Female Lymphocytes for Increased Expression from the Inactive X." Proceedings of the National Academy of Sciences of the United States of America 113 (14): E2029–38.

Wang, Joy Y., and Jennifer A. Doudna. 2023. "CRISPR Technology: A Decade of Genome Editing Is Only the Beginning." Science (New York, N.Y.) 379 (6629): eadd8643.

Wang, Xin Hua, Lin Mei Zhang, Xue Yang, and Shui Zhen Zhou. 2020. "A Pathogenic Missense Variant (c.1617G>A, p.Met539Ile) in UBA1 Causing Infantile X-Linked Spinal Muscular Atrophy (SMAX2)." Frontiers in Pediatrics 8 (February): 64.

Wang, Xu, Kory C. Douglas, John L. Vandeberg, Andrew G. Clark, and Paul B. Samollow. 2014. "Chromosome-Wide Profiling of X-Chromosome Inactivation and Epigenetic States in Fetal Brain and Placenta of the Opossum, Monodelphis Domestica." Genome Research 24 (1): 70–83.

Wang, Xu, Donald C. Miller, Andrew G. Clark, and Douglas F. Antczak. 2012. “Random X Inactivation in the Mule and Horse Placenta.” Genome Research 22 (10): 1855–1863.

Wareham, K. A., M. F. Lyon, P. H. Glenister, and E. D. Williams. 1987. “Age Related Reactivation of an X-Linked Gene.” Nature 327 (6124): 725–727.

Webster, Sarah E., Duncan Vos, Thomas L. Rothstein, and Nichol E. Holodick. 2022. “Modulation of Microbiome Diversity and Cytokine Expression Is Influenced in a Sex-Dependent Manner during Aging.” Frontiers in Microbiomes 1 (October). https://doi.org/10.3389/frmbi.2022.994464.

Wei, Chunyao, Barry Kesner, Hao Yin, and Jeannie T. Lee. 2024. “Imprinted X Chromosome Inactivation at the Gamete-to-Embryo Transition.” Molecular Cell 84 (8): 1442–1459.e7.

Welshons, W. J., and L. B. Russell. 1959. “The Y-Chromosome as the Bearer of Male Determining Factors in the Mouse.” Proceedings of the National Academy of Sciences of the United States of America 45 (4): 560–566.

Williams, R. L., D. J. Hilton, S. Pease, et al. 1988. “Myeloid Leukaemia Inhibitory Factor Maintains the Developmental Potential of Embryonic Stem Cells.” Nature 336 (6200): 684–687.

Wimberger, Sandra, Nina Akrap, Mike Firth, et al. 2023. “Simultaneous Inhibition of DNA-PK and PolΘ Improves Integration Efficiency and Precision of Genome Editing.” Nature Communications 14 (1): 4761.

Winkler, Ivana, Alexander Tolkachov, Fritjof Lammers, et al. 2024. “The Cycling and Aging Mouse Female Reproductive Tract at Single-Cell Resolution.” Cell 187 (4): 981–998.e25.

Wutz, Anton, Theodore P. Rasmussen, and Rudolf Jaenisch. 2002. “Chromosomal Silencing and Localization Are Mediated by Different Domains of Xist RNA.” Nature Genetics 30 (2): 167–174.

Xirocostas, Zoe A., Susan E. Everingham, and Angela T. Moles. 2020. “The Sex with the Reduced Sex Chromosome Dies Earlier: A Comparison across the Tree of Life.” Biology Letters 16 (3): 20190867.

Yagi, Masaki, Satoshi Kishigami, Akito Tanaka, et al. 2017. “Derivation of Ground-State Female ES Cells Maintaining Gamete-Derived DNA Methylation.” Nature 548 (7666): 224–227.

Yamamuro, Tadashi, Tsuyoshi Kawabata, Atsunori Fukuhara, et al. 2020. “Age-Dependent Loss of Adipose Rubicon Promotes Metabolic Disorders via Excess Autophagy.” Nature Communications 11 (1): 4150.

Yang, Lin, Eda Yildirim, James E. Kirby, William Press, and Jeannie T. Lee. 2020. “Widespread Organ Tolerance to Xist Loss and X Reactivation except under Chronic Stress in the Gut.” Proceedings of the National Academy of Sciences of the United States of America 117 (8): 4262–4272.

Yang, Songbai, and Jing Wang. 2015. “Estrogen Activates AMP-Activated Protein Kinase in Human Endothelial Cells via ERβ/Ca(2+)/calmodulin-Dependent Protein Kinase Kinase β Pathway.” Cell Biochemistry and Biophysics 72 (3): 701–707.

Yan, Wenjing, Yongwang Zhong, Xin Hu, et al. 2023. “Auranofin Targets UBA1 and Enhances UBA1 Activity by Facilitating Ubiquitin Trans-Thioesterification to E2 Ubiquitin-Conjugating Enzymes.” Nature Communications 14 (1): 4798.

Yan, Yan, Xinming Wang, Dale Chaput, et al. 2022. “X-Linked Ubiquitin-Specific Peptidase 11 Increases Tauopathy Vulnerability in Women.” Cell 185 (21): 3913–3930.e19.

Yao, Shengze, Yesu Jeon, Barry Kesner, and Jeannie T. Lee. 2025. “Xist RNA Binds Select Autosomal Genes and Depends on Repeat B to Regulate Their Expression.” eLife 13 (RP101197): RP101197.

Yildirim, Eda, James E. Kirby, Diane E. Brown, et al. 2013. “Xist RNA Is a Potent Suppressor of Hematologic Cancer in Mice.” Cell 152 (4): 727–742.

Ying, Qi-Long, Jason Wray, Jennifer Nichols, et al. 2008. “The Ground State of Embryonic Stem Cell Self-Renewal.” Nature 453 (7194): 519–523.

Yousefzadeh, Matthew J., Jing Zhao, Christina Bukata, et al. 2020. “Tissue Specificity of Senescent Cell Accumulation during Physiologic and Accelerated Aging of Mice.” Aging Cell 19 (3): e13094.

Yu, Bingfei, Yanyan Qi, Rui Li, Quanming Shi, Ansuman T. Satpathy, and Howard Y. Chang. 2021. “B Cell-Specific XIST Complex Enforces X-Inactivation and Restrains Atypical B Cells.” Cell 184 (7): 1790–1803.e17.

Zambrowicz, B. P., A. Imamoto, S. Fiering, L. A. Herzenberg, W. G. Kerr, and P. Soriano. 1997. “Disruption of Overlapping Transcripts in the ROSA Beta Geo 26 Gene Trap Strain Leads to Widespread Expression of Beta-Galactosidase in Mouse Embryos and Hematopoietic Cells.” Proceedings of the National Academy of Sciences of the United States of America 94 (8): 3789–3794.

Zekavat, Seyedeh M., Shu-Hong Lin, Alexander G. Bick, et al. 2020. “Hematopoietic Mosaic Chromosomal Alterations and Risk for Infection among 767,891 Individuals without Blood Cancer.” medRxiv : The Preprint Server for Health Sciences, ahead of print, November 16. https://doi.org/10.1101/2020.11.12.20230821.

Zhang, Chunxiao, Taisen Hao, Alessia Bortoluzzi, et al. 2025. “Sex-Dependent Differences in Hematopoietic Stem Cell Aging and Leukemogenic Potential.” Oncogene 44 (2): 64–78.

Zhang, Fan, De Cheng, Kenneth I. Porter, et al. 2025. “Modification of the Telomerase Gene with Human Regulatory Sequences Resets Mouse Telomeres to Human Length.” Nature Communications 16 (1): 1211.

Zhang, Pingze, James H. Catterson, Sebastian Grönke, and Linda Partridge. 2024. “Inhibition of S6K Lowers Age-Related Inflammation and Increases Lifespan through the Endolysosomal System.” Nature Aging 4 (4): 491–509.

Zhang, Xiuying, Huanzi Zhong, Yufeng Li, et al. 2021. “Sex- and Age-Related Trajectories of the Adult Human Gut Microbiota Shared across Populations of Different Ethnicities.” Nature Aging 1 (1): 87–100.

Zhang, Zhen, Amy E. Baxter, Diqiu Ren, et al. 2024. “Efficient Engineering of Human and Mouse Primary Cells Using Peptide-Assisted Genome Editing.” Nature Biotechnology 42 (2): 305–315.

Zhao, Yuhai, Peter N. Alexandrov, Vivian Jaber, and Walter J. Lukiw. 2016. “Deficiency in the Ubiquitin Conjugating Enzyme UBE2A in Alzheimer’s Disease (AD) Is Linked to Deficits in a

Natural Circular miRNA-7 Sponge (circRNA; ciRS-7).” Genes 7 (12): 116.

Zhong, Liangwen, Miriam Gordillo, Xingyi Wang, et al. 2023. “Dual Role of Lipids for Genome Stability and Pluripotency Facilitates Full Potency of Mouse Embryonic Stem Cells.” Protein & Cell 14 (8): 591–602.

Zou, Huiying, Dawei Yu, Xuguang Du, et al. 2019. “No Imprinted XIST Expression in Pigs: Biallelic XIST Expression in Early Embryos and Random X Inactivation in Placentas.” Cellular and Molecular Life Sciences: CMLS 76 (22): 4525–4538.

Zuo, Erwei, Xiaona Huo, Xuan Yao, et al. 2017. “CRISPR/Cas9-Mediated Targeted Chromosome Elimination.” Genome Biology 18 (1): 224.

Żylicz, Jan Jakub, Aurélie Bousard, Kristina Žumer, et al. 2019. “The Implication of Early Chromatin Changes in X Chromosome Inactivation.” Cell 176 (1-2): 182–197.e23.

9. Appendix I

The following pages include the review published during my PhD

Fritz García JHG, Keller Valsecchi CI, Basilicata MF. 2024 Sex as a biological variable in ageing: insights and perspectives on the molecular and cellular hallmarks. *Open Biol*. **14**: 240177. https://doi.org/10.1098/rsob.24.

OPEN BIOLOGY

royalsocietypublishing.org/journal/rsob

Review

Cite this article: Fritz García JHG, Keller Valsecchi CI, Basilicata MF. 2024 Sex as a biological variable in ageing: insights and perspectives on the molecular and cellular hallmarks. *Open Biol.* **14**: 240177.
https://doi.org/10.1098/rsob.240177

Received: 25 June 2024
Accepted: 5 September 2024

Subject Areas:
cellular biology, genetics, molecular biology

Keywords:
sex chromosomes, sex hormones, hallmarks of ageing, ageing, X chromosome, X-chromosome inactivation

Authors for correspondence:
Claudia Isabelle Keller Valsecchi
e-mail: c.keller@imb-mainz.de
M. Felicia Basilicata
e-mail: mfbasilicata@uni-mainz.de

THE ROYAL SOCIETY PUBLISHING

Sex as a biological variable in ageing: insights and perspectives on the molecular and cellular hallmarks

José Héctor Gibrán Fritz García[1], Claudia Isabelle Keller Valsecchi[1] and M. Felicia Basilicata[1,2]

[1]Institute of Molecular Biology (IMB), Mainz, Germany
[2]University Medical Center (UMC), Mainz, Germany

CIKV, 0000-0003-4135-5927; MFB, 0000-0002-1111-9459

Sex-specific differences in lifespan and ageing are observed in various species. In humans, women generally live longer but are frailer and suffer from different age-related diseases compared to men. The hallmarks of ageing, such as genomic instability, telomere attrition or loss of proteostasis, exhibit sex-specific patterns. Sex chromosomes and sex hormones, as well as the epigenetic regulation of the inactive X chromosome, have been shown to affect lifespan and age-related diseases. Here we review the current knowledge on the biological basis of sex-biased ageing. While our review is focused on humans, we also discuss examples of model organisms such as the mouse, fruit fly or the killifish. Understanding these molecular differences is crucial as the elderly population is expected to double worldwide by 2050, making sex-specific approaches in the diagnosis, treatment, therapeutic development and prevention of age-related diseases a pressing need.

1. Introduction

It has become increasingly evident that males and females across species show differences in lifespan (see Glossary) and ageing. In many mammals, females live longer than males, while in birds, males are the longer-lived sex [1]. In humans, women live on average 5 years longer than men [2]. Paradoxically, women are frailer (see Glossary) later in life (usually after the onset of menopause) and do not necessarily have a longer healthspan [3] (see Glossary). Age-associated illnesses are often sex-biased. For example, in 2018, men older than 65 years showed higher death rates of cancer, heart disease, stroke and diabetes, while Alzheimer's disease (AD), influenza and pneumonia showed higher death rates in women [4]. Women are also more susceptible to autoimmunity [5]. Such age-associated sex biases deserve more attention, as the elderly population worldwide is expected to double from 12% to 22% between 2015 and 2050.

Sex is often not reported in the scientific literature, making it hard to link sex-specific effects to ageing, although sex-biased gene expression is widespread in human tissues [6]. With exceptions, most genome-wide association studies (GWAS) omit sex chromosomes [7]. Lastly, the inclusion of women in clinical trials has been historically limited [8], and their under-representation has only recently initiated a callout to understand women's health across their lifespan [9]. The inclusion of women in clinical trials will avoid restricting the development and the application of current therapies, especially when a female-biased disease is encountered [10].

One reason why either sex can be more prone to certain age-associated phenotypes are the sex chromosomes. In mammals, females are XX and males XY, where the presence of the Y chromosome triggers the development of male gonads and secondary sexual traits. The type of sex determination system, whether it involves heterogametic XY males (see Glossary) as in mammals or heterogametic ZW females (see Glossary) as in birds, has been correlated with adult sex ratios (see Glossary) [1,11]. Mammals share evolutionarily conserved sex chromosomes, but in wild populations, not all mammalian females live longer than males. However, when they do, they have a longer median lifespan of around 20% [12]. How the sex chromosome complement impacts longevity is an active area of research [13,14]. Female mammals undergo X-chromosome inactivation (XCI), in which one of the two X chromosomes becomes heterochromatic, leading to the silencing of most of its genes (see box 1). Recently, genetic and epigenetic changes affecting the inactive X of females as well as the Y chromosome of males have been linked to the development of age-associated traits and diseases.

Box 1. The X chromosome and X-chromosome inactivation.

In mammals, sex is determined by the sex chromosomes, with males containing a gene-rich X chromosome and a degenerated, gene-poor Y chromosome; females instead harbour two X chromosomes. *Sry*/*SRY* is the Y-chromosomal male-determining gene, and its expression during embryonic development triggers a signalling cascade for the development of testis from undifferentiated gonads while suppressing ovarian differentiation. An XX genotype results in the expression of genes involved in the development of ovaries [15]. Although the X and Y chromosomes are non-homologous, a handful of X chromosome genes are also present in the Y chromosome. These X–Y pairs are known as gametologues and are mainly located in the pseudoautosomal region. The Y chromosome contains around 60 protein-coding genes of which 17 are gametologues (see Glossary) in humans and 9 in the mouse [16].

The XX versus XY genotype results in a gene dosage imbalance between the sexes with males exhibiting X-linked monoallelic expression. This may disrupt protein stoichiometric ratios and perturb molecular networks [17]. To equilibrate gene expression levels between the sexes, during the embryonic development of female mammals, one X chromosome is chosen for the collective silencing of all its genes. This is referred to as XCI, as reviewed by Galupa & Heard [18].

XCI begins with the upregulation of the master regulator Xist/XIST (which stands for X-inactive specific transcript), a long non-coding RNA transcribed from the future inactive X, coating it in *cis* (see Glossary). Xist then spreads to the rest of the X chromosome and induces a cascade of epigenetic mechanisms, including histone modifications, macroH2A deposition and DNA methylation. This promotes silencing, late-replication and structural reorganization of the X chromosome. The choice of which X to silence is random, but once a decision is made, the inactivated chromosome is propagated mitotically during each cell division.

XCI does not silence all genes as some are able to escape silencing. The mammalian X chromosome contains roughly a thousand of protein coding genes, and the number of escape genes is estimated to be around 20% in humans [19] and 3–8% in mice [20]. Escape from XCI occurs in a highly tissue-specific and, in humans, also in a variable fashion [18,21–23]. Ten human gametologues and four in mice escape inactivation [24]. Despite their high degree of sequence similarity, gametologues often exhibit functional differences between their X and Y versions [25]. These differences can contribute to sex-biased responses in various biological processes [26,27].

Besides the X and Y chromosomes, the action of sex-specific hormones can also contribute to an increase or reduction in the lifespan of one sex [13,28]. Experimental models such as the four core genotype (FCG) mouse model allow researchers to discern the contribution of gonadal sex versus sex chromosomes to biological processes such as ageing (see box 2).

Here we review sex-specific differences in the context of ageing and age-related diseases. Those could arise from social, environmental (not explored in this review) and physiological differences between men and women. We discuss these biological characteristics in the context of the hallmarks of ageing, which are an integrated framework to categorize causes and features of age-associated decline [35,36]. We then focus on how the epigenome of the inactive X and its master regulator *Xist*/*XIST* could contribute to both disease manifestation and resilience.

2. Sex bias and the hallmarks of ageing

Ageing is the progressive deterioration of cellular functions over time, compromising an organism's integrity [35,36]. The proposed hallmarks of ageing comprise cellular and molecular features that contribute to the phenotypic characteristics of the ageing process. They are grouped into three categories and are tightly related to one another [35,36]. The *primary hallmarks* (genome instability, epigenetic alterations, telomere shortening, loss of proteostasis and disrupted autophagy) directly contribute to a decline in cellular function by different means. These are initially counteracted by the *antagonistic hallmarks*, which, over time, become detrimental (cellular senescence, mitochondrial dysfunction and deregulated nutrient sensing). Ultimately, mishandled damage to nucleic acids or proteins leads to stem cell exhaustion, altered cellular communication, chronic inflammation and dysbiosis (see Glossary) (grouped as the *integrative hallmarks*). Sex differences in the hallmarks of ageing have been reviewed by Hägg & Jylhävä [28]. Here, we provide a brief discussion of sex bias in ageing hallmarks (see figure 1), especially in the light of novel insights gained in the last 3 years in humans and other species. When provided, we also report a list of genes that have been correlated with the hallmarks of ageing in a sex-specific fashion (see table 1).

Box 2. The FCG mouse model and ageing studies.

Since sex chromosomes trigger the development of the gonads (XX females develop ovaries, XY males testes), a sex-specific phenotype cannot be unambiguously ascribed to sex hormones secreted by gonads or the cellular karyotype. For this reason, the FCG mouse model was developed. Male gonads in mammals develop due to the presence of a single gene, *Sry*. While *Sry* is found in the Y chromosome, it can induce maleness independently of its chromosomal location. The FCG mouse model makes use of this property, as a transgenic male expressing *Sry* from chromosome 3 develops male gonads independently of the sex chromosome karyotype. Mating of such a male XY^- (Sry^+) mouse, in which *Sry* is transferred to an autosome, with normal XX females results in four offspring genotypes or phenotypes: (i) gonadal males with XX (Sry^+) genotype; (ii) gonadal males with XY^- (Sry^+) genotype; (iii) gonadal females with XX genotype; and (iv) gonadal females with XY^- genotype.

Comparing mice with different gonads, but the same sex chromosome complement, allows researchers to discern the action of sex hormones produced by testis and ovary. On the other hand, sex chromosome complement can be evaluated by comparing mice with the same gonads (XX versus XY) [29]. If in this comparison a difference is detected, other mouse models can help to discern whether those arise from the second X or Y chromosome [30]. Of note, a recent study identified an X-to-Y copy translocation in the FCG model, which impacts the dosage of nine genes [31]. One of these is *Tlr7*, whose excessive dosage leads to autoimmunity. Nonetheless, the FCG model has been a powerful tool to delineate the contribution of gonadal hormones as well as the identification of genes in sex chromosomes that play roles in physiology and disease (for a complete list, see [32]). Not many studies have investigated ageing with the FCG model, but it appears that XX mice, regardless of the gonads, live longer than their XY counterparts and that the presence of ovaries lengthens lifespan only in XX mice [33]. In addition, the extra X chromosome confers resilience to age-dependent cognitive decline [34].

2.1. Genomic instability

Genomic instability is the result of accumulated DNA damage leading to mutations and malfunctions. Cells exhibit various DNA damage repair (DDR) mechanisms and at least some of them act differentially in the sexes and along the ageing process. For example, the repair efficiency of double-strand breaks in peripheral lymphocytes decreases with age in women but not in men [40]. DDR-related proteins have been shown to play sex-specific roles. p53, an autosomal-encoded protein, is a key transcription factor that apart from acting as a tumour suppressor [65] has been shown to regulate the X chromosome status. p53 binds to the murine X inactivation centre and its loss perturbs XCI [66]. Also, the X chromosome encodes p53 regulators such as kinases and deubiquitinases [67]. Since males have just one X chromosome, mutations in those X-encoded p53 regulators can result in a more significant impact in males [68]. This could provide one explanation why age-associated cancer, except for reproductive and thyroid, is male-biased [67,69]. Another relevant DDR factor is the X-encoded *FANCB*. Its pathogenic variants result in accelerated ageing in men [39,70].

Genomic instability can also arise from the expression of transposable elements. The Y chromosome is especially rich in transposons. It has been shown in the fruit fly that a male burden exists when Y heterochromatin loss upon ageing leads to transposon depression [71]. Whether such a 'toxic Y' reduces male lifespan and whether this is conserved has been debated, but recent work suggests this is not the case [72].

Genome instability can impact each sex differently if it affects the sex chromosomes directly. Aneuploid cells (see Glossary) can expand through clonal mosaicism (see Glossary), a process taking place in ageing human lymphocytes and other tissues [42,73]. Sex chromosome aneuploidies in ageing occur at a higher frequency than for any autosome, with loss of the Y chromosome (LOY) and X chromosome (LOX) being the major form of somatic mosaicism in males and females, respectively. LOX occurs with a frequency of less than 3% in women below 40 years, increasing to more than 35% in women older than 80 years [38]. It preferentially affects the inactive X [38,74] and is associated with an increased risk of lymphoid leukaemia and acute tonsillitis [75,76], smoking [38], vitamin B complex deficiency [76] and bacterial-caused pneumonia [76]. LOY is found in different cell types [77], increases from around the age of 50 [78–80] and is correlated with a shorter lifespan [81] and the onset of age-related diseases including AD and bladder and prostate cancers [37,41]. The loss of gametologues via LOY [82,83] or loss-of-function mutations [84] could be a relevant determinant of why cancers are usually deadlier and male-biased. Transplantation of Y-lacking haematopoietic stem cells (HSCs) to recipient male mice leads to cardiac malfunctioning and fibrosis as they age [85]. Genes on the inactive X on the other hand can also provide a genetic reservoir for reduced cancer incidence in women [86]. Whether sex chromosome aneuploidies are drivers or consequences of sex-specific ageing is not well understood. The use of study systems other than humans (e.g. rats [87]), single-cell technologies to study *de novo* somatic mutations [88], as well as recently developed tools that allow the induction of defined aneuploidies in mammalian systems [89,90] will open up new routes to understanding if, how, and why sex chromosome loss impacts ageing.

2.2. Telomere attrition

Telomeres are repetitive DNA sequences located at the end of each chromosome. They associate with proteins to protect free chromosome ends from fusions and from activating DDR pathways [91]. Telomeres shorten at each cell division, and once they are so short that they no longer bind telomere-binding proteins, cells undergo death or replicative senescence (see Glossary) [92]. Telomere attrition (see Glossary) occurs due to the absence of telomerase, a ribonucleoprotein (RNP) complex that adds

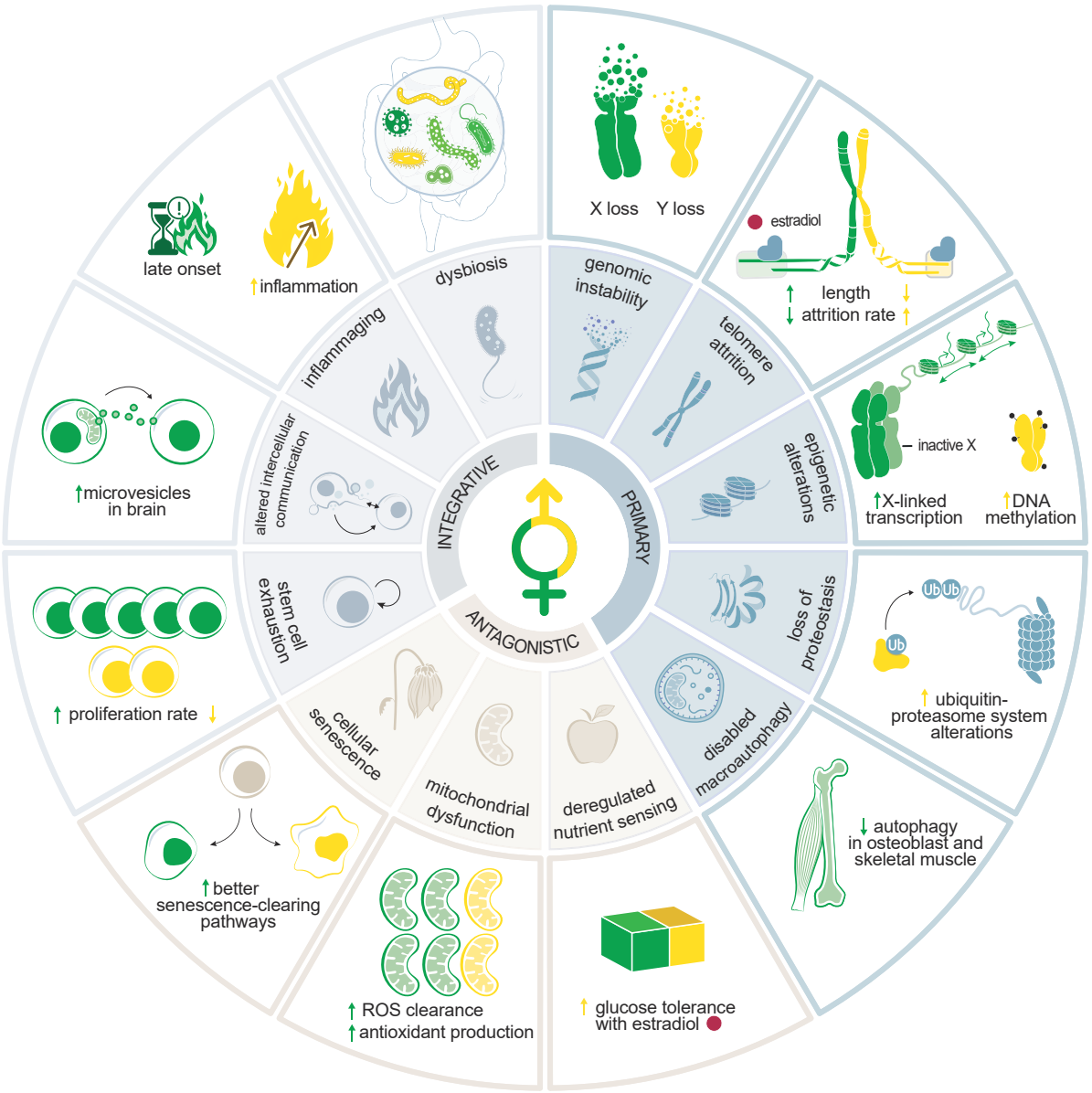

Figure 1. Graphical illustration of the hallmarks of ageing and how they are affected in a sex-specific manner. One example per hallmark (green for females and yellow for males) is illustrated. Primary hallmarks are shaded in light blue. Chromosome instability results in Y chromosome loss in men and X chromosome loss in females. Telomere attrition is faster in males than females, in part due to the oestrogen responsiveness of the *TERT* subunit of the telomerase complex. Epigenetic alterations include hypermethylation of the Y chromosome and relaxation of the heterochromatic inactive X that leads to the upregulation of X-linked genes. Loss of proteostasis affects primarily males, where X-linked mutations reduce lifespan and influence disease onset. Disabled macroautophagy is female-biased with lower activity seen in osteoblasts and skeletal muscle. Antagonistic and integrative hallmarks are shaded in beige and light grey, respectively. Cellular senescence negatively affects males before females. Mitochondrial dysfunction affects males before females and is associated with impaired clearance of reactive oxygen species (ROS) and production of antioxidants. Nutrient sensing: sex effects depend on the modulation of each pathway. The example shows oestradiol, which improves glucose tolerance in males. Integrative hallmarks: Loss of stem cell potential is faster in males. Altered intercellular communication is illustrated by the increase in mitochondrial-derived microvesicles in female aged astrocytes. Inflammaging affects males more than females. Dysbiosis starts later in females, as menopause impacts microbial diversity.

nucleotides to the telomeres. Telomerase activity is repressed in most somatic cell types, and thus telomeres are a key factor in how many times a somatic cell in an organism can divide [93].

It is clear that telomeres shorten during ageing across different tissues, but there has been conflicting data on whether sex is an important factor in telomere homeostasis [94–97]. Mutations in telomerase-associated proteins result in male-biased dyskeratosis congenita, characterized by faster telomere attrition rates and therefore shorter telomere length (TL) [43]. Interestingly, the majority of germline pathogenic mutations causing dyskeratosis congenita occur in the X-linked dyskerin gene (*DKC1*), one of the proteins that stabilizes and positions the telomerase complex [43]. The lower incidence of affected females is due to skewed XCI (see Glossary) [98]. While skewed XCI is tissue-dependent and increases with female age, it is a rare event in newborns and extreme skewing is mainly seen in the context of X-linked pathogenic diseases [99,100].

Besides important X-encoded proteins for telomere homeostasis, chromosome-specific attrition rates can also contribute to a sex bias in age-related diseases [101]. Telomeres on the inactive X undergo faster attrition rates than those on the active X [102]. Chromosomes bearing shorter telomeres and containing large heterochromatin regions, such as the Y or inactive X, are more

Table 1. Genes or loci linked to the ageing hallmarks in a sex-dependent manner in different species. When a locus is reported, we additionally provide the variant or probe used (for GWAS and EWAS). The LOY-related loci identified by Wright *et al*. [37] were also found to be involved in LOX. However the LOX variants had little correlation to LOY in Liu *et al*. [38].

Phenomenon	Species	Bias	Gene/Locus	Location	Ref
Genomic instability					
Decreased DNA damage repair efficiency resulting in Fanconi anemia	*Homo sapiens*	Male	*FANCB*	Chr X	[39]
Decreased DNA damage repair via non-homologous end joining in blood lymphocytes	*H. sapiens*	Female	*ATM*	Chr 11	[40]
	H. sapiens	Female	*BLM*	Chr 15	
	H. sapiens	Female	*XRCC6*	Chr 22	
LOY	*H. sapiens*	Male	*PMF1, PMF1-BGLAP; rs2736609, rs2842873*	Chr 1	[37,41]
	H. sapiens	Male	*TSC22D2, LINC01214; rs59633341, rs4681200*	Chr 3	
	H. sapiens	Male	*SENP7; rs4683900* *SPINK8, FBXW12; rs115854006* *LINC01214; rs4681200* *FAM172BP,TRMT10C; rs13088318*	Chr 3	
	H. sapiens	Male	*NREP, STARD4-AS1; rs56084922, rs56116444*	Chr 5	
	H. sapiens	Male	*CCDC162P; rs13191948* *CD164; rs11251* *QKI; rs381500* *MEAT6; rs4709819*	Chr 6	
	H. sapiens	Male	*MAD1L1; rs4721217, rs4721217*	Chr 7	
	H. sapiens	Male	*RBPMS; rs35091702, rs2979469*	Chr 8	
	H. sapiens	Male	*NPAT; rs4754301* *C11orf65; rs227079*	Chr 11	
	H. sapiens	Male	*WBP4; rs10687116*	Chr 13	
	H. sapiens	Male	*TCL1A, TUNAR; rs1122138, rs1122138* *DLK1, LINC00523; rs137952017, rs72698721*	Chr 14	
	H. sapiens	Male	*CENPN, ATMIN; rs12448368, rs77874075*	Chr 16	
	H. sapiens	Male	*TP53; rs78378222, rs201753350* *FAM117A; rs77522818, rs78997619*	Chr 17	
	H. sapiens	Male	*LINC01478; rs11082396, rs80277818* *BCLN2; rs17758695*	Chr 18	
	H. sapiens	Male	*TPX2; rs60084722*	Chr 20	
LOX	*H. sapiens*	Female	*PHC2; rs10798950*	Chr 1	[38,42]
	H. sapiens	Female	*S1PR1; rs11166573* *LOC100506274; rs16866241* *CPS1; rs66826907* *SP140L; rs725201, rs17327417, rs3731723, rs3086612, rs11885965, rs184226567, rs11686798, rs1678185*	Chr 2	
	H. sapiens	Female	*EOMES; rs2887944* *CX3CR1; rs3732378* *LPP-AS1; rs13080752*	Chr 3	
	H. sapiens	Female	*TADA2B; rs568868093* *CENPU; 4:184696883:C:CT*	Chr 4	
	H. sapiens	Female	*ERAP2; rs3832368*	Chr 5	
	H. sapiens	Female	*JARID2; rs794791* *BTN3A2; rs57760309, rs150289512*	Chr 6	

(*Continued*.)

Table 1. (*Continued.*)

Phenomenon	Species	Bias	Gene/Locus	Location	Ref
			HLA; rs141806003, 6:29866672:A:G *HSPA1A; rs9266234, rs9267283, rs2844455* *C2; rs115378818* *HLA-DQA1; rs7771548, rs146406015* *ITPR3; rs7752348* *CENPQ; rs9395493* *SCML4; rs1739873* *CENPW; rs9372840* *MYB; rs4895441* *SHPRH; rs148401398* *LOC102724152; rs381500*		
	H. sapiens	Female	*MAD1L1; rs2280548*	Chr 7	
	H. sapiens	Female	*CSMD1; rs1827666* *MSC; rs10099390*	Chr 8	
	H. sapiens	Female	*TNFSF8; rs36118932*	Chr 9	
	H. sapiens	Female	*ATM; rs751343*	Chr 11	
	H. sapiens	Female	*KLRB1; rs5796352*	Chr 12	
	H. sapiens	Female	*CSNK1A1L; rs11147640*	Chr 13	
	H. sapiens	Female	*IL27; rs181206* *HEATR3; rs754391850*	Chr 16	
	H. sapiens	Female	*TP53; rs78378222* *PRKAR1A; rs768326149, rs16973034*	Chr 17	
	H. sapiens	Female	*TOMM40; rs113106418* *LILRA1; rs10411397*	Chr 19	
	H. sapiens	Female	*NCOA6; rs2076668*	Chr 20	
	H. sapiens	Female	*GSPT2; 23:51749114:C:CGT* *KLF8; rs6521410, rs141849992* *AMER1; rs181043195* *AR; rs58638231* *PLS3; rs12836051, rs60523627* *DXZ1; rs2942875* *DXZ4; rs11091036*	Chr X	
Telomere attrition					
Faster telomere attrition rate resulting in dyskeratosis congenita	*H. sapiens*	Male	*DKC1*	Chr X	[43]
Epigenetic alterations					
Hypomethyation in muscle, tail, and kidney correlates with decreased expression of androgen receptors	*Ovis aries*, *Mus musculus*	Male	*MKLN1; cg21524116*	Chr 6 (*M. mus*)	[44]
Hypermethylation in the blood	*H. sapiens*	Male	*NLGN4Y; cg03055837, cg04691144, cg27443332, cg03706273* *LOC100101121, TTTY23; cg00311963* *DDX3Y; cg14180491* *TBL1Y; cg01707559* *TTTY20; cg06636270* *TMSB4Y; cg26198148*	Chr Y	[45,46]

(*Continued.*)

Table 1. (*Continued.*)

Phenomenon	Species	Bias	Gene/Locus	Location	Ref
			TTTY14; cg03244189, cg13845521, cg11816202, cg15345074		
Hypomethylation in the blood	*H. sapiens*	Male	*TTTY15; cg25032547* *DDX3Y; cg17816615* *E1F1AY; cg01988452, cg13308744* *TTTY13; cg14467015*	Chr Y	
	H. sapiens	Female	*GAGE10; cg15833111*	Chr X	[47]
Age-dependent loss in hematopoietic stem cells results in increase X-linked expression, hypomethylation and higher chromatin accesbility	*M. musculus*	Female	*Xist/XIST*	Chr X	[48]
Loss of Proteostasis					
Decrease or loss-of-function of the E1 ubiquitin-activating enzyme leads to X-linked infantile spinal muscular atrophy and shorter lifespan	*H. sapiens*	Male	*UBA1*	Chr X	[49]
Decrease or loss-of-function of the E2 ubiquitin-conjugating 2A enzyme leads to neurodegenerative diseases	*H. sapiens*	Males if it is a germline pathogenic variant; in aging, depending on the neurodegenerative disease	*UBE2A*	Chr X	[50]
WT Ubiquilin−2 aggregates in synucleinopathies	*M. musculus, H. sapiens*	No formally tested	*UBQLN2*	Chr X	[51]
Germline mutations lead to ALS and FTD	*H. sapiens*	Earlier onset in males	*UBQLN2*	Chr X	[52]
FMRP mutations lead to adult-onset neurodegenerative disorder, possibly to its role in the ubiquitin pathway	*H. sapiens*	Males	*FMR1*	Chr X	[53,54]
Tau aggregation by increased expression of the USP11 deubiquitinase in the female brain	*M. musculus, H. sapiens*	Females	*USP11*	Chr X	[55]
Disabled macroautophagy					
Decreased number of autophagic vesicles in the aged osteoblasts assessed by LC3-II protein levels	*M. musculus*	Female	*Map1lc3b*	Chr 8	[56]
Decreased autophagic activity in the aged osteoblasts is due, in part, to lower number of autophagic vesicles, assessed by LC3-II protein levels	*M. musculus*	Female	*Map1lc3b*	Chr 8	[57]
Pathogenic germline variants can lead to impaired autophagy in the Danon disease	*M. musculus*	Males are more affected but a later onset is seen in females, resulting in a shorter male lifespan	*LAMP2*	Chr X	[58]
ALS/FTD-related pathogenic UBQLN2 mutations impair	*H. sapiens*	Earlier onset in males	*UBQLN2*	Chr X	[59]

(*Continued.*)

Table 1. (*Continued.*)

Phenomenon	Species	Bias	Gene/Locus	Location	Ref
ubiquitin-proteasome-driven mitophagy					
Cellular senescence and inflammaging					
Higher expression in dendritic cells, natural killers, T cells, B cells and macrophages promotes inflammation and oxidative stress	*H. sapiens*	Male	*CXCR4*	Chr 2	[60]
	H. sapiens	Male	*HLA-DRB5*	Chr 6	
	H. sapiens	Male	*DDIT4*	Chr 10	
	H. sapiens	Male	*JUNB, ZFP36*	Chr 19	
Higher expression, related to higher activity of T cells	*H. sapiens*	Females	*CCR4*	Chr 3	
	H. sapiens	Females	*CYBA*	Chr 16	
	H. sapiens	Females	*IL—2RG*	Chr X	
	H. sapiens	Females	*MZB1*	Chr 5	
	H. sapiens	Females	*XBP1*	Chr 22	
Decreased inflammation in monoctyes and macrophages	*M. musculus, H. sapiens*	Females	*Xist/XIST*	Chr X	[61]
Dysbiosis					
KO mice (resembling FXS) have a misregulated gut microbiome. FXS is more prevalent in males	*M. musculus*	No formally tested but fragile X syndrome is more prevalent in human males	*Fmr1*	Chr X	[62]
Increased expression of these genes is correlated with a stronger immune responses in undisrupted microbiota	*M. musculus*	Females	*Kdm6a, Eif2s3x*	Chr X	[63]
Stem cell exhaustion					
Faster attrition rate impairs stem cell proliferation leading to bone marrow failure	*H. sapiens*	Male	*DKC1*	Chr X	[43]
Altered intercellular communication					
Higher expression in astrocytes of mitochondria-derived microvesicles	*M. musculus*	Females	*TSG101*	Chr 7	[64]
	M. musculus	Females	*Anxa2, Hspa8*	Chr 9	

ALS, amyotrophic lateral sclerosis; EWAS, Epigenome-wide association studies; FTD, frontotemporal dementia; FXS, fragile X syndrome; GWAS, Genome-wide association studies; LOX, loss of the X chromosome; LOY, loss of the Y chromosome.

easily lost, leading to aneuploidy and/or LOX/LOY [103]. Finally, telomere shortening disrupts XCI maintenance by reducing the deposition of H3K27me3, allowing for the reactivation of genes that under normal XCI dynamics are silenced [104].

Recently, mouse models with human-like telomeres [105] and comparable human somatic expression levels of telomerase [106] have been developed, facilitating mechanistic approaches for studying telomere attrition rates and sex differences in human ageing.

2.3. Epigenetic alterations

Although there are multiple uses of the term epigenetics, we herein use it to refer to modifications that alter gene expression across multiple cell divisions without changing the primary DNA sequence. Epigenetic regulators include non-coding RNAs, histones and their associated post-translational modifications and DNA methylation (DNAme). DNAme at cytosine residues is one of the most widely studied epigenetic marks [107]. Interestingly, DNAme appears to be one of the most reliable biomarkers to estimate how physiological conditions ('biological age') differ from an individual's chronological age [108,109]. Mathematical modelling has led to the generation of various 'epigenetic clocks' that identify specific methylated cytosine sites correlating with

accelerated ageing in males [110]. More recently, 'new clocks' have identified evolutionarily conserved sites exhibiting age-related changes across different mammalian species [111]. Some of these methylated sites can become hypomethylated with age, which correlates with higher expression levels of androgen receptors across mammalian species [44]. Also, the Y chromosome becomes hypermethylated with age [45–47]. However, mechanistic experiments that causally connect locus-specific methylation changes with ageing and sex are still lacking.

XCI is another paradigm of epigenetic regulation (see box 1), and, perhaps unsurprisingly, disrupted XCI and misregulation of its master regulator *Xist*/*XIST* have been implicated in sex differences in several ageing hallmarks. Increasing evidence marks the immune system not only as being at the heart of several ageing processes but also as one of the most sensitive systems with regard to disruption of XCI. As such, *Xist*/*XIST* regulation and epigenome remodelling of the X during ageing deserve special attention (see §4).

2.4. Loss of proteostasis

Proteostasis refers to the regulation of a balanced proteome through processes such as protein synthesis, folding, localization and degradation [112]. Ageing disrupts proteostasis, leading to increased discrepancies between mRNA and protein abundance [113] and sex-specific alterations in the tissue proteome of mice [114,115]. The brain contains the most long-lived proteins with females exhibiting slower turnover rates of these proteins than males [116]. Although this could be seen as a 'benefit' of a slow ageing process, it could be detrimental since spontaneously damaged proteins will be present for longer in females. Of interest, many long-lived proteins in the brain are related to female-biased AD [117].

Mechanistically, such observations could be explained by sex-specific alterations in the protein synthesis machinery. For example, protein levels of the ribosomal large subunit complex are higher in the aged female liver [114]. Inefficient handling of misfolded proteins and protein aggregates may also play a role. Long-lived organisms resist protein damage [118], have an active proteasome [119], exhibit higher expression of chaperones and proteasome subunits [120] and show enhanced mitochondrial detoxification of oxidative species [121]. Proteasome activity varies between males and females in a tissue-specific manner. Higher protein degradation activity can be detected in the murine male kidney, murine female small intestine and spinal cord [122] and human female blood cells [123].

For proteotoxic stress occurring in the endoplasmic reticulum and mitochondria, the unfolded protein response (UPR) serves as a protective mechanism that can differ between males and females (reviewed in the context of age-associated diseases by Wodrich *et al*. [124] and gonadal ageing by Okan *et al*. [125] and Rahmani *et al*. [125,126]). For example, female pancreatic β cells in mice demonstrate greater resilience to endoplasmic reticulum stress (see Glossary) compared to their male counterparts [127]. In nematodes, the gonadal-to-soma axis is required for UPR activation in the mitochondria with XX hermaphrodites (see Glossary) being more responsive than XO males [128].

One explanation for why these processes are sex-biased could be the X-linkage of members of the ubiquitin–proteasome system (UPS; see table 1). Loss-of-function mutations or decreased function either shorten lifespan primarily in men [49] or the disease onset is earlier in men [52]; however, female-biased vulnerabilities exist [55]. Deficiency and misregulation of X-encoded UPS proteins are correlated to neurodegeneration [50,51] and earlier cognitive decline in X-linked disorders [53,54].

Currently, there is no systematic study of how and whether the X chromosomal location of proteostasis pathway genes affects lifespan in the two sexes. This could for example be addressed by investigating the highly conserved UPS and UPR system in different species with different sex chromosome complements.

2.5. Disabled macroautophagy

Macroautophagy, the main form of autophagy, is the delivery of cytoplasmic components to the lysosome for their degradation and recycling [129]. This process becomes defective during ageing. Autophagic activity is lower in females than in male fruit flies, promoting disruption of the epithelial gut structure and barrier function [130]. In mammals, basal autophagic activity tends to be lower in murine female skeletal muscle and adipose tissues [56,130]. Age-related changes in autophagic activity have been reported in murine female osteoblasts and skeletal muscle [56,57]. As reviewed in [131], some autophagy-related genes and modulators of the autophagy signalling pathway in the brain are X-encoded in mammals but it is unknown whether their chromosomal location contributes to the lower autophagic activity seen in different female tissues.

Chaperone-mediated autophagy is another form of autophagy that declines during ageing. In this process, some proteins are delivered to the lysosomes by binding to chaperones, instead of being membrane-encapsulated [132]. The X-encoded factor LAMP2A is a central regulator of chaperone-mediated autophagy and is thought to be involved in the age-related decline of this pathway. Indeed, mutations in the *LAMP2* gene lead to Danon disease, in which males are more affected and have a shorter lifespan [58]. Moreover, the X-encoded ubiquilin 2 protein impairs autophagy of the mitochondria when mutated [59]. The enrichment of these X-linked genes as key regulators of such pathways provides a rationale for exploring autophagy in sex-related processes. This is of relevance in age-induced XCI relaxation, which has been previously addressed by [104] and will be further discussed in §4.1.

2.6. Cellular senescence and inflammaging

Cellular senescence refers to the permanent arrest of cell division. While senescence can prevent further damage and is therefore initially protective, accumulation of senescent cells is harmful. Male mice exhibit a higher number of senescent cells across their lifespan than females [133], and this can be attributed to more efficient clearing of senescent cells by the female immune system [134]. Accumulation of senescent cells in the human immune system, known as immunosenescence, decreases the capacity of immune cells to clear aberrant cells. This, in turn, appears to promote the production of proinflammatory molecules, such as interleukin 6 and 18, which accumulate prematurely in ageing men [135]. Over time, the constant state of low-grade chronic inflammation is known as inflammaging [136]. Inflammaging has tissue-specific outcomes and is, for example, greater in the female cortex of the ageing brain [137,138]. Fibrosis and inflammation also play a major role in the ageing of the female reproductive tract [139], a property that is modulated by cycling and pregnancy numbers.

Ageing amplifies the sex differences in immune cell types found in young individuals and affects gene expression programmes in a sex-specific manner. For instance, while monocyte numbers do not change between the sexes during ageing, their chromatin accessibility and gene expression are higher in males [60,135]. Another mechanism that shows sex specificity is attributed to the X chromosome. Upon inflammation in monocytes and macrophages, *Xist*/*XIST* surprisingly shows a cytoplasmic localization. Here, this long non-coding RNA interacts with p65 in order to dampen the proinflammatory NF-κB complex [61]. Many questions are left unanswered including how *Xist*/*XIST* senses inflammation and how this nuclear RNA can translocate to the cytoplasm. More studies are needed to uncover whether *Xist*/*XIST*'s role in inflammation diseases is more general [140].

2.7. Mitochondrial dysfunction

Mitochondria and the metabolites they produce are a central focus of ageing research, as mitochondrial activity declines over the lifespan [36]. While reduced energy production in ageing can help limit reactive oxygen species (ROS; see Glossary) as their levels decrease too, ROS clearance pathways are also impaired, thus leading to higher oxidative stress. Mitochondrial numbers decrease upon ageing, with lower numbers observed in men [141]. Females exhibit refined mitochondrial processes that can contribute to their lifespan lengthening while delaying disease. Those include higher energy production, higher content of antioxidants to clear ROS and better responses to mitochondrial-induced stress [142]. This can be, for example, observed in the sexually dimorphic bioenergetic profiles of immune cells [143,144] or expression changes in genes important for mitochondrial function in the heart [145]. The FCG model (see box 2) revealed that the Y chromosome, independently of the sex hormones, can be responsible for upregulating *Hk2* and *Pdk4*, both of which are nuclear-encoded mitochondrial genes [146]. However, if this is relevant to sex-specific differences in ageing remains to be analysed.

The mitochondria's crucial role in energy-demanding tissues is underscored by mitochondrial DNA (mtDNA) mutations (e.g. induced by ROS) occurring in ageing. How mtDNA mutational load affects the sexes needs further investigation, but interestingly, those processes have been associated with the property of mutated mitochondria to become 'selfish' and negatively affect the fitness of the ageing host [147]. Of note, mitochondria are maternally inherited, and assumptions that female-specific processes have evolved to maintain mitochondrial function and mtDNA have been proposed [148]. Thus, the question of whether and how mitochondrial haplotypes selected in females contribute to sex-specific ageing will be an intriguing area of study.

2.8. Deregulated nutrient sensing

As our bodies age, they handle nutrient sensing, uptake and metabolism in increasingly complex ways. Dietary restriction can extend lifespan in some animals, but its effectiveness diminishes with age [149]. Inhibition of the kinase mammalian target of rapamycin (mTOR) pathway by rapamycin acts as one of the major nutrient-sensing pathways. By inhibiting mTOR, rapamycin mimics caloric restriction and increases lifespan from yeast to worms to mice. Interestingly, it interacts with sex in different ways. In the fasted state, the mTOR pathway generally exhibits higher basal activity in females than in males [150]. In Drosophila, the activation of the mTOR/S6K enhances inflammation through atypical NF-κB activation in fat cells, while its inhibition extends female lifespan. This is not through the downstream autophagic flux, which responds similarly between the sexes [151]. One of the major downstream targets regulated by mTOR is adenosine monophosphate-activated protein kinase (AMPK), which is activated in response to low cellular energy levels. In the killifish, constant AMPK activation appears to benefit females. The constant genetic activation of the AMPKγ1 isoform generates a youth-like response to fed-fasted feeding switches in the adipose tissue of old females [152]. Conversely, when AMPK is activated through direct inhibition of the nucleotide salvage pathway, this extends lifespan in males through improved liver function [153]. In mice, interfering with AMPK produces mixed results with regards to which sex profits from the interventions, potentially due to variations in genetic background and the specific tissues analysed [150]. Since the evolutionary origins of the X and Y chromosomes in killifish, fruit fly and mammals, and accordingly, their gene compositions are entirely different [154], it is unlikely that sex-biased effects on mTOR arise from X-linkage.

Indeed, sex hormones influence how the body interprets nutrient signals. For example, oestradiol (see Glossary), the female sex hormone, improves glucose tolerance in males but not females [155]. It would be interesting to understand the molecular basis of these sex-specific differences in nutrient sensing, but because hormones, X chromosomes and dietary requirements differ for various model organisms, it will likely be challenging to extrapolate the findings to humans.

2.9. Dysbiosis

The commensal bacteria found in the mammalian gastrointestinal tract are important for nutrient absorption and digestion, protection against pathogens and synthesis of beneficial metabolites. The composition and function of the intestinal microbiome change considerably during ageing, which in turn influences its interaction with the immune system and thus correlates with e.g. increased susceptibility to infectious diseases and reduced vaccination response.

Compared to males, the female gut microbiome is more diverse [156] and harbours, for example, species that ensure better glucose metabolism [157]. This greater abundance of beneficial bacteria in the female gut is kept until menopause [158]. After menopause, the female gut microbiome becomes similar to men [159]. Depletion of the gut microbiome in mice significantly alters sexually dimorphic gene expression, particularly in the liver. Germ-free male mice show downregulation of male-biased genes and upregulation of female-biased genes, while germ-free female mice exhibit attenuated female-biased gene expression. Those genes belong to metabolic pathways regulated by sex hormones and growth hormonal signalling. The gut microbiome thus appears to be crucial to maintaining proper sexual differentiation of gene expression and metabolism in mice [160]. The transit time (see Glossary) is also associated with the gut microbiome and varies between the sexes [161].

Sex-dependent changes in microbial diversity can, for example, influence cytokine (see Glossary) production [162]. Since microbial diversity is known to be altered in, e.g. Fragile X syndrome [62], genes encoded by sex chromosomes may be causally related to sex-dependent dysbiosis upon ageing. In a recent study, this idea was investigated using the FCG mouse model. XX mice showed a better immune response to dead bacteria than XY mice, regardless of gonadal sex. Although clearance of the gut microbiome by administration of antibiotics impaired this effect, it was restored after recolonization of the intestine with bacteria that produce short-chain fatty acids, a known class of immunomodulators. At the molecular level, these effects were associated with expression changes in the X-linked genes Kdm6a and Eif2s3x, which both belong to the class of XCI escapee [63]. Some X chromosome escape genes have been linked to promoting acute proinflammatory cellular responses, as observed in sex-biased human glioblastoma [86]. Alternatively, Y-linked gametologues could positively influence the immune response in XY individuals. For example, functional divergence has been demonstrated to occur in the context of the Uty paralogue of Kdm6a through a protective activity against pulmonary hypertension [26,27,163]. These hypotheses are yet to be tested in the context of the gut-microbiota axis.

2.10. Stem cell exhaustion

Tissue-residing stem cells are important to renew tissues such as the gut, skin or blood. Their function declines with age and many stem cell populations face decreased potential during ageing [164,165]. HSCs are the go-to cell type for tissue stem cell biology as their derived mature cells (e.g. erythrocytes or macrophages) are largely short-lived and cannot proliferate. Ageing results in decreased HSC potential [166], cessation of proliferation in up to 30% of its population [167] and HSC size increase, which is negatively associated with functionality [168]. Cell cycle analysis indicates that aged HSCs are in a more quiescent state than young ones [169]. Given that proliferation is central to stem cell biology, it is unsurprising that the functional decline of stem cells can be linked to primary hallmarks, such as DNA damage [170] and telomere attrition. For instance, bone marrow failure is the main cause of death in dyskeratosis congenita [43].

How is stem cell function different between males and females and how does it impact ageing? The adult intestinal stem cells of the fruit fly show intrinsic sex differences reflecting on the expression of genes involved in growth and metabolism [171–173] impacting the cell cycle and thus susceptibility to cancer [68]. Differences associated with the cell cycle are also observed in rodents, where haematopoietic, neural and muscle stem cells proliferate faster in females [174]. It will be important to study and analyse sexes separately in the recently developed stem cell tracing single-cell gene expression technologies (e.g. [167] used both male and female individuals together). Different stem cell-containing tissues need to be studied and ideally involve comparisons of humans to other systems whenever possible.

2.11. Altered intercellular communication

Cell–cell interactions can impact ageing by activating inflammatory pathways leading to enhanced immunosenescence [60]. Yet, there has been little research into sex-biased changes in intercellular communication with ageing. One observation relates to cell–cell communication occurring through extracellular vesicles. These vesicles are secreted by cells and transfer different macromolecules to others [175]. Through increased levels of biogenesis factors (e.g. Annexin 2, Alix, TSG101 and HSC70), microvesicle numbers increase upon ageing in female but not male mouse brains. These vesicles are of mitochondrial origin and are produced by astrocytes [64]. The content of these vesicles, the target cells, as well as the molecular nature of the sex bias, remains obscure. Extracellular vesicles have also been correlated with female-dependent neuroinflammation in ageing [176]. Finally, other forms of perturbed intercellular communication have been reported between (e.g. granulosa cells and the ageing oocyte [177]).

3. The roles of sex hormones in human ageing

The major sex hormones are testosterone and oestradiol, which are important for the development of sexual organs and traits. Both are present in males and females but in different amounts. Testosterone is the major male sex hormone and

oestradiol—metabolized from testosterone by the enzyme aromatase—is the major female sex hormone. Humans experience a 'mini-puberty' (see Glossary) in early infancy, and both hormones are detected circulating in the human body at low levels. However, their main peaks start during puberty between 8 and 13 years in girls and 9 and 14 years in boys. In the mouse, this corresponds to 4–6 weeks postpartum in females and 7–11 weeks in males [178,179]. In men, testosterone decreases steadily from around the age of 30 years and is accompanied by an increase in oestradiol levels. Eventually, this can result in a state referred to as andropause and is characterized by fatigue, insomnia, mood changes, irritability and lower sexual desire. Between 40 and 49 years, the frequency of andropause among men is 0.1%, increasing to 5.1% by 79 years [180]. Oestradiol in females is dynamic with constant cycling during menstruation after puberty. Between 35 and 45 years of age, females enter perimenopause, characterized by irregular hormonal changes. After this—post-menopause—oestradiol levels drop abruptly [181].

Sex hormones exert their effects by binding to membrane-bound or intracellular receptors, which are expressed in a variety of cell types, tissues and even organelles [182,183]. They regulate brain sexual differentiation [184], change chromosomal three-dimensional conformation [185] and induce sex-biased expression profiles, to some extent through hormone-related transcription factors [6]. The roles of sex hormones in healthspan and lifespan are actively investigated (comprehensively reviewed by Ng & Hazrati [186]). Nonetheless, it appears that sex hormones are protective, a property from which both sexes can 'profit'. For instance, premature menopause is associated with a shorter lifespan and higher mortality rates [187]. In mouse skeletal muscle cells, oestradiol is present in mitochondria, reducing oxidative stress and increasing mitochondrial respiration [188]. In males, the adipose tissue is an inflammatory hub, and testosterone alleviates this by reducing fat mass [189].

If both sex hormones hold anti-ageing properties, why do men age faster? The decline in testosterone in men starts earlier than the oestradiol decline in women. Such a decline in males does not trigger specific diseases but rather increases the risk of developing them. For example, in men with andropause, there is a co-occurrence with diabetes, osteoporosis and increased fat mass [190]. In females, many of the hallmarks of ageing worsen during peri- and post-menopause. For instance, levels of the antioxidant glutathione are higher in the female brain during the reproductive age, offering protection against ROS. Glutathione decline leads to the remodelling of metabolic pathways that expose females to mitochondrial dysfunction [191]. Possibly, oestradiol could be also more protective than testosterone. However, the oestradiol pulses during the reproductive age of mice come at a price as the constant remodelling of the female reproductive organs in each cycle results in age-dependent fibrosis and inflammation [139].

The supplementation of sex hormones, also referred to as hormonal therapy (HT; see Glossary), is an opportunity for ameliorating ageing-induced symptomatology. This is of particular interest in females given the sudden oestradiol decrease, but can also be applied to men [192,193]. Ideally, HT is provided early enough so that its protective effects can be sufficiently sustained, usually before 60 years [194]. The cellular response upon HT is cell-type-specific. Oestrogen therapy in post-menopausal women reduces the production of proinflammatory cytokines [195] while increasing B cell counts [196]. In mice, the mammary tissue responds rather negatively to exogenous oestrogen by increasing the risk of developing breast cancer [197,198]. Hormonal phases influence the onset and incidence of colorectal cancer, with oestrogen supplementation being associated with a lower risk of developing the disease in post-menopausal women [199,200]. More research is needed to understand how different human cell types respond to age-related HT, including testosterone effects. An example includes the development of a hormonal signalling map as it has been recently done in the mouse lemur [201]. While animal models offer insights, establishing clear parallels with human responses is crucial for developing more effective, personalized HTs while reducing side effects.

Additionally, many issues still need to be addressed and properly designed case-control studies with the appropriate control subjects are needed. For instance, many females undergo hormonal changes when they use contraceptives for birth control [202]. How they affect female lifespan is not clear, but combinatorial therapies decrease the risk of developing colorectal, endometrial, ovarian, lymphatic and haematopoietic cancer, with the effects persisting for at least 30 years in past users [203]. How the constant use of hormones can modify male healthspan, including the risk of cardiovascular disease and death, is less well studied, but bodybuilders, who consume androgens as part of their activities, are an ideal case study to do so [204]. Further investigations are also needed to determine if these beneficial effects persist with the newer generation of birth control pills. When needed, the use of emerging organisms in ageing research can provide deeper mechanistic insights into these processes [205].

4. Balancing the seX: opposing effects of the X chromosome

XCI (see box 1) provides expression equilibration of X-linked genes between the sexes but can also benefit females. Although XCI is usually random, it can become skewed to one of the parental chromosomes, which is relevant when genes are mutated in a heterozygous fashion. This can prevent the expression of pathogenic variants, a possibility that males do not possess (for a detailed discussion see [206]). XCI can also buffer the effect of cancer mutations occurring on the X [207,208]. Lastly, the biallelic expression of female escapees can provide resilience, for example, if they encode tumour-suppressor genes [84]. The two X chromosomes are beneficial to female lifespan and healthspan, but, nonetheless, can also affect females negatively (see figure 2).

4.1. Moonlighting roles of *Xist/XIST* beyond triggering XCI

Xist/XIST establishes XCI, but once this repressive state is induced, it is dispensable for maintenance, making XCI a *bona fide* epigenetic mechanism [209,210]. Nonetheless, there are exceptions to the rule, with ageing being one process associated with XCI relaxation in some loci of human skin fibroblasts [211] and whole tissue murine spleen and kidney [212]. Cells of the

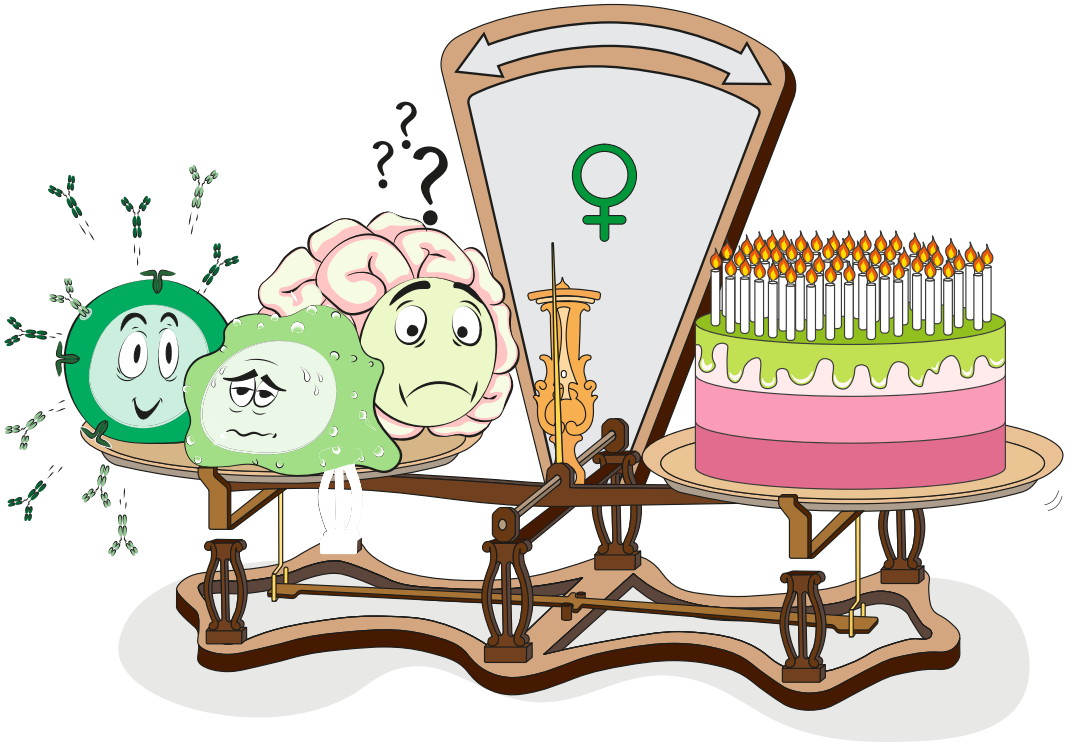

Figure 2. Artistic illustration of the opposing effects of the double X chromosome dosage in females. The biallelic expression of some genes on the second (and inactive) X chromosome in female mammals extends their lifespan and consequently, females celebrate more birthdays (right-hand plate). While their lifespan is longer, having that additional X chromosome comes at the expense of a worsened healthspan (frailty), and thus having a higher risk of autoimmunity and specific neurological disorders (left-hand plate).

female immune system are especially sensitive to *Xist*/*XIST* loss, resulting in differentiation defects during haematopoiesis and aggressive blood cancer [48,213]. Aged HSCs show perturbed *Xist* localization resulting in hypomethylation, chromatin accessibility changes and increased variability in gene expression [214]. In mature naive lymphocytes, *Xist*/*XIST* becomes dispersed and only re-associates with the inactive X upon stimulation. Nonetheless, the spatial redistribution does not result in a global re-expression of X-linked genes as one would perhaps expect: female naive lymphocytes show expression profiles highly similar to males, with only few genes being bi-allelically expressed [215,216]. Similarly, in a mouse model with mildly impaired *Xist* function, phenotypes become penetrant in an age-related fashion with escapees being the primary targets [217]. One prominent escape gene and regulator of the innate immune system is *Tlr7*. Its expression in *Xist*/*XIST*-depleted B cells leads to the generation of a female-specific B cell population that accumulates with age and can also be observed in autoimmune disorders [218].

Consistent with this, misregulation of *Xist* RNA is also observed in autoimmunity [219–221]. *Xist* deletion in B cells is sufficient to induce features of autoimmune diseases [222]. Intriguingly, *Xist* may exert female-biased autoimmunity unrelated to its role in XCI. *Xist* alone serves as a ligand to trigger autoimmunity pathways [223]. Moreover, RNPs associated with *Xist*/XIST RNA can serve as autoantigens, which leads to the production of autoantibodies [224]. While autoimmune diseases such as systemic lupus erythematosus or Sjörgen syndrome are rather rare in the elderly population, autoantibodies increase with age, presumably as a result of tissue damage and apoptosis. While strong evidence supports the role of *Xist*/*XIST* in autoimmunity, there are contradictory changes of *Xist*/*XIST* expression in the brain [225–227], which are yet to be linked to possible age-related neurological illnesses.

In summary, these examples demonstrate that the roles of *Xist* can go beyond canonical XCI. Within the canonical Xist-RNP, *Xist* may regulate autosomal genes [228]. Besides that, it may act as a ligand on its own [224] and inhibit the action of other regulatory factors in compartments other than the nucleus [61]. Since *Xist* is an abundant transcript in females, these possibilities are certainly worthwhile studying in the context of ageing and should encompass tissues other than the immune system.

4.2. Two Xs are better than one: escaping provides resilience

How can the X-linkage of genes regulating any of the hallmarks discussed above be responsible for sex bias in ageing? This question becomes striking for the immune system, as 172 immune-related genes are found on the human X (15% out of all X-linked genes), making it the chromosome containing the highest density of such genes [229,230]. The female immune response is more powerful than that of males, and females contain more circulating immune cells, but this renders women more prone to autoimmunity [231]. Their susceptibility appears to arise from the XX karyotype as demonstrated using the FCG model [232].

Besides Tlr7, the X-linked histone demethylases Kdm6a and Kdm5c appear to influence sex-specific ageing by being escape genes [19,20]. Kdm6a escapes XCI leading to sex-biased expression in, e.g. $CD4^+$ T cells from mice and humans. Conditional deletion of Kdm6a in $CD4^+$ T female cells alleviates neuropathology in multiple sclerosis mouse models by a general decrease in proinflammatory cytokines [233]. XX, compared to XY and XO, mice are more resilient to AD, and this has been correlated with Kdm6a, where overexpression in males attenuates amyloid beta-dependent cognitive decline [234]. More recently, overexpression of catalytically dead Kdm6a in the hippocampus of male mice improved memory and learning upon ageing [235]. Kdm5c is another X-linked demethylase responsible for sex-specific phenotypes. Kdm5c and Kdm6a have been proposed to have a protective role against coronary heart disease in young females [236,237]. However, when a double dose of Kdm5c is expressed in murine adipocytes, this leads to higher weight gain and body fat after a high-fat diet [238], thus highlighting the context-specific benefits and detriments of escape.

Due to the often subtle dosage effects between XX and XY individuals, there is an incomplete understanding of how escape from XCI contributes to sexual dimorphism in age-related diseases. Because escape appears to be highly tissue-specific and can occur in a variable fashion, such studies will be challenging but clearly necessary to advance tailored therapies for men and women.

5. Concluding remarks and future perspectives

Sex differences in lifespan and ageing involve a combination of factors including the X chromosome and hormones. Because males and females age differently, it is imperative to investigate the fundamental basis of sexual dimorphism across that process. The inclusion of both sexes in scientific studies, independently of the study system, is essential to understanding how ageing affects each sex (e.g. reviewed by Lushchak *et al*. [239]). A step towards closing this gap is the policy established by the National Institute of Health to consider sex as a biological variable [240]. In addition, exploring sex hormones within the framework of ageing and life history will be fruitful. For example, in Drosophila, sex steroids affect intestinal physiology [241], while pregnancy transiently remodels the female mouse brain [242]. In the killifish, ablation of the germline leads to an enhanced DDR in females, while extending lifespan and improving metabolic functions in males [205]. Pregnancy can also protect against age-related fibrosis and inflammation caused by reproductive cycling in humans [139], thus underscoring its relevance as a biological variable in future studies. Equally important will be to integrate the X and Y chromosomes in GWAS, which will allow for the identification of sex-linked alleles contributing to age-related diseases.

Research using humans is challenging, with a limited number of deeply mechanistic experiments being feasible [243]. Thus, except for a handful of examples (LOY as a driver in uveal cancer [244] and leading to age-related cardiac dysfunction [85]; Xist KO leading to autoimmunity [217]), many of the phenotypes observed during ageing (e.g. LOX, changes in methylation loci, Xist downregulation and XCI skewing) lack direct evidence of a causative impact on ageing. They could also reflect an adaptation to other processes occurring along the ageing process. Besides further focus on mechanisms, extending the ageing field to samples and organs other than the blood and the haematopoietic system will be also necessary. For instance, the observation of non-canonical regulation of Xist/XIST in lymphocytes has been recently recapitulated in mouse and human lung alveolar type 2 cells, which display a high degree of XCI escape [245]. XCI seems apparently more plastic in humans than in mice and sex-specific programmes govern function in many human organs [6].

Ageing is the common functional decline every human faces, and yet we still do not understand how to successfully tackle it. More research is needed in order to provide therapies for healthy ageing that every man and woman can benefit from.

Glossary

- Adult sex ratio: the proportion of male-to-female individuals in an adult population.
- Aneuploidy: alterations in chromosome numbers that deviate from the euploid complement (e.g., two copies for human autosomes).
- Clonal mosaicism: amplification of cells harboring a different genotype than the inherited germline genome as a result of unrepaired mutations.
- Cytokine: a group of secreted peptides or proteins that have an effect on target cells by typically affecting their growth, proliferation or differentiation.
- *cis*: on the same chromosome where a given gene or regulatory molecule (e.g., *Xist*/*XIST* non-coding RNA) is encoded.
- Dysbiosis: also known as dysbacteria, refers to an imbalance in the intestinal flora
- Endoplasmic reticulum stress: accumulation of unfolded or misfolded proteins in the endoplasmic reticulum
- Frailty: the condition of vulnerability to worse health outcomes.
- Gametologues: Genes that have homologues on the X and Y chromosomes.
- Healthspan: the length of time an organism lives in good health, free from major limitations.
- Hermaphrodites: organisms harboring male and female gonads.
- Heterogametic sex: the sex of a species with two different sex chromosomes (males in the XY and females in the ZW determination systems).
- Homogametic sex: the sex of a species with two homologous sex chromosomes (females in the XX and males in the ZZ determination systems)
- Hormonal therapy: the use of hormones for medical treatment.

- Lifespan: the period of time for which an organism lives.
- Mini-puberty: activation of the hypothalamic-pituitary-gonadal axis between birth and the first few months of life in humans.
- Oestradiol: main active form of estrogen during the female reproductive time (note that other estrogen-derived molecules exist).
- Reactive oxygen species: highly active chemicals with unpaired electrons arising from cellular metabolism. Examples include superoxide (O_2^-), hydrogen peroxide (H_2O_2) and nitric oxide (NO).
- Replicative senescence: the phenomenon of an irreversible block to cell proliferation after a cell has completed a defined number of cell cycles (also known as the Hayflick limit).
- Skewed XCI: non-random inactivation of the X chromosome, i.e., when one of the two parental X chromosomes is preferred for inactivation.
- Telomere attrition: time-dependent telomere length shortening.
- Transit time: the time it takes for food to travel through the gut.

Ethics. This work did not require ethical approval from a human subject or animal welfare committee.
Data accessibility. This article has no additional data.
Declaration of AI use. We have not used AI-assisted technologies in creating this article.
Authors' contributions. J.H.G.F.G.: conceptualization, investigation, writing—original draft, writing—review and editing; C.I.K.V.: conceptualization, funding acquisition, supervision, writing—review and editing; M.F.B.: conceptualization, funding acquisition, supervision, writing—review and editing.

All authors gave final approval for publication and agreed to be held accountable for the work performed therein.

Conflict of interests. We declare we have no competing interests.
Funding. J.H.G.F.G. is part of the 'Science of Healthy Ageing Research Programme' (SHARP) initiative funded by Rhineland-Palatinate's Ministry of Science, Education and Culture. C.I.K.V. is supported by the Deutsche Forschungsgemeinschaft (DFG, German Research Foundation)—Individual Project Grant 513744403, Scientific Network Grant 531902894, GRK GenEvo 407023052, GRK 4R 491145305, Forschungsinitiative Rheinland-Pfalz (ReALity) and institutional funding from the IMB. M.F.B. received financial support from the intramural High Potentials Grant program of the University Medical Center Mainz, by DFG GRK 4R 491145305 and Forschungsinitiative Rheinland-Pfalz (ReALity).
Acknowledgements. We apologize to colleagues whose work could not be covered in this review due to space constraints. We thank Katrina Woolcock (Life Science Editors) and Katharina Papsdorf for their comments on the manuscript.

References

1. Xirocostas ZA, Everingham SE, Moles AT. 2020 The sex with the reduced sex chromosome dies earlier: a comparison across the tree of life. *Biol. Lett*. **16**, 20190867. (doi:10.1098/rsbl.2019.0867)
2. Rochelle TL, Yeung DKY, Bond MH, Li LMW. 2015 Predictors of the gender gap in life expectancy across 54 nations. *Psychol. Health Med*. **20**, 129–138. (doi:10.1080/13548506.2014.936884)
3. Gordon EH, Hubbard RE. 2020 Differences in frailty in older men and women. *Med. J. Aust*. **212**, 183–188. (doi:10.5694/mja2.50466)
4. Heron M. 2021 Deaths: leading causes for 2018. *Natl. Vital Stat. Rep.* **70**, 1–115. (doi:10.15620/cdc:104186)
5. Mauvais-Jarvis F *et al*. 2020 Sex and gender: modifiers of health, disease, and medicine. *Lancet* **396**, 565–582. (doi:10.1016/S0140-6736(20)31561-0)
6. Oliva M *et al*. 2020 The impact of sex on gene expression across human tissues. *Science* **369**, eaba3066. (doi:10.1126/science.aba3066)
7. Sun L, Wang Z, Lu T, Manolio TA, Paterson AD. 2023 eXclusionarY: 10 years later, where are the sex chromosomes in GWASs? *Am. J. Hum. Genet.* **110**, 903–912. (doi:10.1016/j.ajhg.2023.04.009)
8. Mazure CM, Jones DP. 2015 Twenty years and still counting: including women as participants and studying sex and gender in biomedical research. *BMC Womens. Health* **15**, 94. (doi:10.1186/s12905-015-0251-9)
9. The White House. 2024 Executive order on advancing women's health research and innovation. See https://www.whitehouse.gov/briefing-room/presidential-actions/2024/03/18/executive-order-on-advancing-womens-health-research-and-innovation/ (accessed 9 August 2024).
10. Sosinsky AZ, Rich-Edwards JW, Wiley A, Wright K, Spagnolo PA, Joffe H. 2022 Enrollment of female participants in United States drug and device phase 1-3 clinical trials between 2016 and 2019. *Contemp. Clin. Trials.* **115**, 106718. (doi:10.1016/j.cct.2022.106718)
11. Pipoly I, Bókony V, Kirkpatrick M, Donald PF, Székely T, Liker A. 2015 The genetic sex-determination system predicts adult sex ratios in tetrapods. *Nature* **527**, 91–94. (doi:10.1038/nature15380)
12. Lemaître JF *et al*. 2020 Sex differences in adult lifespan and aging rates of mortality across wild mammals. *Proc. Natl Acad. Sci. USA* **117**, 8546–8553. (doi:10.1073/pnas.1911999117)
13. Austad SN, Fischer KE. 2016 Sex differences in lifespan. *Cell Metab*. **23**, 1022–1033. (doi:10.1016/j.cmet.2016.05.019)
14. Connallon T, Beasley IJ, McDonough Y, Ruzicka F. 2022 How much does the unguarded X contribute to sex differences in life span? *Evol. Lett*. **6**, 319–329. (doi:10.1002/evl3.292)
15. Kumar C, Roy JK. 2024 Decoding the epigenetic mechanism of mammalian sex determination. *Exp. Cell Res.* **439**, 114011. (doi:10.1016/j.yexcr.2024.114011)
16. Bellott DW *et al*. 2014 Mammalian Y chromosomes retain widely expressed dosage-sensitive regulators. *Nature* **508**, 494–499. (doi:10.1038/nature13206)
17. Gu L, Walters JR. 2017 Evolution of sex chromosome dosage compensation in animals: a beautiful theory, undermined by facts and bedeviled by details. *Genome Biol. Evol.* **9**, 2461–2476. (doi:10.1093/gbe/evx154)
18. Galupa R, Heard E. 2018 X-chromosome inactivation: a crossroads between chromosome architecture and gene regulation. *Annu. Rev. Genet.* **52**, 535–566. (doi:10.1146/annurev-genet-120116-024611)
19. Tukiainen T *et al*. 2017 Landscape of X chromosome inactivation across human tissues. *Nature* **550**, 244–248. (doi:10.1038/nature24265)
20. Berletch JB, Ma W, Yang F, Shendure J, Noble WS, Disteche CM, Deng X. 2015 Escape from X inactivation varies in mouse tissues. *PLoS Genet.* **11**, e1005079. (doi:10.1371/journal.pgen.1005079)

21. Fang H, Disteche CM, Berletch JB. 2019 X inactivation and escape: epigenetic and structural features. *Front. Cell Dev. Biol.* **7**, 219. (doi:10.3389/fcell.2019.00219)
22. Peeters SB, Posynick BJ, Brown CJ. 2023 Out of the silence: insights into how genes escape X-chromosome inactivation. *Epigenomes* **7**, 29. (doi:10.3390/epigenomes7040029)
23. Käseberg S *et al*. 2023 Dynamic X-chromosomal reactivation enhances female brain resilience. bioRxiv. (doi:10.1101/2023.06.17.545424)
24. Owens MC, Yanas A, Liu KF. 2024 Sex chromosome-encoded protein homologs: current progress and open questions. *Nat. Struct. Mol. Biol.* **31**, 1156–1166. (doi:10.1038/s41594-024-01362-y)
25. Shen H *et al*. 2022 Sexually dimorphic RNA helicases DDX3X and DDX3Y differentially regulate RNA metabolism through phase separation. *Mol. Cell.* **82**, 2588–2603. (doi:10.1016/j.molcel.2022.04.022)
26. Cecalev D, Viçoso B, Galupa R. 2024 Compensation of gene dosage on the mammalian X. *Development* **151**, dev202891. (doi:10.1242/dev.202891)
27. DeCasien AR, Tsai K, Liu S, Thomas A, Raznahan A. 2024 Evolutionary divergence between homologous X-Y chromosome genes shapes sex-biased biology. *Genomics*. (doi:10.1101/2024.03.27.586985)
28. Hägg S, Jylhävä J. 2021 Sex differences in biological aging with a focus on human studies. *eLife* **10**, e63425. (doi:10.7554/eLife.63425)
29. De Vries GJ *et al*. 2002 A model system for study of sex chromosome effects on sexually dimorphic neural and behavioral traits. *J. Neurosci.* **22**, 9005–9014. (doi:10.1523/JNEUROSCI.22-20-09005.2002)
30. Eicher EM, Hale DW, Hunt PA, Lee BK, Tucker PK, King TR, Eppig JT, Washburn LL. 1991 The mouse Y* chromosome involves a complex rearrangement, including interstitial positioning of the pseudoautosomal region. *Cytogenet. Cell Genet.* **57**, 221–230. (doi:10.1159/000133152)
31. Panten J *et al*. 2024 Four-core genotypes mice harbour a 3.2MB X-Y translocation that perturbs Tlr7 dosage. bioRxiv. (doi:10.1101/2023.12.04.569933)
32. Arnold AP. 2020 Four Core genotypes and XY* mouse models: update on impact on SABV research. *Neurosci. Biobehav. Rev.* **119**, 1–8. (doi:10.1016/j.neubiorev.2020.09.021)
33. Davis EJ, Lobach I, Dubal DB. 2019 Female XX sex chromosomes increase survival and extend lifespan in aging mice. *Aging Cell* **18**, e12871. (doi:10.1111/acel.12871)
34. Marino F, Wang D, Merrihew GE, MacCoss MJ, Dubal DB. 2024 A second X chromosome improves cognition in aging male and female mice. *bioRxiv* 2024.07.26.605328. (doi:10.1101/2024.07.26.605328)
35. López-Otín C, Blasco MA, Partridge L, Serrano M, Kroemer G. 2013 The hallmarks of aging. *Cell* **153**, 1194–1217. (doi:10.1016/j.cell.2013.05.039)
36. López-Otín C, Blasco MA, Partridge L, Serrano M, Kroemer G. 2023 Hallmarks of aging: an expanding universe. *Cell* **186**, 243–278. (doi:10.1016/j.cell.2022.11.001)
37. Wright DJ *et al*. 2017 Genetic variants associated with mosaic Y chromosome loss highlight cell cycle genes and overlap with cancer susceptibility. *Nat. Genet.* **49**, 674–679. (doi:10.1038/ng.3821)
38. Liu A *et al*. 2024 Genetic drivers and cellular selection of female mosaic X chromosome loss. *Nature* **631**, 134–141. (doi:10.1038/s41586-024-07533-7)
39. Jung M *et al*. 2020 Association of clinical severity with FANCB variant type in Fanconi anemia. *Blood* **135**, 1588–1602. (doi:10.1182/blood.2019003249)
40. Rall-Scharpf M, Friedl TWP, Biechonski S, Denkinger M, Milyavsky M, Wiesmüller L. 2021 Sex-specific differences in DNA double-strand break repair of cycling human lymphocytes during aging. *Aging* **13**, 21066–21089. (doi:10.18632/aging.203519)
41. Terao C *et al*. 2019 GWAS of mosaic loss of chromosome Y highlights genetic effects on blood cell differentiation. *Nat. Commun.* **10**, 4719. (doi:10.1038/s41467-019-12705-5)
42. Loh PR *et al*. 2018 Insights into clonal haematopoiesis from 8,342 mosaic chromosomal alterations. *Nature* **559**, 350–355. (doi:10.1038/s41586-018-0321-x)
43. AlSabbagh MM. 2020 Dyskeratosis congenita: a literature review. *J. Dtsch. Dermatol. Ges*. **18**, 943–967. (doi:10.1111/ddg.14268)
44. Sugrue VJ *et al*. 2021 Castration delays epigenetic aging and feminizes DNA methylation at androgen-regulated loci. *eLife* **10**, e64932. (doi:10.7554/eLife.64932)
45. Lund JB *et al*. 2020 Age-dependent DNA methylation patterns on the Y chromosome in elderly males. *Aging Cell* **19**, e12907. (doi:10.1111/acel.12907)
46. Li G *et al*. 2022 Age-related DNA methylation on Y chromosome and their associations with total mortality among Chinese males. *Aging Cell* **21**, e13563. (doi:10.1111/acel.13563)
47. McCartney DL *et al*. 2019 An epigenome-wide association study of sex-specific chronological ageing. *Genome Med*. **12**, 1. (doi:10.1186/s13073-019-0693-z)
48. Yildirim E, Kirby JE, Brown DE, Mercier FE, Sadreyev RI, Scadden DT, Lee JT. 2013 Xist RNA is a potent suppressor of hematologic cancer in mice. *Cell* **152**, 727–742. (doi:10.1016/j.cell.2013.01.034)
49. Yan W *et al*. 2023 Auranofin targets UBA1 and enhances UBA1 activity by facilitating ubiquitin trans-thioesterification to E2 ubiquitin-conjugating enzymes. *Nat. Commun*. **14**, 4798. (doi:10.1038/s41467-023-40537-x)
50. Zhao Y, Alexandrov PN, Jaber V, Lukiw WJ. 2016 Deficiency in the ubiquitin conjugating enzyme UBE2A in Alzheimer's Disease (AD) is linked to deficits in a natural circular miRNA-7 Sponge (circRNA; ciRS-7). *Genes.* **7**, 116. (doi:10.3390/genes7120116)
51. Sandoval-Pistorius SS *et al*. 2023 Ubiquilin-2 regulates pathological alpha-synuclein. *Sci. Rep*. **13**, 293. (doi:10.1038/s41598-022-26899-0)
52. Deng HX *et al*. 2011 Mutations in UBQLN2 cause dominant X-linked juvenile and adult-onset ALS and ALS/dementia. *Nature* **477**, 211–215. (doi:10.1038/nature10353)
53. Klusek J, Fairchild A, Moser C, Mailick MR, Thurman AJ, Abbeduto L. 2022 Family history of FXTAS is associated with age-related cognitive-linguistic decline among mothers with the FMR1 premutation. *J. Neurodev. Disord*. **14**, 7. (doi:10.1186/s11689-022-09415-3)
54. Shimizu H, Hohjoh H. 2023 FMRP, FXR1 protein and Dlg4 mRNA, which are associated with fragile X syndrome, are involved in the ubiquitin–proteasome system. *Sci. Rep*. **13**. (doi:10.1038/s41598-023-29152-4)
55. Yan Y, Wang X, Chaput D, Shin MK, Koh Y, Gan L, Pieper AA, Woo JA, Kang DE. 2022 X-linked ubiquitin-specific peptidase 11 increases tauopathy vulnerability in women. *Cell* **185**, 3913–3930.(doi:10.1016/j.cell.2022.09.002)
56. Oliván S, Calvo AC, Manzano R, Zaragoza P, Osta R. 2014 Sex differences in constitutive autophagy. *Biomed. Res. Int.* **2014**, 652817. (doi:10.1155/2014/652817)
57. Camuzard O *et al*. 2016 Sex-specific autophagy modulation in osteoblastic lineage: a critical function to counteract bone loss in female. *Oncotarget* **7**, 66416–66428. (doi:10.18632/oncotarget.12013)
58. Rowland TJ, Sweet ME, Mestroni L, Taylor MRG. 2016 Danon disease—dysregulation of autophagy in a multisystem disorder with cardiomyopathy. *J. Cell. Sci*. **129**, 2135–2143. (doi:10.1242/jcs.184770)
59. Ma Q *et al*. 2023 UBQLN2 and HSP70 participate in parkin-mediated mitophagy by facilitating outer mitochondrial membrane rupture. *EMBO Rep.* **24**, e55859. (doi:10.15252/embr.202255859)
60. Huang Z *et al*. 2021 Effects of sex and aging on the immune cell landscape as assessed by single-cell transcriptomic analysis. *Proc. Natl Acad. Sci. USA* **118**, e2023216118. (doi:10.1073/pnas.2023216118)
61. Shenoda BB *et al*. 2021 Xist attenuates acute inflammatory response by female cells. *Cell. Mol. Life Sci*. **78**, 299–316. (doi:10.1007/s00018-020-03500-3)
62. Altimiras F, Garcia JA, Palacios-García I, Hurley MJ, Deacon R, González B, Cogram P. 2021 Altered gut microbiota in a fragile X syndrome mouse model. *Front. Neurosci*. **15**, 653120. (doi:10.3389/fnins.2021.653120)
63. Amato-Menker CJ, Hopen Q, Pettit A, Gandhi J, Hu G, Schafer R, Franko J. 2024 XX sex chromosome complement modulates immune responses to heat-killed *Streptococcus pneumoniae* immunization in a microbiome-dependent manner. *Biol. Sex Differ*. **15**, 21. (doi:10.1186/s13293-024-00597-0)

64. Kim Y, Pérez-González R, Miller C, Kurz M, D'Acunzo P, Goulbourne CN, Levy E. 2022 Sex differentially alters secretion of brain extracellular vesicles during aging: a potential mechanism for maintaining brain homeostasis. *Neurochem. Res.* **47**, 3428–3439. (doi:10.1007/s11064-022-03701-1)
65. Hernández Borrero LJ, El-Deiry WS. 2021 Tumor suppressor p53: biology, signaling pathways, and therapeutic targeting. *Biochim. Biophys. Acta Rev. Cancer* **1876**, 188556. (doi:10.1016/j.bbcan.2021.188556)
66. Delbridge ARD *et al*. 2019 Loss of p53 causes stochastic aberrant X-chromosome inactivation and female-specific neural tube defects. *Cell Rep*. **27**, 442–454.(doi:10.1016/j.celrep.2019.03.048)
67. Haupt S, Caramia F, Herschtal A, Soussi T, Lozano G, Chen H, Liang H, Speed TP, Haupt Y. 2019 Identification of cancer sex-disparity in the functional integrity of p53 and its X chromosome network. *Nat. Commun*. **10**, 5385. (doi:10.1038/s41467-019-13266-3)
68. Siudeja K *et al*. 2015 Frequent somatic mutation in adult intestinal stem cells drives neoplasia and genetic mosaicism during aging. *Cell Stem Cell* **17**, 663–674. (doi:10.1016/j.stem.2015.09.016)
69. Clocchiatti A, Cora E, Zhang Y, Dotto GP. 2016 Sexual dimorphism in cancer. *Nat. Rev. Cancer* **16**, 330–339. (doi:10.1038/nrc.2016.30)
70. Brosh RM Jr, Bellani M, Liu Y, Seidman MM. 2017 Fanconi anemia: a DNA repair disorder characterized by accelerated decline of the hematopoietic stem cell compartment and other features of aging. *Ageing Res. Rev*. **33**, 67–75. (doi:10.1016/j.arr.2016.05.005)
71. Brown EJ, Nguyen AH, Bachtrog D. 2020 The Y chromosome may contribute to sex-specific ageing in *Drosophila*. *Nat. Ecol. Evol*. **4**, 853–862. (doi:10.1038/s41559-020-1179-5)
72. Delanoue R, Clot C, Leray C, Pihl T, Hudry B. 2023 Y chromosome toxicity does not contribute to sex-specific differences in longevity. *Nat. Ecol. Evol*. **7**, 1245–1256. (doi:10.1038/s41559-023-02089-7)
73. Blokzijl F *et al*. 2016 Tissue-specific mutation accumulation in human adult stem cells during life. *Nature* **538**, 260–264. (doi:10.1038/nature19768)
74. Machiela MJ *et al*. 2016 Female chromosome X mosaicism is age-related and preferentially affects the inactivated X chromosome. *Nat. Commun.* **7**, 11843. (doi:10.1038/ncomms11843)
75. Lin SH *et al*. 2021 Incident disease associations with mosaic chromosomal alterations on autosomes, X and Y chromosomes: insights from a phenome-wide association study in the UK Biobank. *Cell Biosci.* **11**, 143. (doi:10.1186/s13578-021-00651-z)
76. Zekavat SM *et al*. 2020 Hematopoietic mosaic chromosomal alterations and risk for infection among 767,891 individuals without blood cancer. *medRxiv* 2020.11.12.20230821. (doi:10.1101/2020.11.12.20230821)
77. Gutiérrez-Hurtado IA, Sánchez-Méndez AD, Becerra-Loaiza DS, Rangel-Villalobos H, Torres-Carrillo N, Gallegos-Arreola MP, Aguilar-Velázquez JA. 2024 Loss of the Y chromosome: a review of molecular mechanisms, age inference, implications men's health.. *Int. J. Mol. Sci.* **25**. (doi:10.3390/ijms25084230)
78. Pierre RV, Hoagland HC. 1972 Age-associated aneuploidy: loss of Y chromosome from human bone marrow cells with aging. *Cancer* **30**, 889–894. (doi:10.1002/1097-0142(197210)30:4<889::aid-cncr2820300405>3.0.co;2-1)
79. Herens C, Brasseur E, Jamar M, Vierset L, Schoenen I, Koulischer L. 1999 Loss of the Y chromosome in bone marrow cells: results on 1907 consecutive cases of leukaemia and preleukaemia. *Clin. Lab. Haematol.* **21**, 17–20. (doi:10.1046/j.1365-2257.1999.00173.x)
80. Guttenbach M, Koschorz B, Bernthaler U, Grimm T, Schmid M. 1995 Sex chromosome loss and aging: in situ hybridization studies on human interphase nuclei. *Am. J. Hum. Genet.* **57**, 1143–1150.
81. Forsberg LA *et al*. 2014 Mosaic loss of chromosome Y in peripheral blood is associated with shorter survival and higher risk of cancer. *Nat. Genet.* **46**, 624–628. (doi:10.1038/ng.2966)
82. Li J *et al*. 2023 Histone demethylase KDM5D upregulation drives sex differences in colon cancer. *Nature* **619**, 632–639. (doi:10.1038/s41586-023-06254-7)
83. Abdel-Hafiz HA, Schafer JM, Chen X, Xiao T, Gauntner TD, Li Z, Theodorescu D. 2023 Y chromosome loss in cancer drives growth by evasion of adaptive immunity. *Nature* **619**, 624–631. (doi:10.1038/s41586-023-06234-x)
84. Dunford A *et al*. 2017 Tumor-suppressor genes that escape from X-inactivation contribute to cancer sex bias. *Nat. Genet.* **49**, 10–16. (doi:10.1038/ng.3726)
85. Sano S *et al*. 2022 Hematopoietic loss of Y chromosome leads to cardiac fibrosis and heart failure mortality. *Science* **377**, 292–297. (doi:10.1126/science.abn3100)
86. Tharp ME *et al*. 2024 The inactive X chromosome drives sex differences in microglial inflammatory activity in human glioblastoma. *bioRxiv* 2024.06.06.597433. (doi:10.1101/2024.06.06.597433)
87. Orta AH *et al*. 2021 Rats exhibit age-related mosaic loss of chromosome Y. *Commun. Biol*. **4**, 1418. (doi:10.1038/s42003-021-02936-y)
88. Muyas F, Sauer CM, Valle-Inclán JE, Li R, Rahbari R, Mitchell TJ, Hormoz S, Cortés-Ciriano I. 2024 De novo detection of somatic mutations in high-throughput single-cell profiling data sets. *Nat. Biotechnol*. **42**, 758–767. (doi:10.1038/s41587-023-01863-z)
89. Truong MA, Cané-Gasull P, de Vries SG, Nijenhuis W, Wardenaar R, Kapitein LC, Foijer F, Lens SM. 2023 A kinesin-based approach for inducing chromosome-specific mis-segregation in human cells. *EMBO J*. **42**, e111559. (doi:10.15252/embj.2022111559)
90. Bosco N *et al*. 2023 KaryoCreate: A CRISPR-based technology to study chromosome-specific aneuploidy by targeting human centromeres. *Cell* **186**, 1985–2001.(doi:10.1016/j.cell.2023.03.029)
91. Benetos A, Okuda K, Lajemi M, Kimura M, Thomas F, Skurnick J, Labat C, Bean K, Aviv A. 2001 Telomere length as an indicator of biological aging: the gender effect and relation with pulse pressure and pulse wave velocity. *Hypertension* **37**, 381–385. (doi:10.1161/01.hyp.37.2.381)
92. Allsopp RC, Chang E, Kashefi-Aazam M, Rogaev EI, Piatyszek MA, Shay JW, Harley CB. 1995 Telomere shortening is associated with cell division in vitro and in vivo. *Exp. Cell Res*. **220**, 194–200. (doi:10.1006/excr.1995.1306)
93. Leão R, Apolónio JD, Lee D, Figueiredo A, Tabori U, Castelo-Branco P. 2018 Mechanisms of human telomerase reverse transcriptase (hTERT) regulation: clinical impacts in cancer. *J. Biomed. Sci*. **25**, 22. (doi:10.1186/s12929-018-0422-8)
94. Gardner M *et al*. 2014 Gender and telomere length: systematic review and meta-analysis. *Exp. Gerontol*. **51**, 15–27. (doi:10.1016/j.exger.2013.12.004)
95. Demanelis K *et al*. 2020 Determinants of telomere length across human tissues. *Science* **369**, eaaz6876. (doi:10.1126/science.aaz6876)
96. Gutierrez-Rodrigues F, Alves-Paiva RM, Scatena NF, Martinez EZ, Scheucher PS, Calado RT. 2022 Association between leukocyte telomere length and sex by quantile regression analysis. *Hematol. Transfus. Cell Ther*. **44**, 346–351. (doi:10.1016/j.htct.2020.12.005)
97. Ye Q, Apsley AT, Etzel L, Hastings WJ, Kozlosky JT, Walker C, Wolf SE, Shalev I. 2023 Telomere length and chronological age across the human lifespan: a systematic review and meta-analysis of 414 study samples including 743,019 individuals. *Ageing Res. Rev*. **90**, 102031. (doi:10.1016/j.arr.2023.102031)
98. Xu J, Khincha PP, Giri N, Alter BP, Savage SA, Wong JMY. 2016 Investigation of chromosome X inactivation and clinical phenotypes in female carriers of DKC1 mutations. *Am. J. Hematol*. **91**, 1215–1220. (doi:10.1002/ajh.24545)
99. Peeters SB, Yang C, Brown CJ. 2016 Have humans lost control: the elusive X-controlling element. *Semin. Cell Dev. Biol*. **56**, 71–77. (doi:10.1016/j.semcdb.2016.01.044)
100. Orstavik KH. 2009 X chromosome inactivation in clinical practice. *Hum. Genet*. **126**, 363–373. (doi:10.1007/s00439-009-0670-5)

101. Mayer S *et al*. 2006 Sex-specific telomere length profiles and age-dependent erosion dynamics of individual chromosome arms in humans. *Cytogenet. Genome Res*. **112**, 194–201. (doi:10.1159/000089870)
102. Surrallés J, Hande MP, Marcos R, Lansdorp PM. 1999 Accelerated telomere shortening in the human inactive X chromosome. *Am. J. Hum. Genet*. **65**, 1617–1622. (doi:10.1086/302665)
103. Leach NT, Rehder C, Jensen K, Holt S, Jackson-Cook C. 2004 Human chromosomes with shorter telomeres and large heterochromatin regions have a higher frequency of acquired somatic cell aneuploidy. *Mech. Ageing Dev*. **125**, 563–573. (doi:10.1016/j.mad.2004.06.006)
104. Schoeftner S, Blanco R, Lopez de Silanes I, Muñoz P, Gómez-López G, Flores JM, Blasco MA. 2009 Telomere shortening relaxes X chromosome inactivation and forces global transcriptome alterations. *Proc. Natl Acad. Sci. USA* **106**, 19393–19398. (doi:10.1073/pnas.0909265106)
105. Smoom R *et al*. 2023 Telomouse-a mouse model with human-length telomeres generated by a single amino acid change in RTEL1. *Nat. Commun*. **14**, 6708. (doi:10.1038/s41467-023-42534-6)
106. Cheng D, Zhang F, Porter KI, Wang S, Zhang H, Davis CJ, Robertson GP, Zhu J. 2024 Humanization of the mouse Tert gene reset telomeres to human length. *Res. Sq*. rs.3.rs-3617723. (doi:10.21203/rs.3.rs-3617723/v1)
107. Sergeeva A, Davydova K, Perenkov A, Vedunova M. 2023 Mechanisms of human DNA methylation, alteration of methylation patterns in physiological processes and oncology. *Gene* **875**, 147487. (doi:10.1016/j.gene.2023.147487)
108. Duan R, Fu Q, Sun Y, Li Q. 2022 Epigenetic clock: a promising biomarker and practical tool in aging. *Ageing Res. Rev.* **81**, 101743. (doi:10.1016/j.arr.2022.101743)
109. Ying K *et al*. 2024 Causality-enriched epigenetic age uncouples damage and adaptation. *Nat. Aging*. **4**, 231–246. (doi:10.1038/s43587-023-00557-0)
110. Noroozi R, Ghafouri-Fard S, Pisarek A, Rudnicka J, Spólnicka M, Branicki W, Taheri M, Pośpiech E. 2021 DNA methylation-based age clocks: from age prediction to age reversion. *Ageing Res. Rev.* **68**, 101314. (doi:10.1016/j.arr.2021.101314)
111. Lu AT *et al*. 2023 Universal DNA methylation age across mammalian tissues. *Nat. Aging* **3**, 1144–1166. (doi:10.1038/s43587-023-00462-6)
112. Dormann D, Lemke EA. 2024 Adding intrinsically disordered proteins to biological ageing clocks. *Nat. Cell Biol*. **26**, 851–858. (doi:10.1038/s41556-024-01423-w)
113. Llewellyn J, Hubbard SJ, Swift J. 2024 Translation is an emerging constraint on protein homeostasis in ageing. *Trends Cell Biol*. **34**, 646–656. (doi:10.1016/j.tcb.2024.02.001)
114. Keele GR, Zhang JG, Szpyt J, Korstanje R, Gygi SP, Churchill GA, Schweppe DK. 2023 Global and tissue-specific aging effects on murine proteomes. *Cell Rep*. **42**, 112715. (doi:10.1016/j.celrep.2023.112715)
115. Di Fraia D *et al*. 2024 Impaired biogenesis of basic proteins impacts multiple hallmarks of the aging brain. *bioRxiv* 2023.07.20.549210. (doi:10.1101/2023.07.20.549210)
116. Rao NR, Upadhyay A, Savas JN. 2024 Derailed protein turnover in the aging mammalian brain. *Mol. Syst. Biol*. **20**, 120–139. (doi:10.1038/s44320-023-00009-2)
117. Liu X, Novak B, Namendorf C, Steigenberger B, Zhang Y, Turck CW. 2024 Long-lived proteins and DNA as candidate predictive biomarkers for tissue associated diseases. *iScience* **27**, 109642. (doi:10.1016/j.isci.2024.109642)
118. Pickering AM, Lehr M, Kohler WJ, Han ML, Miller RA. 2015 Fibroblasts from longer-lived species of primates, rodents, bats, carnivores, and birds resist protein damage. *J. Gerontol. A Biol. Sci. Med. Sci*. **70**, 791–799. (doi:10.1093/gerona/glu115)
119. Chondrogianni N, Petropoulos I, Franceschi C, Friguet B, Gonos ES. 2000 Fibroblast cultures from healthy centenarians have an active proteasome. *Exp. Gerontol*. **35**, 721–728. (doi:10.1016/s0531-5565(00)00137-6)
120. Lewis KN, Wason E, Edrey YH, Kristan DM, Nevo E, Buffenstein R. 2015 Regulation of Nrf2 signaling and longevity in naturally long-lived rodents. *Proc. Natl Acad. Sci. USA* **112**, 3722–3727. (doi:10.1073/pnas.1417566112)
121. Munro D, Baldy C, Pamenter ME, Treberg JR. 2019 The exceptional longevity of the naked mole-rat may be explained by mitochondrial antioxidant defenses. *Aging Cell* **18**, e12916. (doi:10.1111/acel.12916)
122. Jenkins EC, Shah N, Gomez M, Casalena G, Zhao D, Kenny TC, Guariglia SR, Manfredi G, Germain D. 2020 Proteasome mapping reveals sexual dimorphism in tissue-specific sensitivity to protein aggregations. *EMBO Rep.* **21**, e48978. (doi:10.15252/embr.201948978)
123. Kammerl IE, Flexeder C, Karrasch S, Thorand B, Heier M, Peters A, Schulz H, Meiners S. 2021 Blood immunoproteasome activity is regulated by sex, age and in chronic inflammatory diseases: a first population-based study. *Cells* **10**, 3336. (doi:10.3390/cells10123336)
124. Wodrich APK, Scott AW, Shukla AK, Harris BT, Giniger E. 2022 The unfolded protein responses in health, aging, and neurodegeneration: recent advances and future considerations. *Front. Mol. Neurosci*. **15**, 831116. (doi:10.3389/fnmol.2022.831116)
125. Okan A, Demir N, Sozen B. 2021 Unfolded protein response triggers differential apoptotic mechanisms in ovaries and early embryos exposed to maternal type 1 diabetes. *Sci. Rep*. **11**, 12759. (doi:10.1038/s41598-021-92093-3)
126. Rahmani M, Tavalaee M, R Drevet J, Nasr-Esfahani MH. 2023 Role of endoplasmic reticulum stress in the male reproductive system. *Cell J.* **25**, 437–446. (doi:10.22074/CELLJ.2023.1983074.1205)
127. Brownrigg GP *et al*. 2023 Sex differences in islet stress responses support female β cell resilience. *Mol. Metab*. **69**, 101678. (doi:10.1016/j.molmet.2023.101678)
128. Charmpilas N, Sotiriou A, Axarlis K, Tavernarakis N, Hoppe T. 2024 Reproductive regulation of the mitochondrial stress response in *Caenorhabditis elegans*. *Cell Rep*. **43**, 114336. (doi:10.1016/j.celrep.2024.114336)
129. Levine B, Kroemer G. 2019 Biological functions of autophagy genes: a disease perspective. *Cell* **176**, 11–42. (doi:10.1016/j.cell.2018.09.048)
130. Regan JC, Lu YX, Ureña E, Meilenbrock RL, Catterson JH, Kißler D, Fröhlich J, Funk E, Partridge L. 2022 Sexual identity of enterocytes regulates autophagy to determine intestinal health, lifespan and responses to rapamycin. *Nat. Aging.* **2**, 1145–1158. (doi:10.1038/s43587-022-00308-7)
131. Noh B, McCullough LD, Moruno-Manchon JF. 2023 Sex-biased autophagy as a potential mechanism mediating sex differences in ischemic stroke outcome. *Neural Regen. Res.* **18**, 31–37. (doi:10.4103/1673-5374.340406)
132. Cuervo AM, Dice JF. 2000 Age-related decline in chaperone-mediated autophagy. *J. Biol. Chem.* **275**, 31505–31513. (doi:10.1074/jbc.M002102200)
133. Yousefzadeh MJ *et al*. 2020 Tissue specificity of senescent cell accumulation during physiologic and accelerated aging of mice. *Aging Cell* **19**, e13094. (doi:10.1111/acel.13094)
134. Olivieri F, Marchegiani F, Matacchione G, Giuliani A, Ramini D, Fazioli F, Sabbatinelli J, Bonafè M. 2023 Sex/gender-related differences in inflammaging. *Mech. Ageing Dev*. **211**, 111792. (doi:10.1016/j.mad.2023.111792)
135. Márquez EJ *et al*. 2020 Sexual-dimorphism in human immune system aging. *Nat. Commun*. **11**, 751. (doi:10.1038/s41467-020-14396-9)
136. Franceschi C, Bonafè M, Valensin S, Olivieri F, De Luca M, Ottaviani E, De Benedictis G. 2000 Inflamm-aging: an evolutionary perspective on immunosenescence. *Ann. NY Acad. Sci.* **908**, 244–254. (doi:10.1111/j.1749-6632.2000.tb06651.x)
137. Cyr B, de Rivero Vaccari JP. 2023 Sex differences in the inflammatory profile in the brain of young and aged mice. *Cells* **12**, 1372. (doi:10.3390/cells12101372)
138. Kang S *et al*. 2024 Microglia undergo sex-dimorphic transcriptional and metabolic rewiring during aging. *J. Neuroinflammation* **21**, 150. (doi:10.1186/s12974-024-03130-7)
139. Winkler I *et al*. 2024 The cycling and aging mouse female reproductive tract at single-cell resolution. *Cell* **187**, 981–998.(doi:10.1016/j.cell.2024.01.021)

140. Zhang C, Gao R, Zhou R, Chen H, Liu C, Zhu T, Chen C. 2022 The emerging power and promise of non-coding RNAs in chronic pain. *Front. Mol. Neurosci*. **15**, 1037929. (doi:10.3389/fnmol.2022.1037929)
141. Hägg S, Jylhävä J, Wang Y, Czene K, Grassmann F. 2021 Deciphering the genetic and epidemiological landscape of mitochondrial DNA abundance. *Hum. Genet*. **140**, 849–861. (doi:10.1007/s00439-020-02249-w)
142. Ventura-Clapier R *et al*. 2017 Sex in basic research: concepts in the cardiovascular field. *Cardiovasc. Res*. **113**, 711–724. (doi:10.1093/cvr/cvx066)
143. Sarver DC, Saqib M, Chen F, Wong GW. 2024 Mitochondrial respiration atlas reveals differential changes in mitochondrial function across sex and age. *bioRxiv*. (doi:10.1101/2024.03.26.586781)
144. Mahapatra G, Gao Z, Bateman JR, Lockhart SN, Bergstrom J, Piloso JE, Craft S, Molina AJA. 2024 Peripheral blood cells from older adults exhibit sex-associated differences in mitochondrial function. *J. Gerontol. A Biol. Sci. Med. Sci.* **79**, glae098. (doi:10.1093/gerona/glae098)
145. Han Y, Wennersten SA, Wright JM, Ludwig RW, Lau E, Lam MPY. 2022 Proteogenomics reveals sex-biased aging genes and coordinated splicing in cardiac aging. *Am. J. Physiol. Heart Circ. Physiol.* **323**, H538–H558. (doi:10.1152/ajpheart.00244.2022)
146. Chen X, McClusky R, Itoh Y, Reue K, Arnold AP. 2013 X and Y chromosome complement influence adiposity and metabolism in mice. *Endocrinology* **154**, 1092–1104. (doi:10.1210/en.2012-2098)
147. Campbell P *et al*. 2023 Mitochondrial mutation, drift and selection during human development and ageing. *Research Square*. (doi:10.21203/rs.3.rs-3083262/v1)
148. Edmands S. 2024 Mother's curse effects on lifespan and aging. *Front. Aging.* **5**, 1361396. (doi:10.3389/fragi.2024.1361396)
149. Mitchell SJ *et al*. 2016 Effects of sex, strain, and energy intake on hallmarks of aging in mice. *Cell Metab*. **23**, 1093–1112. (doi:10.1016/j.cmet.2016.05.027)
150. Baar EL, Carbajal KA, Ong IM, Lamming DW. 2016 Sex- and tissue-specific changes in mTOR signaling with age in C57BL/6J mice. *Aging Cell* **15**, 155–166. (doi:10.1111/acel.12425)
151. Zhang P, Catterson JH, Grönke S, Partridge L. 2024 Inhibition of S6K lowers age-related inflammation and increases lifespan through the endolysosomal system. *Nat. Aging* **4**, 491–509. (doi:10.1038/s43587-024-00578-3)
152. Ripa R *et al*. 2023 Refeeding-associated $AMPK_{\gamma 1}$ complex activity is a hallmark of health and longevity. *Nat. Aging* **3**, 1544–1560. (doi:10.1038/s43587-023-00521-y)
153. Astre G *et al*. 2023 Genetic perturbation of AMP biosynthesis extends lifespan and restores metabolic health in a naturally short-lived vertebrate. *Dev. Cell* **58**, 1350–1364.(doi:10.1016/j.devcel.2023.05.015)
154. Reichwald K *et al*. 2015 Insights into sex chromosome evolution and aging from the genome of a short-lived fish. *Cell* **163**, 1527–1538. (doi:10.1016/j.cell.2015.10.071)
155. Garratt M, Bower B, Garcia GG, Miller RA. 2017 Sex differences in lifespan extension with acarbose and 17-α estradiol: gonadal hormones underlie male-specific improvements in glucose tolerance and mTORC 2 signaling . *Aging Cell* **16**, 1256–1266. (doi:10.1111/acel.12656)
156. de la Cuesta-Zuluaga J *et al*. 2019 Age- and sex-dependent patterns of gut microbial diversity in human adults. *mSystems* **4**, mSystems (doi:10.1128/mSystems.00261-19)
157. Sinha T *et al*. 2019 Analysis of 1135 gut metagenomes identifies sex-specific resistome profiles. *Gut Microbes* **10**, 358–366. (doi:10.1080/19490976.2018.1528822)
158. Zhang X *et al*. 2021 Sex- and age-related trajectories of the adult human gut microbiota shared across populations of different ethnicities. *Nat. Aging* **1**, 87–100. (doi:10.1038/s43587-020-00014-2)
159. Mayneris-Perxachs J, Arnoriaga-Rodríguez M, Luque-Córdoba D, Priego-Capote F, Pérez-Brocal V, Moya A, Burokas A, Maldonado R, Fernández-Real JM. 2020 Gut microbiota steroid sexual dimorphism and its impact on gonadal steroids: influences of obesity and menopausal status. *Microbiome* **8**, 136. (doi:10.1186/s40168-020-00913-x)
160. Weger BD *et al*. 2019 The mouse microbiome is required for sex-specific diurnal rhythms of gene expression and metabolism. *Cell Metab*. **29**, 362–382.(doi:10.1016/j.cmet.2018.09.023)
161. Kim YS, Unno T, Kim BY, Park MS. 2020 Sex differences in gut microbiota. *World J. Mens. Health* **38**, 48. (doi:10.5534/wjmh.190009)
162. Webster SE, Vos D, Rothstein TL, Holodick NE. 2022 Modulation of microbiome diversity and cytokine expression is influenced in a sex-dependent manner during aging. *Front. Microbiom*. **1**. (doi:10.3389/frmbi.2022.994464)
163. Cunningham CM *et al*. 2022 Y-chromosome gene, Uty, protects against pulmonary hypertension by reducing proinflammatory chemokines. *Am. J. Respir. Crit. Care Med*. **206**, 186–196. (doi:10.1164/rccm.202110-2309OC)
164. Navarro Negredo P, Yeo RW, Brunet A. 2020 Aging and rejuvenation of neural stem cells and their niches. *Cell Stem Cell* **27**, 202–223. (doi:10.1016/j.stem.2020.07.002)
165. Nalapareddy K, Zheng Y, Geiger H. 2022 Aging of intestinal stem cells. *Stem Cell Rep.* **17**, 734–740. (doi:10.1016/j.stemcr.2022.02.003)
166. Orkin SH, Zon LI. 2008 Hematopoiesis: an evolving paradigm for stem cell biology. *Cell* **132**, 631–644. (doi:10.1016/j.cell.2008.01.025)
167. Scherer M *et al*. 2024 Somatic epimutations enable single-cell lineage tracing in native hematopoiesis across the murine and human lifespan. *bioRxiv* 2024.04.01.587514. (doi:10.1101/2024.04.01.587514)
168. Lengefeld J *et al*. 2021 Cell size is a determinant of stem cell potential during aging. *Sci. Adv*. **7**, eabk0271. (doi:10.1126/sciadv.abk0271)
169. Lv J *et al*. 2024 An aging-related immune landscape in the hematopoietic immune system. *Immun. Ageing* **21**, 3. (doi:10.1186/s12979-023-00403-2)
170. Walter D *et al*. 2015 Exit from dormancy provokes DNA-damage-induced attrition in haematopoietic stem cells. *Nature* **520**, 549–552. (doi:10.1038/nature14131)
171. Regan JC, Khericha M, Dobson AJ, Bolukbasi E, Rattanavirotkul N, Partridge L. 2016 Sex difference in pathology of the ageing gut mediates the greater response of female lifespan to dietary restriction. *eLife* **5**, e10956. (doi:10.7554/eLife.10956)
172. Hudry B, Khadayate S, Miguel-Aliaga I. 2016 The sexual identity of adult intestinal stem cells controls organ size and plasticity. *Nature* **530**, 344–348. (doi:10.1038/nature16953)
173. Kim SK, Tsao DD, Suh GSB, Miguel-Aliaga I. 2021 Discovering signaling mechanisms governing metabolism and metabolic diseases with *Drosophila*. *Cell Metab*. **33**, 1279–1292. (doi:10.1016/j.cmet.2021.05.018)
174. Dulken B, Brunet A. 2015 Stem cell aging and sex: are we missing something? *Cell Stem Cell* **16**, 588–590. (doi:10.1016/j.stem.2015.05.006)
175. Mathieu M, Martin-Jaular L, Lavieu G, Théry C. 2019 Specificities of secretion and uptake of exosomes and other extracellular vesicles for cell-to-cell communication. *Nat. Cell Biol.* **21**, 9–17. (doi:10.1038/s41556-018-0250-9)
176. Li Y, Khan N, Ritzel RM, Lei Z, Allen S, Faden AI, Wu J. 2023 Sexually dimorphic extracellular vesicle responses after chronic spinal cord injury are associated with neuroinflammation and neurodegeneration in the aged brain. *J. Neuroinflammation* **20**, 197. (doi:10.1186/s12974-023-02881-z)
177. Zhang H *et al*. 2022 Melatonin improves the quality of maternally aged oocytes by maintaining intercellular communication and antioxidant metabolite supply. *Redox Biol.* **49**, 102215. (doi:10.1016/j.redox.2021.102215)
178. Prevot V. 2015 Puberty in mice and rats. In *Knobil and Neill's physiology of reproduction* (eds TM Plant, AJ Zeleznik), pp. 1395–1439, 4th edition. San Diego, CA: Academic Press. (doi:10.1016/B978-0-12-397175-3.00030-2)
179. Howard SR. 2021 Interpretation of reproductive hormones before, during and after the pubertal transition-Identifying health and disordered puberty. *Clin. Endocrinol.* **95**, 702–715. (doi:10.1111/cen.14578)
180. Wu FCW *et al*. 2010 Identification of late-onset hypogonadism in middle-aged and elderly men. *N. Engl. J. Med.* **363**, 123–135. (doi:10.1056/NEJMoa0911101)

181. Voskuhl R, Itoh Y. 2022 The X factor in neurodegeneration. *J. Exp. Med*. **219**, e20211488. (doi:10.1084/jem.20211488)
182. Jia M, Dahlman-Wright K, Gustafsson JÅ. 2015 Estrogen receptor alpha and beta in health and disease. *Best Pract. Res. Clin. Endocrinol. Metab*. **29**, 557–568. (doi:10.1016/j.beem.2015.04.008)
183. Davey RA, Grossmann M. 2016 Androgen receptor structure, function and biology: from bench to bedside. *Clin. Biochem. Rev.* **37**, 3–15.
184. Gegenhuber B, Wu MV, Bronstein R, Tollkuhn J. 2022 Gene regulation by gonadal hormone receptors underlies brain sex differences. *Nature* **606**, 153–159. (doi:10.1038/s41586-022-04686-1)
185. Rocks D, Shukla M, Ouldibbat L, Finnemann SC, Kalluchi A, Rowley MJ, Kundakovic M. 2022 Sex-specific multi-level 3D genome dynamics in the mouse brain. *Nat. Commun*. **13**, 3438. (doi:10.1038/s41467-022-30961-w)
186. Ng M, Hazrati LN. 2022 Evidence of sex differences in cellular senescence. *Neurobiol. Aging* **120**, 88–104. (doi:10.1016/j.neurobiolaging.2022.08.014)
187. Xing Z, Alman AC, Kirby RS. 2023 Premature menopause and all-cause mortality and life span among women older than 40 years in the NHANES I epidemiologic follow-up study: propensity score matching analysis. *J. Womens. Health* **32**, 950–959. (doi:10.1089/jwh.2023.0189)
188. Torres MJ *et al*. 2018 17β-Estradiol directly lowers mitochondrial membrane microviscosity and improves bioenergetic function in skeletal muscle. *Cell Metab.* **27**, 167–179. (doi:10.1016/j.cmet.2017.10.003)
189. Bianchi VE. 2019 The anti-Inflammatory effects of testosterone. *J. Endocrin. Soc*. **3**, 91–107. (doi:10.1210/js.2018-00186)
190. Dudek P, Kozakowski J, Zgliczyński W. 2017 Late-onset hypogonadism. *Prz. Menopauzalny* **16**, 66–69. (doi:10.5114/pm.2017.68595)
191. Grimm A, Mensah-Nyagan AG, Eckert A. 2016 Alzheimer, mitochondria and gender. *Neurosci. Biobehav. Rev.* **67**, 89–101. (doi:10.1016/j.neubiorev.2016.04.012)
192. Bhasin S. 2021 Testosterone replacement in aging men: an evidence-based patient-centric perspective. *J. Clin. Invest*. **131**. (doi:10.1172/JCI146607)
193. Sehl ME, Ganz PA. 2018 Potential mechanisms of age acceleration caused by estrogen deprivation: do endocrine therapies carry the same risks? *JNCI Cancer Spectrum* **2**, ky035. (doi:10.1093/jncics/pky035)
194. Rocca WA, Grossardt BR, Shuster LT. 2014 Oophorectomy, estrogen, and dementia: a 2014 update. *Mol. Cell. Endocrinol.* **389**, 7–12. (doi:10.1016/j.mce.2014.01.020)
195. Deguchi K *et al*. 2001 Postmenopausal changes in production of type 1 and type 2 cytokines and the effects of hormone replacement therapy. *Menopause* **8**, 266–273. (doi:10.1097/00042192-200107000-00008)
196. Kamada M *et al*. 2001 B cell subsets in postmenopausal women and the effect of hormone replacement therapy. *Maturitas* **37**, 173–179. (doi:10.1016/s0378-5122(00)00180-8)
197. Tower H *et al*. 2022 Estrogen-induced immune changes within the normal mammary gland. *Sci. Rep.* **12**, 18986. (doi:10.1038/s41598-022-21871-4)
198. Kanaya N *et al*. 2019 Single-cell RNA-sequencing analysis of estrogen- and endocrine-disrupting chemical-induced reorganization of mouse mammary gland. *Commun. Biol.* **2**, 406. (doi:10.1038/s42003-019-0618-9)
199. Kim SE, Paik HY, Yoon H, Lee JE, Kim N, Sung MK. 2015 Sex- and gender-specific disparities in colorectal cancer risk. *World J. Gastroenterol.* **21**, 5167–5175. (doi:10.3748/wjg.v21.i17.5167)
200. Jang YC, Huang HL, Leung CY. 2019 Association of hormone replacement therapy with mortality in colorectal cancer survivor: a systematic review and meta-analysis. *BMC Cancer* **19**, 1199. (doi:10.1186/s12885-019-6428-0)
201. Liu S *et al*. 2024 An organism-wide atlas of hormonal signaling based on the mouse lemur single-cell transcriptome. *Nat. Commun.* **15**, 2188. (doi:10.1038/s41467-024-46070-9)
202. Mielke MM, Miller VM. 2021 Improving clinical outcomes through attention to sex and hormones in research. *Nat. Rev. Endocrinol.* **17**, 625–635. (doi:10.1038/s41574-021-00531-z)
203. Iversen L, Sivasubramaniam S, Lee AJ, Fielding S, Hannaford PC. 2017 Lifetime cancer risk and combined oral contraceptives: the royal college of general practitioners' oral contraception study. *Am. J. Obstet. Gynecol.* **216**, 580. (doi:10.1016/j.ajog.2017.02.002)
204. Smoliga JM, Wilber ZT, Robinson BT. 2023 Premature death in bodybuilders: what do we know? *Sports Med*. **53**, 933–948. (doi:10.1007/s40279-022-01801-0)
205. Moses E *et al*. 2024 The killifish germline regulates longevity and somatic repair in a sex-specific manner. *Nat. Aging* **4**, 791–813. (doi:10.1038/s43587-024-00632-0)
206. Migeon BR. 2020 X-linked diseases: susceptible females. *Genet. Med*. **22**, 1156–1174. (doi:10.1038/s41436-020-0779-4)
207. Edgren G, Liang L, Adami HO, Chang ET. 2012 Enigmatic sex disparities in cancer incidence. *Eur. J. Epidemiol*. **27**, 187–196. (doi:10.1007/s10654-011-9647-5)
208. Jäger N *et al*. 2013 Hypermutation of the inactive X chromosome Is a frequent event in cancer. *Cell* **155**, 567–581. (doi:10.1016/j.cell.2013.09.042)
209. Brown CJ, Willard HF. 1994 The human X-inactivation centre is not required for maintenance of X-chromosome inactivation. *Nature* **368**, 154–156. (doi:10.1038/368154a0)
210. Wutz A, Jaenisch R. 2000 A shift from reversible to irreversible X inactivation is triggered during ES cell differentiation. *Mol. Cell.* **5**, 695–705. (doi:10.1016/s1097-2765(00)80248-8)
211. Migeon BR, Axelman J, Beggs AH. 1988 Effect of ageing on reactivation of the human X-linked HPRT locus. *Nature* **335**, 93–96. (doi:10.1038/335093a0)
212. Bennett-Baker PE, Wilkowski J, Burke DT. 2003 Age-associated activation of epigenetically repressed genes in the mouse. *Genetics* **165**, 2055–2062. (doi:10.1093/genetics/165.4.2055)
213. Yang T, Ou J, Yildirim E. 2022 Xist exerts gene-specific silencing during XCI maintenance and impacts lineage-specific cell differentiation and proliferation during hematopoiesis. *Nat. Commun.* **13**, 4464. (doi:10.1038/s41467-022-32273-5)
214. Grigoryan A, Pospiech J, Krämer S, Lipka D, Liehr T, Geiger H, Kimura H, Mulaw MA, Florian MC. 2021 Attrition of X chromosome inactivation in aged hematopoietic stem cells. *Stem Cell Rep.* **16**, 708–716. (doi:10.1016/j.stemcr.2021.03.007)
215. Sierra I, Nguyen SC, Barnett RJ, Cook AL, Ryu HS, Beethem ZT, Philips-Cremins JE, Joyce EF, Anguera MC. 2022 Remodeling and compaction of the inactive X is regulated by xist during female B cell activation. *bioRxiv*. (doi:10.1101/2022.10.19.512821)
216. Forsyth KS *et al*. 2024 NF-κB signaling is required for X-chromosome inactivation maintenance following T cell activation. *Sci. Immunol.* **9**, eado0398. (doi:10.1126/sciimmunol.ado0398)
217. Huret C *et al*. 2024 Altered X-chromosome inactivation predisposes to autoimmunity. *Sci. Adv*. **10**, eadn6537. (doi:10.1126/sciadv.adn6537)
218. Yu B, Qi Y, Li R, Shi Q, Satpathy AT, Chang HY. 2021 B cell-specific XIST complex enforces X-inactivation and restrains atypical B cells. *Cell* **184**, 1790–1803. (doi:10.1016/j.cell.2021.02.015)
219. Wang J, Syrett CM, Kramer MC, Basu A, Atchison ML, Anguera MC. 2016 Unusual maintenance of X chromosome inactivation predisposes female lymphocytes for increased expression from the inactive X. *Proc. Natl Acad. Sci. USA* **113**, E2029–E2038. (doi:10.1073/pnas.1520113113)
220. Miquel CH, Faz-Lopez B, Guéry JC. 2023 Influence of X chromosome in sex-biased autoimmune diseases. *J. Autoimmun.* **137**, 102992. (doi:10.1016/j.jaut.2023.102992)
221. Jiwrajka N, Toothacre NE, Beethem ZT, Sting S, Forsyth KS, Dubin AH, Driscoll A, Stohl W, Anguera MC. 2023 Impaired dynamic X-chromosome inactivation maintenance in T cells is a feature of spontaneous murine SLE that is exacerbated in female-biased models. *J. Autoimmun.* **139**, 103084. (doi:10.1016/j.jaut.2023.103084)
222. Lovell CD, Jiwrajka N, Amerman HK, Cancro MP, Anguera MC. 2024 *Xist* deletion in B cells results in systemic lupus erythematosus phenotypes. *bioRxiv* 2024.05.15.594175. (doi:10.1101/2024.05.15.594175)

223. Crawford JD *et al*. 2023 The XIST lncRNA is a sex-specific reservoir of TLR7 ligands in SLE. *JCI Insight* **8**, e169344. (doi:10.1172/jci.insight.169344)
224. Dou DR *et al*. 2024 Xist ribonucleoproteins promote female sex-biased autoimmunity. *Cell* **187**, 733–749. (doi:10.1016/j.cell.2023.12.037)
225. Hajdarovic KH, Yu D, Hassell LA, Evans S, Packer S, Neretti N, Webb AE. 2022 Single-cell analysis of the aging female mouse hypothalamus. *Nat. Aging* **2**, 662–678. (doi:10.1038/s43587-022-00246-4)
226. Mancino S, Seneviratne J, Mupo A, Krueger F, Oxley D, Eckersley-Maslin MA, da Rocha ST. 2024 Exploring the stability of genomic imprinting and X-chromosome inactivation in the aged brain. *AgingBio* **2**, e20240030. (doi:10.59368/agingbio.20240030)
227. Wen X, Luo Z, Zhao W, Calandrelli R, Nguyen TC, Wan X, Charles Richard JL, Zhong S. 2024 Single-cell multiplex chromatin and RNA interactions in ageing human brain. *Nature* **628**, 648–656. (doi:10.1038/s41586-024-07239-w)
228. Dror I *et al*. 2024 XIST directly regulates X-linked and autosomal genes in naive human pluripotent cells. *Cell* **187**, 110–129. (doi:10.1016/j.cell.2023.11.033)
229. Youness A, Miquel CH, Guéry JC. 2021 Escape from X chromosome Inactivation and the female predominance in autoimmune diseases. *Int. J. Mol. Sci.* **22**, 1114. (doi:10.3390/ijms22031114)
230. Bost C, Arleevskaya MI, Brooks WH, Plaza S, Guery JC, Renaudineau Y. 2022 Long non-coding RNA Xist contribution in systemic lupus erythematosus and rheumatoid arthritis. *Clin. Immunol.* **236**, 108937. (doi:10.1016/j.clim.2022.108937)
231. Forsyth KS, Jiwrajka N, Lovell CD, Toothacre NE, Anguera MC. 2024 The conneXion between sex and immune responses. *Nat. Rev. Immunol.* **24**, 487–502. (doi:10.1038/s41577-024-00996-9)
232. Smith-Bouvier DL, Divekar AA, Sasidhar M, Du S, Tiwari-Woodruff SK, King JK, Arnold AP, Singh RR, Voskuhl RR. 2008 A role for sex chromosome complement in the female bias in autoimmune disease. *J. Exp. Med.* **205**, 1099–1108. (doi:10.1084/jem.20070850)
233. Itoh Y, Golden LC, Itoh N, Matsukawa MA, Ren E, Tse V, Arnold AP, Voskuhl RR. 2019 The X-linked histone demethylase Kdm6a in CD4+ T lymphocytes modulates autoimmunity. *J. Clin. Invest.* **129**, 3852–3863. (doi:10.1172/JCI126250)
234. Davis EJ *et al*. 2020 A second X chromosome contributes to resilience in a mouse model of Alzheimer's disease. *Sci. Transl. Med.* **12**, eaaz5677. (doi:10.1126/scitranslmed.aaz5677)
235. Shaw CK, Abdulai-Saiku S, Marino F, Wang D, Davis EJ, Panning B, Dubal DB. 2023 X Chromosome factor Kdm6a enhances cognition independent of its demethylase function in the aging XY male brain. *J. Gerontol. A Biol. Sci. Med. Sci.* **78**, 938–943. (doi:10.1093/gerona/glad007)
236. Li J, Chen X, McClusky R, Ruiz-Sundstrom M, Itoh Y, Umar S, Arnold AP, Eghbali M. 2014 The number of X chromosomes influences protection from cardiac ischaemia/reperfusion injury in mice: one X is better than two. *Cardiovasc. Res.* **102**, 375–384. (doi:10.1093/cvr/cvu064)
237. Qi S, Al Mamun A, Ngwa C, Romana S, Ritzel R, Arnold AP, McCullough LD, Liu F. 2021 X chromosome escapee genes are involved in ischemic sexual dimorphism through epigenetic modification of inflammatory signals. *J. Neuroinflamm.* **18**, 70. (doi:10.1186/s12974-021-02120-3)
238. Link JC *et al*. 2020 X chromosome dosage of histone demethylase KDM5C determines sex differences in adiposity. *J. Clin. Invest.* **130**, 5688–5702. (doi:10.1172/JCI140223)
239. Lushchak O, Strilbytska O, Storey KB. 2023 Gender-specific effects of pro-longevity interventions in *Drosophila*. *Mech. Ageing Dev.* **209**, 111754. (doi:10.1016/j.mad.2022.111754)
240. Arnegard ME, Whitten LA, Hunter C, Clayton JA. 2020 Sex as a biological variable: a 5-year progress report and call to action. *J. Womens. Health* **29**, 858–864. (doi:10.1089/jwh.2019.8247)
241. Ahmed SMH, Maldera JA, Krunic D, Paiva-Silva GO, Pénalva C, Teleman AA, Edgar BA. 2020 Fitness trade-offs incurred by ovary-to-gut steroid signalling in *Drosophila*. *Nature* **584**, 415–419. (doi:10.1038/s41586-020-2462-y)
242. Chaker Z, Segalada C, Kretz JA, Acar IE, Delgado AC, Crotet V, Moor AE, Doetsch F. 2023 Pregnancy-responsive pools of adult neural stem cells for transient neurogenesis in mothers. *Science* **382**, 958–963. (doi:10.1126/science.abo5199)
243. Viuff M *et al*. 2023 X chromosome dosage and the genetic impact across human tissues. *Genome Med.* **15**, 21. (doi:10.1186/s13073-023-01169-4)
244. Qi M, Pang J, Mitsiades I, Lane AA, Rheinbay E. 2023 Loss of chromosome Y in primary tumors. *Cell* **186**, S0092-8674(23)00646-3. (doi:10.1016/j.cell.2023.06.006)
245. Sierra I, Pyfrom S, Weiner A, Zhao G, Driscoll A, Yu X, Gregory BD, Vaughan AE, Anguera MC. 2023 Unusual X chromosome inactivation maintenance in female alveolar type 2 cells is correlated with increased numbers of X-linked escape genes and sex-biased gene expression. *Stem Cell Rep.* **18**, 489–502. (doi:10.1016/j.stemcr.2022.12.005)

[redacted]

[redacted]